

Conductional remodeling and arrhythmias in the diseased heart



Magda Fontes

Conductional remodeling and arrhythmias in the diseased heart
Copyright © 2015 Magda Fontes

ISBN: 978-90-393-6384-3

Cover Photo: Fibrosis staining on cryosection of a mouse heart

Layout: Magda Fontes

Printed by: Gildeprint Drukkerijen, The Netherlands

Conductional remodeling and arrhythmias in the diseased heart

Geleidingsveranderingen en ritmestoornissen in het zieke hart
(met een samenvatting in het Nederlands)

Remodelação da condução e arritmias no coração com patologia associada
(com um resumo em Português)

Proefschrift

ter verkrijging van de graad van doctor aan de Universiteit Utrecht op gezag van de rector magnificus, prof.dr. G.J. van der Zwaan, ingevolge het besluit van het college voor promoties in het openbaar te verdedigen op donderdag 3 september 2015 des ochtends te 10.30 uur

door

Magda Sofia Cristóvão Martins Castro Fontes

geboren op 12 november 1987
te Lissabon, Portugal

Promotoren: Prof. dr. M.A. Vos
Prof. dr. H.V.M. van Rijen

Copromotoren: Dr. M.F.A. Bierhuizen
Dr. T.P. de Boer

The research described in this thesis was supported by the Dutch Heart Foundation (DHF 2009B72) and by the Netherlands CardioVascular Research Initiative: the Dutch Heart Foundation, Dutch Federation of University Medical Centers, the Netherlands Organisation for Health Research and Development and the Royal Netherlands Academy of Sciences (CVON-PREDICT).

Financial support by the Dutch Heart Foundation and the Heart & Lung Foundation Utrecht for the publication of this thesis is gratefully acknowledged.

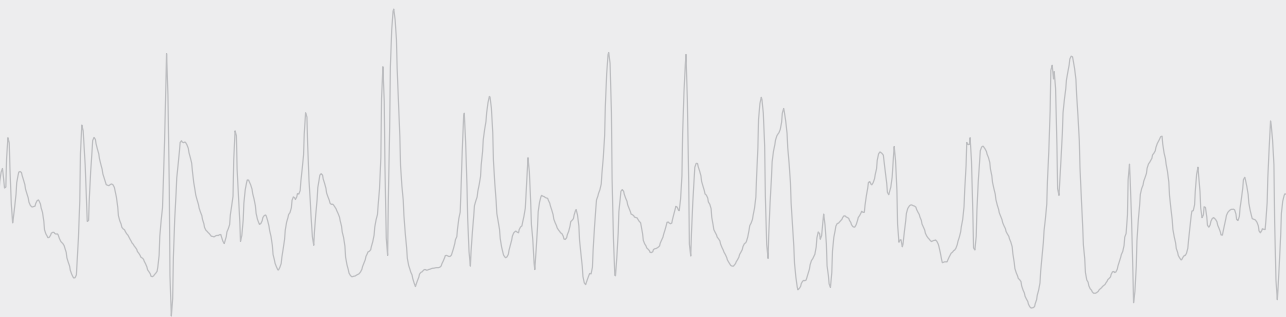
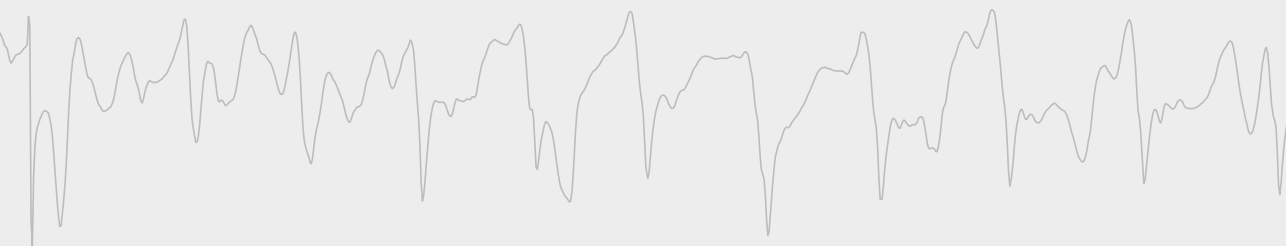
Additional financial support by the Dutch Kidney Foundation and ChipSoft B.V. for the publication of this thesis is gratefully acknowledged.

"Above all else, guard your heart,
for it is the wellspring of life"

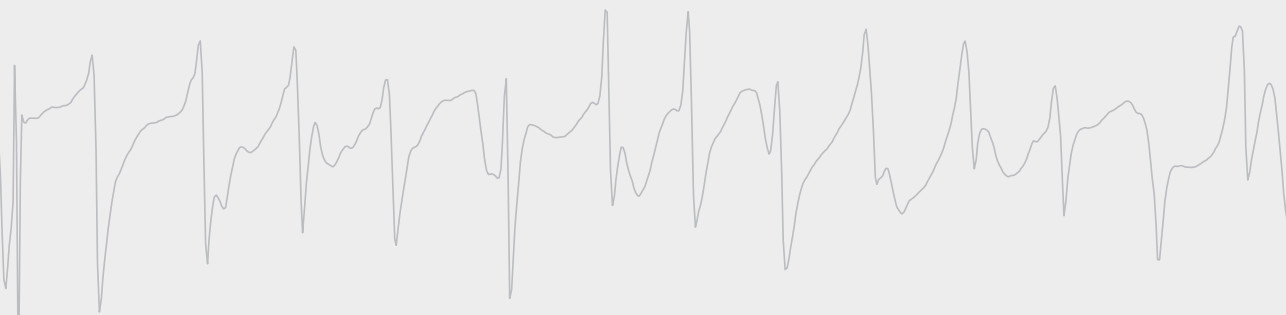
Proverbs 4:23

Contents

Chapter 1	General introduction	9
Chapter 2	Functional consequences of abnormal Cx43 expression in the heart <i>Biochim et Biophys Acta 2012; 1818(8): 2020-9</i>	17
Chapter 3	Arrhythmogenic remodeling in murine models of deoxycorticosterone acetate-salt-induced and 5/6-subtotal nephrectomy-salt-induced cardiorenal disease <i>Cardiorenal Med 2015; 5: 208-18</i>	45
Chapter 4	Calmodulin/CaMKII inhibition augments the localization of cardiac Connexin43 in the intercalated disk: consequences for conduction velocity and arrhythmogenesis <i>Submitted</i>	61
Chapter 5	Changes in Cx43 and Nav1.5 expression precede the occurrence of substantial fibrosis in calcineurin-induced murine cardiac hypertrophy <i>PLoS One 2014; 9(1): e87226</i>	87
Chapter 6	CTGF knockout does not affect cardiac hypertrophy and fibrosis formation upon chronic pressure overload <i>Submitted</i>	109
Chapter 7	General discussion	133
Addendum	Summary in English	149
	Samenvatting in het Nederlands	152
	Resumo em Português	155
	Acknowledgements	158
	List of publications	162
	Curriculum Vitae	165



Magda S.C. Fontes





Chapter 1



General introduction



INTRODUCTION

Societal and clinical background

Cardiovascular disease (CVD) is the main cause of death in Western Society posing an increasing global public health problem, particularly taking into account the increase in elderly populations. In Europe alone, CVD accounts for over 4 million deaths each year, reflecting 47% of all deaths in Europe.¹ An important player in CVD is heart failure, which is a complex syndrome defined by insufficient pump function of the heart due to cardiac structural and functional abnormalities. Although defined as a functional disease, up to 50% of deaths in heart failure patients occurs unexpectedly, due to sudden cardiac death,² caused by fatal cardiac arrhythmias. Heart failure is also one of the final outcomes in the cardiorenal syndrome. This syndrome is characterized by the influence of the diseased heart on the kidney or by the influence of the diseased kidney on the heart, finally causing failure of both organs. Patients with renal failure have an increased risk for CVD, with up to 25% of deaths in dialysis patients being caused by sudden cardiac death.³ Ventricular tachyarrhythmias are responsible for the vast majority of sudden cardiac death events,⁴ however, the underlying mechanisms that lead to these arrhythmias are insufficiently understood. Furthermore, several cardiac pathologies like myocardial infarction and dilated, hypertrophic, and arrhythmogenic cardiomyopathy are characterized by increased susceptibility to arrhythmias. For this reason, more effort is needed to unravel the pathophysiological mechanisms of cardiac arrhythmias in the diseased heart.

Conductional remodeling and calcium signaling in cardiac disease

Under normal conditions, the electrical activation pattern of the heart is initiated in the sinoatrial node, conducted to the atria, slowed in the atrioventricular node, further propagated through the conduction system, and finally terminating by activation of the ventricles. Any disturbance of this normal electrical impulse initiation and/or propagation can result in cardiac arrhythmias. Abnormalities of electrical impulse initiation are associated with cellular disturbances resulting from abnormal automaticity and triggered activity. While abnormal automaticity is when spontaneous irregular electrical activation patterns arise, triggered activity is when premature electrical activation arises from early or delayed afterdepolarizations resulting in premature ventricular contractions. Abnormalities of electrical impulse propagation, the most common mechanism of arrhythmia, are associated with cardiac network disturbances eventually resulting in conduction block and reentry.⁵ This multicellular process occurs when there is repetitive propagation of activation waves that circulate around refractory tissue areas or rotate around a core as spiral waves.⁶

Three main parameters are responsible for proper electrical impulse propagation throughout the heart: 1. electrical cell-to-cell coupling between cardiomyocytes, 2. connective tissue architecture, and 3. excitability of individual cardiomyocytes.

Cell-to-cell coupling

Gap junctions, intercellular channels located between two adjacent cells, mediate electrical coupling and communication between cardiomyocytes.⁷ Gap junctions are formed by two hemichannels, each composed of six connexin proteins. The main connexin isoforms present in the heart are Connexin40 (Cx40), Connexin43 (Cx43), and Connexin45 (Cx45), with Cx43 protein being the most prominent isoform in the working myocardium. Cx43 is mainly located at the cell poles of cardiomyocytes in specialized structures termed intercalated disks. Disturbances in the expression or localization of Cx43 affects cell-to-cell coupling, which can then contribute to conduction slowing. In addition, posttranslational modifications of Cx43 like phosphorylation are also essential for proper maintenance of cell-to-cell coupling. In the diseased heart, Cx43 can typically be downregulated (up to 50%) and/or heterogeneously be redistributed from the intercalated disks to the lateral sides of the cardiomyocytes (called lateralization) and/or less phosphorylated.⁸

Connective tissue architecture

The connective tissue architecture is mainly mediated by the amount of collagen fibers within the extracellular matrix (ECM). The ECM regulates several cellular processes, including the contractility of the heart. The main component of the human cardiac ECM is collagen, mainly collagen type I (85%) and type III (11%). Collagen, produced by fibroblasts and myofibroblasts, has a long half-life of 80-120 days.⁹ A proper balance between synthesis and degradation of collagen is therefore crucial for the normal distribution of thin collagen fibers throughout the healthy heart. If this balance is disturbed it can lead to an excessive deposition and/or decreased degradation of collagen, resulting, together with other ECM components, in accumulation of connective tissue in the ECM (i.e. fibrosis). Fibrosis can result in increased myocardial stiffness, and because cardiomyocytes are embedded in the ECM it can then also impair the electrical coupling between cardiomyocytes. Fibrosis is therefore one of the main contributors to pathological cardiac remodeling and can be found in different cardiac diseases such as hypertension, hypertrophic cardiomyopathy and myocardial infarction.⁹

There are several factors such as cytokines and proteases that can directly or indirectly promote or prevent ECM remodeling and formation of cardiac fibrosis. One of such examples is connective tissue growth factor (CTGF), a matricellular protein secreted into the ECM by both cardiomyocytes and fibroblasts.^{10,11} For decades it was believed that CTGF acted as a potent pro-fibrotic factor, as it was increased, for example, in heart

failure patients and in injury-induced animal models of cardiac fibrosis and hypertrophy.¹² However, recent studies revealed contradicting findings about the role of CTGF as a pro-fibrotic factor.¹³⁻¹⁵ These studies therefore suggest that the role of CTGF in cardiac remodeling remains very elusive.

Excitability of cardiomyocytes

The excitability of cardiomyocytes is mainly mediated by the sodium channel composed of the protein Na_v1.5. The cardiac voltage-dependent sodium channel Na_v1.5 is responsible for a large sodium inward current, resulting in rapid upstroke of the cardiomyocyte action potential (due to very rapid depolarization of its membrane) and subsequent contraction of the cardiomyocyte by activation of the L-type calcium current and excitation-contraction machinery. Mutations in the gene encoding Na_v1.5 have been associated with arrhythmias in several cardiac diseases, such as Brugada syndrome, atrial fibrillation and long QT syndrome.¹⁶ Frequently observed changes in the diseased heart include downregulation of Na_v1.5. Alternatively, even in the setting of unchanged protein levels for Na_v1.5, also channel kinetics may be altered frequently resulting in a reduction of peak sodium current, and an increase in late sodium current.¹⁷⁻¹⁹

Calcium signaling proteins

An additional parameter very relevant for arrhythmogenesis is calcium homeostasis. The maintenance of intracellular calcium concentration is very important for several processes in the heart, such as action potential generation and excitation-contraction coupling. Furthermore, intracellular calcium is involved in several signaling pathways that require binding of calcium, i.e. as second messengers. One of such calcium signaling proteins is calmodulin (CaM). When calcium binds to CaM in the cytoplasm it forms a complex that can subsequently activate different signaling proteins like calcineurin A (CnA) and calcium-calmodulin protein kinase II (CaMKII). Expression and activity of CnA and CaMKII are both upregulated in heart failure patients and closely relate to hypertrophy and arrhythmias.²⁰⁻²³

Aim and research question

The central aim of this thesis was to study different aspects of conductional remodeling in relation to enhanced arrhythmogenesis in the diseased heart. This brings us to the central research questions of this thesis:

- *How, and which changes in expression and localization of conductional parameters can be translated into an arrhythmogenic substrate?*
- *Can modification of one of those parameters prevent arrhythmias?*

To explore these questions, a combination of genetically modified murine models, and models of applied (cardiac) disease have been analyzed with combined electrophysiological and molecular techniques to unravel key players of arrhythmogenesis in the diseased heart.

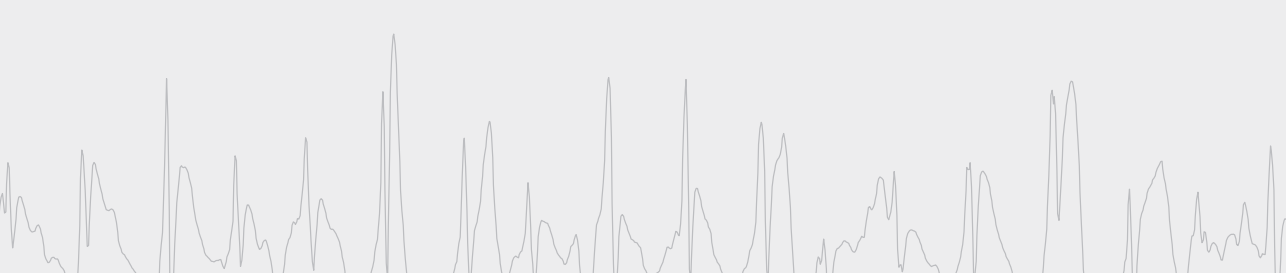


OUTLINE OF THIS THESIS

In **Chapter 2**, we review Cx43 remodeling in different cardiomyopathies in human and animal studies, together with a description of the consequences for conduction, fibrosis and arrhythmias. In **Chapter 3** conductional remodeling is investigated and correlated with enhanced arrhythmogenesis in two mouse models of renal dysfunction with different etiologies. Some studies have shown an interaction between CaM/CaMKII and Cx43 (mostly in Cx43 gating properties). Therefore, we hypothesize in **Chapter 4** that acute and chronic inhibition of CaM/CaMKII can effect Cx43 localization, conduction velocity, and arrhythmogenesis by applying several methodologies in different animal models. Additionally, since CaM is also involved in CnA activation, we further looked into this CnA mechanism. Previously, we studied an accelerated mouse model of hypertrophy by CnA upregulation and showed that these hearts were arrhythmogenic at 4 weeks old.²⁴ In **Chapter 5**, we examined in the same mouse model the temporal changes in conductional parameters Cx43, fibrosis, and Nav1.5 during postnatal development, which ultimately lead to arrhythmias. One of the factors generally involved in fibrosis development is CTGF. Therefore, in **Chapter 6**, we hypothesize that fibrosis formation can be prevented upon chronic pressure overload in a mouse model of conditional CTGF knockout and that other structural and electrophysiological parameters can also be affected. Finally, in **Chapter 7** the results and conclusions from preceding chapters are summarized and discussed, together with suggestions for future perspectives.

REFERENCES

1. Nichols M, Townsend N, Luengo-Fernandez R, Leal J, Gray A, Scarborough P, Rayner M. European cardiovascular disease statistics 2012. *European Heart Network, Brussels and European Society of Cardiology, Sophia Antipolis*. 2012
2. Mosterd A, Hoes AW. Clinical epidemiology of heart failure. *Heart*. 2007;93:1137-1146
3. Whitman IR, Feldman HI, Deo R. CKD and sudden cardiac death: Epidemiology, mechanisms, and therapeutic approaches. *J Am Soc Nephrol*. 2012;23:1929-1939
4. Deo R, Albert CM. Epidemiology and genetics of sudden cardiac death. *Circulation*. 2012;125:620-637
5. Kleber AG, Rudy Y. Basic mechanisms of cardiac impulse propagation and associated arrhythmias. *Physiol Rev*. 2004;84:431-488
6. Akar FG, Hajjar RJ. Gene therapies for arrhythmias in heart failure. *Pflügers Arch*. 2014;466:1211-1217
7. van Veen AA, van Rijen HV, Opthof T. Cardiac gap junction channels: Modulation of expression and channel properties. *Cardiovasc Res*. 2001;51:217-229
8. Severs NJ, Bruce AF, Dupont E, Rothery S. Remodelling of gap junctions and connexin expression in diseased myocardium. *Cardiovasc Res*. 2008;80:9-19
9. de Jong S, van Veen TA, de Bakker JM, Vos MA, van Rijen HV. Biomarkers of myocardial fibrosis. *J Cardiovasc Pharmacol*. 2011;57:522-535
10. Chen MM, Lam A, Abraham JA, Schreiner GF, Joly AH. CTGF expression is induced by TGF-beta in cardiac fibroblasts and cardiac myocytes: A potential role in heart fibrosis. *J Mol Cell Cardiol*. 2000;32:1805-1819
11. Creemers EE, Pinto YM. Molecular mechanisms that control interstitial fibrosis in the pressure-overloaded heart. *Cardiovasc Res*. 2011;89:265-272
12. Koitabashi N, Arai M, Kogure S, Niwano K, Watanabe A, Aoki Y, Maeno T, Nishida T, Kubota S, Takigawa M, Kurabayashi M. Increased connective tissue growth factor relative to brain natriuretic peptide as a determinant of myocardial fibrosis. *Hypertension*. 2007;49:1120-1127
13. Gravning J, Orn S, Kaasboll OJ, Martinov VN, Manhenke C, Dickstein K, Edvardsen T, Attramadal H, Ahmed MS. Myocardial connective tissue growth factor (CCN2/CTGF) attenuates left ventricular remodeling after myocardial infarction. *PLoS One*. 2012;7:e52120
14. Panek AN, Posch MG, Alenina N, Ghadge SK, Erdmann B, Popova E, Perrot A, Geier C, Dietz R, Morano I, Bader M, Ozcelik C. Connective tissue growth factor overexpression in cardiomyocytes promotes cardiac hypertrophy and protection against pressure overload. *PLoS One*. 2009;4:e6743
15. Accornero F, van Berlo JH, Correll RN, Elrod JW, Sargent MA, York A, Rabinowitz JE, Leask A, Molkentin JD. Genetic analysis of connective tissue growth factor as an effector of transforming growth factor beta signaling and cardiac remodeling. *Mol Cell Biol*. 2015;35:2154-2164
16. Shy D, Gillet L, Abriel H. Cardiac sodium channel $\text{Na}_v1.5$ distribution in myocytes via interacting proteins: The multiple pool model. *Biochim Biophys Acta*. 2013;1833:886-894
17. Valdivia CR, Chu WW, Pu J, Foell JD, Haworth RA, Wolff MR, Kamp TJ, Makielski JC. Increased late sodium current in myocytes from a canine heart failure model and from failing human heart. *J Mol Cell Cardiol*. 2005;38:475-483
18. Borlak J, Thum T. Hallmarks of ion channel gene expression in end-stage heart failure. *FASEB J*. 2003;17:1592-1608


19. Soltysinska E, Olesen SP, Christ T, Wettwer E, Varro A, Grunnet M, Jespersen T. Transmural expression of ion channels and transporters in human nondiseased and end-stage failing hearts. *Pflügers Arch.* 2009;459:11-23
20. Anderson ME, Brown JH, Bers DM. CaMKII in myocardial hypertrophy and heart failure. *J Mol Cell Cardiol.* 2011;51:468-473
21. Hoch B, Meyer R, Hetzer R, Krause EG, Karczewski P. Identification and expression of delta-isoforms of the multifunctional Ca^{2+} /calmodulin-dependent protein kinase in failing and nonfailing human myocardium. *Circ Res.* 1999;84:713-721
22. Kirchhefer U, Schmitz W, Scholz H, Neumann J. Activity of cAMP-dependent protein kinase and Ca^{2+} /calmodulin-dependent protein kinase in failing and nonfailing human hearts. *Cardiovasc Res.* 1999;42:254-261
23. Molkentin JD, Lu JR, Antos CL, Markham B, Richardson J, Robbins J, Grant SR, Olson EN. A calcineurin-dependent transcriptional pathway for cardiac hypertrophy. *Cell.* 1998;93:215-228
24. Bierhuizen MF, Boulaksil M, van Stuijvenberg L, van der Nagel R, Jansen AT, Mutsaers NA, Yildirim C, van Veen TA, de Windt LJ, Vos MA, van Rijen HV. In calcineurin-induced cardiac hypertrophy expression of $\text{Nav}1.5$, Cx40 and Cx43 is reduced by different mechanisms. *J Mol Cell Cardiol.* 2008;45:373-384



Magda S.C. Fontes¹, Toon A.B. van Veen¹, Jacques M.T. de Bakker^{1,2}, Harold V.M. van Rijen¹


¹ *Department of Medical Physiology, University Medical Center, Utrecht, The Netherlands*

² *Interuniversity Cardiology Institute of the Netherlands, Utrecht, The Netherlands*





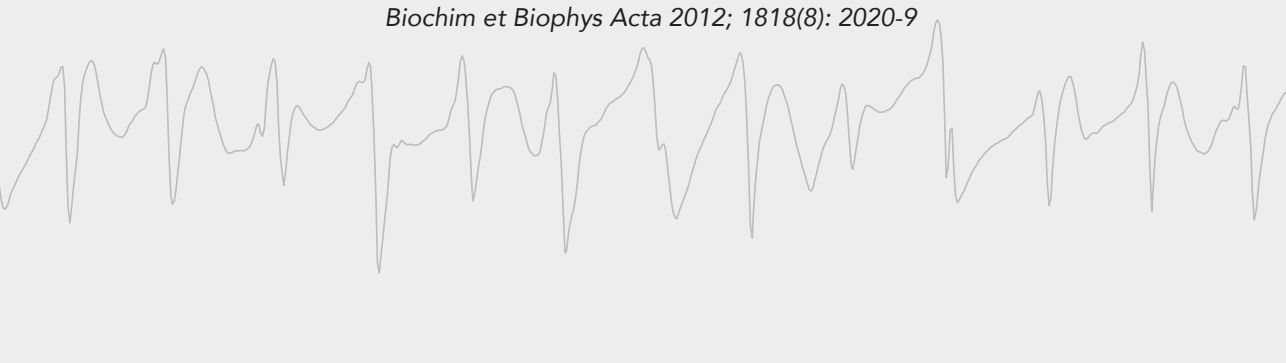
Chapter 2



Functional consequences of abnormal Cx43 expression in the heart



Biochim et Biophys Acta 2012; 1818(8): 2020-9



ABSTRACT

The major gap junction protein expressed in the heart, connexin43 (Cx43), is highly remodeled in the diseased heart. Usually, Cx43 is down-regulated and heterogeneously redistributed to the lateral sides of cardiomyocytes. Reverse remodeling of the impaired Cx43 expression could restore normal cardiac function and normalize electrical stability. In this review, the reduced and heterogeneous Cx43 expression in the heart will be addressed in hypertrophic, dilated and ischemic cardiomyopathy together with its functional consequences of conduction velocity slowing, dispersed impulse conduction, its interaction with fibrosis and propensity to generate arrhythmias. Finally, different therapies are discussed. Treatments aimed to improve the Cx43 expression levels show new potentially anti-arrhythmic therapies during heart failure, but those in the context of acute ischemia can be anti-arrhythmogenic at the cost of larger infarct sizes.

INTRODUCTION

The electrical activation pattern of the heart normally starts in the sinoatrial node (SAN) is then conducted along the atria, delayed in the atrioventricular node (AVN), proceeds through the atrioventricular conduction system and finally ends in the ventricles. Along this pathway, all myocytes are individually activated by intercellular currents that flow through gap junctions.

In the heart, 3 main gap junction proteins are found in the conductive and working myocardial cells: Connexin40 (Cx40), Connexin43 (Cx43), and Connexin45 (Cx45) (Figure 1). Cx40 is expressed in atrial myocytes, in the AVN, His-bundle and ventricular conduction system.¹⁻⁶ Cx43 is by far the most abundant, and is extensively expressed between atrial and ventricular myocytes and to lower degree in parts of the ventricular conduction system.^{3,5,7-14} The expression of Cx45 is restricted to the SAN, the AVN, His-bundle and ventricular conduction system.^{5,15-18}

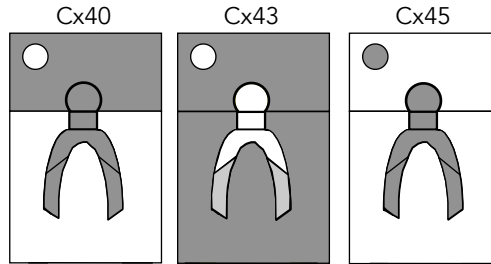


Figure 1. Summary expression patterns of Cx40, Cx43 and Cx45 in the mammalian heart (redrawn after¹³²).

Normally, gap junctions (Cx43) between ventricular myocytes are expressed in a polarized way. Gap junctions are mainly localized at intercalated disks (IDs) at the cell poles, and have relatively low density at lateral sides.^{12,13,19-22} As a consequence, electrical conduction can propagate in both longitudinal and transverse directions. This conduction velocity (CV) is normally higher in the longitudinal than in the transverse direction, giving rise to the phenomenon of anisotropy.^{23,24}

Changes in cardiac workload, either by extrinsic factors, such as pressure or volume overload, or by intrinsic factors such as myocardial infarction or familial hypertrophic cardiomyopathy, generally induce hypertrophic growth of individual myocytes. The classic view is that hypertrophic growth of myocytes counteracts the increased wall tension (Laplace's law), and is therefore often called compensated hypertrophy.^{25,26} Although called compensatory, a prolonged state of hypertrophy increases the risk for progression into heart failure (decompensated hypertrophy). Heart failure has a high morbidity and mortality, which is strongly determined by the high propensity of remodeled hearts to fatal ventricular tachyarrhythmias.²⁷⁻³³

The cardiac remodeling process is governed by structural and electrical changes that decrease the electrical stability of the heart. A hallmark of the electrical changes with regard to impulse conduction is a change in electrical coupling due to abnormal expression of Cx43-constituted gap junctions. Cx43 protein expression is typically down-regulated and channels are often heterogeneously redistributed. This abnormal Cx43 expression is often associated with abnormal conduction and arrhythmias, although there seems to be a large reserve before reduced intercellular coupling becomes arrhythmogenic.³⁴⁻³⁶

In previous reviews we focused on the structure, properties and knockout animal models of Cx43, while in the current review we will focus on Cx43 remodeling in hypertrophic, dilated and ischemic cardiomyopathies and their functional consequences, both in human and animal studies (Table 1).³⁷⁻³⁹

ELECTRICAL COUPLING, IMPULSE CONDUCTION AND ARRHYTHMIAS

Electrical coupling is essential for normal impulse propagation through the heart, together with proper excitability of the cardiomyocytes and normal tissue architecture. Reduced electrical coupling can increase the propensity for arrhythmias by facilitating reentry activity. ‘Circulating excitation’ was first recognized by George Mines as a possible mechanism of arrhythmias⁴⁰ and he already showed that: ‘The circumstances under which the phenomenon made its appearance were such as to produce the favourable conditions of slow conduction and short refractory period’. The relation between CV, the effective refractory period (ERP) and reentry was later captured in the term ‘wavelength’ (λ) which is the distance of the impulse traveled during the refractory period ($\lambda = CV \times ERP^{41}$). Usually, λ is too large to facilitate reentry. In a mouse heart, e.g., CV is ~40cm/s and ERP is ~50ms,⁴² resulting in a λ of 2cm, which is too large to fit on a mouse heart. Conditions that shorten the refractory period or decrease CV will result in a shorter λ , which may fit more easily on the heart, thus increasing the propensity for reentrant arrhythmias. Conversely, conditions that prolong refractoriness or increase CV are expected to prolong the wavelength and reduce arrhythmogeneity.^{41,43}

Reduced expression of Cx43, leading to reduced intercellular coupling is usually associated with reduced CV. However, the relationship between electrical coupling and CV is not linear,⁴⁴ and solid reductions in Cx43 expression are required for reduction of CV. Mice heterozygously deficient for Cx43 showed 50% reduction in Cx43 expression that was associated in some studies with reduced CV, but in others with no effect in the CV.^{42,45-49} Reduction of about 90% in Cx43 expression resulted in about 50% decrease in the CV.^{42,50} While 50% reduction in Cx43 may lead to some conduction slowing, high levels of electrical uncoupling are needed to increase arrhythmogeneity. Abnormal tissue

architecture, e.g. due to increase of collagen deposition (fibrosis), may have synergistic effects together with reduced Cx43 expression and lead to conduction slowing as reviewed by ⁵¹.

HYPERTROPHIC CARDIOMYOPATHY

2

Hypertrophic cardiomyopathy (HCM) is categorized as concentric hypertrophy, with thickening of the left ventricular (LV) wall without a significant dilation of the LV cavity, and is also characterized by cardiomyocyte hypertrophy, myofibrillar disarray, and fibrosis (Figure 2).^{27,52} HCM is usually associated with pressure overload due to aortic stenosis or chronic hypertension.²⁷

In LV biopsies of HCM patients with valvular aortic stenosis, Cx43 was subject to a remodeling process between compensated and decompensated hypertrophy. As mentioned above, compensated hypertrophy reflects proper working myocardium (e.g. ejection fraction > 50%), which may progress to a failing myocardium, decompensated hypertrophy (e.g. ejection fraction < 30%). While compensated hypertrophy had increased levels and increased lateral Cx43 expression, decompensated hypertrophy revealed a heterogeneous reduction of Cx43.⁵³ In other human studies, besides myofibre disarray, a Cx43 redistribution from IDs to the lateral sides of cardiomyocytes, resulting in reduced Cx43 at the IDs, was reported.^{21,54,55} The reduction of Cx43 was not associated with a change in the number of IDs, although they presented an abnormal organization as well as abnormal desmosome organization.⁵⁵ In contrast with the above observation of a Cx43 down-regulation, an increase of Cx43 expression levels in LV biopsies from HCM patients was recently reported for the first time.⁵⁴

Some animal models of HCM showed changes in Cx43 expression similar to that found in humans. A study of transgenic rabbits bearing a mutation in Troponin I that causes HCM in humans, revealed typical HCM characteristics such as cardiomyocyte disarray, fibrosis, and Cx43 disorganization. This disorganization was reflected by a heterogeneous redistribution of Cx43 together with increased levels and increased phosphorylation of Cx43. In these transgenic rabbits no ECG abnormalities were detected, except an altered repolarization phase. The heterogeneous expression of Cx43 did not lead to enhanced arrhythmogeneity, perhaps due to the overall increased levels of Cx43.⁵⁶ Cx43 up-regulation was also detected in another rabbit model of HCM (β -myosin heavy chain-Q403), but only in the midmyocardium. No effect on action potential duration, conduction velocities and anisotropy was detected.⁵⁷

In a guinea pig model with chronic aortic stenosis a reduction in the expression of Cx43, remodeling of IDs and alteration in myocyte shape was observed after transition from compensated to decompensated LV hypertrophy.⁵⁸

Table 1. Abnormal Cx43 expression in heart remodeling.

Cardiomyopathy	Origin	Expression	Cx43		Fibrosis	CV	Arrhythmias	Comments	References
			Phosphorylation	Distribution					
HCM									
Human		↑ LV (early stage) ↓ LV (late stage)		↑				Myofiber disarray, remodeling of IDs	[21]
		↓ LV		↑ LV					[53]
		↑ LV		↑ LV					[55]
									[54]
Rabbit		↑ (Midmyocardial)	↑	↑		=		Cardiomyocyte disarray, altered repolarization phase	[56]
Guinea Pig		↓ LV				=		↑ LV transmural fiber rotation, normal APD	[57]
		↓ RV (IDs)		↑ RV				Altered ventricular myocyte shape, remodeling of IDs	[58]
		↓ LV		↑ LV					[59]
		= RV		↑ RV					[60]
		↑ (early stage) ↓ (late stage)	↑ (early stage) ↓ (late stage)		↑ (late stage) ↓ (late stage)		↑ APD	[59-61]	
		↓		↑	=	↑			[62]
		↓		↑					[67, 68]
		↓ LV		↑ LV					[66]
		↓ LV (distant from fibrosis)		↑ LV (areas of fibrosis)					[64]
		↓ LV		↑ LV					[65]
		↑ (early stage) ↓ (late stage)			↑ (late stage)			Expansion of cardiomyocytes myofilaments	[54]
	Pig								[80]
Dog		↓ LV	↓	↑ LV		↓	↑	No change in action potential upstroke velocity	[69]
		↓	↓	↑		↓			[75]
Rabbit		↑		↑ LV		↓		↑ QRS interval	[81]
		↓	↑		Heterogeneous		=	Regional conduction block	[77]
Mouse		↓				↓		↓ Fractional shortening	[78]
		=	↑ (VT+)		↑	↓ RV CV _L Heterogeneous	↑ (44%)	↑ PQ, QT and QRS prolongation	[79]

Table 1. Abnormal Cx43 expression in heart remodeling. (continued)

Cardiomyopathy	Origin	Cx43				Fibrosis	CV	Arrhythmias	Comments	References
		Expression	Phosphorylation	Heterogeneous	Distribution					
Human		↓ (distant from BZ)		↑ (BZ) = (distant from BZ)	↑ (BZ)				Altered myocyte orientation and cell shape in BZ	[85, 95]
		↓ LV					= CV _L ↓ CV _R		↑ Refractory period	[86]
		↓ LV		↑ LV					Change in cell size distribution	[55]
		↓ (distant from BZ)		↑ (BZ) = (distant from BZ)					↑ Cx40	[64]
		↓								[65]
ICM	Dog	↓		↑		↑ (BZ)			Cardiomyocyte disarray	[96]
		↓	↓							[87]
							= CV _L ↓ CV _R	↑		[100]
				↑	↑	↑ (BZ)		↑		[101]
										[104]
Pig	Rabbit	↓		↑			Heterogeneous			[88]
										[89]
							↓			[90]
										[105]
										[106]

Abbreviations: HCM, hypertrophic cardiomyopathy; DCM, dilated cardiomyopathy; ICM, ischemic cardiomyopathy; ↑, increased; ↓, decreased; ↓, more decreased than ↑; =, unchanged; LV, left ventricle; RV, right ventricle; CV_L, longitudinal conduction velocity; CV_R, transversal conduction velocity; VT+, occurrence of ventricular tachycardia; BZ, border zone; ID, intercalated disk; APD, action potential duration.

Finally, a rat model of HCM (monocrotaline-induced pulmonary hypertension or pressure overload) showed, in both right and left ventricle, a normal distribution of desmoplakin in the IDs and normal levels of total Cx43, although there was redistribution of Cx43 from the IDs to the cytoplasm and lateral sides of myocytes, and increased dephosphorylated Cx43.⁵⁹⁻⁶¹ Furthermore, measurements of CV in the right ventricle revealed a decrease in the longitudinal direction when compared with control, while transversal CV remained unchanged, resulting in reduced anisotropic ratio.⁵⁹ Reduced longitudinal CV probably resulted from reduced Cx43 at IDs, while unchanged transversal CV probably resulted from non-functional lateral Cx43, which may reflect the increase in dephosphorylation of Cx43. In another rat model of pressure overload by ascending aortic banding, a reduction in Cx43 expression, an increase in dephosphorylated Cx43 and a reduction in CV in the late stage of hypertrophy was found.⁶² However, as described above in a human HCM study, in early stages of hypertrophy the typical increase of Cx43 was observed, but also an increase in phosphorylation of Cx43, and slowing of CV that was less severe than observed in the late stage. In this animal model of pressure overload it was possible to induce sustained ventricular tachyarrhythmia.⁶²

Reports from HCM patients and different animal models revealed an increase and lateralization of Cx43 together with slowing of CV in early, compensated stage of hypertrophy that was followed by a reduction of Cx43, resulting in development of arrhythmias.

DILATED CARDIOMYOPATHY

Dilated cardiomyopathy (DCM) is characterized by eccentric hypertrophy, with thickening of the LV wall in conjunction with an increase in the diameter of the LV cavity (Figure 2). It is usually associated with volume overload, as aortic or mitral valve regurgitation and anemia or as muscle dysfunction.^{27,29,63}

Left ventricular biopsies from patients with DCM showed heterogeneous down-regulation of Cx43 expression, with a greater loss in the IDs compared to the lateral sides.^{54,64,65} In small areas of replacement fibrosis there was a redistribution of Cx43, whereas in areas distant from this region, Cx43 was normally distributed in the IDs.⁶⁵ Hearts from DCM patients who died suddenly also showed reduction and redistribution of Cx43 expression in both ventricles.⁶⁶ Since the control hearts used in this study were from patients without DCM, no correlation could be made between reduction of Cx43 and sudden cardiac death in DCM patients. In order to find more about the substrate of arrhythmias, DCM patients were subdivided in patients with ventricular tachycardia (VT+) or without VT (VT-) and in patients with late ventricular potentials (LP+) or without LP (LP-). Left ventricular ejection fraction was similar in VT and LP groups and the amount of fibrosis was not measured in VT groups but it was similar in LP groups. VT+ and LP+ patients

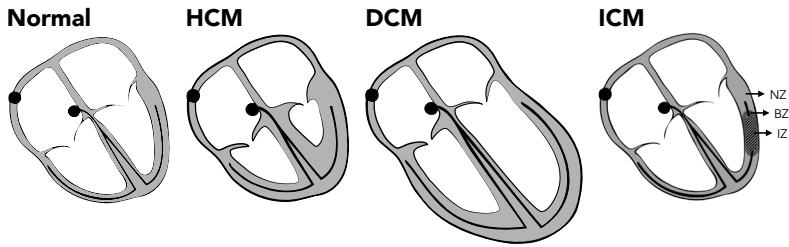


Figure 2. Morphologic differences between normal and cardiomyopathic hearts.

From left to right: normal, hypertrophic cardiomyopathy (HCM), dilated cardiomyopathy (DCM), and ischemic cardiomyopathy (ICM). In ICM a border zone (BZ) is present between the infarct zone (IZ) and the normal zone (NZ).

showed a reduced and heterogeneous distribution of Cx43 when compared with VT- and LP-, and LP+ patients presented high susceptibility for ventricular tachycardia.^{67,68} This suggests that heterogeneous reduction of Cx43, which is related with the presence of ventricular tachycardia and late ventricular potentials, may play a role in development of ventricular arrhythmias in DCM patients, possibly reflecting the patient's arrhythmic risk.

Several animal models of DCM showed similar reductions in Cx43 expression. In a canine pacing-tachycardia model of DCM, epicardial and endocardial CVs in both ventricles were decreased by more than 20%.⁶⁹ In the epicardial and endocardial LV, Cx43 expression levels were decreased by 40% with Cx43 being more expressed in epicardial than in the endocardial tissue. Contrarily, epicardial CV was further decreased when compared with endocardial CV. In both ventricles, there was lateralization and dephosphorylation of Cx43 as well as prolongation of the QRS interval although no change was detected in the action potential upstroke velocity or in fibrosis. The propensity for induced polymorphic ventricular tachycardia was increased in this model and associated with decreased wavelength.⁶⁹ In this study, the decreased epicardial CV did not seem to correlate with the increased epicardial Cx43 expression (when compared with endocardial Cx43 expression) or with reduced excitability because the action potential upstroke velocity was unchanged. The prolongation of the QRS interval can result from the remodeling of potassium currents in the failing heart like the reduction in the inward rectifier K^+ current, but also from the down-regulation in the peak of the Ca^{2+} -independent transient outward current, although Na^+ current remained unchanged.^{70,71} In addition, QRS prolongation might be due to enlargement of the heart without any effect on the absolute value of CV.⁷² Interestingly, another study on the same preparation has shown that Cx43 heterogeneity also leads to transmural heterogeneity of action potential duration, which may also be part of the arrhythmogenic substrate.^{73,74} In the mentioned canine model it was demonstrated that the reduction of Cx43 precedes the slowing of CV, perhaps because reduction of Cx43 alone is not sufficient for conduction slowing.^{42,49,75} The development of fibrosis, in conjunction with reduced Cx43 may

be needed for conduction slowing.⁷⁶ The increase in dephosphorylation of Cx43 was associated with later stages of heart failure while Cx43 lateralization appears in an even later stage, when the CV is significantly reduced.⁷⁵

A mouse model of DCM induced by forced retinoic acid signaling revealed a prolongation of the QRS interval, decreased conduction velocity, increased conduction heterogeneity, regional conduction block but these mice were not susceptible to ventricular arrhythmias. A reduction of Cx43 was accompanied by Cx43 lateralization in the border zones of the affected intramural area in the LV free wall.^{77,78} The heterogeneous reduction of Cx43 may play a role in the appearance of the regional conduction block. The reduction in Cx43 presumably was followed by a reduction in other intercellular junction proteins, β -catenin and N-cadherin. Besides, there was heterogeneous re-expression of the hypertrophic markers like α -skeletal actin and β -MHC and in some severely affected mice low levels of Cx40 re-expression were found.⁷⁷ Since Cx40 expression levels were low, compensation by this connexin isoform can presumably be excluded. A murine model of longstanding pressure overload subjected to transverse aortic constriction (TAC) showed an increase in LV end-diastolic and end-systolic volumes, a decrease in fractional shortening, and a rapid structural and electrical remodeling. Electrical remodeling was reflected by gradual decrease in PQ, QT and QRS prolongation and by reduced longitudinal CV in the right ventricle. Structural remodeling was reflected by heterogeneous expression of Cx43 and increased interstitial fibrosis in TAC mice while Cx43 expression levels were similar to control hearts. In this study 44% of the TAC mice were susceptible to induce polymorphic ventricular tachycardia. The only difference found in TAC mice with and without arrhythmias was a more pronounced heterogeneity of Cx43 expression in the arrhythmogenic TAC mice.⁷⁹ Thus, the arrhythmias found in this animal model of pressure overload seemed to be associated with heterogeneous expression of Cx43, which may lead to functional block and unstable reentry, resulting in polymorphic ventricular tachyarrhythmias.

Interestingly, in a pig model of DCM, expression of Cx43 was increased in the early stage of hypertrophy, but with its progression into heart failure, the levels of Cx43 decreased, cardiomyocytes myofilaments expanded and fibrosis increased.⁸⁰ Up-regulation of Cx43 in acute stages of hypertrophy in DCM but also in HCM may represent an immediate compensatory response of the heart to increased workload. A rabbit model of DCM due to surgically aortic regurgitation showed an increase in expression of Cx43 over time compared with control hearts in which expression of Cx43 remained similar up to 2.5 years.⁸¹ This is the opposite to what was found in other animal models of DCM in which Cx43 expression decreased over time. The overall up-regulation of Cx43 in these previous studies could also result from beta-adrenergic stimulation. After 24 hours of beta-adrenergic stimulation, an increase in Cx43 expression was observed in cultured neonatal rat cardiomyocytes, as well as an increase in gap junction currents.⁸² However,

in a different study on the same preparation, 24 hours of beta-adrenergic stimulation lead to an increase in CV but had no effect on expression or distribution of Cx43, other than a slight increase in phosphorylated Cx43.⁸³

In DCM, heterogeneous reduction of Cx43 seems to be closely related with the presence of ventricular tachycardia in both patient and animal models, perhaps because the concomitant development of fibrosis is prerequisite for CV slowing. Besides that, prolongation of the QRS interval is possibly related with disturbances in ion channels.

ISCHEMIC CARDIOMYOPATHY

Ischemic cardiomyopathy (ICM) usually results from coronary artery disease and can be divided in an acute phase followed by a chronic phase. The acute ischemia is associated with gap junction closure thus with reduced intercellular coupling. The chronic phase refers to healing/healed infarcts that corresponds to the tissue that is recovering from the suffered ischemia and since it is a late stage, is associated with changes in the Cx43-constituent gap junction expression and/or trafficking. After acute myocardial infarction, there is the formation of a compact infarct scar surrounded by a border zone (BZ) that separates the infarct scar from normal tissue (Figure 2).^{27,29} The BZ is composed of damaged but still viable muscle fibers, with abnormal physiological properties.⁸⁴

The presence of myocyte bridges extended across infarcted areas and coupled by gap junctions, suggests the existence of impulse propagation between areas of healthy myocardium, although in some cases those bridges were made up from a single myocyte.⁸⁵ Impulse propagation in these conditions caused transversal CV slowing due to a “zigzag” course of activation performed by impulses between healthy myocardium, although the longitudinal CV remained unchanged.⁸⁶

Acute myocardial infarction and changes in gap junction function

In a canine model of infarction, active membrane properties were largely affected in acute ischemia, followed by a partial recovery of the surviving myocytes, with the action potential duration remaining reduced.⁸⁴ One hour after ischemia, Cx43 was dephosphorylated and heterogeneously reduced in infarcted areas, and after acute ischemia small amounts of Cx43 were detected at the lateral sides of cardiomyocytes, although the signal at IDs was practically gone.⁸⁷ In an isolated perfused rabbit heart model of ischemia/reperfusion, the reduction of Cx43 over time is in accordance with that described in the canine model. Besides a redistribution of Cx43, another intercellular junction protein N-cadherin was reduced and structure integrity was altered. Despite these disturbances, epicardial CV anisotropy was unchanged.⁸⁸ In arterially blood-perfused rabbit papillary muscles there was an increased extracellular longitudinal

resistance during the acute, reversible phase of myocardial ischemia, while intracellular longitudinal resistance remained unchanged, resulting in unaffected electrical coupling. During this phase, the increased extracellular resistance most likely contributed to the small slowing of CV observed. On the other hand, after 15-20 minutes of ischemia, increased intracellular longitudinal resistance resulted in rapid electrical uncoupling. This probably leads to CV slowing that may be an important factor for the occurrence of arrhythmias during this phase of ischemia.⁸⁹ In an isolated perfused adult rat heart model of ischemia/reperfusion a progressive dephosphorylation of Cx43 over time during ischemia was observed together with progressive electrical uncoupling and progressive reduction in total Cx43 immunofluorescent signal, while in control hearts practically all Cx43 remained phosphorylated. Although the total amount of Cx43 did not change, the decrease in total Cx43 immunofluorescent signal and increase in dephosphorylated Cx43 at IDs were probably related with the electrical uncoupling. After reperfusion, the functional recovery was associated with an increase in the phosphorylation of Cx43. These observations lead the authors to suggest that uncoupling induced by ischemia was also associated with a translocation of Cx43 from gap junctions to intracellular sites, although this was not demonstrated.⁹⁰ In neonatal rat ventricular myocyte monolayers with induced acute regional ischemia/reperfusion, a slower CV was observed after a slow recovery from Cx43 dephosphorylation during early reperfusion.⁹¹ This slow recovery from Cx43 dephosphorylation may be a fundamental factor for the creation of a highly arrhythmogenic substrate by prolonging slow conduction after recovery of the membrane excitability. Different studies indicated the following serine positions of Cx43, Ser297/368, Ser325/328/330 or Ser365, as being phosphorylated in normal conditions and dephosphorylated during ischemia.⁹²⁻⁹⁴ However, the functional consequences of (de)phosphorylation at these different sites are not known, nor the relation of dephosphorylated Cx43 with the redistribution of Cx43 from IDs to the lateral sides of myocytes.

Chronic myocardial infarction and gap junction remodeling

Areas of the BZ in human healed infarcts revealed alterations in myocyte orientation and in cell shape with more rounded or attenuated forms being present, enlargement or multiple nuclei, and disorientation of the individual myofilaments in the intact myofibrils.⁸⁵ Contrarily, areas of myocardium distant from the healed infarct appeared to be well-preserved with arrangement of fibers, IDs and an overall cellular structure resembling that of normal myocardium.^{85,95} In areas of the BZ of healed infarcts a heterogeneous redistribution of Cx43 to the lateral sides of myocytes was detected in contrast with areas distant from healed infarcts, where the number of IDs remained the same as in control heart and Cx43 was confined to well-defined IDs.^{55,64,65,85,95} Although these regions distant from the infarct scars (called normal zone) revealed normal Cx43 distribution, the amount

of Cx43 was reduced and the cell size distribution was changed.^{55,64,65,95} Up-regulation of Cx40 detected in the endocardium may represent a compensatory response to the decrease in Cx43.⁶⁴

The BZ of infarcted canine hearts was characterized by reduced and altered kinetics of sodium current, slower CV and down-regulation of Cx43, with lateral Cx43 being more reduced than in IDs.^{84,88,96,97} These observations suggest an increased axial resistivity in the transverse direction, possibly contributing this way to the development of reentrant arrhythmias.⁹⁶ Cx43 remodeling that resulted in a relative myocyte uncoupling was described together with an increase in interstitial fibrosis, distorted muscle fibers and myocyte disarray, pointing to a non-uniform anisotropic structure.^{84,96,98} Concerning the electrical remodeling, another canine model of infarction presented a reduction in transverse coupling conductance⁹⁹ which is in accordance with decreased transverse CV,¹⁰⁰ while longitudinal coupling and CV remained unchanged. Surprisingly, no reduction in Cx43 expression was detected, suggesting the presence of non-functional gap junctions, an increase in gap junction proteins dephosphorylation, or changes in other ion channels which e.g. alter the passive membrane properties.⁹⁹ The decrease in transverse conductance and CV (longitudinally oriented lines of apparent block) most probably contributed to the occurrence of reentry in this model of infarction and this is a key factor in the development of ventricular tachycardia.¹⁰⁰ Moreover, the abnormal redistribution and lateralization of Cx43 observed in the epicardial BZ occurred before the presence of increased fibrosis indicating an early post-infarction remodeling. This disturbance in Cx43 distribution was associated with the location of the central common pathways of the figure-of-8 reentry.¹⁰¹ Cabo and coworkers¹⁰² described some differences between the central common pathway (CCP) and outer pathway (OP) of the reentrant circuit in the canine epicardial BZ. The CV in OP myocytes was reduced with transversal CV more reduced than the longitudinal one, leading to an increase in the anisotropic ratio. In these cells the transversal gap junctional conductance decreased while the longitudinal conductance remained normal when compared to control tissue. In OP myocytes there was no Cx43 lateralization. Instead, in CCP myocytes a lateralization of Cx43 was observed. In these cells, transversal and longitudinal gap junctional conductances were similar to that of normal tissue as well as the anisotropic ratio, which reflects the equal reduction in transversal and longitudinal CVs. The decrease in longitudinal CV was bigger in CCP than in OP myocytes.¹⁰² These changes can result from the heterogeneous remodeling of ion channels in the epicardial BZ. A previous study from the same group showed a reduction in sodium and calcium current densities in CCP and OP myocytes.¹⁰³ Thus, a combined effect of altered Cx43 and ion channel expression may explain the differences in the observed CVs. In the acute and reversible phase of myocardial ischemia in isolated porcine hearts, there was also a heterogeneous reduction in longitudinal and transversal CV and a shorter amplitude of the action potentials, which seem to be initiated by the rapid Na⁺ inward current.¹⁰⁴ In another rat model of myocardial ischemia, Cx43 was

observed in well-defined IDs.¹⁰⁵ In acute ischemia Cx43, desmoplakin and cadherin expressions in the BZ of the infarct were reduced and redistributed to the lateral borders of cardiomyocytes, which further deteriorated during the chronic phase.^{105,106} The IDs were remodeled, changing its form into tentacle-like structures in the BZ of the infarct, which was followed by the temporally presence of small amounts of Cx43 expression at the lateral sides of cardiomyocytes and by the increased deposition of extracellular matrix proteins like β 1-integrin.^{105,106} These changes may contribute to alterations of the CVs in the BZs of the infarct.

In ICM practically all the animal models presented a heterogeneous redistribution and reduction of Cx43 in the BZ of the infarcts, usually followed by slowing of CV either in the longitudinal or transverse direction, and by an ongoing increases in fibrosis. In the canine model of infarction the occurrence of reentrant arrhythmias and a decrease in the sodium current was also reported.

THERAPIES

As described above, expression of Cx43 in the heart is strongly remodeled in different forms of cardiomyopathy. Therefore, several attempts have been made to improve electrical coupling and, as a final goal, to reduce arrhythmogenesis which is frequently present in these diseases.

Some of the treatments already used in rat, rabbit, guinea pig or canine models of different cardiomyopathies are: rotigaptide, which increases gap junction intercellular communication; diltiazem, an L-type calcium channel blocker; estrogen; sotalol, a potassium channel blocker; omega-3 fatty acids, unsaturated fatty acids; atorvastatin, a member of statin class of drugs; gap26, a synthetic structural mimetic peptide deriving from the first extracellular loop of Cx43; losartan, which is an antagonist of angiotensin II type 1 receptor; apocynin, which is an inhibitor of nicotinamide adenine dinucleotide phosphate (NADPH) oxidase, a major source of reactive oxygen species in the heart; and targeted external heavy ion beam irradiation (THIR) (Table 2).

Losartan reduced LV hypertrophy and Cx43 disorganization, as Cx43 remained mainly at IDs.⁶⁰ Inhibition of the renin-angiotensin-aldosterone system in other studies also resulted in prevention of gap junction remodeling, suppression of fibrosis, normalization of impulse conduction, and increased electrical stability.^{107,108} THIR increased LV lateralization and expression of Cx43, which in normal heart lasted up to one year after a single THIR treatment and improved conductivity, decreased spatial heterogeneity of repolarization, and reduced the vulnerability for ventricular arrhythmias after myocardial infarction.^{109,110} Estrogen reduced Cx43 dephosphorylation, myocyte apoptosis and infarct size, and reduced the vulnerability to ventricular arrhythmias.¹¹¹⁻¹¹³ Diltiazem improved LV function and reduced Cx43 dephosphorylation after reperfusion.¹¹⁴ Apocynin reduced the

Table 2. Therapy treatments to reverse the abnormal Cx43 expression in heart remodeling.

Therapy	Tissue origin	Expression	Cx43		Fibrosis	CV	Arrhythmias	Comments	References
			Phosphorylation	Distribution					
Losartan	Rat			↑					[60]
	Rabbit							↑ Spatial heterogeneity of repolarization	[109]
Estrogen	Rat	↑	↑				↑	↑ Myocyte apoptosis	[111]
								↓ Infarct size, ↓ free radicals	[113]
Diltiazem	Rat	↑	↑				↓	↑ LV function	[112]
Apocynin	Rabbit	↑	↑		↓		↓	↑ SERCA2a expression and activity, ↓ QRS interval, ↓ ERP, ↓ MAP duration at 90% repolarization	[114]
	Guinea								[115, 116]
Sotalol	Pig							Recovery of electrical coupling, ↓ APD	[117]
Omega-3 fatty acids	Rabbit					↑	↓	↑ ERP	[118]
	Rat	↑					↓	= Hypertrophy	[119]
Atorvastatin	Rat		↓				↓	Preservation of cardiomyocytes and gap junctions integrity	[120]
								Preservation of cardiomyocytes and gap junctions integrity	[120]
Gap26	Rat							↓ Infarct size	[121]
Rotigaptide							↓	↑ Conductance	[122]
								= ERP, surface ECG, mean arterial pressure or infarct size	
	Canine	↑ (gap junctions in general)					↓	↓ Infarct size	[123]
		↑ (EBZ)						= Surface ECG, blood pressure	[124]
	Human (ex-vivo)	↑ (EBZ)						↑ ERP	[125]
						↑ CV		Destabilized transverse conduction curves	

Abbreviations: THIR, targeted external heavy ion beam irradiation; ↑, increased; ↓, decreased; =, no effect; LV, left ventricle; CV, longitudinal conduction velocity; EBZ, epicardial border zone; ERP, effective refractory period; MAP, monophasic action potential; APD, action potential duration; ECG, electrocardiography.

vulnerability for ventricular arrhythmias, increased Cx43 expression and phosphorylation, decreased interstitial fibrosis and increased SERCA2a expression and activity.^{115,116} The improvement in cardiac dysfunction was also characterized by shortening of QRS interval, ERP and monophasic action potential duration at 90% repolarization.¹¹⁵ Sotalol prevented ischemia-induced electrical uncoupling although there was still shortening of the action potential duration and also improved electrical coupling after acute ischemia.¹¹⁷ In another study sotalol increased CV and the ERP, and the propensity for induced ventricular tachycardia was markedly decreased.¹¹⁸ Omega-3 fatty acids and atorvastatin increased Cx43 expression although there was a decrease in the phosphorylation of Cx43, preserved the integrity of cardiomyocytes and gap junctions, and decreased the propensity for induced ventricular fibrillation, although fibrosis was not reduced.^{119,120} Gap26 protected the heart against ischemic injury by reducing the infarct size by half, either when applied before or during ischemia.¹²¹ Rotigaptide reduced the infarct size, enhanced gap junctional conductance and suppressed reentrant ventricular tachycardia during ischemia, although no effect was observed in ERP, surface ECG parameters and blood pressure.^{122,123} In epicardial BZ, rotigaptide increased Cx43 but had no effect on Cx43 phosphorylation or lateralization. However, rotigaptide in the epicardial BZ did not suppress ventricular tachycardia and did not improve CV, although the ERP was decreased.¹²⁴ Since Cx43 in epicardial BZ was not totally recovered, this could reflect the non-improvement of CV and in prevention of arrhythmias. In explanted perfused hearts from patients with end-stage heart failure, rotigaptide resulted in decreased ERP, increased longitudinal CV and normalized longitudinal conduction curves, although with destabilized transversal conduction curves.¹²⁵

Although most of the studies associate the improvement of electrical coupling as being anti-arrhythmogenic, some studies demonstrate the opposite after coronary occlusion: mice with 50% reduction of Cx43 presented an infarct size smaller than in normal mice;¹²⁶ mice with a deletion of the carboxyl terminal domain of Cx43 showed an increase in the infarct size;¹²⁷ and mice expressing Cx32, which is a connexin isoform pH- and voltage-independent, presented an increase in infarct size compared with control mice.^{128,129} The effect on arrhythmogeneity was found to be beneficial¹²⁹ or absent.¹²⁸ Therefore, improving intercellular coupling during acute ischemia can have anti-arrhythmic effects, but will also lead to increased infarct size after coronary occlusion.

These findings suggest that strategies that suppress Cx43 remodeling can be potential new anti-arrhythmic targets, especially in the context of heart failure associated arrhythmias. The opportunities for treatment of ischemia related arrhythmias are more limited, because reduction of arrhythmogeneity is achieved at the cost of increased infarct size.

CONCLUSIONS

Abnormal Cx43 expression in the heart has been reported in several forms of cardiomyopathies as hypertrophic, dilated and ischemic cardiomyopathy. Generally, Cx43 is down-regulated and heterogeneously redistributed throughout the heart, and in some cases it is lateralized. This abnormal Cx43 expression is often followed by a reduction in the CV, which then seems to be accompanied by an increase in fibrosis. All these disturbances may lead somehow to the development of arrhythmias (Figure 3). In addition, ventricular tachycardia seems to be associated with the heterogeneous reduction of Cx43. One of the explanations for conduction slowing is the Cx43 redistribution and the decrease in the phosphorylation of Cx43, but other factors can also be involved like altered repolarization phase and a reduction in the sodium current. An interesting factor in the ischemic heart is the up-regulation of Cx43 in fibroblasts,¹³⁰ that can also play a role in the disturbance of the CVs. Prolongation of the QRS interval can possibly be related with disturbances in ion channels and prolongation of the action potential duration can possibly be related with the decrease in the intercellular coupling conductance.¹³¹ In addition to the general down-regulation of Cx43, in some cases Cx43 is up-regulated in early, compensated stage of hypertrophy but followed by a down-regulation, which could reflect a compensatory mechanism to the workload.

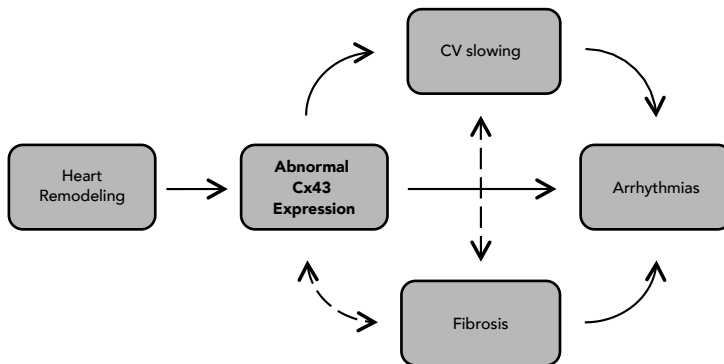


Figure 3. Functional consequences of abnormal Cx43 expression after heart remodeling.

Several approaches that successively improved Cx43 expression levels or Cx43 conductance and reduced the vulnerability for ventricular arrhythmias open the opportunity for potentially new anti-arrhythmic therapies for heart failure.

In conclusion, the functional consequences of reduced and heterogeneous Cx43 expression in the heart are slow and dispersed impulse conduction, which may increase the propensity to generate arrhythmias, especially when combined with increased fibrosis. Treatments aimed to improve the Cx43 expression levels show new potentially

anti-arrhythmic therapies during heart failure, but those in the context of acute ischemia can be anti-arrhythmogenic at the cost of larger infarct sizes.

FUNDING SOURCES

This work was supported by the Netherlands Heart Foundation, grant 2009B072.

REFERENCES

1. Gros D, Jarry-Guichard T, Ten Velde I, de Mazière A, van Kempen MJ, Davoust J, Briand JP, Moorman AF, Jongsma HJ. Restricted distribution of connexin40, a gap junctional protein, in mammalian heart. *Circ Res*. 1994;74:839-851
2. Delorme B, Dahl E, Jarry-Guichard T, Marics I, Briand JP, Willecke K, Gros D, Theveniau-Ruissy M. Developmental regulation of connexin 40 gene expression in mouse heart correlates with the differentiation of the conduction system. *Dev Dyn*. 1995;204:358-371
3. Delorme B, Dahl E, Jarry-Guichard T, Briand JP, Willecke K, Gros D, Theveniau-Ruissy M. Expression pattern of connexin gene products at the early developmental stages of the mouse cardiovascular system. *Circ Res*. 1997;81:423-437
4. Miquerol L, Meysen S, Mangoni M, Bois P, van Rijen HV, Abran P, Jongsma HJ, Nargeot J, Gros D. Architectural and functional asymmetry of the His-Purkinje system of the murine heart. *Cardiovasc Res*. 2004;63:77-86
5. van Veen TA, van Rijen HV, van Kempen MJ, Miquerol L, Opthof T, Gros D, Vos MA, Jongsma HJ, de Bakker JM. Discontinuous conduction in mouse bundle branches is caused by bundle architecture. *Circulation*. 2005;112:2235-2244
6. Davis LM, Rodefeld ME, Green K, Beyer EC, Saffitz JE. Gap junction protein phenotypes of the human heart and conduction system. *J Cardiovasc Electrophysiol*. 1995;6:813-822
7. Beyer EC, Paul DL, Goodenough DA. Connexin43: A protein from rat heart homologous to a gap junction protein from liver. *J Cell Biol*. 1987;105:2621-2629
8. Beyer EC, Kistler J, Paul DL, Goodenough DA. Antisera directed against connexin43 peptides react with a 43-kD protein localized to gap junctions in myocardium and other tissues. *J Cell Biol*. 1989;108:595-605
9. Yancey SB, John SA, Lal R, Austin BJ, Revel JP. The 43-kD polypeptide of heart gap junctions: Immunolocalization, topology, and functional domains. *J Cell Biol*. 1989;108:2241-2254
10. Kanter HL, Saffitz JE, Beyer EC. Cardiac myocytes express multiple gap junction proteins. *Circ Res*. 1992;70:438-444
11. Gourdie RG, Green CR, Severs NJ. Gap junction distribution in adult mammalian myocardium revealed by an anti-peptide antibody and laser scanning confocal microscopy. *J Cell Sci*. 1991;99 (Pt 1):41-55
12. van Kempen MJ, Fromaget C, Gros D, Moorman AF, Lamers WH. Spatial distribution of connexin43, the major cardiac gap junction protein, in the developing and adult rat heart. *Circ Res*. 1991;68:1638-1651
13. Fromaget C, El Auomari A, Gros D. Distribution pattern of connexin43, a gap junctional protein, during the differentiation of mouse heart myocytes. *Differentiation*. 1992;51:9-20
14. Manjunath CK, Page E. Cell biology and protein composition of cardiac gap junctions. *Am J Physiol*. 1985;248:H783-791
15. Coppen SR, Dupont E, Rothery S, Severs NJ. Connexin45 expression is preferentially associated with the ventricular conduction system in mouse and rat heart. *Circ Res*. 1998;82:232-243
16. Coppen SR, Kodama I, Boyett MR, Dobrzynski H, Takagishi Y, Honjo H, Yeh HI, Severs NJ. Connexin45, a major connexin of the rabbit sinoatrial node, is co-expressed with connexin43 in a restricted zone at the nodal-crista terminalis border. *J Histochem Cytochem*. 1999;47:907-918
17. Honjo H, Boyett MR, Coppen SR, Takagishi Y, Opthof T, Severs NJ, Kodama I. Heterogeneous expression of connexins in rabbit sinoatrial node cells: Correlation between connexin isotype

- p and cell size.
- Cardiovasc Res.*
- 2002;53:89-96
18. Verheijck EE, van Kempen MJ, Veereschild M, Lurvink J, Jongsma HJ, Bouman LN. Electrophysiological features of the mouse sinoatrial node in relation to connexin distribution. *Cardiovasc Res.* 2001;52:40-50
 19. Severs NJ. Gap junction shape and orientation at the cardiac intercalated disk. *Circ Res.* 1989;65:1458-1462
 20. Hoyt RH, Cohen ML, Saffitz JE. Distribution and three-dimensional structure of intercellular junctions in canine myocardium. *Circ Res.* 1989;64:563-574
 21. Sepp R, Severs NJ, Gourdie RG. Altered patterns of intercellular junction distribution in human patients with hypertrophic cardiomyopathy. *Heart.* 1996;76:412-417
 22. Luque EA, Veenstra RD, Beyer EC, Lemanski LF. Localization and distribution of gap junctions in normal and cardiomyopathic hamster heart. *J Morphol.* 1994;222:203-213
 23. Spach MS, Miller WT, 3rd, Geselowitz DB, Barr RC, Kootsey JM, Johnson EA. The discontinuous nature of propagation in normal canine cardiac muscle. Evidence for recurrent discontinuities of intracellular resistance that affect the membrane currents. *Circ Res.* 1981;48:39-54
 24. Saffitz JE, Kanter HL, Green KG, Tolley TK, Beyer EC. Tissue-specific determinants of anisotropic conduction velocity in canine atrial and ventricular myocardium. *Circ Res.* 1994;74:1065-1070
 25. Lorell BH, Carabello BA. Left ventricular hypertrophy: Pathogenesis, detection, and prognosis. *Circulation.* 2000;102:470-479
 26. Grossman W, Jones D, McLaurin LP. Wall stress and patterns of hypertrophy in the human left ventricle. *J Clin Invest.* 1975;56:56-64
 27. Lips DJ, deWindt LJ, van Kraaij DJ, Doevendans PA. Molecular determinants of myocardial hypertrophy and failure: Alternative pathways for beneficial and maladaptive hypertrophy. *Eur Heart J.* 2003;24:883-896
 28. Frey N, Olson EN. Cardiac hypertrophy: The good, the bad, and the ugly. *Annu Rev Physiol.* 2003;65:45-79
 29. Stevenson WG, Sweeney MO. Arrhythmias and sudden death in heart failure. *Jpn Circ J.* 1997;61:727-740
 30. Zipes DP, Wellens HJ. Sudden cardiac death. *Circulation.* 1998;98:2334-2351
 31. Levy D, Garrison RJ, Savage DD, Kannel WB, Castelli WP. Prognostic implications of echocardiographically determined left ventricular mass in the Framingham Heart Study. *N Engl J Med.* 1990;322:1561-1566
 32. Levy D, Kenchiah S, Larson MG, Benjamin EJ, Kupka MJ, Ho KK, Murabito JM, Vasan RS. Long-term trends in the incidence of and survival with heart failure. *N Engl J Med.* 2002;347:1397-1402
 33. Ghali JK, Kadakia S, Cooper RS, Liao YL. Impact of left ventricular hypertrophy on ventricular arrhythmias in the absence of coronary artery disease. *J Am Coll Cardiol.* 1991;17:1277-1282
 34. van Rijen HV, van Veen TA, Gros D, Wilders R, de Bakker JM. Connexins and cardiac arrhythmias. *Adv Cardiol.* 2006;42:150-160
 35. Stein M, Boulaksil M, Engelen MA, van Veen TA, Hauer RN, de Bakker JM, van Rijen HV. Conduction reserve and arrhythmias. *Neth Heart J.* 2006;14:113-116
 36. van Rijen HV, de Bakker JM, van Veen TA. Hypoxia, electrical uncoupling, and conduction slowing: Role of conduction reserve. *Cardiovasc Res.* 2005;66:9-11

37. Jansen JA, van Veen TA, de Bakker JM, van Rijen HV. Cardiac connexins and impulse propagation. *J Mol Cell Cardiol.* 2010;48:76-82
38. Noorman M, van der Heyden MA, van Veen TA, Cox MG, Hauer RN, de Bakker JM, van Rijen HV. Cardiac cell-cell junctions in health and disease: Electrical versus mechanical coupling. *J Mol Cell Cardiol.* 2009;47:23-31
39. van Veen AA, van Rijen HV, Opthof T. Cardiac gap junction channels: Modulation of expression and channel properties. *Cardiovasc Res.* 2001;51:217-229
40. Mines GR. On dynamic equilibrium in the heart. *J Physiol.* 1913;46:349-383
41. Wiener N, Rosenblueth A. The mathematical formulation of the problem of conduction of impulses in a network of connected excitable elements, specifically in cardiac muscle. *Arch Inst Cardiol Mex.* 1946;16:205-265
42. van Rijen HV, Eckardt D, Degen J, Theis M, Ott T, Willecke K, Jongsma HJ, Opthof T, de Bakker JM. Slow conduction and enhanced anisotropy increase the propensity for ventricular tachyarrhythmias in adult mice with induced deletion of connexin43. *Circulation.* 2004;109:1048-1055
43. Rensma PL, Allesie MA, Lammers WJ, Bonke FI, Schalij MJ. Length of excitation wave and susceptibility to reentrant atrial arrhythmias in normal conscious dogs. *Circ Res.* 1988;62:395-410
44. Jongsma HJ, Wilders R. Gap junctions in cardiovascular disease. *Circ Res.* 2000;86:1193-1197
45. Eloff BC, Lerner DL, Yamada KA, Schuessler RB, Saffitz JE, Rosenbaum DS. High resolution optical mapping reveals conduction slowing in connexin43 deficient mice. *Cardiovasc Res.* 2001;51:681-690
46. Guerrero PA, Schuessler RB, Beyer EC, Saffitz JE. Mice heterozygous for a Cx43 null mutation exhibit a cardiac conduction defect. *Circulation.* 1996;94 Suppl.1:8
47. Guerrero PA, Schuessler RB, Davis LM, Beyer EC, Johnson CM, Yamada KA, Saffitz JE. Slow ventricular conduction in mice heterozygous for a connexin43 null mutation. *J Clin Invest.* 1997;99:1991-1998
48. Thomas SA, Schuessler RB, Berul CI, Beardslee MA, Beyer EC, Mendelsohn ME, Saffitz JE. Disparate effects of deficient expression of connexin43 on atrial and ventricular conduction: Evidence for chamber-specific molecular determinants of conduction. *Circulation.* 1998;97:686-691
49. Morley GE, Vaidya D, Samie FH, Lo C, Delmar M, Jalife J. Characterization of conduction in the ventricles of normal and heterozygous Cx43 knockout mice using optical mapping. *J Cardiovasc Electrophysiol.* 1999;10:1361-1375
50. Gutstein DE, Morley GE, Tamaddon H, Vaidya D, Schneider MD, Chen J, Chien KR, Stuhlmann H, Fishman GI. Conduction slowing and sudden arrhythmic death in mice with cardiac-restricted inactivation of connexin43. *Circ Res.* 2001;88:333-339
51. de Jong S, van Veen TA, van Rijen HV, de Bakker JM. Fibrosis and cardiac arrhythmias. *J Cardiovasc Pharmacol.* 2010;57:630-638
52. Ommen SR, Nishimura RA. Hypertrophic cardiomyopathy. *Current problems in cardiology.* 2004;29:239-291
53. Kostin S, Dammer S, Hein S, Klovekorn WP, Bauer EP, Schaper J. Connexin 43 expression and distribution in compensated and decompensated cardiac hypertrophy in patients with aortic stenosis. *Cardiovasc Res.* 2004;62:426-436
54. Salameh A, Krautblatter S, Karl S, Blanke K, Gomez DR, Dhein S, Pfeiffer D, Janousek J. The signal transduction cascade regulating the expression of the gap junction protein connexin43

- by beta-adrenoceptors. *Br J Pharmacol.* 2009;158:198-208
55. Peters NS, Green CR, Poole-Wilson PA, Severs NJ. Reduced content of connexin43 gap junctions in ventricular myocardium from hypertrophied and ischemic human hearts. *Circulation.* 1993;88:864-875
 56. Sanbe A, James J, Tuzcu V, Nas S, Martin L, Gulick J, Osinska H, Sakthivel S, Klevitsky R, Ginsburg KS, Bers DM, Zinman B, Lakatta EG, Robbins J. Transgenic rabbit model for human troponin I-based hypertrophic cardiomyopathy. *Circulation.* 2005;111:2330-2338
 57. Ripplinger CM, Li W, Hadley J, Chen J, Rothenberg F, Lombardi R, Wickline SA, Marian AJ, Efimov IR. Enhanced transmural fiber rotation and connexin 43 heterogeneity are associated with an increased upper limit of vulnerability in a transgenic rabbit model of human hypertrophic cardiomyopathy. *Circ Res.* 2007;101:1049-1057
 58. Wang X, Gerdes AM. Chronic pressure overload cardiac hypertrophy and failure in guinea pigs: III. Intercalated disc remodeling. *J Mol Cell Cardiol.* 1999;31:333-343
 59. Uzzaman M, Honjo H, Takagishi Y, Emdad L, Magee AI, Severs NJ, Kodama I. Remodeling of gap junctional coupling in hypertrophied right ventricles of rats with monocrotaline-induced pulmonary hypertension. *Circ Res.* 2000;86:871-878
 60. Emdad L, Uzzaman M, Takagishi Y, Honjo H, Uchida T, Severs NJ, Kodama I, Murata Y. Gap junction remodeling in hypertrophied left ventricles of aortic-banded rats: Prevention by angiotensin II type 1 receptor blockade. *J Mol Cell Cardiol.* 2001;33:219-231
 61. Sasano C, Honjo H, Takagishi Y, Uzzaman M, Emdad L, Shimizu A, Murata Y, Kamiya K, Kodama I. Internalization and dephosphorylation of connexin43 in hypertrophied right ventricles of rats with pulmonary hypertension. *Circ J.* 2007;71:382-389
 62. Jin H, Chemaly ER, Lee A, Kho C, Hadri L, Hajjar RJ, Akar FG. Mechanoelectrical remodeling and arrhythmias during progression of hypertrophy. *FASEB J.* 2010;24:451-463
 63. Katz AM. *Heart failure: Pathophysiology, molecular biology, and clinical management.* Philadelphia: Lippincott Williams & Wilkins; 2000.
 64. Dupont E, Matsushita T, Kaba RA, Vozzi C, Coppen SR, Khan N, Kaprielian R, Yacoub MH, Severs NJ. Altered connexin expression in human congestive heart failure. *J Mol Cell Cardiol.* 2001;33:359-371
 65. Kostin S, Rieger M, Dammer S, Hein S, Richter M, Klovekorn WP, Bauer EP, Schaper J. Gap junction remodeling and altered connexin43 expression in the failing human heart. *Mol Cell Biochem.* 2003;242:135-144
 66. Chen X, Zhang Y. Myocardial Cx43 expression in the cases of sudden death due to dilated cardiomyopathy. *Forensic Sci Int.* 2006;162:170-173
 67. Kitamura H, Ohnishi Y, Yoshida A, Okajima K, Azumi H, Ishida A, Galeano EJ, Kubo S, Hayashi Y, Itoh H, Yokoyama M. Heterogeneous loss of connexin43 protein in nonischemic dilated cardiomyopathy with ventricular tachycardia. *J Cardiovasc Electrophysiol.* 2002;13:865-870
 68. Kitamura H, Yoshida A, Ohnishi Y, Okajima K, Ishida A, Galeano EJ, Kubo S, Fukuzawa K, Takano T, Yokoyama M. Correlation of connexin43 expression and late ventricular potentials in nonischemic dilated cardiomyopathy. *Circ J.* 2003;67:1017-1021
 69. Akar FG, Spragg DD, Tunin RS, Kass DA, Tomaselli GF. Mechanisms underlying conduction slowing and arrhythmogenesis in nonischemic dilated cardiomyopathy. *Circ Res.* 2004;95:717-725
 70. Akar FG, Wu RC, Juang GJ, Tian Y, Burysek M, Disilvestre D, Xiong W, Armondas AA, Tomaselli GF. Molecular mechanisms underlying K⁺ current downregulation in canine tachycardia-induced heart failure. *Am J Physiol Heart Circ Physiol.* 2005;288:H2887-2896

71. Kääh S, Nuss HB, Chiamvimomvat N, O'Rourke B, Pak PH, Kass DA, Marban E, Tomaselli GF. Ionic mechanism of action potential prolongation in ventricular myocytes from dogs with pacing-induced heart failure. *Circ Res*. 1996;78:262-273
72. Wiegerinck RF, Verkerk AO, Belterman CN, van Veen TA, Baartscheer A, Opthof T, Wilders R, de Bakker JM, Coronel R. Larger cell size in rabbits with heart failure increases myocardial conduction velocity and QRS duration. *Circulation*. 2006;113:806-813
73. Poelzing S, Akar FG, Baron E, Rosenbaum DS. Heterogeneous connexin43 expression produces electrophysiological heterogeneities across ventricular wall. *Am J Physiol Heart Circ Physiol*. 2004;286:H2001-2009
74. Poelzing S, Rosenbaum DS. Altered connexin43 expression produces arrhythmia substrate in heart failure. *Am J Physiol Heart Circ Physiol*. 2004;287:H1762-1770
75. Akar FG, Nass RD, Hahn S, Cingolani E, Shah M, Hesketh GG, DiSilvestre D, Tunin RS, Kass DA, Tomaselli GF. Dynamic changes in conduction velocity and gap junction properties during development of pacing-induced heart failure. *Am J Physiol Heart Circ Physiol*. 2007;293:H1223-1230
76. Jansen JA, van Veen AA, Bosch AA, van der Nagel R, Vos MA, de Bakker JM, van Rijen HV. Arrhythmia vulnerability of aged haploinsufficient Cx43 mice is determined by heterogeneous downregulation of Cx43 combined with increased fibrosis. *Circulation*. 2008;118:S494
77. van Veen TA, van Rijen HV, Wiegerinck RF, Opthof T, Colbert MC, Clement S, de Bakker JM, Jongsma HJ. Remodeling of gap junctions in mouse hearts hypertrophied by forced retinoic acid signaling. *J Mol Cell Cardiol*. 2002;34:1411-1423
78. Hall DG, Morley GE, Vaidya D, Ard M, Kimball TR, Witt SA, Colbert MC. Early onset heart failure in transgenic mice with dilated cardiomyopathy. *Pediatr Res*. 2000;48:36-42
79. Boulaksil M, Noorman M, Engelen MA, van Veen TA, Vos MA, de Bakker JM, van Rijen HV. Longitudinal arrhythmogenic remodelling in a mouse model of longstanding pressure overload. *Neth Heart J*. 2010;18:509-515
80. Formigli L, Ibba-Manneschi L, Perna AM, Pacini A, Polidori L, Nediani C, Modesti PA, Nosi D, Tani A, Celli A, Neri-Serneri GG, Quercioli F, Zecchi-Orlandini S. Altered Cx43 expression during myocardial adaptation to acute and chronic volume overloading. *Histol Histopathol*. 2003;18:359-369
81. Goldfine SM, Walcott B, Brink PR, Magid NM, Borer JS. Myocardial connexin43 expression in left ventricular hypertrophy resulting from aortic regurgitation. *Cardiovasc Pathol*. 1999;8:1-6
82. Salameh A, Frenzel C, Boldt A, Rassler B, Glawe I, Schulte J, Muhlberg K, Zimmer HG, Pfeiffer D, Dhein S. Subchronic alpha- and beta-adrenergic regulation of cardiac gap junction protein expression. *FASEB J*. 2006;20:365-367
83. de Boer TP, van Rijen HV, van der Heyden MA, Kok B, Opthof T, Vos MA, Jongsma HJ, de Bakker JM, van Veen TA. Beta-, not alpha-adrenergic stimulation enhances conduction velocity in cultures of neonatal cardiomyocytes. *Circ J*. 2007;71:973-981
84. Ursell PC, Gardner PI, Albala A, Fenoglio JJ, Wit AL. Structural and electrophysiological changes in the epicardial border zone of canine myocardial infarcts during infarct healing. *Circ Res*. 1985;56:436-451
85. Smith JH, Green CR, Peters NS, Rothery S, Severs NJ. Altered patterns of gap junction distribution in ischemic heart disease. An immunohistochemical study of human myocardium using laser scanning confocal microscopy. *Am J Pathol*. 1991;139:801-821
86. de Bakker JM, van Capelle FJ, Janse MJ, Tasseron S, Vermeulen JT, de Jonge N, Lahpor JR. Slow conduction in the infarcted human heart. 'Zigzag' course of activation. *Circulation*. 1993;88:915-926

87. Huang XD, Sandusky GE, Zipes DP. Heterogeneous loss of connexin43 protein in ischemic dog hearts. *J Cardiovasc Electrophysiol.* 1999;10:79-91
88. Tansey EE, Kwaku KF, Hammer PE, Cowan DB, Federman M, Levitsky S, McCully JD. Reduction and redistribution of gap and adherens junction proteins after ischemia and reperfusion. *Ann Thorac Surg.* 2006;82:1472-1479
89. Kleber AG, Riegger CB, Janse MJ. Electrical uncoupling and increase of extracellular resistance after induction of ischemia in isolated, arterially perfused rabbit papillary muscle. *Circ Res.* 1987;61:271-279
90. Beardslee MA, Lerner DL, Tadros PN, Laing JG, Beyer EC, Yamada KA, Kleber AG, Schuessler RB, Saffitz JE. Dephosphorylation and intracellular redistribution of ventricular connexin43 during electrical uncoupling induced by ischemia. *Circ Res.* 2000;87:656-662
91. de Diego C, Pai RK, Chen F, Xie LH, De Leeuw J, Weiss JN, Valderrabano M. Electrophysiological consequences of acute regional ischemia/reperfusion in neonatal rat ventricular myocyte monolayers. *Circulation.* 2008;118:2330-2337
92. Axelsen LN, Stahlhut M, Mohammed S, Larsen BD, Nielsen MS, Holstein-Rathlou NH, Andersen S, Jensen ON, Hennan JK, Kjolbye AL. Identification of ischemia-regulated phosphorylation sites in connexin43: A possible target for the antiarrhythmic peptide analogue rotigaptide (ZP123). *J Mol Cell Cardiol.* 2006;40:790-798
93. Lampe PD, Cooper CD, King TJ, Burt JM. Analysis of Connexin43 phosphorylated at S325, S328 and S330 in normoxic and ischemic heart. *J Cell Sci.* 2006;119:3435-3442
94. Solan JL, Marquez-Rosado L, Sorgen PL, Thornton PJ, Gafken PR, Lampe PD. Phosphorylation at S365 is a gatekeeper event that changes the structure of Cx43 and prevents down-regulation by PKC. *J Cell Biol.* 2007;179:1301-1309
95. Severs NJ. Gap junction alterations in the failing heart. *Eur Heart J.* 1994;15 Suppl D:53-57
96. Luke RA, Saffitz JE. Remodeling of ventricular conduction pathways in healed canine infarct border zones. *J Clin Invest.* 1991;87:1594-1602
97. Pu J, Boyden PA. Alterations of Na⁺ currents in myocytes from epicardial border zone of the infarcted heart. A possible ionic mechanism for reduced excitability and postrepolarization refractoriness. *Circ Res.* 1997;81:110-119
98. Whittaker P, Boughner DR, Kloner RA. Analysis of healing after myocardial infarction using polarized light microscopy. *Am J Pathol.* 1989;134:879-893
99. Yao JA, Hussain W, Patel P, Peters NS, Boyden PA, Wit AL. Remodeling of gap junctional channel function in epicardial border zone of healing canine infarcts. *Circ Res.* 2003;92:437-443
100. Dillon SM, Allesie MA, Ursell PC, Wit AL. Influences of anisotropic tissue structure on reentrant circuits in the epicardial border zone of subacute canine infarcts. *Circ Res.* 1988;63:182-206
101. Peters NS, Coromilas J, Severs NJ, Wit AL. Disturbed Connexin43 gap junction distribution correlates with the location of reentrant circuits in the epicardial border zone of healing canine infarcts that cause ventricular tachycardia. *Circulation.* 1997;95:988-996
102. Cabo C, Yao J, Boyden PA, Chen S, Hussain W, Duffy HS, Ciaccio EJ, Peters NS, Wit AL. Heterogeneous gap junction remodeling in reentrant circuits in the epicardial border zone of the healing canine infarct. *Cardiovasc Res.* 2006;72:241-249
103. Baba S, Dun W, Cabo C, Boyden PA. Remodeling in cells from different regions of the reentrant circuit during ventricular tachycardia. *Circulation.* 2005;112:2386-2396
104. Kleber AG, Janse MJ, Wilms-Schopmann FJ, Wilde AA, Coronel R. Changes in conduction velocity during acute ischemia in ventricular myocardium of the isolated porcine heart.

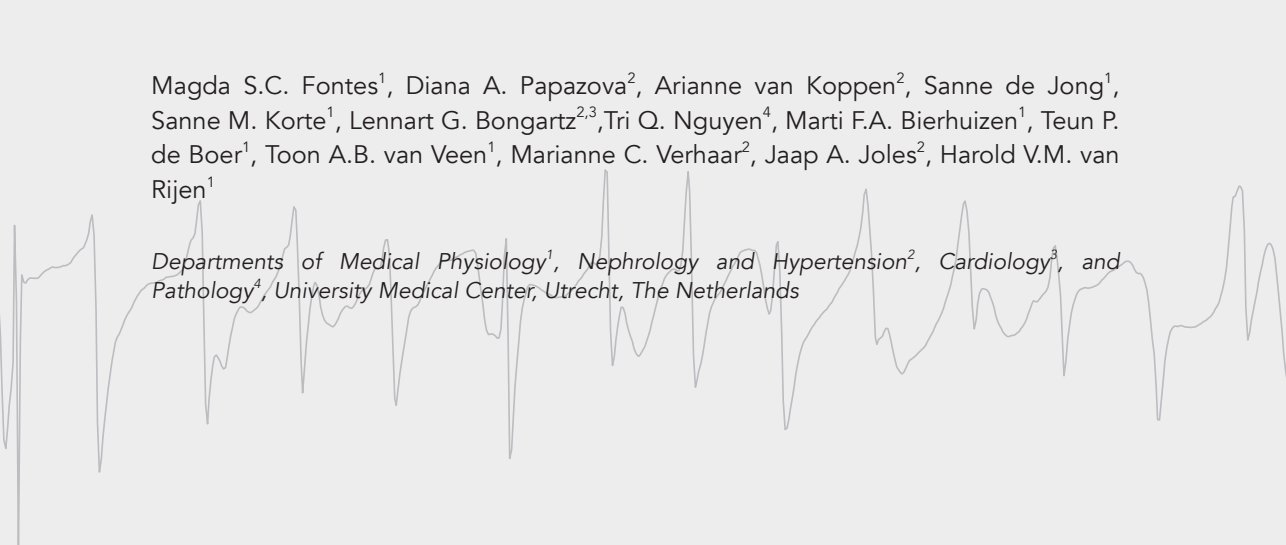
- Circulation*. 1986;73:189-198
105. Matsushita T, Takamatsu T. Ischaemia-induced temporal expression of connexin43 in rat heart. *Virchows Arch*. 1997;431:453-458
 106. Matsushita T, Oyamada M, Fujimoto K, Yasuda Y, Masuda S, Wada Y, Oka T, Takamatsu T. Remodeling of cell-cell and cell-extracellular matrix interactions at the border zone of rat myocardial infarcts. *Circ Res*. 1999;85:1046-1055
 107. Qu J, Volpicelli FM, Garcia LI, Sandeep N, Zhang J, Marquez-Rosado L, Lampe PD, Fishman GI. Gap junction remodeling and spironolactone-dependent reverse remodeling in the hypertrophied heart. *Circ Res*. 2009;104:365-371
 108. Stein M, Boulaksil M, Jansen JA, Herold E, Noorman M, Joles JA, van Veen TA, Houtman MJ, Engelen MA, Hauer RN, de Bakker JM, van Rijen HV. Reduction of fibrosis-related arrhythmias by chronic renin-angiotensin-aldosterone system inhibitors in an aged mouse model. *Am J Physiol Heart Circ Physiol*. 2010;299:H310-321
 109. Amino M, Yoshioka K, Tanabe T, Tanaka E, Mori H, Furusawa Y, Zareba W, Yamazaki M, Nakagawa H, Honjo H, Yasui K, Kamiya K, Kodama I. Heavy ion radiation up-regulates Cx43 and ameliorates arrhythmogenic substrates in hearts after myocardial infarction. *Cardiovasc Res*. 2006;72:412-421
 110. Amino M, Yoshioka K, Fujibayashi D, Hashida T, Furusawa Y, Zareba W, Ikari Y, Tanaka E, Mori H, Inokuchi S, Kodama I, Tanabe T. Year-long upregulation of connexin43 in rabbit hearts by heavy ion irradiation. *Am J Physiol Heart Circ Physiol*. 2010;298:H1014-1021
 111. Wang Y, Wang Q, Zhao Y, Gong D, Wang D, Li C, Zhao H. Protective effects of estrogen against reperfusion arrhythmias following severe myocardial ischemia in rats. *Circ J*. 2010;74:634-643
 112. Chen CC, Lin CC, Lee TM. 17beta-estradiol decreases vulnerability to ventricular arrhythmias by preserving Connexin43 protein in infarcted rats. *Eur J Pharmacol*. 2010;629:73-81
 113. Lee TM, Lin MS, Chou TF, Tsai CH, Chang NC. Adjunctive 17beta-estradiol administration reduces infarct size by altered expression of canine myocardial connexin43 protein. *Cardiovasc Res*. 2004;63:109-117
 114. Matsushita S, Kurihara H, Watanabe M, Okada T, Sakai T, Amano A. Inhibition of connexin43 dephosphorylation is involved in protective effects of diltiazem on cardiac function during hypoxic injury. *Histol Histopathol*. 2011;26:315-322
 115. Liu Y, Huang H, Xia W, Tang Y, Yuan M, Tang Q, Huang C. Inhibition of NADPH oxidase up-regulates connexin 43 and ameliorates electrical remodeling in rabbits with heart failure. *Biomed Pharmacother*. 2010:[Epub ahead of print]
 116. Liu Y, Huang H, Xia W, Tang Y, Li H, Huang C. NADPH oxidase inhibition ameliorates cardiac dysfunction in rabbits with heart failure. *Mol Cell Biochem*. 2010;343:143-153
 117. Manoach M, Tribulova N, Imanaga I. The protective effect of D-sotalol against hypoxia-induced myocardial uncoupling. *Heart Vessels*. 1996;11:281-288
 118. Hill BC, Hunt AJ, Courtney KR. Reentrant tachycardia in a thin layer of ventricular subepicardium: Effects of d-sotalol and lidocaine. *J Cardiovasc Pharmacol*. 1990;16:871-880
 119. Mitasikova M, Smidova S, Macsaliova A, Knezl V, Dlugosova K, Okruhlicova L, Weismann P, Tribulova N. Aged male and female spontaneously hypertensive rats benefit from n-3 polyunsaturated fatty acids supplementation. *Physiol Res*. 2008;57 Suppl 2:S39-48
 120. Bacova B, Radosinska J, Knezl V, Kolenova L, Weismann P, Navarova J, Barancik M, Mitasikova M, Tribulova N. Omega-3 fatty acids and atorvastatin suppress ventricular fibrillation inducibility in hypertriglyceridemic rat hearts: Implication of intracellular coupling protein, connexin-43. *J Physiol Pharmacol*. 2010;61:717-723

121. Hawat G, Benderdour M, Rousseau G, Baroudi G. Connexin 43 mimetic peptide Gap26 confers protection to intact heart against myocardial ischemia injury. *Pflugers Arch.* 2010;460:583-592
122. Xing D, Kjolbye AL, Nielsen MS, Petersen JS, Harlow KW, Holstein-Rathlou NH, Martins JB. ZP123 increases gap junctional conductance and prevents reentrant ventricular tachycardia during myocardial ischemia in open chest dogs. *J Cardiovasc Electrophysiol.* 2003;14:510-520
123. Hennan JK, Swillo RE, Morgan GA, Keith JC, Jr., Schaub RG, Smith RP, Feldman HS, Haugan K, Kantrowitz J, Wang PJ, Abu-Qare A, Butera J, Larsen BD, Crandall DL. Rotigaptide (ZP123) prevents spontaneous ventricular arrhythmias and reduces infarct size during myocardial ischemia/reperfusion injury in open-chest dogs. *J Pharmacol Exp Ther.* 2006;317:236-243
124. Macia E, Dolmatova E, Cabo C, Sosinsky AZ, Dun W, Coromilas J, Ciaccio EJ, Boyden PA, Wit AL, Duffy HS. Characterization of gap junction remodeling in epicardial border zone of healing canine infarcts and electrophysiological effects of partial reversal by rotigaptide. *Circ Arrhythm Electrophysiol.* 2011;4:344-351
125. Wiegerinck RF, de Bakker JM, Opthof T, de Jonge N, Kirkels H, Wilms-Schopman FJ, Coronel R. The effect of enhanced gap junctional conductance on ventricular conduction in explanted hearts from patients with heart failure. *Basic Res Cardiol.* 2009;104:321-332
126. Kanno S, Kovacs A, Yamada KA, Saffitz JE. Connexin43 as a determinant of myocardial infarct size following coronary occlusion in mice. *J Am Coll Cardiol.* 2003;41:681-686
127. Maass K, Chase SE, Lin X, Delmar M. Cx43 CT domain influences infarct size and susceptibility to ventricular tachyarrhythmias in acute myocardial infarction. *Cardiovasc Res.* 2009;84:361-367
128. Prestia KA, Sosunov EA, Anyukhovskiy EP, Dolmatova E, Kelly CW, Brink PR, Robinson RB, Rosen MR, Duffy HS. Increased cell-cell coupling increases infarct size and does not decrease incidence of ventricular tachycardia in mice. *Front Physiol.* 2011;2:1
129. Anyukhovskiy EP, Sosunov EA, Kryukova YN, Prestia K, Ozgen N, Rivaud M, Cohen IS, Robinson RB, Rosen MR. Expression of skeletal muscle sodium channel (Na_v1.4) or connexin32 prevents reperfusion arrhythmias in murine heart. *Cardiovasc Res.* 2011;89:41-50
130. Zhang Y, Kanter EM, Yamada KA. Remodeling of cardiac fibroblasts following myocardial infarction results in increased gap junction intercellular communication. *Cardiovasc Pathol.* 2010;19:e233-240
131. Conrath CE, Wilders R, Coronel R, de Bakker JM, Taggart P, de Groot JR, Opthof T. Intercellular coupling through gap junctions masks M cells in the human heart. *Cardiovasc Res.* 2004;62:407-414
132. van Kempen MJ, ten Velde I, Wessels A, Oosthoek PW, Gros D, Jongsma HJ, Moorman AF, Lamers WH. Differential connexin expression accommodates cardiac function in different species. *Microsc Res Tech.* 1995;31:420-436




Magda S.C. Fontes¹, Diana A. Papazova², Arianne van Koppen², Sanne de Jong¹,
Sanne M. Korte¹, Lennart G. Bongartz^{2,3}, Tri Q. Nguyen⁴, Marti F.A. Bierhuizen¹, Teun P.
de Boer¹, Toon A.B. van Veen¹, Marianne C. Verhaar², Jaap A. Joles², Harold V.M. van
Rijen¹

*Departments of Medical Physiology¹, Nephrology and Hypertension², Cardiology³, and
Pathology⁴, University Medical Center, Utrecht, The Netherlands*

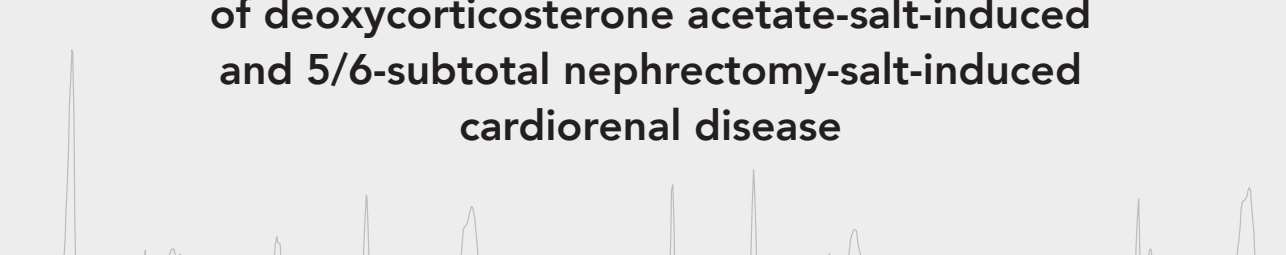




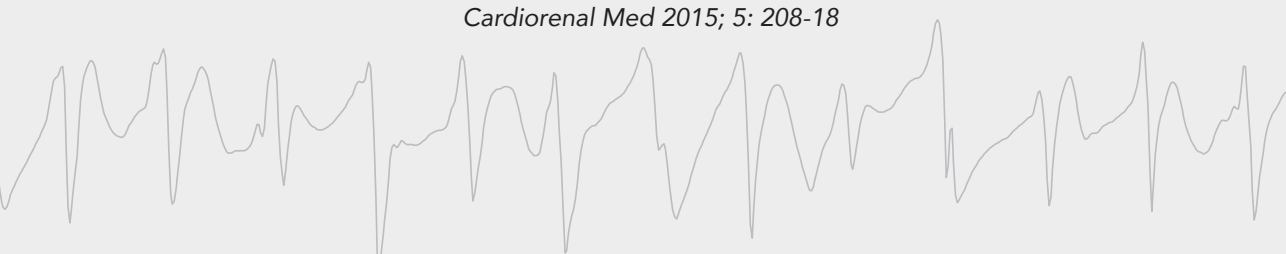
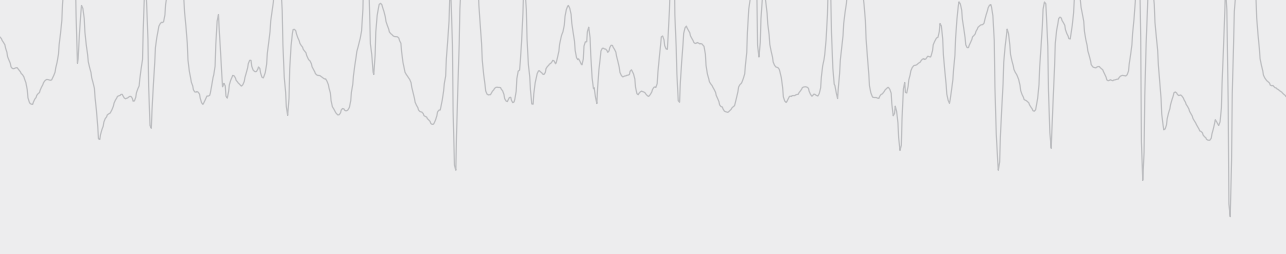
Chapter 3



**Arrhythmogenic remodeling in murine models
of deoxycorticosterone acetate-salt-induced
and 5/6-subtotal nephrectomy-salt-induced
cardiorenal disease**



Cardiorenal Med 2015; 5: 208-18



ABSTRACT

Background

Renal failure is associated with adverse cardiac remodeling and sudden cardiac death. The mechanism leading to enhanced arrhythmogenicity in the cardiorenal syndrome is unclear. The aim of this study was to characterize electrophysiological and tissue alterations correlated with enhanced arrhythmogenicity in two distinct mouse models of renal failure.

Methods

Thirty-week-old 129Sv mice received a high-salt diet and deoxycorticosterone acetate (DOCA) for 8 weeks, followed by an additional period of high-salt diet for 27 weeks (DOCA-salt aged model). Adult CD-1 mice were submitted to 5/6-subtotal nephrectomy (SNx) and treated for 11 weeks with a high-salt diet (SNx-salt adult model). Vulnerability to arrhythmia as well as conduction velocities (CVs) of the hearts were determined *ex vivo* with epicardial mapping. Subsequently, the hearts were characterized for Connexin43 (Cx43) and fibrosis.

Results

DOCA-salt and SNx-salt mice developed renal dysfunction characterized by albuminuria. Heart, lung and kidney weights were increased in DOCA-salt mice. Both DOCA-salt and SNx-salt mice were highly susceptible to ventricular arrhythmias. DOCA-salt mice had a significant decrease in both longitudinal and transversal CV in the left ventricle. Histological analysis revealed a significant reduction in Cx43 expression as well as an increase in interstitial fibrosis in both DOCA-salt and SNx-salt mice.

Conclusion

DOCA-salt and SNx-salt treatment induced renal dysfunction, which resulted in structural and electrical cardiac remodeling and enhanced arrhythmogenicity. The reduced Cx43 expression and increased fibrosis levels in these hearts are likely candidates for the formation of the arrhythmogenic substrate.

INTRODUCTION

The cardiorenal syndrome is a condition characterized by the influence of a diseased kidney on the heart and vice versa, which can lead to progression of failure of both organs.¹ Patients with renal failure have an increased mortality risk due to cardiovascular disease.² Around 25% of all mortality of dialysis patients is caused by sudden cardiac death, mostly arising from arrhythmias such as ventricular tachycardia or fibrillation.³⁻⁵ The mechanism leading to enhanced arrhythmogenicity in the cardiorenal syndrome is unclear.

Cardiac arrhythmias can be caused by three basic mechanisms: enhanced automaticity, triggered activity or reentry.⁶ Reentry-based arrhythmias are responsible for the majority of ventricular arrhythmias and are often observed in dialysis patients.^{3,6} Typical electrophysiological characteristics of reentry are slow impulse conduction, conduction block and a lower effective refractory period. Hearts prone to reentrant arrhythmias typically show reduced levels and a heterogeneous distribution of the gap junction protein Connexin43 (Cx43) as well as the presence of fibrotic tissue.⁶⁻⁸

The aim of this study was to characterize electrophysiological alterations and cardiac remodeling correlated with enhanced arrhythmogenicity on the background of renal failure. Therefore, two mouse models of renal dysfunction with different etiologies were tested: (1) an aldosterone-induced hypertension model using deoxycorticosterone acetate (DOCA) in combination with a high-salt diet in aged mice (DOCA-salt aged model), and (2) a more severe model using 5/6-subtotal nephrectomy (SNx) in combination with a high-salt diet in adult mice (SNx-salt adult model).

METHODS

Ethics statement and animal housing

All the experimental protocols were performed in accordance with the national guidelines and approved by the local Ethical Animal Experimental Committee of the University of Utrecht, The Netherlands (approval No. 2010.II.11.201 and 2012.II.10.154). All animals were housed under standard conditions in a light-, temperature- and humidity-controlled environment.

Animal models of renal dysfunction

DOCA-salt aged mice

Thirty-week-old male 129Sv mice were used (Harlan Laboratories, Horst, The Netherlands). Renal dysfunction was induced in mice (experimental week 0) by the combination of a DOCA pellet (3.3 mg/day) and a high-salt diet (chow containing 3% NaCl) for a period of 8 weeks ($n=7$). At experimental week 8, the DOCA pellet was removed and the high-salt diet withdrawn. At experimental week 11, the high-salt diet (6% NaCl) was continued until termination at experimental week 38 (68-week-old mice). Untreated age-matched mice were used as controls ($n=4$).

SNx-salt adult mice

Adult (8-week-old) male CD-1 mice were used (Charles River Laboratories, Sulzfeld, Germany). SNx was performed in two steps. At week -1, the right kidney was surgically removed (uninephrectomy), followed by removal of the poles from the left kidney at week 0. To the SNx-salt group, a high-salt diet (chow containing 6% NaCl) was given from week 1 until sacrifice at week 11 ($n=5$), whereas 9 mice underwent only SNx (SNx group).

Renal function and arterial pressure evaluation

To collect 16-hour urine, mice were placed in metabolic cages with food and water; values are expressed as per 24 h. Albumin was measured with a mouse albumin ELISA kit (Bethyl Laboratories Inc., Montgomery, USA). Systolic blood pressure and mean arterial pressure were measured using tail-cuff plethysmography and a catheter directly inserted into the femoral artery, respectively. Blood samples were collected by cheek puncture. Plasma urea was determined by DiaSys Urea CT FS (DiaSys Diagnostic Systems, Holzheim, Germany).

Echocardiography and epicardial mapping of Langendorff perfused hearts

Echocardiography was performed to determine cardiac function using a Vevo 2100 device (VisualSonics Inc., Toronto, Canada) with an MS550D transducer. Before termination, the mice were anesthetized with 4-5% isoflurane in oxygen and air. Next, the heart was excised and attached to a Langendorff retrograde perfusion setup. The heart was continuously perfused with a carbogen-gassed buffer at 37°C, composed of (in mM): NaCl 116, KCl 5, MgSO₄ 1.1, NaH₂PO₄ 0.35, NaHCO₃ 27, glucose 10, mannitol 16 and CaCl₂ 1.8. Extracellular electrograms were recorded during stimulation (2x stimulation threshold) from the center of a 19x13 multielectrode grid, both from the left

ventricle (LV) and right ventricle (RV), as described previously.⁹ The conduction velocity was determined off-line from the recorded electrograms, as described previously,⁷ using custom-made software based on MATLAB (The MathWorks Inc., Natick, USA). Susceptibility to arrhythmia was provoked by programmed electrical stimulation using a standardized protocol published earlier.⁷

Immunohistochemistry and histology

After the epicardial mapping procedure, the hearts were snap frozen in liquid nitrogen. For immunohistochemistry and fibrosis detection, cryosections of the heart (10 μ m thickness) were prepared. Immunolabeling was performed to assess the subcellular distribution of Cx43, as described previously,⁹ using rabbit polyclonal anti-Cx43 (71-0700; Invitrogen, Carlsbad, USA) and mouse monoclonal anti-N-cadherin (C1821; Sigma-Aldrich, Saint Louis, USA) antibodies. Cx43 levels were expressed as the area immunolabeled for Cx43 normalized to control. For cardiac fibrosis detection, cryosections were fixed with 4% paraformaldehyde and stained with Picrosirius red as described previously.¹⁰ The cryosections were visualized by light microscopy (Nikon Eclipse 80i; Nikon Europe B.V., Amstelveen, The Netherlands) and digitally analyzed using ImageJ software. The percentage of fibrosis was calculated as the area stained by Picrosirius red relative to the total tissue area.

Statistical analysis

Data are presented as means \pm standard errors of the mean and analyzed by Student's t test or Fisher's exact test using GraphPad Prism 6 software (La Jolla, California, USA). Differences were considered statistically significant if $p < 0.05$. Animals that did not complete the experiment were excluded from analysis.

RESULTS

Arrhythmogenic remodeling in DOCA-salt aged mice

Renal dysfunction, morphological and echocardiographic data

DOCA-salt treatment of aged mice resulted in renal dysfunction confirmed by a significant increase of albumin in the urine (4.8 ± 1.4 vs. 0.1 ± 0.02 mg/24h, $p < 0.05$, Figure 1A). DOCA-salt mice developed hypertension, detected by an increase in systolic blood pressure as compared with aged control mice (135 ± 5 vs. 88 ± 8 mmHg, $p < 0.01$, Figure 1B). Plasma urea was not elevated or different between the two groups of mice (11.1 ± 1.0 vs. 11.0 ± 0.9 mmol/L, *n.s.*, Figure 1C).

DOCA-salt mice presented with cardiac hypertrophy, backward failure (indicated by increased lung weight) and enlargement of the kidneys, as shown in Figures 1D-F. Secondly, cardiac function was impaired in DOCA-salt mice as assessed by echocardiography, which showed a decrease in fractional shortening (22.5 ± 1.2 vs. $29.9 \pm 1.6\%$, $p < 0.01$, Figure 1G).

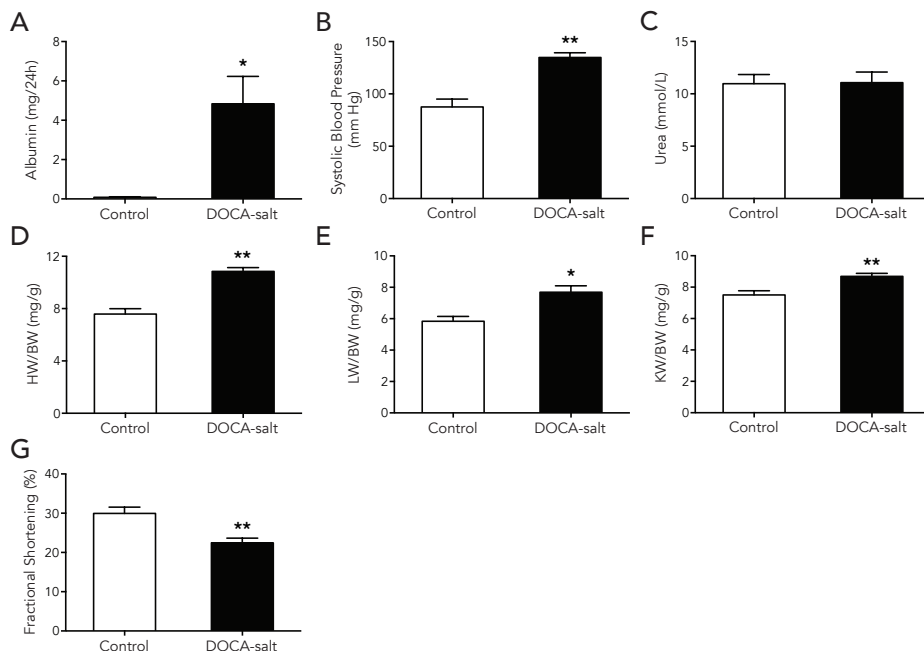


Figure 1. Urinary albumin, systolic blood pressure, plasma urea, as well as tissue and echocardiographic parameters in control (n=4) and DOCA-salt (n=7) aged mice.

* $p < 0.05$, ** $p < 0.01$ vs. control. **A:** Albumin measured in 24-hour urine samples. **B:** Systolic blood pressure measured by tail-cuff plethysmography. **C:** Urea measured in plasma samples. **D:** Heart weight-to-body weight ratio (HW/BW). **E:** Lung weight-to-body weight ratio (LW/BW). **F:** Kidney weight-to-body weight ratio (KW/BW; average of both kidneys). **G:** Fractional shortening.

Arrhythmia induction and conduction velocity

Isolated Langendorff perfused DOCA-salt mouse hearts were highly arrhythmogenic. An example of a polymorphic tachyarrhythmia is shown in Figure 2A. Arrhythmias were induced in 86% (6/7) of the DOCA-salt hearts as compared with 0% of control hearts ($p < 0.05$, Figure 2B). Epicardial activation maps generated during ventricular tachyarrhythmias (VT) showed no signs of reentry activity (Figure 2C).

Conduction velocities (CVs) were obtained from paced epicardial activation maps for the LVs and RVs (Figure 2D). Longitudinal and transverse CVs in the RV were similar

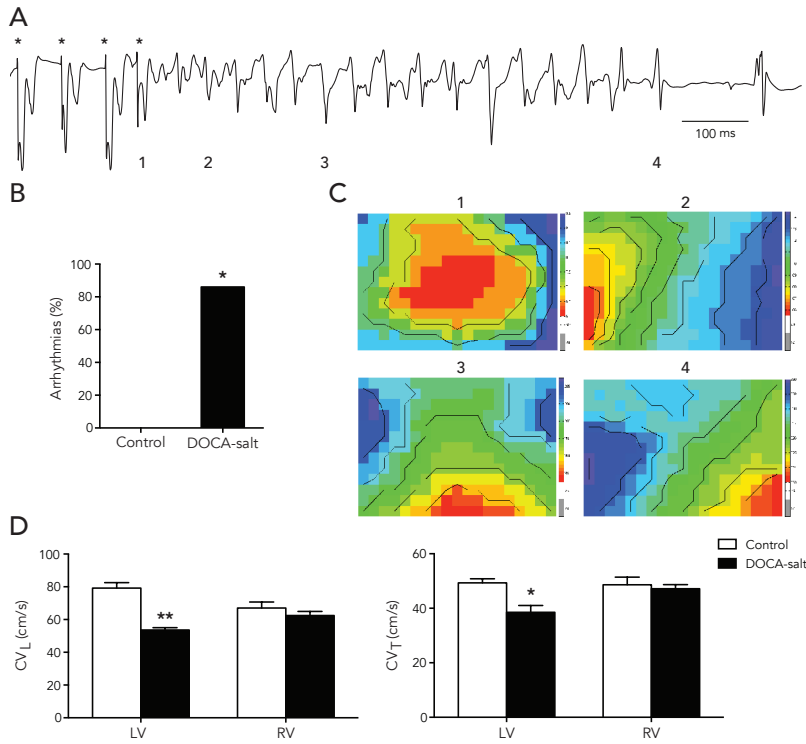


Figure 2. Arrhythmias and CV induced in perfused control and DOCA-salt aged mice.

A: Representative epicardial electrogram of a stimulation-induced polymorphic VT in DOCA-salt mice. Asterisks (*) indicate the last 4 burst-paced (60 ms) complexes. **B:** Incidence of arrhythmias in control ($n=4$) and DOCA-salt ($n=7$) mice. * $p<0.05$ vs. control. **C:** Activation maps from the 4 numbered VT complexes indicated in the electrogram in **A**. The black isochronal lines of activation are 1 ms apart. Red represents the earliest activation time and blue the latest. **D:** CV measured by epicardial mapping on the LV (control: $n=4$; DOCA-salt: $n=5$) and RV (control: $n=4$; DOCA-salt: $n=7$) in longitudinal (CV_L; left) and transverse (CV_T; right) directions. * $p<0.05$, ** $p<0.01$ vs. control.

between control and DOCA-salt mice. Interestingly, DOCA-salt mice showed a significant decrease in both longitudinal (-32%) and transverse (-22%) CVs in the LV ($p<0.05$, Figure 2D).

Cx43 expression and fibrosis

Cx43 expression was significantly reduced in DOCA-salt mice compared with control mice as assessed by immunohistochemistry (0.6 ± 0.05 vs. 1.0 ± 0.05 , $p<0.01$, Figure 3A). Cardiac fibrosis as assessed by Picrosirius Red staining was significantly increased (3.7-fold) in DOCA-salt aged mice as compared with control mice of similar age ($p<0.01$, Figure 3B).

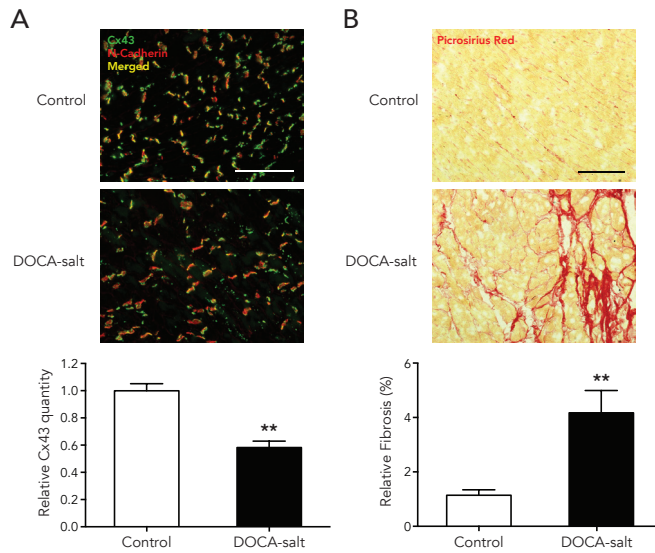


Figure 3. Cx43 expression and fibrosis in isolated control ($n=4$) and DOCA-salt ($n=7$) aged mouse hearts.

**** $p < 0.01$ vs. control.** **A:** Representative pictures of Cx43 (green) and N-cadherin (red) expression in control and DOCA-salt hearts (top). N-cadherin was used as a marker for intercalated disks. Scale bar = 100 μm . Bottom: quantification of Cx43 immunolabeling. **B:** Representative pictures of fibrosis in control and DOCA-salt hearts (top). Scale bar = 100 μm . Bottom: quantification of fibrosis staining.

Arrhythmogenic remodeling in SNx-salt adult mice

Renal dysfunction and morphological data

SNx alone was not sufficient to develop renal dysfunction in adult mice of this strain (data not shown). Therefore, an additional SNx group was created in which salt was given to the food for 10 weeks as an extra renal challenge (SNx-salt).

Renal dysfunction was clearly present in SNx-salt compared to SNx, as indicated by a significant increase in albumin in the urine (186 ± 25 vs. $8 \pm 6 \text{ mg/24h}$, $p < 0.01$, Figure 4A). The mean arterial pressure tended to be higher in SNx-salt mice (97 ± 10 vs. $82 \pm 4 \text{ mmHg}$, $p = 0.16$, Figure 4B). Plasma urea was elevated in both the SNx-salt and the SNx group (21 ± 2 vs. $22 \pm 2 \text{ mmol/L}$, *n.s.*, Figure 4C). Furthermore, there was a tendency towards increased heart, lung and kidney weights in the SNx-salt group (Figures 4D-F).

Arrhythmia induction and conduction velocity

SNx-salt hearts were highly susceptible to polymorphic ventricular arrhythmias (Figure 5A). In the SNx-salt group, 75% of the hearts showed arrhythmias, as compared

with 25% of the SNx hearts (*n.s.*, Figure 5B). The activation maps obtained during the VT showed no signs of reentry activity (Figure 5C). Epicardial CVs were similar in SNx and SNx-salt hearts (Figure 5D).

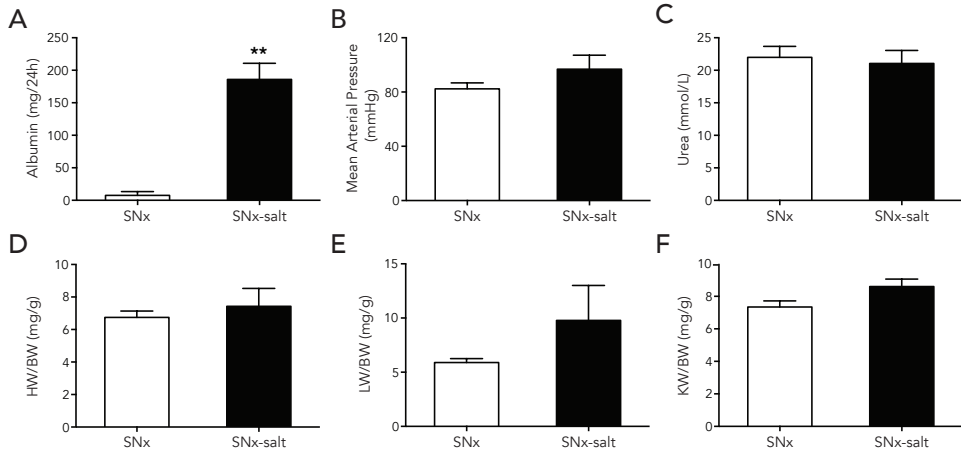


Figure 4. Urinary albumin, mean arterial pressure, plasma urea and tissue parameters in SNx and SNx-salt adult mice.

****** $p < 0.01$ vs. SNx. **A:** Albumin measured in 24-hour urine samples (SNx: $n=5$; SNx-salt: $n=5$). **B:** Mean arterial pressure measured using a catheter inserted into the femoral artery (SNx: $n=9$; SNx-salt: $n=5$). **C:** Urea measured in plasma samples (SNx: $n=9$; SNx-salt: $n=5$). **D:** Heart weight-to-body weight ratio (HW/BW). **E:** Lung weight-to-body weight ratio (LW/BW). **F:** Kidney (remnant) weight-to-body weight ratio (KW/BW). **D-F:** SNx: $n=8$; SNx-salt: $n=5$.

Cx43 expression and fibrosis

Cx43 expression was significantly decreased upon administration of salt to SNx mice (0.6 ± 0.08 vs. 1.0 ± 0.06 , $p < 0.01$, Figure 6A). Additionally, SNx-salt hearts presented with significantly higher levels (1.4-fold) of cardiac fibrosis than SNx hearts ($p < 0.05$, Figure 6B).

DISCUSSION

In this study, the relation between cardiac remodeling and arrhythmogenicity was investigated in two different mouse models of renal dysfunction: aged mice subjected to DOCA and salt (DOCA-salt) and adult mice subjected to SNx and salt (SNx-salt). The main findings of this study are the following: (1) The cardiorenal syndrome was present in both mouse models; renal failure was established with albuminuria in both mouse models, although DOCA-salt, but not SNx-salt, resulted in hypertension, cardiac hypertrophy, and decreased cardiac contractility; (2) Both models presented with a high

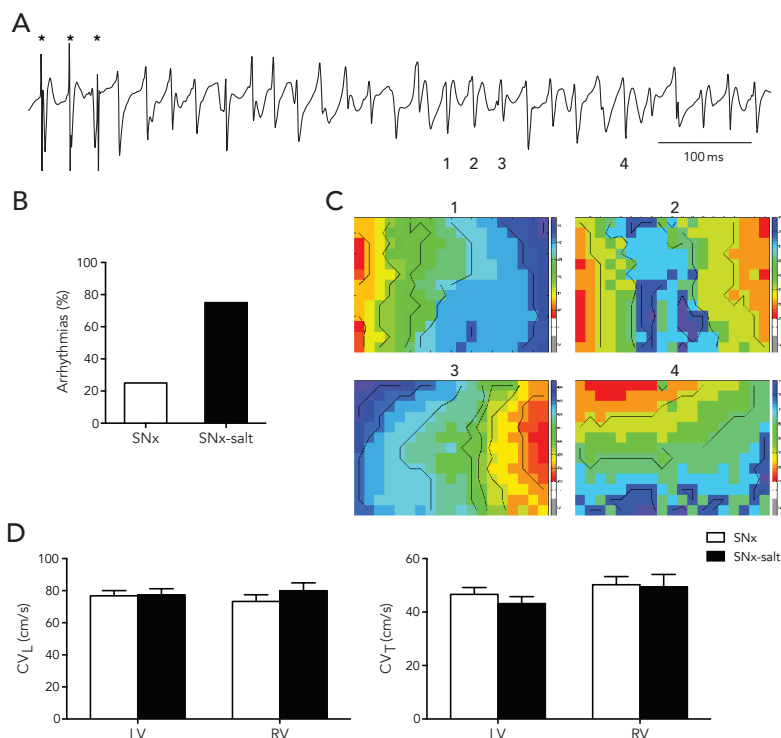


Figure 5. Arrhythmias and CVs induced in perfused SNx and SNx-salt adult mice. **A:** Representative epicardial electrogram of a stimulation-induced polymorphic VT in SNx-salt mice. Asterisks (*) indicate the last 3 burst-paced (30 ms) complexes. **B:** Incidence of arrhythmias in SNx (n=8) and SNx-salt mice (n=4). **C:** Activation maps from the 4 numbered VT complexes indicated in the electrogram in **A**. The black isochronal lines of activation are 1 ms apart. Red represents the earliest activation time and blue the latest. **D:** CV measured by epicardial mapping on the LV (SNx: n=8; SNx-salt: n=3) and RV (SNx: n=8; SNx-salt: n=2) in longitudinal (CV_L; left) and transverse (CV_T; right) directions.

incidence of arrhythmias accompanied by increased interstitial fibrosis and decreased Cx43 expression in the heart.

Induction of the cardiorenal syndrome in mice

Mice are known to be very resistant to induction of renal failure,^{11,12} usually requiring removal of large parts of the kidneys, therefore leaving little renal tissue for analysis. In order to retain both kidneys, we opted for the DOCA-salt mouse model and combined it with aging as an alternative trigger to the commonly used uninephrectomy,¹³ as aging increases the susceptibility for development of hypertension as well as renal and cardiac failure.¹⁴⁻¹⁶ In our model, treating mice with DOCA-salt caused hypertension and albuminuria, confirming renal dysfunction. Besides renal injury, the combination of DOCA (which mimics aldosterone) and a high-salt diet induced cardiac remodeling

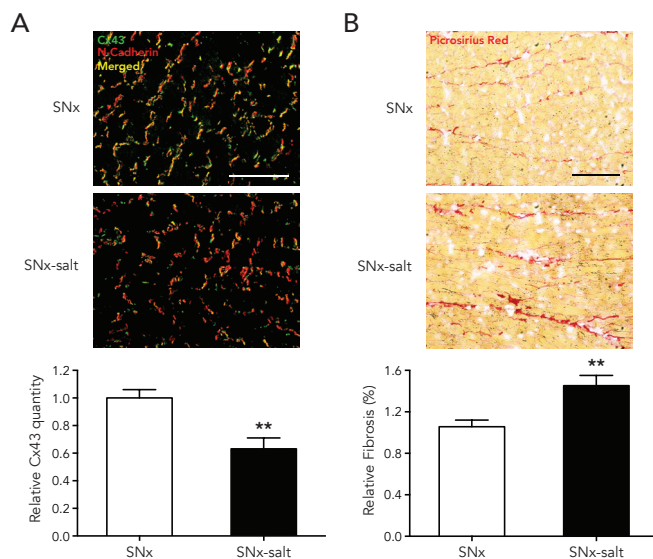


Figure 6. Cx43 expression and fibrosis in isolated SNx (n=9) and SNx-salt (n=5) adult mouse hearts. ** $p < 0.01$ vs. SNx. **A:** Representative pictures of Cx43 (green) and N-cadherin (red) expression in SNx and SNx-salt hearts (top). N-cadherin was used as a marker for intercalated disks. Scale bar = 100 μ m. Bottom: quantification of Cx43 immunolabeling. **B:** Representative pictures of fibrosis in SNx and SNx-salt hearts (top). Scale bar = 100 μ m. Bottom: quantification of fibrosis staining.

as evidenced by hypertrophy, decreased fractional shortening, cardiac fibrosis, and reduced Cx43 expression. Several studies suggested that the development of cardiac hypertrophy and fibrosis in the DOCA-salt model is at least partly independent of the extent of hypertension.¹⁷⁻¹⁹ Therefore, renal dysfunction but not hypertension may be the key factor causing cardiac remodeling.

The second model of renal failure was based on SNx in CD-1 mice. Although it is known that the susceptibility to developing renal failure is dependent on the strain of mouse used,^{11,12} a study has shown that both CD-1 mice and 129S3 mice (a substrain of 129Sv) developed renal failure after SNx.²⁰ In our mouse model, however, SNx alone was not sufficient to result in hypertension or renal dysfunction, requiring the addition of another trigger. Therefore, we used a combination of SNx with a high-salt diet. The follow-up time of 11 weeks was limited by the progressive worsening of the clinical condition of the animals. The addition of a high-salt diet did not induce significant hypertension, but as the mean arterial pressure was determined under anesthesia, blood pressure might have been underestimated. Although no significant differences were found between SNx and SNx-salt mice with respect to heart, lung or kidney weights, SNx-salt mice were more susceptible to arrhythmias than SNx mice. The low percentage of arrhythmias in the SNx group suggests that these mice were in an early stage of cardiac remodeling, which was further enhanced in the SNx-salt group.

Both mouse models used in this study showed renal dysfunction and cardiac remodeling. In addition, they were highly susceptible to arrhythmias; therefore, they at least phenotypically reflect the cardiorenal syndrome in patients. Furthermore, the presence of similar and severe arrhythmias in both models without significant hypertension, left ventricular hypertrophy and uremia in the SNx-salt model suggests that hypertension, left ventricular hypertrophy and uremia per se are presumably not prerequisites for arrhythmias in the cardiorenal syndrome. More subtle changes within the heart are probably required, as discussed below.

Development of the arrhythmogenic substrate in the cardiorenal syndrome

Both models of the cardiorenal syndrome exhibited high levels of arrhythmias. The high susceptibility to cardiac arrhythmias in our mouse models was accompanied by cardiac remodeling with reduced Cx43 expression and increased fibrosis. Previous studies have shown that reduced or abnormal Cx43 expression and/or increased fibrosis are strongly associated with arrhythmias in patients,²¹⁻²³ as well as in dog^{24,25} and mouse models of cardiac remodeling and failure.^{7,21,26} Furthermore, in a mouse model of cardiac pressure overload, the involvement of abnormal Cx43 expression in the arrhythmogenic substrate was associated with dispersion in CV, rather than conduction slowing, suggesting a triggered activity mechanism.²¹ In the LV of DOCA-salt aged hearts, CV was slowed both along and parallel to the fiber orientation, which may have contributed to the arrhythmogenic substrate. In SNx-salt hearts, however, arrhythmogenicity was also high, with comparable polymorphic VTs and activation patterns, albeit without conduction slowing. It seems therefore that conduction slowing is not a prerequisite for arrhythmias in this model. Triggered activity as an arrhythmia mechanism was shown earlier in a chronic kidney disease rat model.²⁷ This is well supported by the high-resolution epicardial activation mapping in our study, which did not show evident signs of reentry, making a triggered activity a very likely mechanism for the arrhythmias.

Clinical implications

Our data using cardiorenal syndrome mouse models show that under conditions of excess mineralocorticoid hormone and high salt, or upon the combination of SNx and high salt, there is an increased susceptibility to arrhythmias. Previously, we demonstrated that chronic treatment of aged arrhythmogenic mice with the aldosterone antagonist eplerenone significantly decreased cardiac fibrosis, restored normal levels of Cx43 in the heart and, most importantly, reduced the amount of arrhythmias.⁸ A similar result was obtained in the context of pressure-overloaded mouse hearts treated with spironolactone, which normalized Cx43 expression, reduced fibrosis and restored normal impulse conduction.²⁸ Inhibiting the aldosterone pathway may therefore be a therapeutic

avenue to suppress the development of the arrhythmogenic substrate in cardiorenal syndrome patients.

Conclusion

In conclusion, our data provide evidence that renal dysfunction in the high-salt DOCA and SNx models causes pronounced structural and electrical cardiac remodeling and a markedly enhanced susceptibility to arrhythmias. The reduced Cx43 expression and increased fibrosis levels in these hearts are likely candidates for the formation of the arrhythmogenic substrate.

3

ACKNOWLEDGMENTS

We thank Krista den Ouden, Paula Martens and Myrthe den Toom for their excellent technical assistance.


FUNDING SOURCES

This study was supported by Dutch Heart Foundation grant NHS 2009B072. M.C.V. is supported by the Netherlands Organization for Scientific Research (NWO) Vidi grant 016.096.359.

REFERENCES

1. Ronco C, Haapio M, House AA, Anavekar N, Bellomo R. Cardiorenal Syndrome. *J Am Coll Cardiol*. 2008;52:1527-1539
2. McCullough PA, Jurkovitz CT, Pergola PE, McGill JB, Brown WW, Collins AJ, Chen SC, Li S, Singh A, Norris KC, Klag MJ, Bakris GL, Investigators K. Independent components of chronic kidney disease as a cardiovascular risk state: Results from the Kidney Early Evaluation Program (KEEP). *Arch Intern Med*. 2007;167:1122-1129
3. Davis TR, Young BA, Eisenberg MS, Rea TD, Copass MK, Cobb LA. Outcome of cardiac arrests attended by emergency medical services staff at community outpatient dialysis centers. *Kidney Int*. 2008;73:933-939
4. Whitman IR, Feldman HI, Deo R. CKD and sudden cardiac death: Epidemiology, mechanisms, and therapeutic approaches. *J Am Soc Nephrol*. 2012;23:1929-1939
5. Tonelli M, Wiebe N, Culleton B, House A, Rabbat C, Fok M, McAlister F, Garg AX. Chronic kidney disease and mortality risk: A systematic review. *J Am Soc Nephrol*. 2006;17:2034-2047
6. Gaztanaga L, Marchlinski FE, Betensky BP. Mechanisms of cardiac arrhythmias. *Rev Esp Cardiol (Engl Ed)*. 2012;65:174-185
7. Jansen JA, van Veen TA, de Jong S, van der Nagel R, van Stuijvenberg L, Driessen H, Labzowski R, Oefner CM, Bosch AA, Nguyen TQ, Goldschmeding R, Vos MA, de Bakker JM, van Rijen HV. Reduced Cx43 expression triggers increased fibrosis due to enhanced fibroblast activity. *Circ Arrhythm Electrophysiol*. 2012;5:380-390
8. Stein M, Boulaksil M, Jansen JA, Herold E, Noorman M, Joles JA, van Veen TA, Houtman MJ, Engelen MA, Hauer RN, de Bakker JM, van Rijen HV. Reduction of fibrosis-related arrhythmias by chronic renin-angiotensin-aldosterone system inhibitors in an aged mouse model. *Am J Physiol Heart Circ Physiol*. 2010;299:H310-321
9. van Veen TA, van Rijen HV, Wiegerinck RF, Opthof T, Colbert MC, Clement S, de Bakker JM, Jongsma HJ. Remodeling of gap junctions in mouse hearts hypertrophied by forced retinoic acid signaling. *J Mol Cell Cardiol*. 2002;34:1411-1423
10. Sweat F, Puchter H, Rosenthal SI. Sirius Red F3Ba as a stain for connective tissue. *Arch Pathol*. 1964;1964:69-72
11. Ishola DA, Jr., van der Giezen DM, Hahnel B, Goldschmeding R, Kriz W, Koomans HA, Joles JA. In mice, proteinuria and renal inflammatory responses to albumin overload are strain-dependent. *Nephrol Dial Transplant*. 2006;21:591-597
12. Ma LJ, Fogo AB. Model of robust induction of glomerulosclerosis in mice: Importance of genetic background. *Kidney Int*. 2003;64:350-355
13. Hartner A, Cordasic N, Klanke B, Veelken R, Hilgers KF. Strain differences in the development of hypertension and glomerular lesions induced by deoxycorticosterone acetate salt in mice. *Nephrol Dial Transplant*. 2003;18:1999-2004
14. Esposito C, Dal Canton A. Functional changes in the aging kidney. *Journal of nephrology*. 2010;23 Suppl 15:S41-45
15. Acelajado MC, Oparil S. Hypertension in the elderly. *Clin Geriatr Med*. 2009;25:391-412
16. Bolignano D, Mattace-Raso F, Sijbrands EJ, Zoccali C. The aging kidney revisited: A systematic review. *Ageing research reviews*. 2014;14:65-80
17. Young M, Head G, Funder J. Determinants of cardiac fibrosis in experimental hypermineralocorticoid states. *Am J Physiol*. 1995;269:E657-662
18. Peng H, Carretero OA, Alfie ME, Masura JA, Rhaleb NE. Effects of angiotensin-converting

- enzyme inhibitor and angiotensin type 1 receptor antagonist in deoxycorticosterone acetate-salt hypertensive mice lacking Ren-2 gene. *Hypertension*. 2001;37:974-980
19. Loch D, Hoey A, Morisseau C, Hammock BO, Brown L. Prevention of hypertension in DOCA-salt rats by an inhibitor of soluble epoxide hydrolase. *Cell Biochem Biophys*. 2007;47:87-98
 20. Leelahavanichkul A, Yan Q, Hu X, Eisner C, Huang Y, Chen R, Mizel D, Zhou H, Wright EC, Kopp JB, Schnermann J, Yuen PS, Star RA. Angiotensin II overcomes strain-dependent resistance of rapid CKD progression in a new remnant kidney mouse model. *Kidney Int*. 2010;78:1136-1153
 21. Boulaksil M, Winckels SK, Engelen MA, Stein M, van Veen TA, Jansen JA, Linnenbank AC, Bierhuizen MF, Groenewegen WA, van Oosterhout MF, Kirkels JH, de Jonge N, Varro A, Vos MA, de Bakker JM, van Rijen HV. Heterogeneous Connexin43 distribution in heart failure is associated with dispersed conduction and enhanced susceptibility to ventricular arrhythmias. *Eur J Heart Fail*. 2010;12:913-921
 22. Kitamura H, Ohnishi Y, Yoshida A, Okajima K, Azumi H, Ishida A, Galeano EJ, Kubo S, Hayashi Y, Itoh H, Yokoyama M. Heterogeneous loss of connexin43 protein in nonischemic dilated cardiomyopathy with ventricular tachycardia. *J Cardiovasc Electrophysiol*. 2002;13:865-870
 23. Kostin S, Rieger M, Dammer S, Hein S, Richter M, Klovekorn WP, Bauer EP, Schaper J. Gap junction remodeling and altered connexin43 expression in the failing human heart. *Mol Cell Biochem*. 2003;242:135-144
 24. Burstein B, Comtois P, Michael G, Nishida K, Villeneuve L, Yeh YH, Nattel S. Changes in connexin expression and the atrial fibrillation substrate in congestive heart failure. *Circ Res*. 2009;105:1213-1222
 25. Peters NS, Coromilas J, Severs NJ, Wit AL. Disturbed Connexin43 gap junction distribution correlates with the location of reentrant circuits in the epicardial border zone of healing canine infarcts that cause ventricular tachycardia. *Circulation*. 1997;95:988-996
 26. Iravanian S, Sovari AA, Lardin HA, Liu H, Xiao HD, Dolmatova E, Jiao Z, Harris BS, Witham EA, Gourdie RG, Duffy HS, Bernstein KE, Dudley SC, Jr. Inhibition of renin-angiotensin system (RAS) reduces ventricular tachycardia risk by altering connexin43. *J Mol Med (Berl)*. 2011;89:677-687
 27. Hsueh CH, Chen NX, Lin SF, Chen PS, Gattone VH, 2nd, Allen MR, Fishbein MC, Moe SM. Pathogenesis of arrhythmias in a model of CKD. *J Am Soc Nephrol*. 2014
 28. Qu J, Volpicelli FM, Garcia LI, Sandeep N, Zhang J, Marquez-Rosado L, Lampe PD, Fishman GI. Gap junction remodeling and spironolactone-dependent reverse remodeling in the hypertrophied heart. *Circ Res*. 2009;104:365-371



Hiroki Takanari^{1,2,3,*}, Vincent J.A. Bourgonje^{1,*}, Magda S.C. Fontes^{1,*}, Antonia J.A. Raaijmakers¹, Helen Driessen¹, John A. Jansen, Roel van der Nagel¹, Bart Kok¹, Leonie van Stuijvenberg¹, Mohamed Boulaksil^{1,4}, Yoshio Takemoto², Masatoshi Yamazaki², Yukiomi Tsuji², Haruo Honjo², Kaichiro Kamiya², Itsuo Kodama⁵, Mark E. Anderson⁶, Marcel A.G. van der Heyden¹, Harold V.M. van Rijen¹, Toon A.B. van Veen^{1,¶}, Marc A. Vos^{1,¶}

**,¶ Authors contributed equally*

¹ Department of Medical Physiology, University Medical Center, Utrecht, The Netherlands

² Department of Cardiovascular Research, Research Institute of Environmental Medicine, Nagoya University, Nagoya, Japan

³ Department of Pathophysiology, Oita University School of Medicine, Yufu, Japan

⁴ Department of Cardiology, Radboud University Medical Center, Nijmegen, The Netherlands

⁵ Nagoya University, Nagoya, Japan

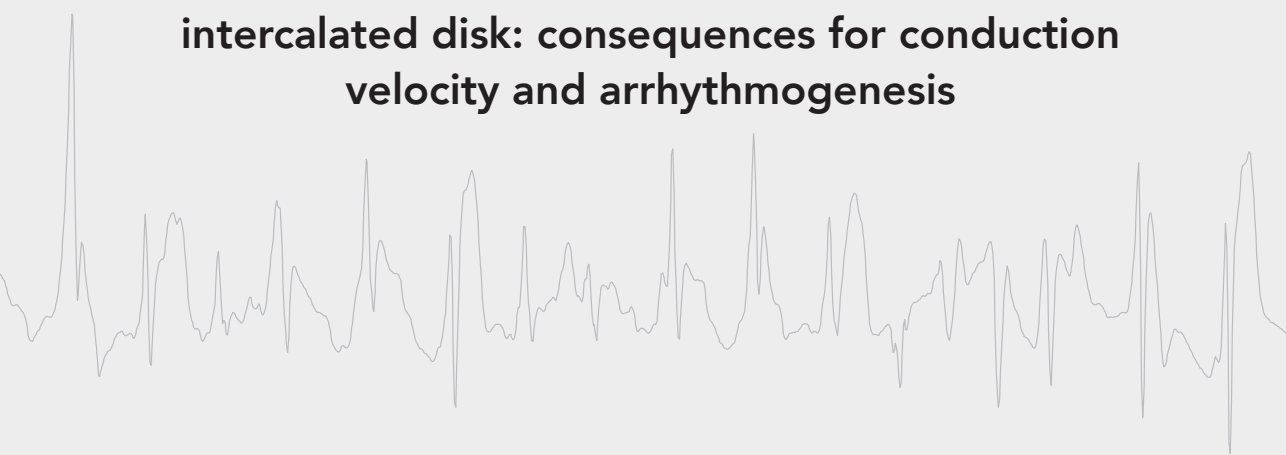
⁶ Division of Cardiology, Department of Medicine, Johns Hopkins University School of Medicine, Baltimore, USA



Chapter 4



**Calmodulin/CaMKII inhibition augments the
localization of cardiac Connexin43 in the
intercalated disk: consequences for conduction
velocity and arrhythmogenesis**



Submitted



ABSTRACT

Background

In healthy hearts, ventricular gap junctions are mainly composed by Connexin43 (Cx43) and localize in the intercalated disk, enabling appropriate electrical coupling. During pathophysiology, Cx43 is heterogeneously downregulated whereas activity of CaM/CaMKII signaling increases. It is unclear if CaM/CaMKII affects Cx43 expression/localization of gap junction channels or impulse propagation. We analyzed different models to assess this.

Methods and Results

AC3-I mice with CaMKII genetically inhibited were subjected to pressure overload (16weeks, TAC vs. sham). Optical and epicardial mapping was performed on Langendorff perfused rabbit and AC3-I mouse hearts, respectively. Junctional Cx43 expression from rabbit/mouse ventricles was evaluated by Western blot after Triton X-100-based fractionation. In mice, conduction velocity (CV) was augmented in AC3-I ($n=11$, $p<0.01$ vs. WT) and preserved after TAC, but impaired in TAC-WT mice (-20%). Cx43 expression was preserved after TAC in AC3-I mice though arrhythmias and fibrosis were still present. W7 (CaM inhibitor, 10 μ M) increased CV (6-9%, $n=6$, $p<0.05$) in rabbits while susceptibility to arrhythmias decreased. Immuno-confocal microscopy revealed enlarged Cx43 cluster sizes at intercalated disks of those hearts. Total Cx43 did not change by W7 ($n=4$), whereas junctional Cx43 increased (+21%, $n=4$, $p<0.01$). This was confirmed in AC3-I mouse hearts when compared to control, and in cultured dog cardiomyocytes. Physiological relevance was shown through increased metabolic coupling in cultured neonatal rat cardiomyocytes.

Conclusion

Both acute and chronic CaM/CaMKII inhibition positively affects conduction properties and localization of Cx43 in intercalated disk. In the absence of fibrosis this reduced the susceptibility for arrhythmias.

INTRODUCTION

Normal cardiac conduction of electrical excitation is essential for the synchronous beating of the heart. This electrical conductivity includes active conduction due to sodium channel activation (depolarization) and passive conduction through gap junction channels, which propagates the electrical charge from one cell to the other. In ventricular tissue, connexin43 (Cx43) is the major component of gap junction channels, and sodium channels mainly consist of the alpha-subunit protein $\text{Na}_v1.5$. Reduced expression and heterogeneous redistribution of Cx43 channels in the heart, as well as lateralization, negatively modifies the conductivity of cardiac tissue in diseased hearts and enhance susceptibility for arrhythmias.¹⁻³ Besides Cx43, disturbed $\text{Na}_v1.5$ expression and localization, and increased cardiac fibrosis are contributing factors,^{2,4} which often act in combination.

Calmodulin (CaM) and the multifunctional Ca^{2+} and calmodulin-dependent protein kinase II (CaMKII) are involved in cardiac arrhythmias, both in drug-induced-arrhythmia models,^{5,6} and in CaMKII overexpression animal models.^{7,8} The available evidence suggests that CaM/CaMKII activation leads to arrhythmias via three potential mechanisms: 1) it can directly phosphorylate ion channels, thereby altering their function in a pro-arrhythmic manner,⁹ 2) prolonged CaMKII activation gives rise to changes in ion channel expression patterns, called electrical remodelling,¹⁰ and 3) long-term CaMKII activation ultimately culminates in cardiac hypertrophy, heart failure,¹¹⁻¹³ apoptosis of cardiomyocytes and fibrosis formation,¹⁴ which may provide the substrate of reentry-based arrhythmias.

There are several studies showing an interaction between CaM/CaMKII and Cx43: 1) Cx43 has a CaM binding site to regulate the gating of Cx43-mediated gap junction channels,^{15,16} 2) CaM inhibition by W7 prevented Ca-CaM-complex induced impairment of gap junctional conductance,¹⁷ and 3) bepridil, which has CaM inhibiting activity, increased the intercellular electrical coupling and terminated reentrant arrhythmias.¹⁸ These studies suggested but did not directly test the hypothesis that CaM and CaMKII can influence the conductive properties of myocardium via modulation of Cx43.

We hypothesized that CaM/CaMKII has not only a direct effect on Cx43 channels by regulating its gating properties but also has an indirect effect by modifying their expression, or subcellular localization in the intercalated disk. To approach this issue, we applied several methodologies in different animal models to determine the effects of both acute and chronic inhibition of CaM/CaMKII on Cx43 localization, conduction velocity, and arrhythmogenesis.

METHODS

Acute experiments

The effect of acute CaM inhibition on cardiac Cx43-based conduction properties (molecular and electrophysiological) was investigated using rabbit hearts. Rat neonatal and canine cardiomyocytes were also used to determine gap-junctional intercellular communication and Cx43 subcellular distribution. All acute experiments were approved by the Institutional Animal Care and Use Committees at Nagoya University, Japan and Utrecht University, The Netherlands.

Optical mapping of Langendorff perfused rabbit hearts

The experimental model and procedures of optical mapping have been described before.^{18,19} For the electrophysiological experiments six rabbit hearts were Langendorff perfused with modified Krebs-Ringer solution, equilibrated with 95% O₂-5% CO₂ at 37°C. Complete atrioventricular block was produced by His bundle destruction. Cryoablation of the left ventricular (LV) endomyocardium was applied to make a thin epicardial layer of ventricular myocardium (~1 mm thick). The hearts were stained with voltage-sensitive dye, di-4-ANEPPS. Motion artifacts due to heartbeat were eliminated by 100 mM of 2, 3-butandione monoxime (BDM). The effect of acute CaM inhibition was tested through application of 10 μ M W7. Hearts were illuminated by green LED lights, and the fluorescent image was recorded with a high-speed video camera at a sampling rate of 1,000 frames/s. Isochrone maps of 4 ms intervals were generated from the filtered image, then conduction velocity (CV) was measured in a square of 18x18 mm around the stimulation site from the center of the LV free wall. CV in longitudinal (CV_L) and transverse directions (CV_T) was calculated from the slope of a linear least-squares fit of the activation time plotted against the distance.

The space constant (λ), an index of intercellular electrical coupling, was estimated from the exponential decay of the electrotonic membrane depolarization in response to subthreshold stimulus as described.^{18,20,21} A magnified image covering a square of 5x5 mm was obtained through a photographic lens with a longer focal distance (Micro-Nikkor 105 mm, f/2.8D, Nikon). A single subthreshold stimulus (20 ms, ~0.8 times threshold) was delivered during electrical diastole after regular (basic cycle length: BCL 400 ms) suprathreshold stimuli (2.0 ms, ~1.2 times threshold) through a teflon-coated platinum wire electrode placed at the center of the LV free wall. Myocardial excitability was reduced by increasing the extracellular K⁺ from 4 to 8 mM in order to induce subthreshold membrane potential responses.

Ventricular tachycardia or ventricular fibrillation (VT/VF) were induced by modified S1-S2 cross-field stimulation and classified by the length of arrhythmias into non-

sustained (<10 s) and sustained (≥ 10 s) VT/VF. When VT/VF sustained for more than 60 seconds, it was terminated by DC shocks. Wave propagation patterns during VT/VF were also analyzed by the phase mapping to detect the movement of phase singularity as the center of spiral-wave reentry.

Western blot and immunohistochemistry

Rabbit hearts were perfused on a Langendorff apparatus for 1 hour with ($n=4$) or without ($n=4$) 10 μM W7 to see the effect of sub-acute CaM inhibition on Cx43 distribution in the hearts. Then the hearts were removed from the set-up and immediately frozen by liquid nitrogen. For protein isolation ($n=8$), the frozen tissue was treated with modified RIPA buffer (10 mM Tris-HCl, 150 mM NaCl, 1% Triton X-100, 0.1% SDS, and 0.5% sodium deoxycholate, pH 7.4). Total protein samples were loaded on 10% SDS-gel and transferred on nitrocellulose membrane. The membrane was blocked by 5% milk and then incubated with mouse monoclonal anti-Cx43 antibody (BD Transduction Laboratories, 610062) to detect total Cx43. Detection was performed using ECL detection kit (GE Healthcare). Fractionation of non-junctional and junctional proteins, based on the Triton X-100 extraction method, was performed as previously described.²²

Immunofluorescence microscopy was performed on cryosections of frozen rabbit hearts ($n=8$), which were fixed by 4% paraformaldehyde (PFA). Cryosections were made in two different planes, longitudinal and transverse, relative to the apical-base axis of the heart. After permeabilization by 0.3% Triton X-100, Cx43 was labeled with mouse monoclonal anti-Cx43 antibody (Millipore, mab3068) and stained with green fluorescence Alexa-Fluor 488 (Molecular Probes, A11006).

Cardiomyocytes isolated from adult normal sinus rhythm dogs were cultured overnight and used to test acute CaM/CaMKII inhibition. Cultured cardiomyocytes were stimulated for 4 hours with either 5 μM of W7 (CaM inhibitor) or 1-10 μM of KN93 (CaMKII inhibitor). Total protein was then isolated and prepared for Western blot using the same procedure as described above. Cx43 was detected using mouse monoclonal anti-Cx43 (BD Transduction Laboratories, The Netherlands, 610062).

Dye transfer assay on cultured rat neonatal cardiomyocytes

The communication through gap junctions was assessed by a dye transfer assay on primary cultures of neonatal rat cardiomyocytes (NRCMs) that were prepared as reported previously.²³ Twenty-four hours after generating a confluent monolayer of NRCMs, either normal culture medium ($n=5$) or medium with 10 μM W7 ($n=5$) was added. Thirty minutes later, Lucifer yellow CH (LY, 2mM) was microinjected into a single NRCM of each monolayer. NRCMs were fixed by 2% PFA 15 minutes after the injection. Confocal images were obtained by laser scanning microscopy (LSM-510, Carl Zeiss), and the number of LY-stained cells was counted.

Chronic experiments

Mice expressing cardiospecific autocamtide-3 related peptide (AC3-I)²⁴ were bred into a C57BL/6 background; we recently confirmed AC3-I mice have reduced CaMKII activity at multiple substrate proteins by comparative phosphoproteomic analysis.²⁵ The chronic experiments were approved by the Institutional Animal Care and Use Committee, Utrecht University, The Netherlands.

Experimental set-up

To evaluate the effect of chronic CaMKII inhibition on Cx43 expression and conduction properties under basic conditions and during chronic pressure overload, 11 AC3-I mice (10-12 weeks of age) underwent sham surgery and another 11 AC3-I mice were subjected to transverse constriction of the aorta (TAC). All mice were followed for 4 months. For comparative reasons, historical data were obtained from TAC experiments in wildtype (WT) animals performed in the same strain of mice, for the same duration of 16 weeks.^{3,4}

AC3-I mice were TAC operated, as previously described.³ Effectiveness of the constriction was confirmed by Doppler echocardiography (pressure gradient: 66 ± 4 mmHg). Sham animals received the same treatment, but without aortic constriction. Sixteen weeks after the surgery, mice were anesthetized by 2.5% isoflurane in O₂ and subjected to the following experiments.

Electrocardiogram and echocardiography

A 3-lead electrocardiogram (ECG) was recorded using PowerLab 4/30 and Dual Bio Amp and analyzed off-line using LabChart 7 Pro (all from ADInstruments Ltd., UK). Echocardiography was performed immediately after ECG analysis, to determine functional and structural characteristics (SONOS 5500, Philips Medical Systems).

Epicardial mapping of Langendorff perfused mouse hearts

After the *in vivo* measurements, the heart was excised and mounted on a Langendorff apparatus for epicardial mapping during retrograde perfusion of the hearts. Perfusion buffer contained (mM) NaCl 116, KCl 5, MgSO₄ 1.1, NaH₂PO₄ 0.35, NaHCO₃ 27, glucose 10, mannitol 16, CaCl₂ 1.8, which was carbogen-gassed at 37°C. A multielectrode 19x13 grid was placed on the epicardial surface of the heart. Stimulation was performed from the center of the grid (2 times stimulation threshold). Analysis of CV was done off-line. The maximal negative dV/dt on the unipolar electrogram was defined as the time of local activation. The combined activation times of the electrodes allowed generation of an activation map, which subsequently could be used to determine CVs. All measurements were analyzed with custom made software based on Matlab (The MathWorks Inc.).

Assessment of arrhythmias was performed in three steps; i) spontaneous arrhythmias, ii) arrhythmias induced by a 16-paced train (BCL 100ms) followed by 1-3 premature stimuli close to the effective refractory period, iii) arrhythmias induced by 2 s of burst pacing at the shortest possible cycle length.

Western blot and histological examination

Hearts were removed from the Langendorff apparatus and immediately frozen in liquid nitrogen. Protein lysate samples were made in a similar fashion as described for rabbit heart tissue. Mouse monoclonal anti-Cx43 antibody (BD Transduction Laboratories, 610062) was used to detect Cx43. To detect Na_v1.5, protein samples were loaded on 7% SDS-gel and incubated with rabbit polyclonal anti-Na_v1.5 antibody (Sigma-Aldrich Corp., USA, S0819). Cryosections were generated (in four-chamber view) for histological analysis and immunohistochemistry. Immunolabeling using rabbit polyclonal anti-Cx43 (Invitrogen, 71-0700) antibodies was performed to assess subcellular distribution of Cx43, as described previously.²⁶ For fibrosis detection, cryosections were fixed with 4% PFA and stained by Picrosirius Red, as previously described.²⁷ Analysis was done in ImageJ and microscopy was performed using an Eclipse 80i (Nikon, Tokyo, Japan).

Statistical analysis

Data were shown as means \pm standard error of the mean (SEM). Statistics were performed by two-way ANOVA with Tukey's HSD post-hoc test, Student's t-test or Fisher exact test when appropriate. Differences were considered significant if $p < 0.05$.

RESULTS

The effect of acute CaM inhibition

Electrophysiology and arrhythmogenicity in rabbit hearts

In perfused rabbit hearts, W7 (10 μ M) significantly increased CV_L and CV_T by 5.8% and 9.1%, respectively (Figure 1A). The space constant (λ), an index of intercellular electrical coupling, was significantly increased by W7 in both longitudinal and transversal directions (λ_L , 1.52 ± 0.16 vs. 1.09 ± 0.08 mm, $n=6$, $p < 0.05$; λ_T , 1.31 ± 0.07 vs. 0.93 ± 0.05 mm, $n=6$, $p < 0.01$, Figure 1B and 1C).

Sustained ventricular arrhythmias (VT or VF) were induced in 6/6 control hearts. With subsequent exposure to 10 μ M W7, incidence of sustained-VT/VF decreased to 4/6 hearts. Total incidence of VT/VF decreased from 53% to 35% by W7 (Figure 2A), and the percentage of sustained VT/VF over total incidence was significantly reduced

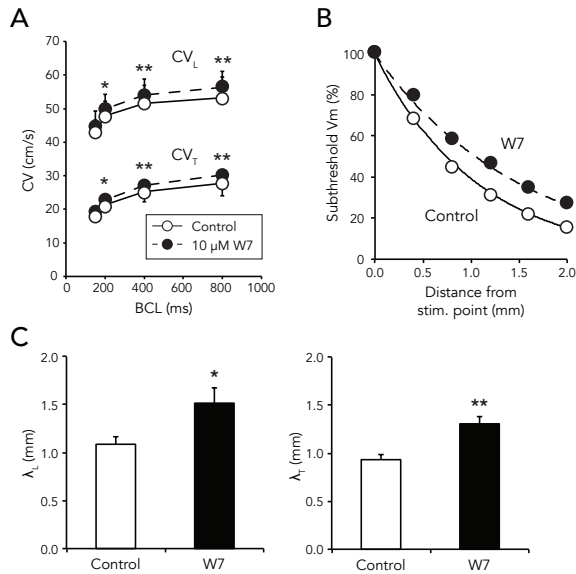


Figure 1. Electrophysiological changes by calmodulin inhibitor W7 in perfused rabbit hearts.

A: Conduction velocity in longitudinal (CV_L) and transverse (CV_T) directions as measured by high-resolution optical mapping. BCL, basic cycle length. **B:** Representative measurement of space constant in the absence (open circle) or presence (closed circle) of 10 μ M W7. The amplitude of membrane voltage (V_m) in response to subthreshold stimulation decreased exponentially depending on the distance from the stimulation site. **C:** Summarized data of space constant measured in longitudinal (λ_L) and transverse (λ_T) directions. * $p < 0.05$, ** $p < 0.01$ vs. control ($n = 6$).

from 82% to 33% ($n = 6$, $p < 0.01$). In 5 hearts, spiral wave reentry before and after application of 10 μ M W7 was clearly seen (Figures 2B-C). Under control conditions (30 s after VT initiation), a stable rotor circulating around a line of functional block (FBL, ~4 mm in length) was observed (Figure 2B). The distant bipolar electrogram showed a monomorphic VT pattern. In the phase map, a phase singularity, the rotational center of spiral wave, moved back and forth along the functional block line (Figure 2D left). On the other hand, in presence of 10 μ M W7, spiral waves changed their circuits in a beat-to-beat manner with a polymorphic VT-pattern (Figure 2C). The shape and length of the functional block line changed with every beat. Consequently, the rotation center drifted upward and collided with the atrioventricular groove, resulting in self-termination of the spiral wave. The phase singularity trajectory during these beats was illustrated in Figure 2D right. Mean length of functional block line extended from 8.2 ± 2.1 mm to 16.7 ± 2.3 mm by 10 μ M of W7 ($p < 0.01$, Figure 2E), revealing a larger spiral wave meandering in presence of W7.

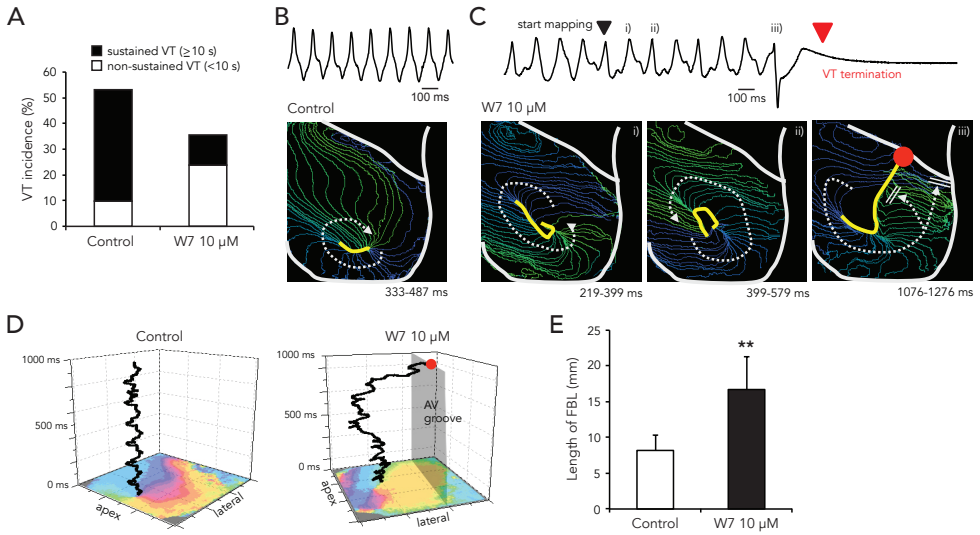


Figure 2. Characteristics of ventricular tachyarrhythmias (VT) induced in perfused rabbit hearts by cross-field stimulation.

A: (Non) sustained VT incidence (white and black bars, respectively) before and after application of 10 μ M W7. **B top:** Electrogram of sustained VT induced in the absence of W7. **bottom:** Isochrone map of VT recorded by high-resolution optical mapping. **C top:** Electrogram of self-terminated VT induced in the presence of 10 μ M W7. **bottom:** Three isochronal maps recorded at three different periods to show the meandering of the circuit of spiral-wave reentry during non-sustained VT. **D:** The trajectory of phase singularity during VTs shown in **B** and **C**. **E:** Mean length of functional block line (FBL) in the absence and presence of 10 μ M W7. ** $p < 0.01$ vs. control ($n = 6$).

Subcellular distribution of Cx43

As expected because of the acute nature of our study, the total amount of Cx43 was not significantly changed by W7 (Figure 3A). Surprisingly, non-junctional Cx43 was significantly decreased (14%) by a 1-hour W7 treatment, whereas junctional Cx43 expression was significantly increased by 21% (Figure 3B). Using immuno-confocal imaging, no apparent changes in Cx43 distribution by W7 were observed in longitudinal sections; whereas Cx43 was well localized to the intercalated disk in both W7-treated and untreated hearts (Figure 3C top). Examining transverse cryosections, we noticed that the total area of intercalated disk was not changed, while the fluorescent signal of Cx43 increased in the intercalated disk (Figure 3C bottom & Table 1). These results suggest that acute CaM inhibition increased the localization of Cx43 to the intercalated disk.

With respect to a physiological meaning of the increased accumulation of junctional Cx43, as depicted in Supplemental Figure 1, an increased number of dye coupled cells can be seen after W7 treatment of monolayers of cultured NRCMs.

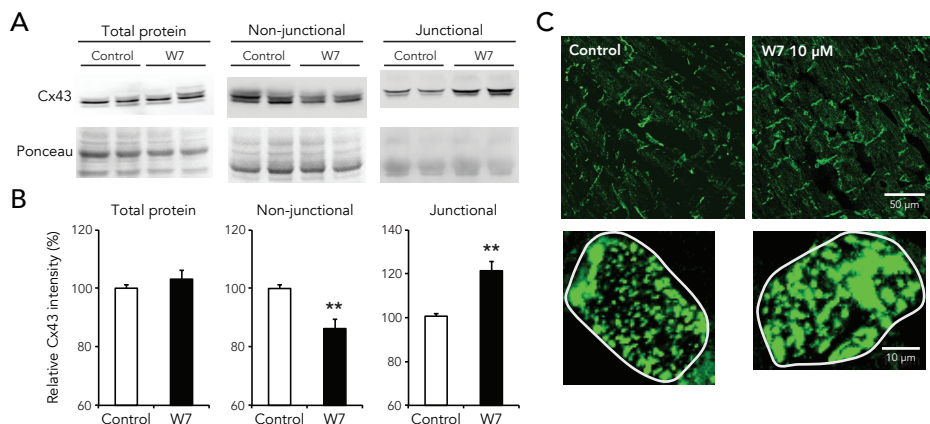


Figure 3. The expression and localization of connexin43 (Cx43) in isolated rabbit hearts perfused for one hour with or without 10 μ M W7.

A: Representative blot of Cx43 in total lysate (**left**), non-junctional (**middle**), or junctional (**right**) fractions. The intensity of the blot signal was normalized by ponceau staining. **B:** Summarized data of Cx43 expression [in total lysate (**left**), non-junctional (**middle**), or junctional (**right**) fractions]. * $p < 0.05$, ** $p < 0.01$ vs. control ($n = 4$). **C:** Representative images of immunohistochemistry labeled for Cx43 (green). Frozen sections of perfused rabbit hearts were made in longitudinal (**top**) and transverse (**bottom**) directions. Scale bars represent 50 μ m and 10 μ m, respectively. Please note the increase in Cx43 labeling.

Table 1. Intercalated disk characteristics from transverse cryosections of rabbit hearts.

	Control	W7 10 μ M	p value (n=3)
Area of intercalated disk (pixels)	3705 \pm 562	3865 \pm 352	0.31
Percentage of Cx43 (%)	30.5 \pm 2.2	51.0 \pm 3.2	<0.01

Values are mean \pm SEM.

A different and more specific inhibitor of CaMKII (KN93) was also tested in a third model of acute inhibition to generalize the effects observed by W7 on Cx43. In isolated and cultured adult dog cardiomyocytes, the effect of W7 on total and junctional Cx43 expression was compared to KN93. In Supplemental Figure 2 is depicted that both drugs increased junctional Cx43 localization in a comparable fashion, without affecting the total Cx43 expression.

The effect of chronic CaMKII inhibition on (diseased) mouse hearts

Morphological, echocardiographic and electrocardiographic data

The basic data of sham- and TAC-operated AC3-I mice are depicted in Tables 2 and 3. Aortic constriction of 16 weeks in TAC AC3-I mice resulted in increased heart and lung weights as compared to sham AC3-I, also when heart weight was corrected

Table 2. Tissue characteristics and echocardiographic measurements of Sham- and TAC-operated AC3-I mice.

	Sham	TAC
N	11	11
Organ weights		
Body weight (g)	27.9 ± 1.1	28.6 ± 1.3
Heart weight (mg)	162.56 ± 9.55	235.90 ± 17.24 †
HW/BW (mg/g)	5.97 ± 0.40	8.29 ± 0.42 †
Tibia length (cm)	1.84 ± 0.02	1.76 ± 0.09
HW/TL (mg/cm)	88.84 ± 5.18	142.08 ± 17.22 *
Liver weight (g)	1.21 ± 0.06	1.21 ± 0.08
Lungs weight (g)	0.183 ± 0.006	0.206 ± 0.005 †
Kidneys weight (g)	0.176 ± 0.010	0.169 ± 0.010
Echocardiography		
IVSd (mm)	0.050 ± 0.001	0.071 ± 0.001 †
LVIDd (mm)	0.318 ± 0.013	0.373 ± 0.018 *
LVPWd (mm)	0.049 ± 0.001	0.071 ± 0.001 †
IVSs (mm)	0.068 ± 0.001	0.089 ± 0.001 †
LVIDs (mm)	0.164 ± 0.007	0.242 ± 0.018 †
LVPWs (mm)	0.067 ± 0.002	0.087 ± 0.002 †
Aortic root diameter (mm)	0.123 ± 0.005	0.149 ± 0.005 †
LVOT diameter (mm)	0.108 ± 0.004	0.131 ± 0.003 †
LA dimension (mm)	0.145 ± 0.007	0.182 ± 0.007 †
Pressure Gradient (mmHg)	2.4 ± 0.2	65.7 ± 4.1 †
Fractional Shortening (%)	48.4 ± 0.8	35.8 ± 1.7 †

Values are mean ± SEM. TAC, transverse aortic constriction; N, number of animals; HW/BW, heart weight to body weight ratio; HW/TL, heart weight to tibia length ratio; IVSd and IVSs, diastolic and systolic interventricular septal thickness, respectively; LV, left ventricle; LVIDd and LVIDs, LV diastolic and systolic internal diameter, respectively; LVPWd and LVPWs diastolic and systolic posterior wall thickness, respectively; LVOT, LV outflow tract; LA, left atrium. * $p < 0.05$, † $p < 0.01$ vs. sham.

for body weight (HW/BW, 8.3 ± 0.4 vs. 6.0 ± 0.4 mg/g, $n=11$, $p < 0.01$, Table 2) or tibia length. Likewise, all echocardiographic parameters were significantly increased with the exception of fractional shortening (FS) which was significantly decreased in TAC AC3-I (FS, 35.8 ± 1.7 vs. 48.4 ± 0.8 %, $n=11$, $p < 0.01$, Table 2). Moreover, heart rate and other electrocardiographic parameters remained unchanged after TAC except for QRS width, which was increased in TAC AC3-I compared to sham AC3-I (QRS, 11.4 ± 0.2 vs. 10.2 ± 0.3 ms, $n=11$, $p < 0.01$, Table 3).

Table 3. Electrocardiographic and electrophysiological measurements of Sham- and TAC-operated AC3-I mice.

	Sham	TAC
N	11	11
Electrocardiography		
Heart Rate (beats/min)	503.7 ± 25.8	536.7 ± 19.8
RR interval (ms)	122.5 ± 6.8	113.5 ± 4.6
PR interval (ms)	44.5 ± 1.1	47.1 ± 1.5
P duration (ms)	11.2 ± 0.2	11.2 ± 0.6
QRS interval (ms)	10.2 ± 0.3	11.4 ± 0.2 †
QT duration (ms)	49.4 ± 0.6	50.6 ± 2.0
QTc duration (ms)	45.0 ± 1.0	47.5 ± 1.7
Echocardiography		
LV CV _L (cm/s)	79.7 ± 4.4	86.2 ± 2.5
LV CV _T (cm/s)	60.0 ± 2.5	53.5 ± 3.5
RV CV _L (cm/s)	74.6 ± 3.8	80.7 ± 4.3
RV CV _T (cm/s)	55.1 ± 3.7	49.6 ± 7.1
LV AR (CV _L /CV _T)	1.34 ± 0.08	1.67 ± 0.17
RV AR (CV _L /CV _T)	1.37 ± 0.05	1.75 ± 0.20
LV ERP (ms)	57.8 ± 3.6	50.0 ± 3.0
RV ERP (ms)	44.5 ± 3.9	41.8 ± 3.0
LV CV Disp index	1.56 ± 0.18	1.59 ± 0.14
RV CV Disp index	1.28 ± 0.22	1.40 ± 0.22

Values are mean ± SEM. TAC, transverse aortic constriction; N, number of hearts; LV and RV, left and right ventricle, respectively; CV_L and CV_T, longitudinal and transversal conduction velocity, respectively; AR, anisotropic ratio; ERP, effective refractory period; CV Disp, dispersion of conduction velocity. † $p < 0.01$ vs. sham.

Conduction velocity and arrhythmia induction

Electrophysiological data obtained from epicardial mapping are shown in Table 3 (bottom). In transgenic AC3-I mice, conduction velocity, both in longitudinal and transverse directions, and both in left and right ventricles, was clearly increased compared to WT mice ($p < 0.01$, Figures 4A-B). Interestingly, the increases in CV seen in sham AC3-I mice were preserved after TAC. A major finding was that the decreases in longitudinal CV normally seen in TAC-WT are completely prevented. These measurements confirmed that CaMKII inhibition resulted in enhanced CV in the TAC model of structural heart disease.

Despite the preservation of conduction velocity, AC3-I mice still showed arrhythmias on the Langendorff set-up after TAC (4/11, sham mice 0/11). Arrhythmias were burst

pacing-induced, polymorphic, and sustained (>15 beats), as exemplified in Figure 4C. The percentage of TAC AC3-I mice with arrhythmias (36.4%) was comparable to TAC-WT populations (historical data in identical C57BL/6 strain), as shown in the studies of Jansen *et al.*⁴ (18.2%) or Boulaksil *et al.*³ (44.4%) (Figure 4D). Importantly, the epicardial activation maps generated during the arrhythmias showed no signs of functional block and CV was preserved in general (Figure 4E).

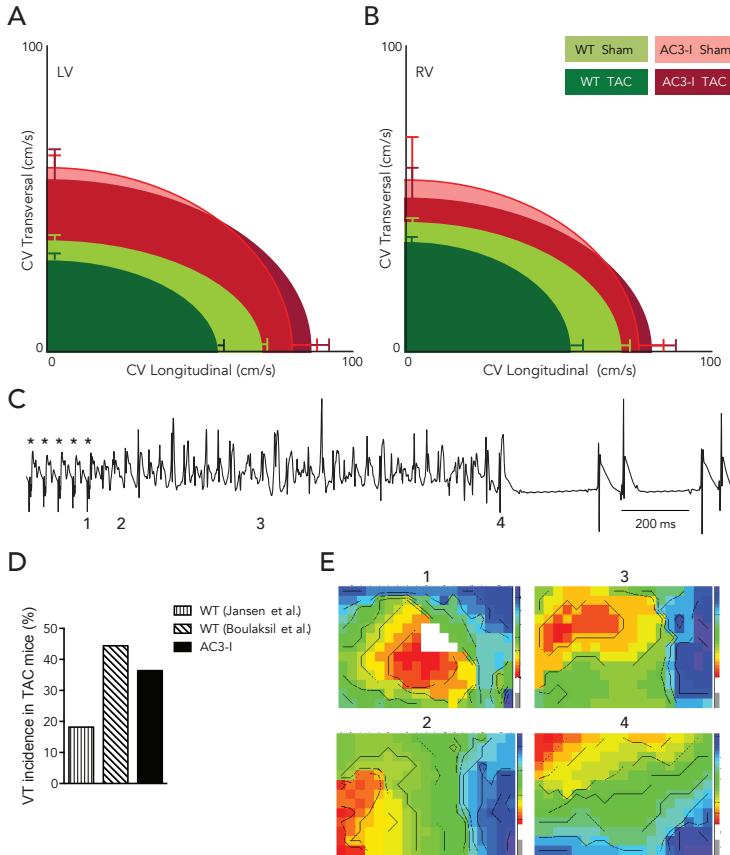


Figure 4. Conduction velocity (CV) and ventricular tachyarrhythmias (VTs) induced in perfused TAC-operated mouse hearts.

A-B: CV in longitudinal and transverse directions measured by epicardial mapping on the left ventricle (LV) and right ventricle (RV), respectively. Sham and TAC AC3-I mice were compared with historical data of sham and TAC WT mice.⁴ Green colors represent WT mice (sham-light green and TAC-dark green) and red colors AC3-I mice (sham-light red and TAC-dark red). Please note that the CV reduction in WT TAC is not present in AC3-I TAC mice. **C:** Representative epicardial electrogram of a polymorphic VT induced by pacing in TAC AC3-I mice. Asterisks (*) indicate the last 5 burst paced (cycle length 40 ms) complexes. **D:** Comparison of the VT incidence in TAC AC3-I mice with TAC WT mice from our previous studies.^{3,4} **E:** Activation maps from 4 numbered VT complexes indicated in the epicardial electrogram in C. Black isochronal lines of activation are 1 ms apart. Red colour represent earliest activation time and blue colour the latest.

Cx43 expression, Na_v1.5 and fibrosis

The total amount of Cx43 expression was not changed in TAC AC3-I hearts when compared with sham AC3-I hearts as shown both by immunohistochemistry (Figures 5A-B) and Western blot (Figures 5C-D). Additionally, there was no significant difference in total Cx43 from chronic CaMKII inhibition of sham AC3-I hearts compared with control mouse hearts from the same C57BL/6 background, although the apparent small increase was close to significance ($p=0.052$, Figures 5C-D). Interestingly, junctional Cx43 expression was significantly increased after CaMKII inhibition in sham AC3-I as compared to control hearts (2.5 ± 0.2 vs. 1.0 ± 0.2 , $p<0.01$), and further increased after TAC AC3-I (2.5 ± 0.2 vs. 3.7 ± 0.3 , $p<0.05$, Figures 5E-F).

Similar to our measurements of total Cx43, there was no change in total Na_v1.5 expression between sham and TAC AC3-I hearts or when compared with control hearts as assessed by Western blot (Figures 5G-H).

Fibrosis did show profound changes when assessed through Picrosirius Red staining. AC3-I mice displayed areas of patchy fibrosis after TAC, and total fibrosis levels were significantly increased, by a factor of four, when compared to sham ($p<0.05$, Figures 5I-J).

DISCUSSION

The central question of this research project was to directly determine if the CaM/CaMKII pathway regulated CV, junctional Cx43 levels and arrhythmogenesis. We discovered that: 1) Conduction properties and the expression of junctional Cx43 (in the intercalated disk) are increased by acute CaM/CaMKII inhibition in rabbit hearts and dog cardiomyocytes, and by chronic CaMKII inhibition in AC3-I transgenic mice, 2) Acute CaM/CaMKII inhibition improved intercellular communication in NRCMs and decreased the incidence of re-entrant arrhythmic episodes in rabbit hearts, 3) Chronic CaMKII inhibition prevented TAC-induced reduction of CV and (junctional) Cx43 expression in AC3-I mice, but failed to prevent structural and contractile remodelling, and had no suppressive effect on ventricular arrhythmias induced by programmed electrical stimulation.

Intercellular coupling and conduction velocity

In normal ventricles, Cx43 protein localizes to the intercalated disk and forms gap junctions that enable cardiomyocytes to transfer excitability and small metabolic solutes. Total Cx43 protein expression was neither affected by acute CaM inhibition in rabbit hearts nor by chronic CaMKII inhibition in transgenic AC3-I mice hearts. However, the expression of junctional Cx43 was increased in both models (Figures 3, 5,

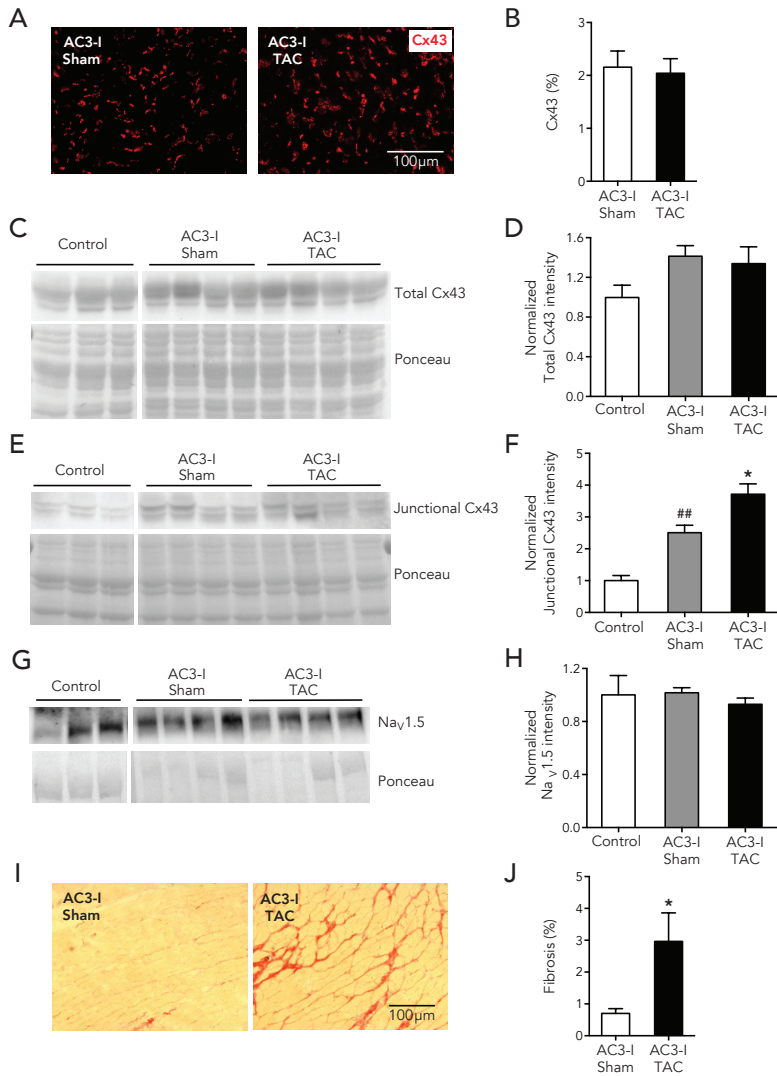


Figure 5. Connexin43 (Cx43) expression, Nav1.5 expression and fibrosis in isolated sham- and TAC-operated AC3-I mouse hearts compared with control mouse hearts from the same C57BL/6 background.

A: Representative pictures of Cx43 expression (red) in sham and TAC AC3-I hearts. Scale bar represents 100 μm. **B:** Quantification of Cx43 immunolabeling exemplified in **A**. Western blots of Cx43 in total lysate (**C**) and in junctional fraction (**E**) with their respective ponceau stainings below. **D and F:** Quantification of the blots (Cx43/ponceau) represented in **C** and **E**, respectively. ^{##} $p < 0.01$ vs. control; ^{*} $p < 0.05$ vs. AC3-I sham. **G:** Western blot of Nav1.5 in total lysate and respective ponceau staining below. **H:** Quantification of the blots (Nav1.5/ponceau) represented in **G**. Control samples (**C**, **E**, and **G**) were loaded on the same membrane as respective AC3-I sham and TAC, but were not adjoining (indicated by white line in between). **I:** Representative pictures of collagen in sham and TAC AC3-I hearts. Scale bar represents 100 μm. **J:** Quantification of collagen exemplified in **I**. ^{*} $p < 0.05$ vs. sham AC3-I.

and Supplemental Figure 2) while the cluster size of Cx43-mediated gap junction was enlarged by treatment with W7 (Figure 3). In line with these observations, similar effects were shown in canine cardiomyocytes using KN93 and W7. We recognize that W7 and KN93 have off target, CaMKII-independent, actions at a number of ion channels that could affect CV.^{5,28,29} However, our findings were confirmed using three mechanistically distinct antagonists, including transgenic AC3-I that has no known CaMKII-independent actions on ion channels. Thus, taken together, our findings support a view that the CaM/CaMKII pathway is an important signal for controlling Cx43 localization and CV in myocardium. Because we did not find a change in total Cx43 expression after W7, KN93 or in mice with transgenic myocardial expression of AC3-I, we speculate that CaMKII is involved in post-translational modification of Cx43 leading to an increased junctional positioning of this gap junction protein.

CaMKII phosphorylation sites have been identified on Cx43,¹⁶ although the physiological implication of this is not yet known. In our chronic inhibition of CaMKII, we found no obvious differences between phosphorylated and non-phosphorylated Cx43 levels (as suggested by the upper and lower Cx43 bands, respectively, in AC3-I sham vs. control groups of Figures 5C and 5E). Beyond phosphorylation, it is possible that other post-translational modifications of Cx43 may be involved (e.g. ubiquitination, SUMOylation, nitrosylation, hydroxylation, acetylation, methylation, and γ -carboxyglutamation).³⁰

That the increased presence of Cx43 signals in the intercalated disk has functional implications was indicated in several ways. The dye transfer assay in neonatal rat cardiomyocytes, indicative for coupling, revealed a higher number of coupled cells after acute CaM inhibition with W7 (Supplemental Figure 1). Support for this observation comes from a recent study, demonstrating that Cx43-mediated gap junction channels are closed by a CaM-dependent mechanism.¹⁵

To speculate, the observed increased coupling and junctional presence of Cx43 could possibly explain the increase in CV observed in both studied models of CaM/CaMKII inhibition. In perfused rabbit hearts, acute treatment with W7 increased CV_L and CV_T (Figure 1). In a similar way, we have demonstrated that chronic CaMKII inhibition in AC3-I transgenic mice improved CV_L and CV_T under baseline conditions (Figure 4). When chronic pressure overload is induced through TAC surgery, CV is generally decreased.^{3,4} Interestingly, upon 16 weeks of pressure overload in our transgenic AC3-I mice of chronic CaMKII inhibition, CV and the junctional levels for Cx43 were preserved. To the best of our knowledge, this is the first time CaM/CaMKII is experimentally linked to regulation of cardiac conduction velocity.

Loss of Cx43 distribution to the intercalated disk is an important characteristic of heart failure that may contribute to abnormal excitation-contraction coupling and

arrhythmia susceptibility. Our findings suggest that the CaM/CaMKII pathway, which is augmented in structural heart disease,³¹ may contribute to this pathological phenotype.

Role of excitability

Another factor that importantly adds to intercellular impulse propagation is the functionality of the sodium channel $\text{Na}_v1.5$. $\text{Na}_v1.5$ can be directly phosphorylated by CaMKII, which alters its gating properties resulting in increased sodium current.^{32,33} Although this suggests that CaMKII inhibition could decrease sodium channel function, we found no difference in $\text{Na}_v1.5$ protein expression between normal and CaMKII inhibited mouse hearts (Figure 5H). It is thus tempting to speculate that $\text{Na}_v1.5$ expression is not contributing to the improved CV seen in AC3-I mice at baseline and that enhanced CV is mainly dependent on increased gap-junctional coupling.

Expression of $\text{Na}_v1.5$ remained also unchanged in TAC AC3-I hearts when analysed after 16 weeks of pressure overload. A recent study that used the same intervention to induce pressure overload showed an increase in $\text{Na}_v1.5$ after 1 and 5 weeks of TAC.³⁴ Furthermore, they showed an increase in late sodium current that could be reversed by inhibiting CaMKII. This, however, most likely reflects an earlier phase of cardiac remodeling that is not comparable to the phase studied in our approach.

Antiarrhythmic effect of acute and chronic CaM/CaMKII inhibition

We demonstrated with the *ex vivo* rabbit model that acute inhibition of CaM by W7 reduces arrhythmias, especially sustained VT/VF. The antiarrhythmic effect of W7 was previously shown in an *in vivo* rabbit model.³⁵ Additionally, we observed that spiral wave reentry arrhythmias in the presence of W7 were self-terminated. In a previous study, we demonstrated that early termination of spiral wave reentry could be explained by destabilization of the spiral waves due to increased intercellular coupling triggered by application of the gap junction opener Rotigaptide.²¹ Here, we show that CaM inhibition results in increased coupling between cultured NRCMs and increased junctional levels of Cx43 in dog cardiomyocytes and rabbits. In addition, our perfused rabbit hearts showed an increase in space constant indicative of increased coupling but also an increase in length of the functional block line. Both factors likely contribute to the destabilization of the spiral waves and therefore to its self-termination.

Previously, we showed that enhancement of gap junction conductance caused a large reduction in the incidence of sustained VT by 58%, with an increase in CV of only 10%.²¹ Additionally, we also showed that reduced (and heterogeneous) expression of Cx43 increases the susceptibility to cardiac arrhythmias.⁴ Here, acute CaM inhibition reduced sustained VT by 60%, while increasing CV by 6-9%. Therefore, the reduction in

sustained VT observed in acute CaM inhibition could be explained by the increase in CV due to the increased gap-junctional Cx43, although a contribution of additional factors that might have been of additive influence for the observed anti-arrhythmic effect of W7 should not be excluded given the rather small effect on CV. The antiarrhythmic effect in this special preparation was however not robust: a number of non-sustained VT/VF remained.

We also investigated potential anti-arrhythmic effects of chronic CaMKII inhibition during pathological pressure overload by TAC surgery, as it has been shown that CaMKII activity is already increased after 1 week of TAC.³⁶ Many studies have demonstrated that acute inhibition of CaMKII through application of the pharmacological agent KN93 has antiarrhythmic effects in different animal models.^{5,37,38} Although CV and junctional levels of Cx43 were increased in AC3-I TAC hearts, against our expectations, chronic CaMKII inhibition did not reduce susceptibility to arrhythmias. We speculate that this discrepancy is due to the unattenuated presence of fibrosis, which is a major proarrhythmic substrate in diseased hearts. Besides fibrosis, mechanical remodeling due to increased LV wall stress and poor mechanical function may also contribute to the presence of arrhythmias.

Although in our previous studies on WT TAC hearts the arrhythmias were reentry-based,^{3,4} in AC3-I TAC mice we found no evidence of reentry-like activity. In fact, arrhythmias had a polymorphic nature suggesting focal-activity possibly starting from early afterdepolarizations.

Structural hypertrophy and fibrosis

TAC surgery induces an increase in HW/BW, dilatation, an increased wall thickness and a reduced fractional shortening (Supplemental Figure 3). In contrast to the effects observed with regard to intercellular coupling, this mechanical and structural remodeling after TAC was not prevented by chronic CaMKII inhibition (Supplemental Figure 3). In several studies, CaMKII has been reported as an important factor for the progression of cardiac hypertrophy and that CaM/CaMKII inhibition could rescue hearts from hypertrophy after 3-8 weeks of TAC.^{14,39,40} However, two recent independent studies using CaMKII knockout mice reported a similar level of hypertrophy compared to WT mice after 3 weeks of TAC.^{41,42} Nonetheless, these studies had opposite findings regarding fibrosis; Kreusser *et al.*⁴² showed preservation of fibrosis while Cheng *et al.*⁴¹ showed a substantial increase in fibrosis compared to WT. We found that fibrosis remained present in our CaMKII inhibition model of 16 weeks of TAC but did not compare hearts with CaMKII inhibition to WT controls. This paradox separating preservation of Cx43/Nav1.5 versus increased fibrosis is new and of great interest. The most striking finding is that CV was improved compared to WT hearts, even in the presence of fibrosis after TAC surgery. The QRS interval prolongation after TAC was also not prevented by CaMKII inhibition,

but this most likely can be explained by the increased cell size due to the observed hypertrophy, as was previously confirmed in a rabbit model.⁴³

Limitations

In our study, we investigated acute CaM/CaMKII inhibition and chronic CaMKII inhibition. CaM activates not only CaMKII but also several Ca^{2+} handling proteins like calcineurin. We have to pay attention to the fact that CaM inhibition and CaMKII inhibition might not be the same and, as discussed above, that the currently available antagonists are suboptimal. Despite these limitations, the results of acute CaM inhibition and chronic CaMKII inhibition are similar: both increased CV and also junctional Cx43 in the intercalated disk. These results suggest a common signal transduction pathway between CaM and CaMKII inhibition that could affect Cx43 and conduction properties.

We speculated about $\text{Na}_v1.5$ not contributing to the increased CV. However, this remark should be taken with caution since we only show results for total $\text{Na}_v1.5$ protein level. We attempted to evaluate the levels of $\text{Na}_v1.5$ in non-junctional and junctional fractions by Western blot, but unfortunately were not successful.

Conclusions

The inhibition of CaM/CaMKII accelerated CV by increasing the localization of Cx43 in the intercalated disk. Acceleration of CV resulted in the prevention of reentry-based arrhythmias. Our present study encourages the possibility that CaM and CaMKII are potential therapeutic targets to reduce arrhythmogenic susceptibility via enhancement of intercellular electrical coupling.

FUNDING SOURCES

We acknowledge the support from the Netherlands CardioVascular Research Initiative: the Dutch Heart Foundation, Dutch Federation of University Medical Centres, the Netherlands Organisation for Health Research and Development and the Royal Netherlands Academy of Sciences (CVON-PREDICT), Dutch Heart Foundation Grant 2009B072, Foundation LeDucq: The Alliance for CaMKII signaling in heart disease, Grant-in Aid for Scientific Research (C) 20590860 and Grant-in-Aid for Scientific Research (C) 26860215 from the Japanese Society for Promotion of Sciences, Grant-in-Aid for Scientific Research on Innovative Areas 22136010 from the Ministry of Education, Culture, Sports, Science and Technology, Japan. We also thank SENSIN Medical Research Foundation and the Japanese Society of Electrophysiology, National Institutes of Health (NIH) Grants R01-HL079031, R01-HL096652, R01-HL070250, and R01-HL071140 for their financial support.

REFERENCES

1. Fontes MS, van Veen TA, de Bakker JM, van Rijen HV. Functional consequences of abnormal Cx43 expression in the heart. *Biochim Biophys Acta*. 2012;1818:2020-2029
2. Jansen JA, Noorman M, Musa H, Stein M, de Jong S, van der Nagel R, Hund TJ, Mohler PJ, Vos MA, van Veen TA, de Bakker JM, Delmar M, van Rijen HV. Reduced heterogeneous expression of Cx43 results in decreased $\text{Na}_v1.5$ expression and reduced sodium current that accounts for arrhythmia vulnerability in conditional Cx43 knockout mice. *Heart Rhythm*. 2012;9:600-607
3. Boulaksil M, Winckels SK, Engelen MA, Stein M, van Veen TA, Jansen JA, Linnenbank AC, Bierhuizen MF, Groenewegen WA, van Oosterhout MF, Kirkels JH, de Jonge N, Varro A, Vos MA, de Bakker JM, van Rijen HV. Heterogeneous Connexin43 distribution in heart failure is associated with dispersed conduction and enhanced susceptibility to ventricular arrhythmias. *Eur J Heart Fail*. 2010;12:913-921
4. Jansen JA, van Veen TA, de Jong S, van der Nagel R, van Stuijvenberg L, Driessen H, Labzowski R, Oefner CM, Bosch AA, Nguyen TQ, Goldschmeding R, Vos MA, de Bakker JM, van Rijen HV. Reduced Cx43 expression triggers increased fibrosis due to enhanced fibroblast activity. *Circ Arrhythm Electrophysiol*. 2012;5:380-390
5. Anderson ME, Braun AP, Wu Y, Lu T, Wu Y, Schulman H, Sung RJ. KN-93, an inhibitor of multifunctional Ca^{2+} /calmodulin-dependent protein kinase, decreases early afterdepolarizations in rabbit heart. *J Pharmacol Exp Ther*. 1998;287:996-1006
6. Bourgonje VJ, Schoenmakers M, Beekman JD, van der Nagel R, Houtman MJ, Miedema LF, Antoons G, Sipido K, de Windt LJ, van Veen TA, Vos MA. Relevance of calmodulin/CaMKII activation for arrhythmogenesis in the AV block dog. *Heart Rhythm*. 2012;9:1875-1883
7. Khoo MS, Li J, Singh MV, Yang Y, Kannankeril P, Wu Y, Grueter CE, Guan X, Oddis CV, Zhang R, Mendes L, Ni G, Madu EC, Yang J, Bass M, Gomez RJ, Wadzinski BE, Olson EN, Colbran RJ, Anderson ME. Death, cardiac dysfunction, and arrhythmias are increased by calmodulin kinase II in calcineurin cardiomyopathy. *Circulation*. 2006;114:1352-1359
8. Maier LS, Zhang T, Chen L, DeSantiago J, Brown JH, Bers DM. Transgenic CaMKII δ C overexpression uniquely alters cardiac myocyte Ca^{2+} handling: Reduced SR Ca^{2+} load and activated SR Ca^{2+} release. *Circ Res*. 2003;92:904-911
9. Wagner S, Dybkova N, Rasenack EC, Jacobshagen C, Fabritz L, Kirchhof P, Maier SK, Zhang T, Hasenfuss G, Brown JH, Bers DM, Maier LS. Ca^{2+} /calmodulin-dependent protein kinase II regulates cardiac Na^+ channels. *J Clin Invest*. 2006;116:3127-3138
10. Wagner S, Hacker E, Grandi E, Weber SL, Dybkova N, Sossalla S, Sowa T, Fabritz L, Kirchhof P, Bers DM, Maier LS. Ca/calmodulin kinase II differentially modulates potassium currents. *Circ Arrhythm Electrophysiol*. 2009;2:285-294
11. Zhang T, Johnson EN, Gu Y, Morissette MR, Sah VP, Gigena MS, Belke DD, Dillmann WH, Rogers TB, Schulman H, Ross J, Jr., Brown JH. The cardiac-specific nuclear delta(B) isoform of Ca^{2+} /calmodulin-dependent protein kinase II induces hypertrophy and dilated cardiomyopathy associated with increased protein phosphatase 2A activity. *J Biol Chem*. 2002;277:1261-1267
12. Hoch B, Meyer R, Hetzer R, Krause EG, Karczewski P. Identification and expression of delta-isoforms of the multifunctional Ca^{2+} /calmodulin-dependent protein kinase in failing and nonfailing human myocardium. *Circ Res*. 1999;84:713-721
13. Kirchhefer U, Schmitz W, Scholz H, Neumann J. Activity of cAMP-dependent protein kinase and Ca^{2+} /calmodulin-dependent protein kinase in failing and nonfailing human hearts. *Cardiovasc Res*. 1999;42:254-261
14. Ling H, Zhang T, Pereira L, Means CK, Cheng H, Gu Y, Dalton ND, Peterson KL, Chen J,

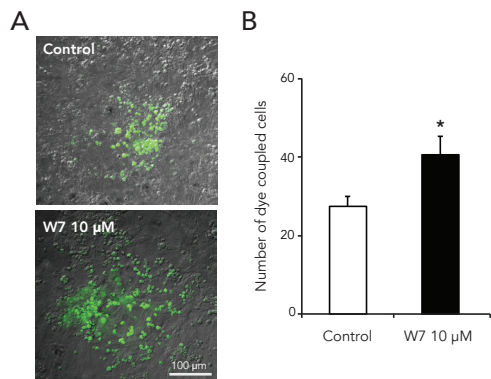
- Bers D, Brown JH. Requirement for Ca^{2+} /calmodulin-dependent kinase II in the transition from pressure overload-induced cardiac hypertrophy to heart failure in mice. *J Clin Invest*. 2009;119:1230-1240
15. Xu Q, Kopp RF, Chen Y, Yang JJ, Roe MW, Veenstra RD. Gating of connexin 43 gap junctions by a cytoplasmic loop calmodulin binding domain. *Am J Physiol Cell Physiol*. 2012;302:C1548-1556
 16. Huang RY, Laing JG, Kanter EM, Berthoud VM, Bao M, Rohrs HW, Townsend RR, Yamada KA. Identification of CaMKII phosphorylation sites in connexin43 by high-resolution mass spectrometry. *J Proteome Res*. 2011;10:1098-1109
 17. Toyama J, Sugiura H, Kamiya K, Kodama I, Terasawa M, Hidaka H. Ca^{2+} -calmodulin mediated modulation of the electrical coupling of ventricular myocytes isolated from guinea pig heart. *J Mol Cell Cardiol*. 1994;26:1007-1015
 18. Takanari H, Honjo H, Takemoto Y, Suzuki T, Kato S, Harada M, Okuno Y, Ashihara T, Opthof T, Sakuma I, Kamiya K, Kodama I. Bepridil facilitates early termination of spiral-wave reentry in two-dimensional cardiac muscle through an increase of intercellular electrical coupling. *J Pharmacol Sci*. 2011;115:15-26
 19. Ishiguro YS, Honjo H, Opthof T, Okuno Y, Nakagawa H, Yamazaki M, Harada M, Takanari H, Suzuki T, Morishima M, Sakuma I, Kamiya K, Kodama I. Early termination of spiral wave reentry by combined blockade of Na^{+} and L-type Ca^{2+} currents in a perfused two-dimensional epicardial layer of rabbit ventricular myocardium. *Heart Rhythm*. 2009;6:684-692
 20. Akar FG, Roth BJ, Rosenbaum DS. Optical measurement of cell-to-cell coupling in intact heart using subthreshold electrical stimulation. *Am J Physiol Heart Circ Physiol*. 2001;281:H533-542
 21. Takemoto Y, Takanari H, Honjo H, Ueda N, Harada M, Kato S, Yamazaki M, Sakuma I, Opthof T, Kodama I, Kamiya K. Inhibition of intercellular coupling stabilizes spiral-wave reentry, whereas enhancement of the coupling destabilizes the reentry in favor of early termination. *Am J Physiol Heart Circ Physiol*. 2012;303:H578-586
 22. Bruce AF, Rothery S, Dupont E, Severs NJ. Gap junction remodelling in human heart failure is associated with increased interaction of connexin43 with ZO-1. *Cardiovasc Res*. 2008;77:757-765
 23. Kinugawa K, Shimizu T, Yao A, Kohmoto O, Serizawa T, Takahashi T. Transcriptional regulation of inducible nitric oxide synthase in cultured neonatal rat cardiac myocytes. *Circ Res*. 1997;81:911-921
 24. Zhang R, Khoo MS, Wu Y, Yang Y, Grueter CE, Ni G, Price EE, Jr, Thiel W, Guatimosim S, Song LS, Madu EC, Shah AN, Vishnivetskaya TA, Atkinson JB, Gurevich VV, Salama G, Lederer WJ, Colbran RJ, Anderson ME. Calmodulin kinase II inhibition protects against structural heart disease. *Nat Med*. 2005;11:409-417
 25. Scholten A, Preisinger C, Corradini E, Bourgonje VJ, Hennrich ML, van Veen TA, Swaminathan PD, Joiner ML, Vos MA, Anderson ME, Heck AJ. Phosphoproteomics study based on in vivo inhibition reveals sites of calmodulin-dependent protein kinase II regulation in the heart. *J Am Heart Assoc*. 2013;2:e000318
 26. van Veen TA, van Rijen HV, Wiegerinck RF, Opthof T, Colbert MC, Clement S, de Bakker JM, Jongsma HJ. Remodeling of gap junctions in mouse hearts hypertrophied by forced retinoic acid signaling. *J Mol Cell Cardiol*. 2002;34:1411-1423
 27. Sweat F, Puchter H, Rosenthal SI. Sirius Red F3Ba as a stain for connective tissue. *Arch Pathol*. 1964;1964:69-72
 28. Ledoux J, Chartier D, Leblanc N. Inhibitors of calmodulin-dependent protein kinase are

- nonspecific blockers of voltage-dependent K⁺ channels in vascular myocytes. *J Pharmacol Exp Ther.* 1999;290:1165-1174
29. Rezazadeh S, Claydon TW, Fedida D. KN-93 (2-[N-(2-hydroxyethyl)]-N-(4-methoxybenzenesulfonyl)]amino-N-(4-chlorocinnamyl)-N-methylbenzylamine), a calcium/calmodulin-dependent protein kinase II inhibitor, is a direct extracellular blocker of voltage-gated potassium channels. *J Pharmacol Exp Ther.* 2006;317:292-299
 30. Axelsen LN, Calloe K, Holstein-Rathlou NH, Nielsen MS. Managing the complexity of communication: Regulation of gap junctions by post-translational modification. *Front Pharmacol.* 2013;4:130
 31. Rokita AG, Anderson ME. New therapeutic targets in cardiology: Arrhythmias and Ca²⁺/calmodulin-dependent kinase II (CaMKII). *Circulation.* 2012;126:2125-2139
 32. Ashpole NM, Herren AW, Ginsburg KS, Brogan JD, Johnson DE, Cummins TR, Bers DM, Hudmon A. Ca²⁺/calmodulin-dependent protein kinase II (CaMKII) regulates cardiac sodium channel Nav1.5 gating by multiple phosphorylation sites. *J Biol Chem.* 2012;287:19856-19869
 33. Yao L, Fan P, Jiang Z, Viatchenko-Karpinski S, Wu Y, Kornyevev D, Hirakawa R, Budas GR, Rajamani S, Shryock JC, Belardinelli L. Nav1.5-dependent persistent Na⁺ influx activates CaMKII in rat ventricular myocytes and N_{132S} mice. *Am J Physiol Cell Physiol.* 2011;301:C577-586
 34. Toischer K, Hartmann N, Wagner S, Fischer TH, Herting J, Danner BC, Sag CM, Hund TJ, Mohler PJ, Belardinelli L, Hasenfuss G, Maier LS, Sossalla S. Role of late sodium current as a potential arrhythmogenic mechanism in the progression of pressure-induced heart disease. *J Mol Cell Cardiol.* 2013;61:111-122
 35. Mazur A, Roden DM, Anderson ME. Systemic administration of calmodulin antagonist W-7 or protein kinase a inhibitor H-8 prevents torsade de pointes in rabbits. *Circulation.* 1999;100:2437-2442
 36. Colomer JM, Mao L, Rockman HA, Means AR. Pressure overload selectively up-regulates Ca²⁺/calmodulin-dependent protein kinase II in vivo. *Mol Endocrinol.* 2003;17:183-192
 37. Bell JR, Curl CL, Ip WT, Delbridge LM. Ca²⁺/calmodulin-dependent protein kinase inhibition suppresses post-ischemic arrhythmogenesis and mediates sinus bradycardic recovery in reperfusion. *Int J Cardiol.* 2012;159:112-118
 38. Liu N, Ruan Y, Denegri M, Bachetti T, Li Y, Colombi B, Napolitano C, Coetzee WA, Priori SG. Calmodulin kinase II inhibition prevents arrhythmias in RyR2(R4496C+/-) mice with catecholaminergic polymorphic ventricular tachycardia. *J Mol Cell Cardiol.* 2011;50:214-222
 39. Lu YM, Huang J, Shioda N, Fukunaga K, Shirasaki Y, Li XM, Han F. CaMKII δ mediates aberrant NCX1 expression and the imbalance of NCX1/SERCA in transverse aortic constriction-induced failing heart. *PLoS One.* 2011;6:e24724
 40. Backs J, Backs T, Neef S, Kreusser MM, Lehmann LH, Patrick DM, Grueter CE, Qi X, Richardson JA, Hill JA, Katus HA, Bassel-Duby R, Maier LS, Olson EN. The delta isoform of CaM kinase II is required for pathological cardiac hypertrophy and remodeling after pressure overload. *Proc Natl Acad Sci U S A.* 2009;106:2342-2347
 41. Cheng J, Xu L, Lai D, Guilbert A, Lim HJ, Keskanokwong T, Wang Y. CaMKII inhibition in heart failure, beneficial, harmful, or both. *Am J Physiol Heart Circ Physiol.* 2012;302:H1454-1465
 42. Kreusser MM, Lehmann LH, Keranov S, Hoting MO, Oehl U, Kohlhaas M, Reil JC, Neumann K, Schneider MD, Hill JA, Dobrev D, Maack C, Maier LS, Grone HJ, Katus HA, Olson EN, Backs J. Cardiac CaM kinase II genes delta and gamma contribute to adverse remodeling but

- redundantly inhibit calcineurin-induced myocardial hypertrophy. *Circulation*. 2014;130:1262-1273
43. Wiegerinck RF, Verkerk AO, Belterman CN, van Veen TA, Baartscheer A, Opthof T, Wilders R, de Bakker JM, Coronel R. Larger cell size in rabbits with heart failure increases myocardial conduction velocity and QRS duration. *Circulation*. 2006;113:806-813

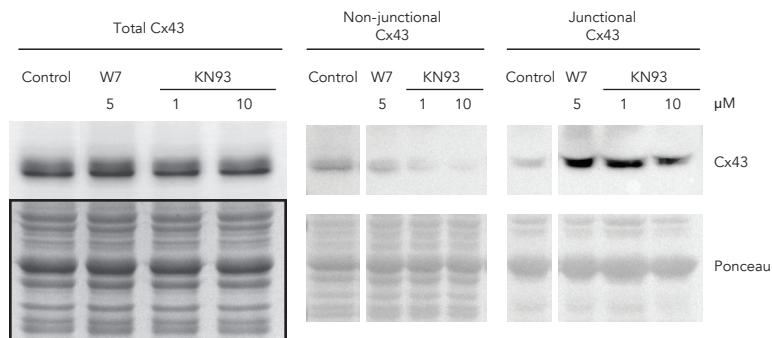
SUPPLEMENTAL MATERIAL

Supplemental Figures



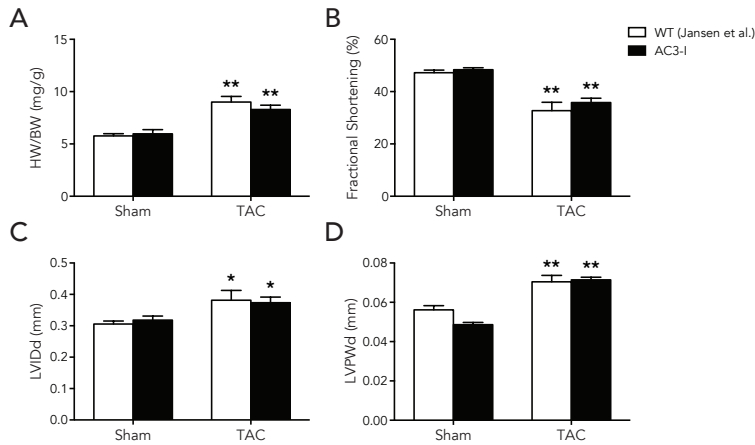
Supplemental Figure 1. Dye transfer assay using a gap-junctional permeable dye, Lucifer yellow.

A: Representative microscopic views of cultured neonatal rat cardiomyocytes 15 minutes after dye injection in normal condition (**top**) or after W7 (10 μ M) for 24 hours (**bottom**). Scale bar represents 100 μ m. **B:** Summarized data of the number of dye-coupled cells ($n=5$). Open column is control and closed is W7. * $p<0.05$ vs. control.



Supplemental Figure 2. Connexin43 (Cx43) subcellular distribution after acute CaM/CaMKII inhibition in cultured adult dog cardiomyocytes in the presence of CaM inhibitor W7 (5 μ M) or CaMKII inhibitor KN93 (1 or 10 μ M).

Western blots of Cx43 in total lysate (**left**) and non-junctional (**middle**) or junctional (**right**) fractions are shown with their respective ponceau staining below. Non-junctional and junctional samples (including their respective controls) were all loaded on the same membrane, but were not adjoining (indicated by white lines in between). Please note an increase in junctional Cx43 protein expression after treatment.

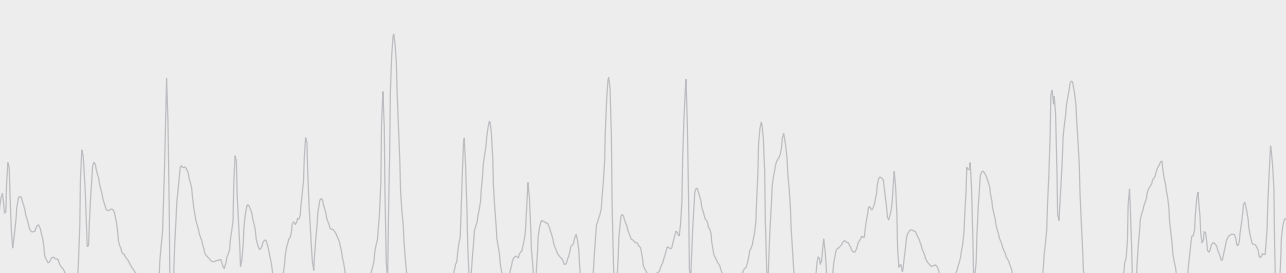




Supplemental Figure 3. Tissue and echocardiographic parameters of sham and TAC AC3-I mice compared with historical data of sham and TAC WT mice¹.

A-D: Heart weight to body weight ratio (HW/BW); fractional shortening, diastolic left ventricular internal diameter (LVIDd) and diastolic left ventricular posterior wall thickness (LVPWd), respectively. Black bars refer to AC3-I mice and white bars to WT mice. * $p < 0.05$, ** $p < 0.01$ vs. respective sham.

References

1. Jansen JA, van Veen TA, de Jong S, van der Nagel R, van Stuijvenberg L, Driessen H, Labzowski R, Oefner CM, Bosch AA, Nguyen TQ, Goldschmeding R, Vos MA, de Bakker JM, van Rijen HV. Reduced Cx43 expression triggers increased fibrosis due to enhanced fibroblast activity. *Circ Arrhythm Electrophysiol.* 2012;5:380-390




Magda S.C. Fontes¹, Antonia J.A. Raaijmakers¹, Tessa van Doorn¹, Bart Kok¹, Sylvia Nieuwenhuis¹, Roel van der Nagel¹, Marc A. Vos¹, Teun P. de Boer¹, Harold V.M. van Rijen¹, Marti F.A. Bierhuizen¹

¹ *Department of Medical Physiology, University Medical Center, Utrecht, The Netherlands*

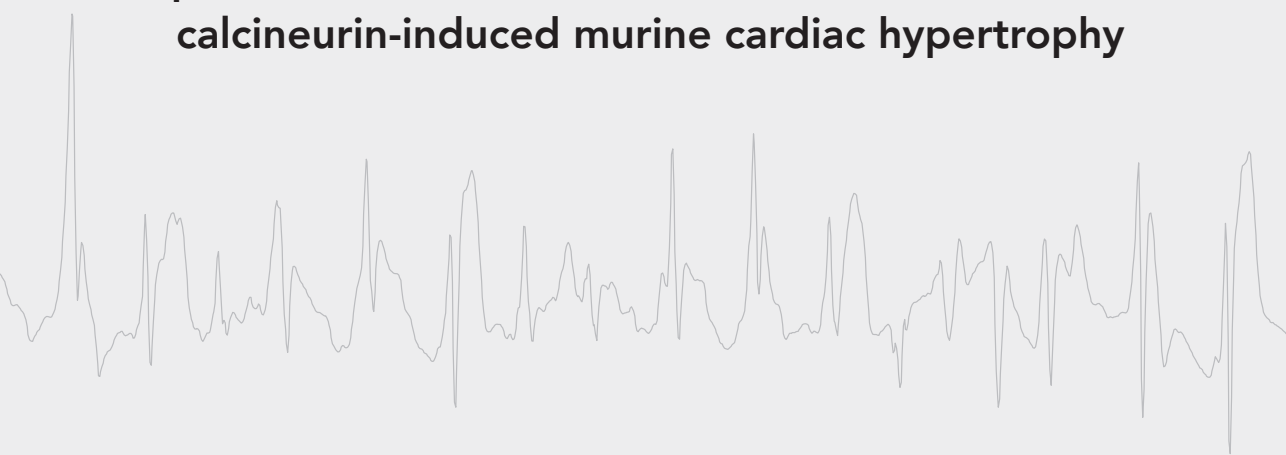





Chapter 5



**Changes in Cx43 and Na_v1.5 expression
precede the occurrence of substantial fibrosis in
calcineurin-induced murine cardiac hypertrophy**



PLoS One 2014; 9(1): e87226



ABSTRACT

In mice, the calcium-dependent phosphatase calcineurin A (CnA) induces a transcriptional pathway leading to pathological cardiac hypertrophy. Interestingly, induction of CnA has been frequently noticed in human hypertrophic and failing hearts. Independently, the arrhythmia vulnerability of such hearts has been regularly associated with remodeling of parameters determining electrical conduction (expression level of connexin43 (Cx43) and $\text{Na}_v1.5$, connective tissue architecture), for which the precise molecular basis and sequence of events is still unknown. Recently, we observed reduced Cx43 and $\text{Na}_v1.5$ expression in 4-week old mouse hearts, overexpressing a constitutively active form of CnA (MHC-CnA model), but the order of events is still unknown. Therefore, three key parameters of conduction (Cx43, $\text{Na}_v1.5$ and connective tissue expression) were characterized in MHC-CnA ventricles versus wild-type (WT) during postnatal development on a weekly basis.

At postnatal week 1, CnA overexpression induced cardiac hypertrophy in MHC-CnA. Moreover, protein and RNA levels of both Cx43 and $\text{Na}_v1.5$ were reduced by at least 50% as compared to WT. Cx43 immunoreactive signal was reduced at week 2 in MHC-CnA. At postnatal week 3, Cx43 was less phosphorylated and RNA level of Cx43 normalized to WT values, although the protein level was still reduced. Additionally, MHC-CnA hearts displayed substantial fibrosis relative to WT, which was accompanied by increased RNA levels for genes previously associated with fibrosis such as *Col1a1*, *Col1a2*, *Col3a1*, *Tgfb1*, *Ctgf*, *Timp1* and microRNA miR-21.

In MHC-CnA, reduction in Cx43 and $\text{Na}_v1.5$ expression thus coincided with overexpression of CnA and hypertrophy development and preceded significant presence of fibrosis. At postnatal week 4 the alterations in conduction parameters observed in the MHC-CnA model lead to abnormal conduction and arrhythmias, similar to those observed in cardiac remodeling in heart failure patients. The MHC-CnA model, therefore, provides for a unique model to resolve the molecular origin of conduction remodeling in detail.

INTRODUCTION

In human cardiac hypertrophy and heart failure, activation of the calcium-dependent phosphatase calcineurin A (CnA) has been frequently observed.^{1,2} In mice, increased intracellular calcium is known to activate CnA, which binds and dephosphorylates members of the nuclear factor of activated T cells (NFAT) transcription factor family. Subsequently, NFAT translocates from the cytoplasm to the nucleus where it potentiates the transcription of multiple hypertrophic marker genes. Transgenic mice overexpressing a constitutively active form of CnA specifically in cardiomyocytes (MHC-CnA) developed cardiac hypertrophy as early as 18 days postnatally, which to varying extent progressed to failure and sudden death.³

Electrical impulse conduction in the heart is mainly determined by three key parameters: electrical coupling between cardiomyocytes, excitability of individual cardiomyocytes and connective tissue architecture.⁴ These parameters of conduction are mainly mediated by connexin43 (Cx43) (major gap junction protein expressed in the heart), by the sodium channel Na_v1.5, and by the amount of collagen fibers, respectively. In arrhythmogenic remodeled hearts, abnormalities in any of these parameters of conduction have been frequently observed. Cx43 is usually downregulated, less phosphorylated and/or redistributed from the intercalated disks to the lateral sides of cardiomyocytes.^{5,6} Downregulation of Na_v1.5 at the protein or RNA level, reduction of peak and increased late sodium current have all been frequently reported, but in contrast also no change in *Scn5a* mRNA, the gene encoding Na_v1.5, has been observed.⁷⁻¹¹ Finally, collagen fiber deposition is usually increased (fibrosis).¹² The precise molecular basis for these changes and the order of events is still largely unknown.

Previously, we associated CnA activation with reduced expression of Cx43 and Na_v1.5 and with increased susceptibility for polymorphic ventricular tachyarrhythmias in 4-week old hypertrophic MHC-CnA hearts.¹³ This model therefore may serve as an accelerated model for the pathophysiological changes seen in heart failure patients.

In the current study, we have exploited the ventricles of this mouse model further to investigate calcineurin-dependent changes in three key conductional parameters (Cx43, Na_v1.5 and connective tissue architecture) during postnatal development, in order to visualize the order of adverse events ultimately leading to arrhythmias.

MATERIALS AND METHODS

Ethics statement

The experimental protocol was performed in accordance with the national guidelines and approved by the local Ethical Animal Experimental Committee (approval

number 2011.II.04.065) of the University of Utrecht (Utrecht, The Netherlands). All efforts were made to minimize suffering.

Animals

Male and female MHC-CnA mice, kindly provided by Dr. E. Olson (University of Texas Southwestern Medical Center, Dallas, TX, USA), were compared with age-matched WT littermates (both C57BL/6 background) at week 0, 1, 2, 3 and 4 after birth. Genotype of mice was determined by polymerase chain reaction (PCR) on DNA isolated from ear or tail biopsy specimens, as described before.¹³ Mice were housed under standard conditions with food and water given *ad libitum* and maintained on a 12 hours light/dark cycle with controlled temperature and humidity.

Heart sampling

Mice were sacrificed directly (0) or 1, 2, 3 and 4 weeks after birth and hearts were rapidly excised and rinsed in cold phosphate buffered saline (PBS). Subsequently the hearts were either immediately frozen in liquid nitrogen (for histology) or the atria were discarded and the ventricles frozen in liquid nitrogen (for real-time quantitative PCR (RT-qPCR) and immunoblotting). Only ventricles (both left and right) were analyzed in all experiments. Tissue samples were stored at -80°C until further use.

Immunohistochemistry and histology

For immunohistochemistry and collagen detection, cryosections of 4 different WT and MHC-CnA hearts (four-chamber view, 10 μm thickness) were prepared from different levels of the heart. Immunolabeling was performed as previously described,¹⁴ antibodies are listed below. After immunolabeling, sections were analyzed with a widefield microscope (Nikon Eclipse 80i; Nikon Europe B.V., Amstelveen, The Netherlands) with epifluorescence equipment. To evaluate the amount of collagen content, sections were fixed with 4% paraformaldehyde (in PBS, 30 minutes at room temperature), stained with Picrosirius Red as described previously¹⁵ and visualized with brightfield microscopy (Nikon Eclipse 80i). An investigator that was blinded to the groups took randomly chosen images from both ventricles of each heart with identical camera settings (gain and exposure time) using NIS Elements BR 3.0 software at 200x magnification. Widefield fluorescence images were deconvoluted using Huygens Essential 4.1 software (Scientific Volume Imaging B.V., Hilversum, The Netherlands) and transformed into 8-bit RGB (i.e. Red Green Blue) stack. Between 36 to 40 images per group (genotype/time point) were used for quantification analysis using ImageJ 1.44o software,¹⁶ in which only pixels positive for Cx43/Na ν 1.5/Fibrosis are taken into account by defining a mask with a fixed threshold value in the 255-leveled green channel. The amount of fibrosis was calculated

as a percentage of the area of each image (expressed in pixels).

Immunoblotting

Total cellular protein lysates were isolated from the ventricles and analyzed by immunoblotting as described before.^{14,17} Briefly, 20 µg of protein lysate (40 µg for Nav1.5 detection) was separated by 7% or 10% (w/v) sodium dodecyl sulfate-polyacrylamide gel electrophoresis (SDS-PAGE) and subsequently electro-transferred onto a nitrocellulose membrane (Bio-Rad Laboratories, Inc., Hercules, CA, USA). Equal loading of protein was assessed by Ponceau S staining. Proteins were detected after incubation with specific primary and secondary antibodies using a standard ECL procedure (GE Healthcare, Buckinghamshire, United Kingdom). Protein levels were expressed as the ratio of protein of interest/correspondent Ponceau S staining and both were quantified using Image Lab 3.0.1 software (Bio-Rad Laboratories, Inc.).

Antibodies

As primary antibodies, the following antibodies were used: mouse monoclonal antibodies against Cx43 (1:250, BD Transduction Laboratories by BD Biosciences, Breda, The Netherlands, immunoblotting), Cx43-NP (1:500, Invitrogen by Life Technologies Corp., Carlsbad, CA, USA) and N-cadherin (1:800, Sigma-Aldrich Corp., Saint Louis, MO, USA); rabbit polyclonal antibodies against Cx43 (1:250, Invitrogen by Life Technologies Corp., immunohistochemistry), Nav1.5 (1:200, Alomone Labs, Jerusalem, Israel, immunoblotting; 1:100, Sigma-Aldrich Corp., immunohistochemistry) and CnA (1:500, Merck Millipore, Billerica, Massachusetts, USA); goat polyclonal antibodies against connective tissue growth factor (CTGF) (1:200, a kind gift of Dr. R. Goldschmeding, Department of Pathology, University Medical Center Utrecht, The Netherlands). Alexa Fluor 594 and fluorescein isothiocyanate (FITC)-conjugated anti-mouse or anti-rabbit whole IgG (1:250, Jackson ImmunoResearch Europe Ltd., Newmarket, United Kingdom) were used as secondary antibodies for immunohistochemistry; horseradish peroxidase (HRP)-conjugated donkey anti-mouse, anti-rabbit (1:7000, Bio-Rad Laboratories, Inc.) or anti-goat (1:7000, Jackson ImmunoResearch Europe Ltd.) as secondary antibodies for immunoblotting.

Real-time quantitative PCR (RT-qPCR)

Total RNA was isolated from WT and MHC-CnA ventricles (n=4) with TRIzol reagent (Invitrogen by Life Technologies Corp.) and subsequently treated with DNase I (Promega, Madison, WI, USA) as previously described.¹⁸ One µg of RNA was converted to cDNA with Reverse Transcriptase (Invitrogen by Life Technologies Corp.) according to the manufacturer's protocol and diluted 10-fold prior to PCR amplification. RT-qPCR

was performed for each gene in a MyiQ2 Real-Time PCR Detection System (Bio-Rad Laboratories, Inc.) using Applied Biosystems TaqMan Gene Expression Assays (for specifics see supplementary Table S1) (Applied Biosystems by Life Technologies Corp.).

For microRNAs (miRNAs) a similar approach was performed as described above for RNA isolation and treatment. TaqMan miRNA Reverse Transcriptase Kit (Applied Biosystems by Life Technologies Corp.) was used to synthesize cDNA from 10 ng of RNA according to the manufacturer's protocol and diluted 10-fold prior to PCR amplification. RT-qPCR amplification was performed using TaqMan miRNA-specific primers (for specifics see supplementary Table S1) (Applied Biosystems by Life Technologies Corp.).

Experiments were carried out in duplicate. Relative expression of MHC-CnA mRNA and miRNA levels was determined using the $2^{-\Delta\Delta C_T}$ method and normalized to WT expression levels, as previously described.¹⁹ Glyceraldehyde 3-phosphate dehydrogenase (*Gapdh*) and U6 snRNA (Applied Biosystems by Life Technologies Corp.) (for specifics see supplementary Table S1) were used as internal controls for mRNA and miRNA levels, respectively, since their levels did not differ between WT and MHC-CnA samples.

Statistical analysis

All results are presented as mean \pm standard error of the mean (SEM). Shapiro-Wilk test was used to check for normality of data. Differences among group averages were evaluated using unpaired Student's t-test (RT-qPCR), confidence interval of the ratio²⁰ (immunoblotting and immunohistochemistry) or two-way ANOVA followed by Tukey-HSD's *post-hoc* test for multiple comparisons (hypertrophy and histology). Differences were considered statistically significant if $p < 0.05$. Data were analyzed using R version 2.15.1.²¹

RESULTS

In the present study the development of both structural and conductional remodeling was investigated in MHC-CnA ventricles at weeks 0, 1, 2, 3, and 4 after birth. Transgenic overexpression of CnA, lacking functional and auto-inhibitory domains (~43kDa) and driven by the α MHC promotor in this MHC-CnA mouse model, was slightly visible right after birth (week 0) and clearly detectable in the ventricles 1 week after birth and persisted in the following weeks (Figure 1A). In the blot of Figure 1A no bands are visible in WT ventricles, since endogenous CnA is only detectable at a higher molecular mass (~58kDa) (supplementary Figure S1). Hypertrophy, assessed by heart weight/body weight (HW/BW) ratio, was present at week 1 in MHC-CnA hearts (1.5-fold increase compared to WT; $p < 0.001$) and increased in the following weeks as shown in Figure 1B.

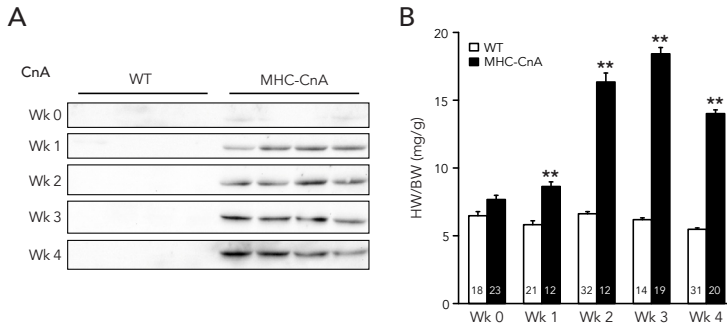


Figure 1. Expression of constitutively active CnA and hypertrophy in WT and MHC-CnA hearts.

A: Protein lysates from four different WT and MHC-CnA ventricles were analyzed for expression of constitutively active CnA (~43kDa) by immunoblotting at weeks (Wk) 0, 1, 2, 3 and 4. **B:** Hypertrophy is indicated by heart weight/body weight (HW/BW) ratio. Number of mice per group is indicated in the bar graph. Values are mean \pm SEM; ** $p < 0.01$ compared to WT.

The slight decrease in HW/BW ratio from week 3 to 4 in MHC-CnA is explained by the smaller increase in HW as compared to BW (supplementary Figure S2).

The protein levels of the sodium channel $\text{Na}_v1.5$, that primarily mediates excitability in the heart, were assessed with immunoblotting (Figure 2A). At week 0 there was no statistically significant difference between WT and MHC-CnA protein expression in the ventricles. From week 1 until week 4 there was a reduction in $\text{Na}_v1.5$ protein level in MHC-CnA by more than 50% (58%, 79%, 74% and 75% relative to WT, respectively), although this reduction was only significant from week 2 to 4 ($p < 0.05$; Figure 2A and B). The protein levels of $\text{Na}_v1.5$ were also assessed with immunohistochemistry (Figure 2C). In MHC-CnA, $\text{Na}_v1.5$ labeling intensity was reduced by 29-43% from week 1 to 4 relative to WT ($p < 0.05$; Figure 2C and D), correlating with the reduction detected by immunoblotting (Figure 2A and B). To determine if the reduction in $\text{Na}_v1.5$ protein expression was accompanied by a reduction in RNA levels, RT-qPCR was performed (Figure 2E). RNA expression for *Scn5a*, the gene encoding $\text{Na}_v1.5$, revealed a trend towards reduced levels in MHC-CnA already at week 0 (by 34%; $p = 0.052$). However, the reduction in RNA expression was only significant from week 1 until week 4 (reduction by 82%, 89%, 76% and 55% relative to WT, respectively; Figure 2E).

The gap junction protein Cx43, primarily mediating electrical coupling in the heart, was also investigated at the different time points (Figure 3A). The analysis of total Cx43 protein levels revealed no difference between WT and MHC-CnA ventricles right after birth (week 0). From week 1 until week 4 there was a reduction in total Cx43 protein expression (69%, 64%, 65% and 78% relative to WT, respectively; Figure 3A and B). Upon immunoblotting, different Cx43 isoforms can be distinguished on the basis of their phosphorylation status. In Figure 3A, P0 is referred to as the least phosphorylated and

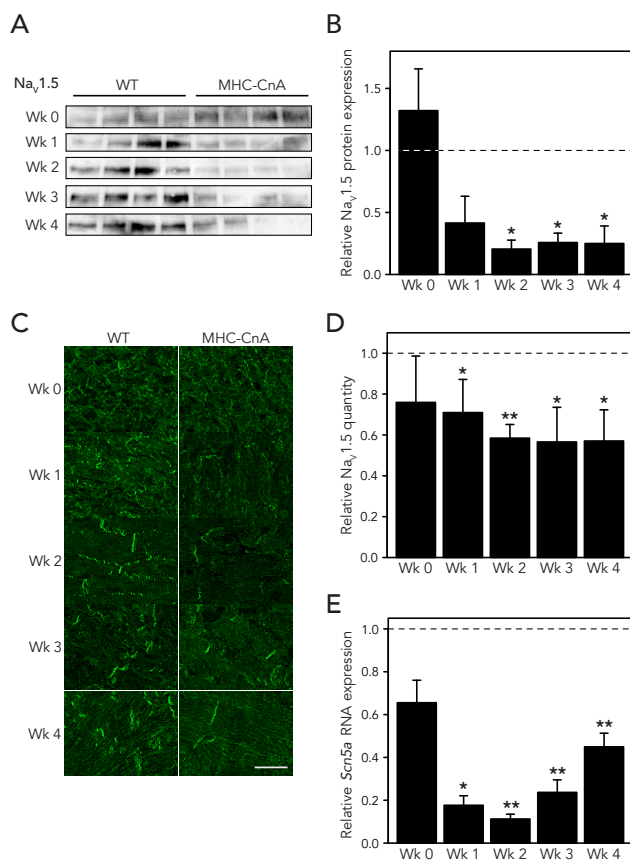


Figure 2. Sodium channel Nav1.5 expression in WT and MHC-CnA ventricles.

A: Protein lysates from four different WT and MHC-CnA ventricles were analyzed for Nav1.5 expression by immunoblotting at weeks (Wk) 0, 1, 2, 3 and 4. **B:** Quantification of the blots (ratio of Protein/Ponceau) represented in **A**. **C:** Representative images from WT and MHC-CnA ventricles immunolabeled for Nav1.5. Scale bar represents 25 μ m. **D:** Quantification of Nav1.5 labeling intensity exemplified in **C**. **E:** Scn5a, the gene encoding Nav1.5, was assessed by TaqMan RT-qPCR. MHC-CnA values (**B**, **D** and **E**) are relative to WT (set to 1). Values are mean \pm SEM; * p <0.05, ** p <0.01 compared to WT.

P2 as the most phosphorylated isoform of Cx43. Moreover, from these blots it appeared that the Cx43 P0 isoform was relatively increased in some of the weeks relative to the other isoforms in MHC-CnA, suggesting reduced phosphorylation of Cx43. Therefore, we investigated the phosphorylation status of Cx43 using Cx43-NP antibody that recognizes the Cx43 P0 isoform specifically when serine residue 368 (Ser368) is non-phosphorylated (Figure 3C). Using Cx43-NP antibody, an increase in the Cx43 P0 isoform was detected at weeks 3 and 4 in MHC-CnA (by 5.7- and 3.6-fold, respectively). Week 1 also presented higher non-phosphorylated levels (by 3.2-fold), although not significant, possibly due to the unexpected increase in one of the WT samples (Figure 3C and D).

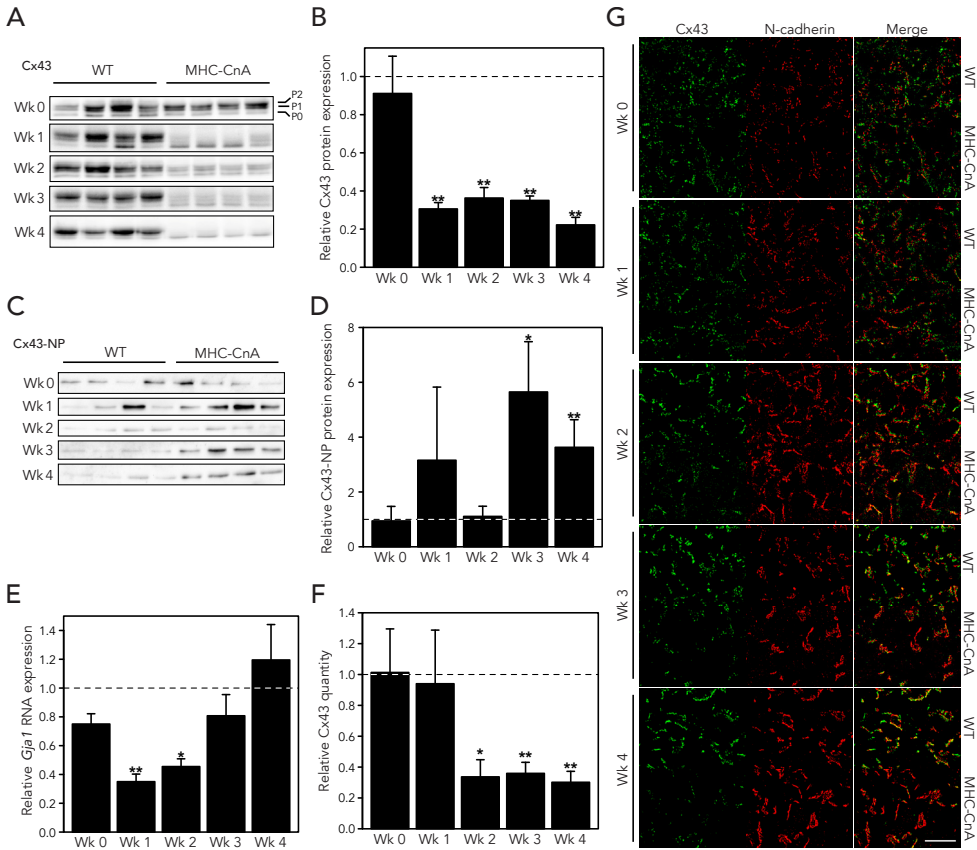


Figure 3. Gap junction Cx43 expression in WT and MHC-CnA ventricles.

Protein lysates from four different WT and MHC-CnA ventricles were analyzed for Cx43 (**A**) and Cx43-NP (**C**) expression by immunoblotting at weeks (Wk) 0, 1, 2, 3 and 4. In **A** P0, P1 and P2 isoforms are indicated, where P2 corresponds to the most phosphorylated isoform and P0 to the least phosphorylated isoform of Cx43. **B**: Quantification of total Cx43 (P0+P1+P2) of the blots (ratio of Protein/Ponceau) represented in **A**. In **C** Cx43-NP antibody recognizes the P0 isoform of Cx43 specifically when Ser368 is non-phosphorylated. **D**: Quantification of the blots (ratio of Protein/Ponceau) represented in **C**. **E**: Gja1, the gene encoding Cx43, was assessed by TaqMan RT-qPCR. **F**: Quantification of Cx43 labeling intensity exemplified in **G**. **G**: Representative images from WT and MHC-CnA ventricles immunolabeled for Cx43 (green) and N-cadherin (red), a marker for intercalated disk. Scale bar represents 25 μ m. MHC-CnA values (**B**, **D**, **E** and **F**) are relative to WT (set to 1). Values are mean \pm SEM; * $p < 0.05$, ** $p < 0.01$ compared to WT.

Additionally, another antibody that also recognizes the Cx43 P0 isoform (Cx43-CT1 antibody) showed in the same way an increase in P0 isoform at weeks 3 and 4, although week 3 was not significant (supplementary Figure S3). To determine if Cx43 RNA levels accompanied the alterations in protein expression, RT-qPCR was performed (Figure 3E). RNA expression for Gja1, the gene encoding Cx43, revealed reduced levels in MHC-CnA ventricles (by 25%) at week 0 compared to WT, though not significant ($p=0.054$).

A significant reduction in RNA levels of *Gja1* was detected at weeks 1 and 2 (by 65% and 55%, respectively), increasing back to WT values in the following weeks (Figure 3E). Figure 3G shows typical examples of Cx43 and N-cadherin immunolabeled sections in WT and MHC-CnA ventricles at weeks 0, 1, 2, 3 and 4. From week 0 to 4 the hearts are developing and the cardiomyocytes transiting from a fusiform-like to a more elongated and mature ("brick stone")-like appearance, as evidenced by the development and formation of the intercalated disks detected with N-cadherin (and Cx43 in the case of the WT hearts). In MHC-CnA, Cx43 labeling intensity was reduced to 30-36% of WT in weeks 2, 3 and 4 ($p < 0.05$; Figure 3F and G), but not in weeks 0 and 1.

Finally, the amount of ventricular fibrosis, primarily determining tissue architecture in the heart, was also investigated (Figure 4A). Picrosirius Red staining for fibrosis revealed a continuous increase in MHC-CnA ventricles from week 2 until week 4. This increase was only significantly different from WT in weeks 3 and 4 ($1.8 \pm 0.3\%$ versus $0.7 \pm 0.1\%$ and $2.3 \pm 0.4\%$ versus $0.8 \pm 0.2\%$, respectively; $p < 0.01$; Figure 4A and B). Interstitial fibrosis found in MHC-CnA ventricles at weeks 3 and 4 was not identified in specific regions of the heart, thus no correlation exists between local fibrosis and reduced Cx43/Na_v1.5 expression. In line with the enhanced interstitial fibrosis in MHC-CnA hearts, development of mRNA expression levels (from week 0 to 4) of several genes involved in connective tissue formation and degradation were analyzed with TaqMan RT-qPCR assays (Figure 4C). Collagen (*Col1a1*, *Col1a2*, *Col3a1*) RNA levels were similar between WT and MHC-CnA ventricles from week 0 until week 2, whereas in weeks 3 and 4 RNA levels increased. Transforming growth factor beta1 (*Tgfb1*) RNA levels were similar between WT and MHC-CnA at weeks 0 and 1, decreased by 30% in MHC-CnA at week 2 and increased by 1.4- and 1.6-fold, respectively, at weeks 3 and 4. *Ctgf* RNA level was increased in MHC-CnA at week 0 (although not significantly), significantly reduced to 44% of WT at week 1, similar to WT at week 2 and significantly increased by 4.6- and 2.8-fold, respectively, at weeks 3 and 4. Similarly, tissue inhibitor of metalloproteinase 1 (*Timp1*) RNA level in MHC-CnA was not different from WT at week 0, significantly reduced at week 1 to 38% of WT, similar to WT at week 2, and significantly increased by 17.4- and 8.8-fold, respectively, at weeks 3 and 4 (Figure 4C). Interestingly, matrix metalloproteinase 2 (*Mmp2*) and matrix metalloproteinase 9 (*Mmp9*) were not different from WT values at week 4 (data not shown). To determine whether the observed increase of *Ctgf* RNA was correlated with the corresponding alteration at the protein level, immunoblotting was performed (Figure 4D). Quantification of CTGF protein expression revealed similar levels in MHC-CnA compared to WT ventricles at weeks 0 and 2, at week 1 a decrease of 70% (but not significant) and at weeks 3 and 4 a significant 10.8- and 54.3-fold increase, respectively (Figure 4E). Figure 4D shows that WT samples at week 1 had higher CTGF expression than in other weeks probably explaining the reduction observed in MHC-CnA at week 1 (Figure 4C and E). In weeks 3 and 4 CTGF protein and RNA levels correlated well: both were increased. Since four miRNAs were previously implicated in the regulation

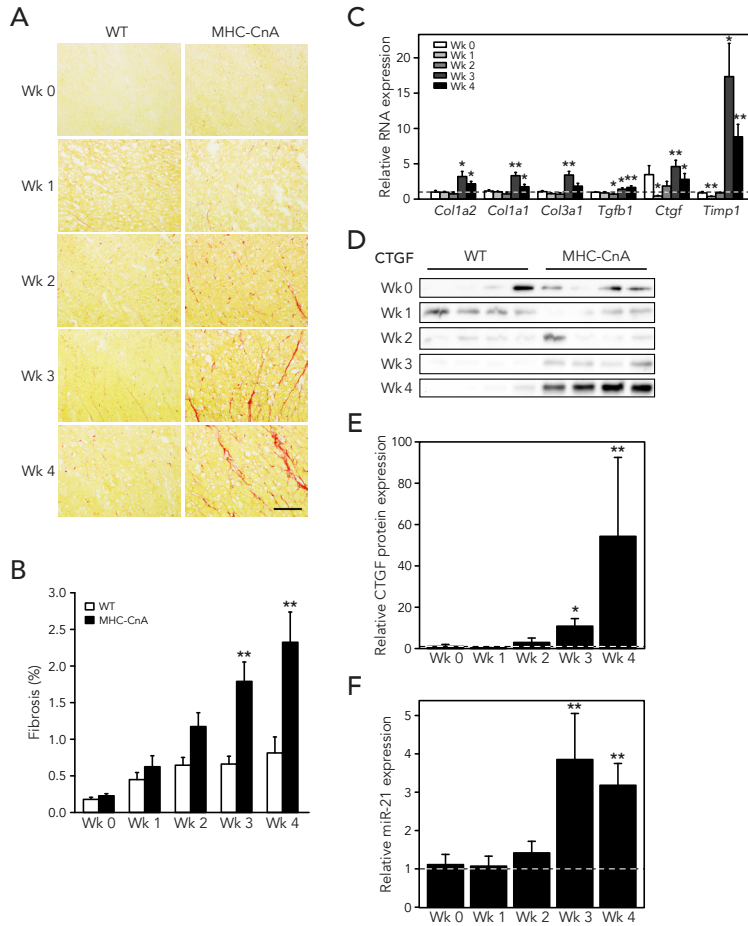


Figure 4. Fibrosis in WT and MHC-CnA ventricles.

A: Picrosirius Red representative images of WT and MHC-CnA ventricles from week (Wk) 0 to 4. Scale bar represents 100 μ m. **B:** Quantification of Picrosirius Red collagen content. **C:** Col1a1, Col1a2, Col3a1, Tgfb1, Ctgf, and Timp1 RNA expression assessed by TaqMan RT-qPCR. **D:** Protein lysates from four different WT and MHC-CnA ventricles were analyzed for CTGF expression by immunoblotting. **E:** Quantification of the blots (ratio of Protein/Ponceau) represented in **D**. MiR-21 miRNA expression assessed by TaqMan RT-qPCR. MHC-CnA values (**C**, **E** and **F**) are relative to WT (set to 1). Values are mean \pm SEM; * p <0.05, ** p <0.01 compared to WT.

of fibrosis, namely miR-21, miR29b, miR-30c and miR-133a,¹² their expression level was also determined. Since only miR-21 was significantly upregulated in MHC-CnA ventricles at week 4 (data not shown), we further investigated miR-21 in the other weeks. MiR-21 in MHC-CnA was similar to WT from week 0 until week 2 and was significantly increased at weeks 3 and 4 (3.9- and 3.2-fold, respectively; p <0.01; Figure 4F), which corresponded to the increase observed in fibrosis (Figure 4A and B).

DISCUSSION

In this study we targeted the development of conductional remodeling in calcineurin-induced cardiac hypertrophy and newly demonstrated that (in MHC-CnA, Figure 5): 1) overexpression of continuously active CnA and cardiac hypertrophy already appeared at postnatal week 1; 2) the appearance of cardiac hypertrophy coincided with reductions in both Nav1.5 and Cx43 protein/RNA expression; 3) the initial reduction in Cx43 RNA (but not protein) expression normalized at postnatal weeks 3 and 4, paralleled by a decrease in Cx43 phosphorylation; 4) fibrosis occurred later than hypertrophy and was significantly detectable from postnatal week 3 onwards, which was further substantiated by increased RNA levels for *Col1a1*, *Col1a2*, *Col3a1*, *Tgfb1*, *Ctgf*, *Timp1* and microRNA miR-21. Overall, many aspects of the conductional remodeling observed in the MHC-CnA model resemble those that have been reported for human cardiac hypertrophy and failure.⁵⁻¹²

The observed association at postnatal weeks 1-4 between Nav1.5 protein/RNA downregulation and the expression of continuously active CnA supports our earlier suggestion for a (NFAT-mediated) transcriptional mechanism for its reduction.¹³ Although involvement of NFAT in *Scn5a* regulation has not yet been reported and NFAT is considered, often in collaboration with either GATA4 or MEF2, an enhancer of gene transcription it is possible that NFAT regulation of *Scn5a* depends on an as yet unidentified co-factor. One potential candidate for this role could be the T-box (Tbx) transcription factor Tbx5 as it was recently suggested to be involved in the regulation of *Scn5a* expression²² and its expression was found to be reduced in MHC-CnA hearts from week 1 onwards (results not shown). Interestingly, Guo *et al.*²³ reported a progressive decrease in sodium current density (I_{Na}) with age in MHC-CnA hearts, which was however not accompanied by a reduction in Nav1.5 protein expression. Although the reason for this discrepancy is not clear, the use of different mouse strains (ICR *versus* C57BL/6), the level of constitutively active CnA expression, the severity of hypertrophy, and the use of different experimental approaches all may have contributed.

As for Nav1.5, the observed reduction in Cx43 protein level correlated with downregulation of *Gja1* RNA expression at postnatal weeks 1 and 2 in MHC-CnA. However, at weeks 3 and 4 the RNA level of *Gja1* normalized to WT values, whereas the protein level remained reduced. This suggests that the initial Cx43 reduction is caused at the transcriptional level, whereas at weeks 3 and 4 another mechanism may be responsible. Analysis of the Cx43 phosphorylation status at Ser368 (Cx43-NP) revealed that Cx43 is less phosphorylated at this site in MHC-CnA at weeks 3 and 4, which may mark Cx43 for preliminary degradation. Since Ser368 is a target for protein kinase C (PKC),²⁴ reduced phosphorylation by PKC may underlie this phenomenon. Alternatively, CnA as a serine/threonine phosphatase itself may be involved in dephosphorylation of

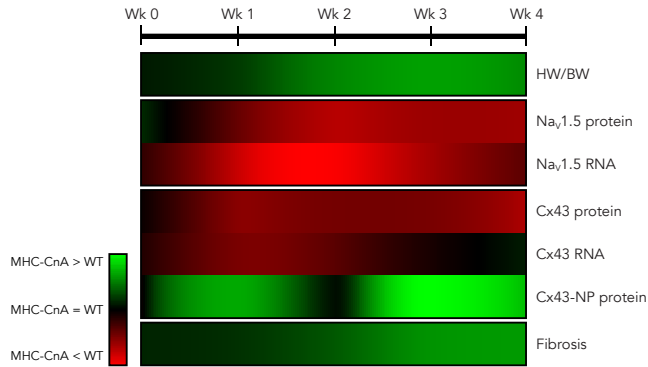


Figure 5. Schematic overview of calcineurin-dependent changes in key conductional parameters of MHC-CnA ventricles during postnatal development.

The conductional parameters are listed on the right of the map. Map illustrates the level of upregulation or downregulation based on the color scheme in the legend. MHC-CnA values are relative to WT (set to 1) from week (Wk) 0 to 4 (on the top of the map). Nav1.5 and Cx43 protein levels reflect values from immunoblotting; Cx43-NP antibody recognizes the P0 isoform of Cx43 specifically when Ser368 is non-phosphorylated; fibrosis levels reflect values from the Picosirius Red staining. HW/BW indicates heart weight/body weight ratio.

Cx43, either directly or indirectly. In line with this, dephosphorylation of Cx43 following myocardial ischemia in rats was inhibited by cyclosporine A, a CnA inhibitor, suggesting involvement of CnA.²⁵ Moreover, in a test-tube experiment purified CnA indeed proved to be able to dephosphorylate Cx43, immunoprecipitated from mouse heart, at the mentioned Ser residue (supplementary Figure S4 and Methods S1). Besides the above-mentioned potential role of (de)phosphorylation, regulation of Cx43 by particular microRNAs may provide for another such mechanism.²⁶⁻²⁸ Cx43 expression is known to be regulated by two miRNAs, miR-1 and miR-206,²⁹ however the expression of these miRNAs was not different between MHC-CnA and WT from week 0 to 4 (data not shown). Decreased expression of mechanical junction proteins plakoglobin, plakophilin or N-cadherin leads to downregulation or altered expression of Cx43 and together it could result in enhanced susceptibility to arrhythmias.³⁰⁻³² However, in 4-week old MHC-CnA hearts, the expression of these proteins was not decreased (data not shown). Taken together, the observed reduction in Cx43 protein level, when *Gja1* RNA level is similar to WT values, is possibly caused by a reduction in the phosphorylation levels which could trigger degradation of Cx43 by an as yet unknown mechanism, or by another pathway yet to be identified.

The increased collagen deposition in MHC-CnA hearts is in agreement with previous results.^{3,33} The increase in cardiac fibrosis can occur by an increase in collagen gene expression or by a decrease in the breakdown of collagen fibers, which is regulated

by different proteolytic enzymes, namely MMP2 and MMP9.^{34,35} Indeed, we showed that RNA expression levels of collagen in MHC-CnA are significantly upregulated at 3 weeks after birth, coinciding with the histological detection of fibrosis in this mouse model. Additionally, the RNA expression levels of TGF- β 1, a known inducer of fibrosis, and CTGF, a known downstream protein of TGF- β ,^{36,37} were increased in MHC-CnA ventricles at weeks 3 and 4 also coinciding with the histological detection of fibrosis. However, in MHC-CnA the RNA levels of *Mmp2* and *Mmp9* did not differ statistically from WT values. Instead, an upregulation of *Timp1*, a known inhibitor of MMPs,³⁴ coincided with occurrence of fibrosis.

Expression analysis of miR-21, miR-29b, miR-30c and miR-133a (all previously implicated in the regulation of fibrosis³⁸⁻⁴¹) revealed that the upregulation of miR-21 at weeks 3 and 4 was the only alteration observed between MHC-CnA and WT. This upregulation of miR-21 was correlated with the histological detection of fibrosis. Recently, an increase in miR-21 was also found in patients with atrial fibrillation or heart failure and in mice with pressure overload or cardiac stress.^{38,42} However, the role of miR-21 in fibrosis development is controversial since it has been disputed by two different groups.^{38,43} Interestingly, MHC-CnA mice interbred with miR-21 deficient mice developed cardiac hypertrophy at the same level as MHC-CnA mice, but unfortunately the level of fibrosis was not compared.⁴³ Altogether, the changes in collagen, TIMP-1, TGF- β 1, CTGF and miR-21 expression observed in the MHC-CnA model correlate and may contribute to the increased collagen deposition detected in these hearts.

Recently it was proposed that reduction in Cx43 expression precedes the development of fibrosis in aging or pressure-overloaded mice hearts.⁴⁴ Interestingly, in the MHC-CnA mouse model increased collagen deposition occurred after the reduction in Cx43 expression. The ability of individual cardiomyocytes to establish gap junctional communication with fibroblasts has been shown in cell cultures, but also in multicellular tissue over extended distances.⁴⁵ This coupling between cardiomyocytes and fibroblasts by Cx43 could potentially be involved in the triggering of collagen deposition; however, the molecular mechanism by which Cx43 reduction may result in excessive fibrosis remains to be elucidated. This combination of reduced Cx43 with excessive fibrosis led to increased susceptibility for ventricular arrhythmias.⁴⁴ Another arrhythmia combination is Na_v1.5 reduction in senescence mice together with the occurrence of extensive fibrosis in a later stage.⁴⁶

One of the limitations with transgenic models using the α -MHC promoter is that it can result in the expression of relatively high levels of transgenic protein, the normal variant of which is expressed at lower levels. Another limitation is that the transgene may already be expressed before birth and thus influence cardiac development. In addition, when cardiac hypertrophy/failure has developed the expression of the transgene may decrease due to the α -MHC to β -MHC shift. The limitation of quantifying

immunohistological images is the fact that this is a subjective method. The quantification of Cx43 labeling intensity (or collagen content) is performed by the use of a threshold that is set equal to all images and the drawback is there might be some images that can be over- or underestimated by the use of this threshold.

In summary, the reduction of Cx43 and Nav1.5 expression coincided with activation of the CnA/NFAT pathway and hypertrophy development, and preceded significant presence of fibrosis. At 4 weeks of age the alterations in conduction parameters observed in the MHC-CnA model lead to abnormal conduction and arrhythmias, similar to those observed in pathophysiological cardiac remodeling in heart failure patients.

FUNDING SOURCES

This study was supported by the Dutch Heart Foundation (grant numbers 2009B072 and 2010T045). The funders had no role in study design, data collection and analysis, decision to publish, or preparation of the manuscript.

REFERENCES

1. Diedrichs H, Chi M, Boelck B, Mehlhorn U, Schwinger RH. Increased regulatory activity of the calcineurin/NFAT pathway in human heart failure. *Eur J Heart Fail*. 2004;6:3-9
2. Haq S, Choukroun G, Lim H, Tymitz KM, del Monte F, Gwathmey J, Grazette L, Michael A, Hajjar R, Force T, Molkentin JD. Differential activation of signal transduction pathways in human hearts with hypertrophy versus advanced heart failure. *Circulation*. 2001;103:670-677
3. Molkentin JD, Lu JR, Antos CL, Markham B, Richardson J, Robbins J, Grant SR, Olson EN. A calcineurin-dependent transcriptional pathway for cardiac hypertrophy. *Cell*. 1998;93:215-228
4. Kleber AG, Rudy Y. Basic mechanisms of cardiac impulse propagation and associated arrhythmias. *Physiol Rev*. 2004;84:431-488
5. Fontes MS, van Veen TA, de Bakker JM, van Rijen HV. Functional consequences of abnormal Cx43 expression in the heart. *Biochim Biophys Acta*. 2012;1818:2020-2029
6. Severs NJ, Bruce AF, Dupont E, Rothery S. Remodelling of gap junctions and connexin expression in diseased myocardium. *Cardiovasc Res*. 2008;80:9-19
7. Borlak J, Thum T. Hallmarks of ion channel gene expression in end-stage heart failure. *FASEB J*. 2003;17:1592-1608
8. Shang LL, Pfahnl AE, Sanyal S, Jiao Z, Allen J, Banach K, Fahrenbach J, Weiss D, Taylor WR, Zafari AM, Dudley SC, Jr. Human heart failure is associated with abnormal C-terminal splicing variants in the cardiac sodium channel. *Circ Res*. 2007;101:1146-1154
9. Valdivia CR, Chu WW, Pu J, Foell JD, Haworth RA, Wolff MR, Kamp TJ, Makielski JC. Increased late sodium current in myocytes from a canine heart failure model and from failing human heart. *J Mol Cell Cardiol*. 2005;38:475-483
10. Soltysinska E, Olesen SP, Christ T, Wettwer E, Varro A, Grunnet M, Jespersen T. Transmural expression of ion channels and transporters in human nondiseased and end-stage failing hearts. *Pflügers Arch*. 2009;459:11-23
11. Rook MB, Evers MM, Vos MA, Bierhuizen MF. Biology of cardiac sodium channel $\text{Na}_v1.5$ expression. *Cardiovasc Res*. 2012;93:12-23
12. Creemers EE, Pinto YM. Molecular mechanisms that control interstitial fibrosis in the pressure-overloaded heart. *Cardiovasc Res*. 2011;89:265-272
13. Bierhuizen MF, Boulaksil M, van Stuijvenberg L, van der Nagel R, Jansen AT, Mutsaers NA, Yildirim C, van Veen TA, de Windt LJ, Vos MA, van Rijen HV. In calcineurin-induced cardiac hypertrophy expression of $\text{Na}_v1.5$, Cx40 and Cx43 is reduced by different mechanisms. *J Mol Cell Cardiol*. 2008;45:373-384
14. van Veen TA, van Rijen HV, Wiegerinck RF, Opthof T, Colbert MC, Clement S, de Bakker JM, Jongsma HJ. Remodeling of gap junctions in mouse hearts hypertrophied by forced retinoic acid signaling. *J Mol Cell Cardiol*. 2002;34:1411-1423
15. Sweat F, Puchter H, Rosenthal SI. Sirius Red F3Ba as a stain for connective tissue. *Arch Pathol*. 1964;1964:69-72
16. Schneider CA, Rasband WS, Eliceiri KW. NIH Image to ImageJ: 25 years of image analysis. *Nat Methods*. 2012;9:671-675
17. de Boer TP, van Veen TA, Bierhuizen MF, Kok B, Rook MB, Boonen KJ, Vos MA, Doevendans PA, de Bakker JM, van der Heyden MA. Connexin43 repression following epithelium-to-mesenchyme transition in embryonal carcinoma cells requires Snail1 transcription factor. *Differentiation*. 2007;75:208-218

18. Teunissen BE, Jansen AT, Mutsaers NA, Vuerhard MJ, Vos MA, Bierhuizen MF. Primary structure, organization, and expression of the rat connexin45 gene. *DNA Cell Biol.* 2007;26:108-115
19. Livak KJ, Schmittgen TD. Analysis of relative gene expression data using real-time quantitative PCR and the 2(-Delta Delta C(T)) method. *Methods.* 2001;25:402-408
20. Fieller EC. The Biological Standardization of Insulin. *Suppl to J R Statist Soc.* 1940;7:1-64
21. R Core Team. R: A language and environment for statistical computing. 2012:ISBN 3-900051-900007-900050, URL <http://www.R-project.org/> Accessed 2013 Dec 30
22. Arnolds DE, Liu F, Fahrenbach JP, Kim GH, Schillinger KJ, Smemo S, McNally EM, Nobrega MA, Patel VV, Moskowitz IP. TBX5 drives Scn5a expression to regulate cardiac conduction system function. *J Clin Invest.* 2012;122:2509-2518
23. Guo J, Zhan S, Somers J, Westenbroek RE, Catterall WA, Roach DE, Sheldon RS, Lees-Miller JP, Li P, Shimoni Y, Duff HJ. Decrease in density of I_{Na} is in the common final pathway to heart block in murine hearts overexpressing calcineurin. *Am J Physiol Heart Circ Physiol.* 2006;291:H2669-2679
24. Marquez-Rosado L, Solan JL, Dunn CA, Norris RP, Lampe PD. Connexin43 phosphorylation in brain, cardiac, endothelial and epithelial tissues. *Biochim Biophys Acta.* 2012;1818:1985-1992
25. Hatanaka K, Kawata H, Toyofuku T, Yoshida K. Down-regulation of connexin43 in early myocardial ischemia and protective effect by ischemic preconditioning in rat hearts in vivo. *Jpn Heart J.* 2004;45:1007-1019
26. Thum T. MicroRNA therapeutics in cardiovascular medicine. *EMBO Mol Med.* 2012;4:3-14
27. van Rooij E, Olson EN. MicroRNA therapeutics for cardiovascular disease: Opportunities and obstacles. *Nat Rev Drug Discov.* 2012;11:860-872
28. Small EM, Olson EN. Pervasive roles of microRNAs in cardiovascular biology. *Nature.* 2011;469:336-342
29. Anderson C, Catoe H, Werner R. MIR-206 regulates connexin43 expression during skeletal muscle development. *Nucleic Acids Res.* 2006;34:5863-5871
30. Fabritz L, Hoogendijk MG, Scicluna BP, van Amersfoort SC, Fortmueller L, Wolf S, Laakmann S, Kreienkamp N, Piccini I, Breithardt G, Noppinger PR, Witt H, Ebnet K, Wichter T, Levkau B, Franke WW, Pieperhoff S, de Bakker JM, Coronel R, Kirchhof P. Load-reducing therapy prevents development of arrhythmogenic right ventricular cardiomyopathy in plakoglobin-deficient mice. *J Am Coll Cardiol.* 2011;57:740-750
31. Oxford EM, Musa H, Maass K, Coombs W, Taffet SM, Delmar M. Connexin43 remodeling caused by inhibition of plakophilin-2 expression in cardiac cells. *Circ Res.* 2007;101:703-711
32. Li J, Patel VV, Kostetskii I, Xiong Y, Chu AF, Jacobson JT, Yu C, Morley GE, Molkentin JD, Radice GL. Cardiac-specific loss of N-cadherin leads to alteration in connexins with conduction slowing and arrhythmogenesis. *Circ Res.* 2005;97:474-481
33. Chu G, Carr AN, Young KB, Lester JW, Yatani A, Sanbe A, Colbert MC, Schwartz SM, Frank KF, Lampe PD, Robbins J, Molkentin JD, Kranias EG. Enhanced myocyte contractility and Ca²⁺ handling in a calcineurin transgenic model of heart failure. *Cardiovasc Res.* 2002;54:105-116
34. Lombardi R, Betocchi S, Losi MA, Tocchetti CG, Aversa M, Miranda M, D'Alessandro G, Cacace A, Ciampi Q, Chiariello M. Myocardial collagen turnover in hypertrophic cardiomyopathy. *Circulation.* 2003;108:1455-1460
35. Pauschinger M, Doerner A, Remppis A, Tannhauser R, Kuhl U, Schultheiss HP. Differential myocardial abundance of collagen type I and type III mRNA in dilated cardiomyopathy: Effects of myocardial inflammation. *Cardiovasc Res.* 1998;37:123-129

36. Daniels A, van Bilsen M, Goldschmeding R, van der Vusse GJ, van Nieuwenhoven FA. Connective tissue growth factor and cardiac fibrosis. *Acta Physiol (Oxf)*. 2009;195:321-338
37. Ruiz-Ortega M, Rodriguez-Vita J, Sanchez-Lopez E, Carvajal G, Egido J. TGF-beta signaling in vascular fibrosis. *Cardiovasc Res*. 2007;74:196-206
38. Thum T, Gross C, Fiedler J, Fischer T, Kissler S, Bussen M, Galuppo P, Just S, Rottbauer W, Frantz S, Castoldi M, Soutschek J, Koteliensky V, Rosenwald A, Basson MA, Licht JD, Pena JT, Rouhanifard SH, Muckenthaler MU, Tuschl T, Martin GR, Bauersachs J, Engelhardt S. MicroRNA-21 contributes to myocardial disease by stimulating MAP kinase signalling in fibroblasts. *Nature*. 2008;456:980-984
39. van Rooij E, Sutherland LB, Thatcher JE, DiMaio JM, Naseem RH, Marshall WS, Hill JA, Olson EN. Dysregulation of microRNAs after myocardial infarction reveals a role of miR-29 in cardiac fibrosis. *Proc Natl Acad Sci U S A*. 2008;105:13027-13032
40. Duisters RF, Tijssen AJ, Schroen B, Leenders JJ, Lentink V, van der Made I, Herias V, van Leeuwen RE, Schellings MW, Barenbrug P, Maessen JG, Heymans S, Pinto YM, Creemers EE. miR-133 and miR-30 regulate connective tissue growth factor: Implications for a role of microRNAs in myocardial matrix remodeling. *Circ Res*. 2009;104:170-178
41. Matkovich SJ, Wang W, Tu Y, Eschenbacher WH, Dorn LE, Condorelli G, Diwan A, Nerbonne JM, Dorn GW, 2nd. MicroRNA-133a protects against myocardial fibrosis and modulates electrical repolarization without affecting hypertrophy in pressure-overloaded adult hearts. *Circ Res*. 2010;106:166-175
42. Adam O, Lohfelme B, Thum T, Gupta SK, Puhl SL, Schafers HJ, Bohm M, Laufs U. Role of miR-21 in the pathogenesis of atrial fibrosis. *Basic Res Cardiol*. 2012;107:278
43. Patrick DM, Montgomery RL, Qi X, Obad S, Kauppinen S, Hill JA, van Rooij E, Olson EN. Stress-dependent cardiac remodeling occurs in the absence of microRNA-21 in mice. *J Clin Invest*. 2010;120:3912-3916
44. Jansen JA, van Veen TA, de Jong S, van der Nagel R, van Stuijvenberg L, Driessen H, Labzowski R, Oefner CM, Bosch AA, Nguyen TQ, Goldschmeding R, Vos MA, de Bakker JM, van Rijen HV. Reduced Cx43 expression triggers increased fibrosis due to enhanced fibroblast activity. *Circ Arrhythm Electrophysiol*. 2012;5:380-390
45. Camelliti P, Green CR, LeGrice I, Kohl P. Fibroblast network in rabbit sinoatrial node: Structural and functional identification of homogeneous and heterogeneous cell coupling. *Circ Res*. 2004;94:828-835
46. Leoni AL, Gavillet B, Rougier JS, Marionneau C, Probst V, Le Scouarnec S, Schott JJ, Demolombe S, Bruneval P, Huang CL, Colledge WH, Grace AA, Le Marec H, Wilde AA, Mohler PJ, Escande D, Abriel H, Charpentier F. Variable Nav1.5 protein expression from the wild-type allele correlates with the penetrance of cardiac conduction disease in the *Scn5a*^{+/-} mouse model. *PLoS One*. 2010;5:e9298

SUPPLEMENTARY MATERIALS

Methods S1

Additional methods of co-immunoprecipitation assay and PP2B dephosphorylation assay with supporting references.

Co-immunoprecipitation assay

The co-immunoprecipitation of Cx43 from an adult mouse heart was performed as described previously.¹ Briefly, heart lysates from a pool of 3 adult mouse hearts were homogenized in lysis buffer and centrifuged at 14000 rpm for 10 min. Immunoprecipitation was performed using 12.5 mg of protein lysate as input. To pre-clear the lysate, the supernatant was exposed to protein A/G agarose beads (Roche Applied Science, Indianapolis, IN, USA) for 1 hour at 4°C, followed by centrifugation at 14000 rpm for 1 min at 4°C. The pre-cleared supernatant was incubated for 4 hours at 4°C with 7 µg of mouse anti-Cx43 (BD Transduction Laboratories by BD Biosciences, Breda, The Netherlands) and exposed to 500 µl protein A/G agarose beads overnight at 4°C. After centrifugation, the antibody-protein A/G agarose complex was washed 5 times in lysis buffer to clear the solvent of unbound material. The final pellet was resuspended in 500 µl of lysis buffer and 20 µl was used for each PP2B dephosphorylation assay.

PP2B dephosphorylation assay

For CnA (PP2B) dephosphorylation assays, two individual experiments were performed. One set of tubes was pre-incubated for 10 min at 30°C with PP2B buffer (Merck Millipore, Billerica, Massachusetts, USA), calmodulin (3.3 nM, Merck Millipore) and a range of PP2B enzyme concentrations (0, 0.1, 0.25, 0.5 and 0.75 Units, Merck Millipore). The other set of tubes was pre-incubated for 10 min at 30°C with PP2B buffer (Merck Millipore), calmodulin (3.3 nM, Merck Millipore) and PP2B enzyme (0.75 Units, Merck Millipore) with or without FK506 (100 µM, Sigma-Aldrich Corp., Saint Louis, MO, USA) and FKBP (10 µM, Sigma-Aldrich Corp.). Pre-incubated solution was added to 20 µl of the immunoprecipitated beads per reaction, incubated for 20 min at 30°C with 800 rpm shaker and centrifuged for 1 min at 1000 rpm. The final pellet was resuspended in 50 µl of blue sample buffer and the protein of interest detected by immunoblotting (see Materials and Methods). The antibodies used for protein detection were mouse monoclonal antibodies against total Cx43 (1:250, BD Transduction Laboratories by BD Biosciences), Cx43-NP (1:500, Invitrogen by Life Technologies Corp., Carlsbad, CA, USA) and Cx43-CT1 (1:500, kindly provided by Dr. P.D. Lampe, Molecular Diagnostics Program, Fred Hutchinson Cancer Research Center, USA).²

Supplemental Table

Table S1. References of the Applied Biosystems assays used in this study.

Gene	Assay ID
<i>Gapdh</i>	Mm99999915_g1
<i>Scn5a</i>	Mm00451971_m1
<i>Gja1</i>	Mm00439105_m1
<i>Col1a1</i>	Mm00801666_g1
<i>Col1a2</i>	Mm00483888_m1
<i>Col3a1</i>	Mm01254476_m1
<i>Ctgf</i>	Mm01192933_g1
<i>Tgfb1</i>	Mm01178820_m1
<i>Timp1</i>	Mm00441818_m1
miRNA	Assay ID
<i>U6 snRNA</i>	001973
<i>hsa-miR-21</i>	000397

Supplemental Figures

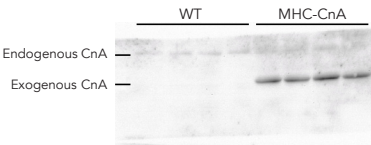


Figure S1. Expression of constitutively active CnA in WT and MHC-CnA hearts at week 2. Protein lysates from four different WT and MHC-CnA ventricles were analyzed for expression of endogenous (~58kDa) and exogenous (~43kDa; constitutively active) CnA by immunoblotting.

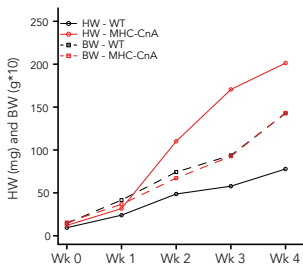


Figure S2. Heart weight (HW) and body weight (BW) in WT and MHC-CnA mice in weeks (Wk) 0, 1, 2, 3 and 4.

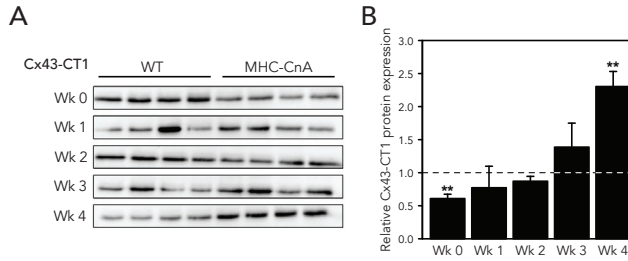


Figure S3. Gap junction Cx43 expression in WT and MHC-CnA ventricles.

Protein lysates from four different WT and MHC-CnA ventricles were analyzed for Cx43-CT1 expression by immunoblotting at weeks (Wk) 0, 1, 2, 3 and 4. In **A** Cx43-CT1 antibody recognizes the P0 isoform of Cx43 specifically when Ser364 and/or Ser365 are non-phosphorylated. **B**: Quantification of the blots (ratio of Protein/Ponceau) represented in **A**. MHC-CnA values are relative to WT (set to 1). Values are mean ± SEM; **p < 0.01 compared to WT.

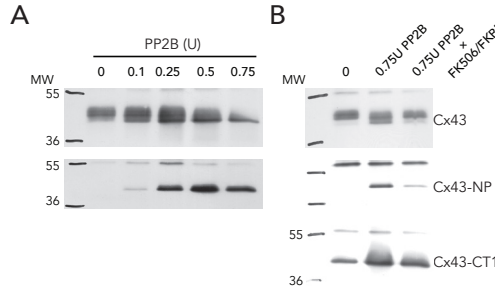
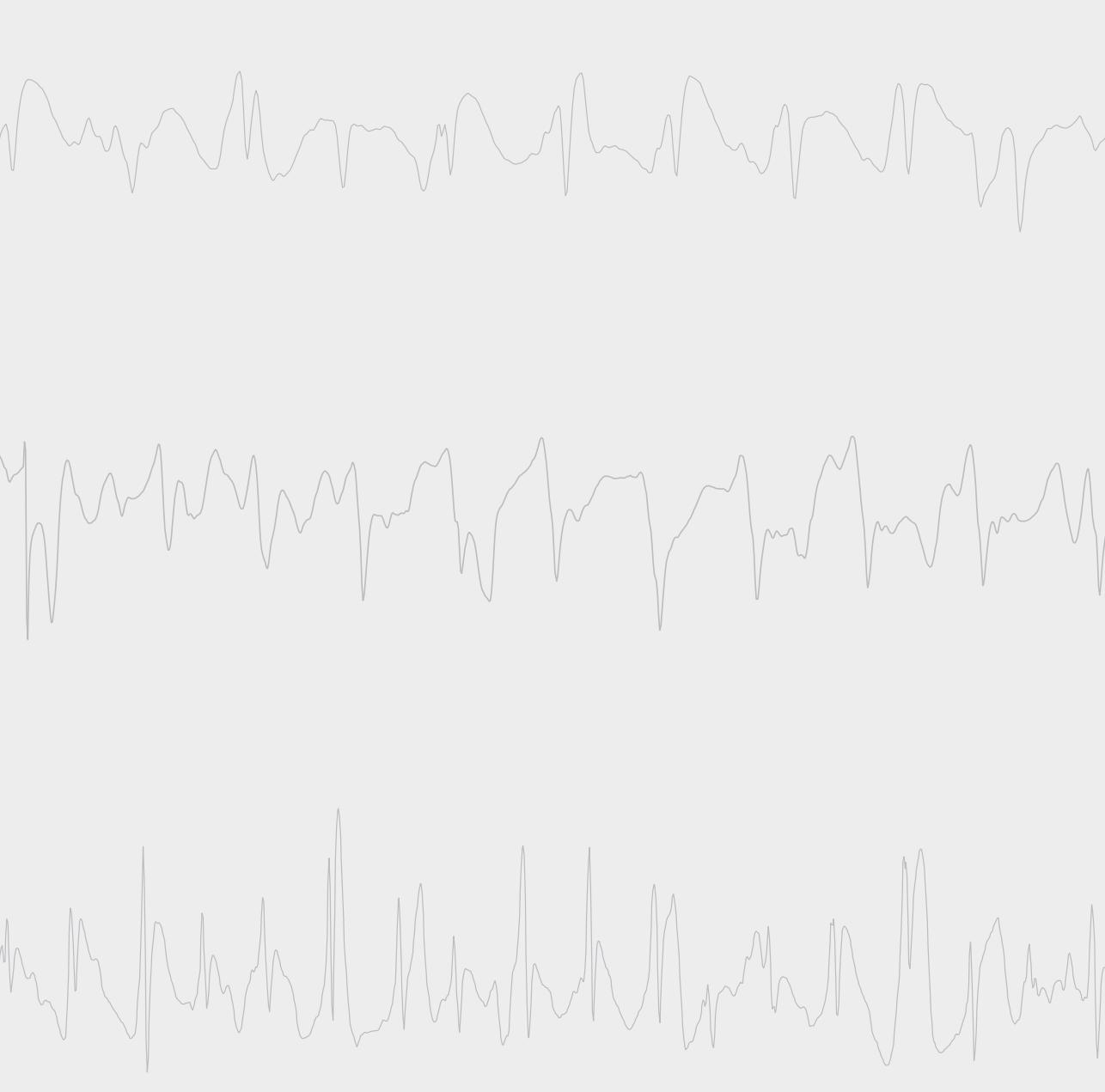


Figure S4. Cx43 immunoprecipitated from adult mouse heart treated with CnA or with CnA and a CnA inhibitor.

A: CnA (PP2B) treatment of Cx43 was analyzed at different concentrations for total Cx43 and Cx43 P0 isoform expression by immunoblotting. Cx43-NP antibody recognizes the P0 isoform of Cx43 specifically when Ser368 is non-phosphorylated. **B**: Treatment of Cx43 with PP2B or PP2B together with a CnA inhibitor (FK506/FKBP) was analyzed for total Cx43 and Cx43 P0 isoform expression by immunoblotting. Cx43-CT1 antibody recognizes the P0 isoform of Cx43 specifically when Ser364 and/or Ser365 are non-phosphorylated.

References

1. Sato PY, Musa H, Coombs W, Guerrero-Serna G, Patino GA, Taffet SM, Isom LL, Delmar M. Loss of plakophilin-2 expression leads to decreased sodium current and slower conduction velocity in cultured cardiac myocytes. *Circ Res*. 2009;105:523-526
2. Sosinsky GE, Solan JL, Gaietta GM, Ngan L, Lee GJ, Mackey MR, Lampe PD. The C-terminus of connexin43 adopts different conformations in the Golgi and gap junction as detected with structure-specific antibodies. *Biochem J*. 2007;408:375-385



Magda S.C. Fontes^{1,*}, Elise L. Kessler^{1,*}, Leonie van Stuijvenberg¹, Maike A. Brans¹,
Lucas L. Falke², Bart Kok¹, Harold V.M. van Rijen¹, Marc A. Vos¹, Roel Goldschmeding²,
Toon A.B. van Veen¹

** Authors contributed equally*

Departments of Medical Physiology¹, and Pathology², University Medical Center, Utrecht, The Netherlands







Chapter 6



**CTGF knockout does not affect cardiac
hypertrophy and fibrosis formation upon chronic
pressure overload**



Submitted



ABSTRACT

Background

One of the main contributors to maladaptive cardiac remodeling is fibrosis. Connective tissue growth factor (CTGF), a matricellular protein that is secreted into the cardiac extracellular matrix by both cardiomyocytes and fibroblasts, is often associated with development of fibrosis. However, recent studies have questioned the role of CTGF as a pro-fibrotic factor. Therefore, we aimed to investigate the effect of CTGF on cardiac fibrosis, and on functional, structural, and electrophysiological parameters in a mouse model of CTGF knockout (KO) and chronic pressure overload.

Methods and results

A new mouse model of global conditional CTGF KO induced by tamoxifen-driven deletion of CTGF, was subjected to 16 weeks of chronic pressure overload via transverse aortic constriction (TAC, control was sham surgery). CTGF KO TAC mice presented with hypertrophic hearts, and echocardiography revealed a decrease in contractility on a similar level as control TAC mice. *Ex vivo* epicardial mapping suggested a decrease in pacing-induced ventricular arrhythmias (0/10 vs. 2/12 in control TAC, *n.s.*) and a tendency towards recovery of the longitudinal conduction velocity of CTGF KO TAC hearts. Picrosirius Red staining on these hearts unveiled increased fibrosis at a similar level as control TAC hearts. Furthermore, genes related to fibrogenesis were also similarly upregulated in both TAC groups. Histological analysis revealed an increase in fibronectin and vimentin protein expression, a significant reduction in connexin43 (Cx43) protein expression, and no difference in Nav1.5 expression of CTGF KO ventricles as compared with sham treated animals.

Conclusion

Conditional CTGF inhibition failed to prevent TAC-induced cardiac fibrosis and hypertrophy. Additionally, no large differences were found in other parameters between CTGF KO and control TAC mice. With no profound effect of CTGF on fibrosis formation, other factors or pathways are likely responsible for fibrosis development.

INTRODUCTION

One of the main contributors to pathological cardiac remodeling is fibrosis.¹ Cardiac fibrosis refers to an accumulation of connective tissue in the extracellular matrix (ECM) that results from excessive deposition and/or decreased degradation of its components, including collagen.² Fibrosis can result in increased myocardial stiffness and impairment of electrical connections between cardiomyocytes, possibly leading to increased susceptibility to arrhythmias.³ Additionally, the normal electrical impulse propagation can be disturbed by direct reduction of cell-to-cell coupling due to reduced or heterogeneously redistributed gap junction proteins, mainly connexin43 (Cx43), or by reduction in excitability of individual cardiomyocytes due to abnormal expression of the sodium channel Nav1.5.^{4,5}

Connective tissue growth factor (CTGF) is a matricellular protein that is e.g. involved in angiogenesis, tissue repair and a variety of types of fibrosis formation including cardiac fibrosis, through the regulation of several factors in ECM homeostasis.^{6,7} Increased levels of CTGF have been found in patients with heart failure, ischemia and coronary artery disease.⁸⁻¹⁰ Similar elevations were observed in injury-induced animal models of cardiac hypertrophy and fibrosis.¹⁰⁻¹⁴ The implication of CTGF in fibrosis development/maintenance, but also the close relationship with the pro-fibrotic cytokine transforming growth factor beta-1 (TGF- β 1), is well documented.^{6,15} Some studies have also reported a decrease in fibrosis after inhibition of CTGF.¹⁶ However, recent studies using transgenic mice overexpressing CTGF pointed towards a cardio-protective effect of CTGF, reporting similar amount of fibrosis after myocardial infarction or pressure overload compared to control mice.¹⁷⁻¹⁹ Very recently, Accornero and colleagues showed that cardiac specific CTGF deletion in mice (or in combination with CTGF deletion from fibroblast) did not affect fibrosis, among other parameters, upon 2 or 8 weeks of pressure overload stimulation.²⁰ These contradicting findings show that the specific role of CTGF in the origin and progression of cardiac fibrosis is therefore not yet fully understood.

Research on CTGF could contribute to important insight into the underlying mechanisms of fibrosis and cardiac disease. In the heart, CTGF is secreted into the ECM by both fibroblasts and cardiomyocytes.⁸ In order to target both cell types, we developed a new mouse model in which CTGF is conditionally knocked out (KO) in all cells of the body. The aim of our study was to investigate the effect of CTGF KO on fibrosis formation in the heart upon 16 weeks of chronic pressure overload, and consequently, the relation with remodeling of functional, structural, and electrophysiological parameters. For the latter ones, special attention has been paid at potential effects on conduction velocity, development of arrhythmias and modulation of the underlying molecular substrate.

METHODS

Generation of conditional CTGF knockout (KO) mice

All experiments were conducted with consent of the Experimental Animal Ethics Committee of the University of Utrecht, The Netherlands. CTGF flox mice, in which a CTGF allele is flanked by loxP sites, were kindly donated by Dr. Andrew Leask (University of Western Ontario, Canada).²¹ To generate time-conditional CTGF full knockout mice, homozygous CTGF flox mice were crossed with mice ubiquitously expressing tamoxifen-inducible Cre recombinase (Cre-ERT2) under the control of the ROSA26 locus (ROSA26CreERT2; The Jackson Laboratory, Maine, USA). ROSA26CreERT2 and CTGF flox mice, both on C57Bl/6J genetic background, were crossbred for five generations and homozygous CTGF^{flox/flox}/ROSA26-ERT/Cre mice were used in this study. Genotype of mice was confirmed by polymerase chain reaction (PCR) using the following primers: CTGF flox forward (5'-AAAGTCGCTCTGAGTTGTTAT-3') and reverse (5'-CCTGATCCTGGCAATTCG-3'); ROSA26CreERT2 forward (5'-AATACCAATGCACTTGCCTGGATGG-3') and reverse (5'-GAAACAGCAATTACTACAACGGGAGTGG-3') and (5'-GGAGCGGGAGAAATGGATATG-3'). All animals were housed under standard conditions with controlled light, humidity and temperature, and with food and water *ad libitum*.

Tamoxifen (T5648; Sigma-Aldrich, St Louis, MO, USA) was dissolved at 10 mg/mL in corn oil (C8267; Sigma-Aldrich). To induce global CTGF gene ablation, adult CTGF^{flox/flox}/ROSA26-ERT/Cre mice (13-14 weeks old) were injected intraperitoneally once a day with 0.1 mL of tamoxifen for 4 consecutive days (designated hereafter as CTGF KO mice). Corresponding littermates were injected with only corn oil for 4 consecutive days (designated as control mice).

Experimental set-up

Two weeks after tamoxifen/vehicle injections, control and CTGF KO mice were subjected to transverse aortic constriction (TAC) or sham surgery as previously performed.²² After surgery, all mice were followed for 16 weeks and the ones that completed the study were further analyzed: control sham (n=10), CTGF KO sham (n=9), control TAC (n=13), and CTGF KO TAC (n=10).

Electrocardiography and echocardiography

At 16 weeks after surgery, mice were anesthetized with isoflurane (2% in O₂) and a 3-lead electrocardiogram (ECG) was recorded using PowerLab 4/30 and Dual Bio Amp (ADInstruments Ltd., UK). At least 100 complexes were averaged and analyzed off-line

using LabChart 7 Pro (ADInstruments Ltd.). Subsequently, transthoracic echocardiography was performed to determine functional and structural parameters using Vevo 2100 System (VisualSonics Inc., Toronto, Canada) equipped with a 22-55MHz transducer (MS550D). Aortic peak velocity was measured by pulsed-wave Doppler with a 13-24MHz transducer (MS250) to confirm proper constriction (pressure gradient approximately 58mmHg) in both TAC operated groups. Analysis off-line and calculations were performed using the Vevo 2100 software.

Epicardial mapping of Langendorff perfused mouse hearts

After transthoracic echocardiography, the chest was opened and the heart rapidly excised and perfused retrogradely on a Langendorff apparatus for epicardial mapping. The perfusion solution was carbogen-gassed at 37°C and extracellular electrograms were recorded using a 19x13 multielectrode grid (0.3mm spacing) placed on the epicardial surface of both the left and right ventricles of the heart as described previously.²³ Epicardial recordings were made during stimulation (2 times stimulation threshold) from the center of the grid at a basic cycle length (BCL) of 120ms. The effective refractory period (ERP) was determined for both ventricles. Local activation times of the recorded electrograms were determined off-line with custom made software based on Matlab (The MathWorks Inc., Natick, USA) and used to calculate conduction velocity (CV), as previously described.⁵ Susceptibility for arrhythmias was tested by programmed electrical stimulation using a standardized protocol as described before.⁵

Immunohistochemistry

After Langendorff experiments, the hearts were snap frozen in liquid nitrogen. Subsequently, serial cryosections of the hearts were generated (10µm thickness, in four-chamber view) for immunohistochemistry and histological analysis. Immunolabeling was performed as described previously,²⁴ using mouse monoclonal antibodies against vimentin (1:200, Sigma-Aldrich) and Cx43 (1:200, BD Transduction Laboratories, Breda, The Netherlands), and rabbit polyclonal antibodies against fibronectin (1:400, Sigma-Aldrich) and pan-cadherin (1:4000, Sigma-Aldrich). Secondary labeling was achieved by appropriate fluorescein isothiocyanate (FITC, 1:250) or Alexa Fluor 594 (1:100) conjugated anti-mouse or anti-rabbit whole IgG antibodies (Jackson ImmunoResearch Europe, Newmarket, United Kingdom).

Immunohistochemistry for CTGF detection was performed as described previously with slight modifications.²⁵ Briefly, heart cryosections of 10µm thickness were fixed with 4% paraformaldehyde (PFA) for 30 minutes, endogenous peroxidase activity was blocked, and heat-based antigen retrieval was performed in citrate buffer. Sections were then incubated overnight with goat polyclonal antibodies against CTGF (1:200,

Santa Cruz Biotechnology, Heidelberg, Germany), followed by incubation of secondary labeling with horseradish peroxidase (HRP)-conjugated rabbit anti-goat IgG (1:100, Dako, Glostrup, Denmark) and goat anti-rabbit BrightVision-HRP (Immunologic BV, Duiven, The Netherlands). Sections were developed with NovaRED (Vector Laboratories, Burlingame, CA, USA), counterstained with hematoxylin and mounted with Pertex (Histolab Products AB, Gothenburg, Sweden).

After immunolabeling, sections were analyzed with an epifluorescence microscope (Nikon Eclipse 80i; Nikon Europe BV, Amstelveen, The Netherlands) and randomly chosen images were taken using NIS Elements BR 3.0 software. Quantification analysis was performed using ImageJ 1.35s software.²⁶

Histology

Frozen cryosections were fixed by 4% PFA for 30 minutes, incubated with xylene and rehydrated in an ethanol series. Subsequently, sections were pre-incubated with 0.2% phosphomolybdic acid (Sigma-Aldrich) and stained with 0.1% Picrosirius red solution for 90 minutes. Afterwards, sections were incubated with 0.01M HCl for 2 minutes, dehydrated in a reverse ethanol series, incubated in xylene and sealed with Pertex (Histolab Products AB).

To quantify fibrosis, all ventricles were analyzed individually under the microscope ($n=10$, $n=9$, $n=13$ and $n=9$ for control sham, CTGF KO sham, control TAC and CTGF KO TAC, respectively) and scored independently by three observers in a double-blind manner into none (0), scant (1), moderate (2), and severe (3) fibrosis as previously described.³

Immunoblotting

Total cellular protein was isolated from ventricular tissue as described previously.²⁴ Protein samples were separated on 7% or 10% SDS-PAGE gel, electro-transferred on nitrocellulose membranes and blocked with 5% milk powder. Equality of protein transfer was assessed by Ponceau S staining. Membranes were incubated with mouse monoclonal antibodies against Cx43 (1:250, BD Transduction Laboratories) and rabbit polyclonal antibodies against fibronectin (1:1000, Sigma-Aldrich), and Nav1.5 (1:200, Sigma-Aldrich). Secondary labeling was performed with HRP-conjugated anti-mouse or anti-rabbit whole IgG antibodies (1:7000, Bio-Rad Laboratories, Hercules, CA, USA). Detection was performed using standard ECL procedure (GE Healthcare, Buckinghamshire, United Kingdom) with ChemiDoc XRS system (BioRad Laboratories). Quantification analysis was performed with ImageJ 1.35s software, where the protein of interest was corrected for correspondent Ponceau S staining.

Real-time quantitative PCR (RT-qPCR)

RT-qPCR on ventricular tissue was performed using TaqMan Gene Expression Assays (Applied Biosystems by Life Technologies Corp., Carlsbad, CA, USA) as described earlier.¹⁴ Relative mRNA expression levels were determined for CTGF, brain natriuretic peptide (BNP), Collagen 1a1, Collagen 1a2, Collagen 3a1, TGF- β 1, plasminogen activator inhibitor-1 (PAI-1), heat shock protein 47 (Hsp47), Cx43 and sodium channel Na_v1.5 (all from Applied Biosystems by Life Technologies Corp.). 60S acidic ribosomal protein P1 (RPLP1) (Applied Biosystems by Life Technologies Corp.) was used as internal control, since the levels did not differ between group samples (for specifics see Supplementary Table 1).

Statistical analysis

Data are expressed as mean \pm standard error of the mean (SEM). Statistical analyses were performed using two-way ANOVA followed by Tukey's multiple comparisons test. The survival data were analyzed using the log-rank test, arrhythmia inducibility analysed with Fisher exact test and fibrosis score analysed using one-way ANOVA with contrast test. All analyses were performed using GraphPad Prism 6.0 (GraphPad Software, La Jolla, CA, USA), except for the ANOVA with contrast test that was performed using SPSS 20.0 (SPSS Inc., Chicago, IL, USA). A value of $p < 0.05$ was considered statistically significant.

RESULTS

In the present study, functional, structural, and electrical remodeling was investigated after chronic pressure overload in a new mouse model of global conditional CTGF knockout. The Kaplan-Meier survival curves in Figure 1A revealed a trend towards higher mortality after 16 weeks of TAC surgery in CTGF KO mice when compared with control mice (52 vs. 28%, *n.s.*). The global conditional gene deletion of CTGF in both sham and TAC groups was confirmed in the ventricles with a reduction of 95-98% on CTGF RNA and protein levels compared with respective controls ($p < 0.05$, Figures 1B-C). CTGF knockout was also confirmed in the atria with a reduction in CTGF protein level of 98% in sham and TAC groups compared with respective controls ($p < 0.01$, Figure 1D). Additionally, in the control TAC group, CTGF was upregulated after surgery: 2.2-fold (mRNA) and 2.7-fold (protein) in the ventricles, and 1.6-fold (protein) in the atria ($p < 0.01$, Figures 1B-D, respectively).

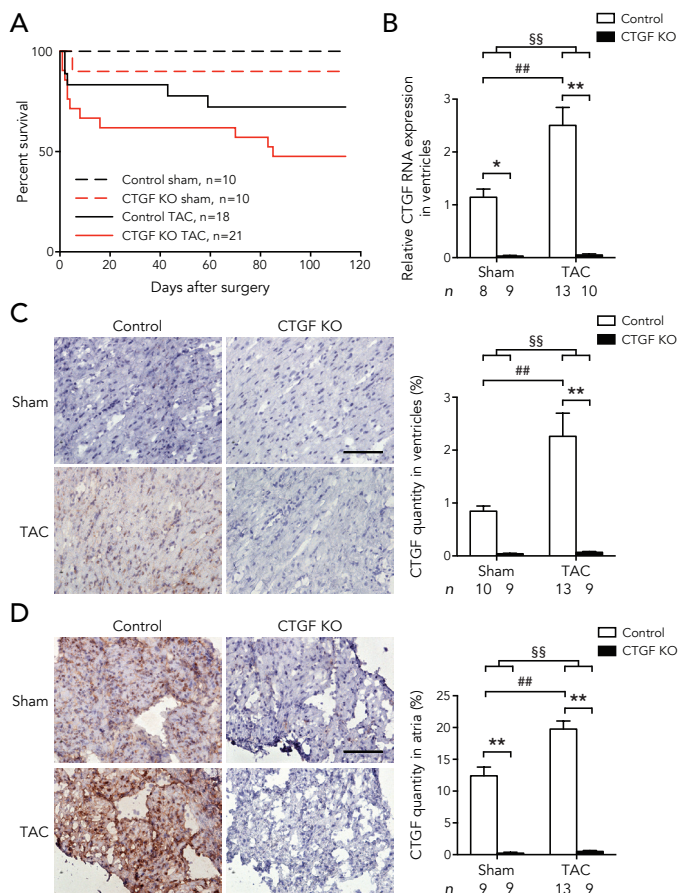


Figure 1. Characterization of CTGF conditional knockout mice after sham or TAC surgery.

A: Kaplan-Meier survival curves of control and tamoxifen-induced conditional knockout of CTGF (CTGF KO) mice. **B:** CTGF RNA expression in the ventricles assessed by TaqMan RT-qPCR in control and CTGF KO mice. Representative images from control and CTGF KO ventricles (**C**) and atria (**D**) immunolabeled for CTGF (left), and respective quantification (right). Scale bar in **C** and **D** represent 100 μ m. Black bars refer to CTGF KO mice and white bars to control mice; n indicates the number of mice per group. * $p < 0.05$, ** $p < 0.01$, ## $p < 0.01$, §§ $p < 0.01$.

Morphological, echocardiographic and electrocardiographic data

Sixteen weeks of pressure overload resulted in cardiac hypertrophy of CTGF KO mice to the same extent as the control mice, as evidenced by the increase of heart weight to body weight ratio and the increase of the hypertrophic marker BNP ($p < 0.05$, Figures 2C-D). Moreover, no significant changes were found in lungs, liver or kidney weights (Table 1). Echocardiography revealed impaired cardiac contractility after TAC in control, as well as in CTGF KO mice (Figure 2A), with decreased fractional shortening compared to respective sham groups (22% in control TAC and 23% in CTGF KO TAC vs. $\pm 31\%$ in

both sham groups, $p < 0.05$, Figure 2B and Table 1). Furthermore, electrocardiographic parameters remained unchanged after TAC except for QRS and QTc intervals. These were significantly increased in control, but not in CTGF KO mice, where there was only a tendency of increased values (Table 2).

Arrhythmia induction and conduction velocity

Isolated Langendorff-perfused control hearts were arrhythmogenic upon TAC, with sustained (>15 beats) polymorphic ventricular tachyarrhythmia (VT) as shown in Figure 3A. Epicardial activation maps generated during VT revealed irregular activation

Table 1. Tissue characteristics and echocardiographic measurements for Sham- and TAC-operated mice.

	Sham		TAC	
	Control	CTGF KO	Control	CTGF KO
<i>n</i>	10	9	13	10
Organ weights				
Body weight (g)	26.0 \pm 1.2	27.4 \pm 1.3	27.8 \pm 1.5	25.7 \pm 1.0
Heart weight (mg) ^{§§}	144.1 \pm 7.6	161.3 \pm 8.5	205.2 \pm 15.3***#	201.7 \pm 8.7**
HW/BW (mg/g) ^{§§}	5.5 \pm 0.1	5.9 \pm 0.3	7.4 \pm 0.4***#	7.9 \pm 0.4***#
LuW/BW (mg/g)	5.7 \pm 0.2	5.7 \pm 0.4	5.7 \pm 0.3	6.2 \pm 0.2
LiW/BW (mg/g)	3.8 \pm 0.1	4.0 \pm 0.1	3.6 \pm 0.1	3.9 \pm 0.1
KW/BW (mg/g)	5.3 \pm 0.2	5.4 \pm 0.1	5.2 \pm 0.2	5.6 \pm 0.2
Echocardiography				
LVID,s (mm)	2.8 \pm 0.1	2.4 \pm 0.2	3.2 \pm 0.2	2.9 \pm 0.2
LVID,d (mm)	4.0 \pm 0.1	3.6 \pm 0.2	4.1 \pm 0.2	3.8 \pm 0.2
LV Vol,s (μ L) [§]	30.9 \pm 4.0	22.5 \pm 4.0	46.0 \pm 8.2	35.0 \pm 6.4
LV Vol,d (μ L)	69.7 \pm 5.8	56.9 \pm 6.6	77.6 \pm 10.2	63.8 \pm 9.3
SV (μ L) [§]	38.8 \pm 2.3	34.4 \pm 3.7	31.6 \pm 2.7	28.7 \pm 3.6
EF (%) ^{§§}	56.8 \pm 2.2	61.7 \pm 2.9	45.0 \pm 3.2***#	47.1 \pm 2.9##
FS (%) ^{§§}	29.5 \pm 1.4	32.8 \pm 2.0	22.3 \pm 1.8***#	23.3 \pm 1.7##
CO (mL/min)	16.1 \pm 1.0	14.1 \pm 2.1	14.5 \pm 1.7	11.8 \pm 1.9
LV mass (mg) ^{§§}	111.3 \pm 9.8	110.7 \pm 9.7	167.9 \pm 15.2*#	162.4 \pm 16.4

Values are mean \pm SEM. TAC, transverse aortic constriction; *n*, number of animals; HW/BW, heart weight to body weight ratio; LuW/BW, lungs weight to body weight ratio; LiW/BW, liver weight to body weight ratio; KW/BW, average kidneys weight to body weight ratio; LV, left ventricle; LVID,s and LVID,d, LV systolic and diastolic internal diameter, respectively; LV Vol,s and LV Vol,d, LV systolic and diastolic volume, respectively; SV, stroke volume; EF, ejection fraction; FS, fractional shortening; CO, cardiac output. * $p < 0.05$ vs. control sham, ** $p < 0.01$ vs. control sham, # $p < 0.05$ vs. CTGF KO sham, ## $p < 0.01$ vs. CTGF KO sham, § $p < 0.05$ sham vs. TAC, §§ $p < 0.01$ sham vs. TAC.

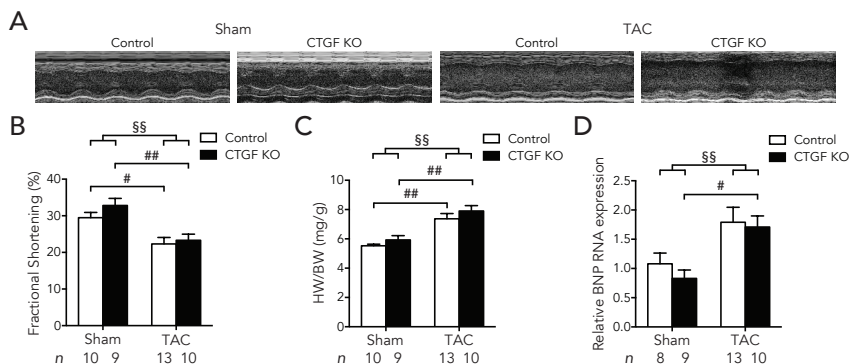


Figure 2. Tissue and echocardiographic parameters at 16 weeks of sham and TAC CTGF KO mice compared with controls.

A: Typical examples of M-mode echocardiograms. **B and C:** Fractional shortening and heart weight to body weight ratio (HW/BW), respectively. **D:** BNP RNA expression in the ventricles assessed by TaqMan RT-qPCR in control and CTGF KO mice. Black bars refer to CTGF KO mice and white bars to control mice; n indicates the number of mice per group. # $p < 0.05$, ## $p < 0.01$, \$\$ $p < 0.01$. BNP, brain natriuretic peptide.

patterns (Figure 3B). Additionally, one control TAC mouse showed 20 premature ventricular contractions (PVC) in 1 minute of electrocardiography recording (data not shown), although this mouse was not susceptible to arrhythmias in the Langendorff set-up. Arrhythmias were burst paced-induced in 17% (2/12) of the control TAC hearts compared to 0% of CTGF KO TAC hearts and both sham groups (n.s., Figure 3C). The electrophysiological parameters obtained from epicardial activation maps of the left and right ventricles (LV and RV) are summarized in Table 2 (bottom). The transversal conduction velocity (CV_T) in the LV was significantly decreased by 18% in control TAC and by 21% in CTGF KO TAC hearts (44.0 ± 1.9 and 42.0 ± 2.1 respectively vs. 53.4 ± 1.7 cm/s in control sham, $p < 0.01$, Figure 3D and Table 2). Interestingly, the decrease in longitudinal CV seen in the RV of control TAC hearts was not found in the CTGF KO TAC hearts (Figure 3D and Table 2). This lead to an increase in the anisotropic ratio in the LV of CTGF KO TAC hearts compared to respective sham hearts (1.80 ± 0.09 vs. 1.59 ± 0.13 in CTGF KO sham, $p < 0.05$, Table 2).

Fibrosis, Cx43 and $Na_v1.5$ expression

The amount of ventricular fibrosis as assessed by Picosirius Red staining was quantified by 3 independent observers that scored all hearts into 4 categories (0-3) depending on the severity of fibrosis (Figure 4A). This scoring revealed a significant 1.7-fold increase of fibrosis in control hearts after pressure overload by TAC surgery compared with control sham ($p < 0.05$, Figure 4B). Interestingly, the amount of fibrosis in the absence of CTGF was not different from control, showing a comparable increase

Table 2. Electrocardiographic and electrophysiological measurements for Sham- and TAC-operated mice.

	Sham		TAC	
	Control	CTGF KO	Control	CTGF KO
<i>n</i>	10	9	13	10
Electrocardiography				
HR (beats/min)	455.8 ± 13.6	479.8 ± 30.1	461.4 ± 19.2	465.0 ± 28.7
RR interval (ms)	132.7 ± 4.0	130.4 ± 11.0	132.9 ± 5.7	134.5 ± 9.9
PR interval (ms)	38.0 ± 0.8	45.9 ± 6.4	41.9 ± 2.5	46.2 ± 4.3
P duration (ms)	9.7 ± 0.3	11.6 ± 0.9	10.9 ± 0.6	12.7 ± 1.2
QRS interval (ms) ^{§§}	10.1 ± 0.2	11.3 ± 0.6	12.2 ± 0.4**	12.5 ± 0.4**
QT duration (ms) ^{§§}	46.3 ± 1.3	52.2 ± 3.8	58.0 ± 3.0*	58.5 ± 2.9*
QTc duration (ms) ^{§§}	40.2 ± 1.1	45.7 ± 1.5	50.5 ± 2.4**	50.8 ± 1.8**
<i>n</i>	10	7/8	11/12	9/10
Electrophysiology				
LV CV _L (cm/s)	73.2 ± 1.9	74.1 ± 3.0	63.8 ± 3.6	72.0 ± 1.6
LV CV _T (cm/s) ^{§§}	53.4 ± 1.7	47.7 ± 2.5	44.0 ± 1.9**	42.0 ± 2.1**
RV CV _L (cm/s) ^{§§}	73.8 ± 2.5	77.1 ± 2.8	63.7 ± 2.0*##	71.2 ± 2.1
RV CV _T (cm/s) ^{§§}	58.4 ± 1.7	58.2 ± 3.1	49.1 ± 1.6	51.9 ± 3.9
LV AR (CV _L /CV _T)	1.38 ± 0.05	1.59 ± 0.13	1.46 ± 0.06	1.80 ± 0.09**†
RV AR (CV _L /CV _T)	1.27 ± 0.04	1.36 ± 0.11	1.31 ± 0.05	1.43 ± 0.10
LV ERP (ms)	65.0 ± 2.7	61.3 ± 5.8	74.0 ± 5.6	64.4 ± 4.7
RV ERP (ms)	51.0 ± 3.1	51.3 ± 4.0	51.8 ± 4.6	49.0 ± 4.1

Values are mean ± SEM. TAC, transverse aortic constriction; *n*, number of animals/hearts; HR, heart rate; LV and RV, left and right ventricle, respectively; CV_L and CV_T, longitudinal and transversal conduction velocity, respectively; AR, anisotropic ratio; ERP, effective refractory period. * *p*<0.05 vs. control sham, ** *p*<0.01 vs. control sham, ## *p*<0.01 vs. CTGF KO sham, † *p*<0.05 vs. control TAC, §§ *p*<0.01 sham vs. TAC.

after TAC (1.6-fold vs. CTGF KO sham, *n.s.*, Figure 4B). Subsequently, the mRNA expression levels of several genes involved in connective tissue were analyzed (Figure 4C). Collagen (1a1, 1a2 and 3a1) RNA levels were increased after TAC surgery (*p*<0.05) although individual comparisons did not show significant differences (except collagen 1a2 between control sham and TAC). TGF-β1 RNA levels were similar between control and CTGF KO hearts, with an increase after TAC (*p*<0.05). PAI-1 and Hsp47 RNA levels, as gene targets of TGF-β1, did also not reveal any differences between control and CTGF KO hearts, although a significant increase was observed after TAC (*p*<0.05). Levels of the extracellular matrix protein fibronectin and intermediate filament protein vimentin were also investigated. Fibronectin protein levels showed no statistical difference between the groups when assessed by immunoblotting (Supplementary Figures 1A-B), however, there was an increase in TAC groups when assessed by immunohistochemistry (*p*<0.01,

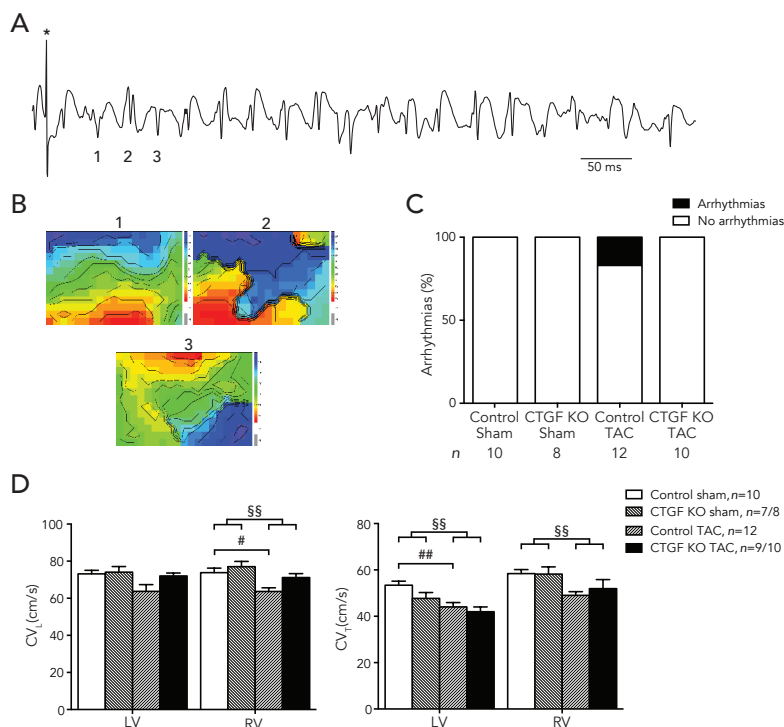


Figure 3. Arrhythmias and conduction velocity (CV) induced in perfused sham and TAC CTGF KO mouse hearts compared with controls.

A: Representative epicardial electrogram of an induced polymorphic ventricular tachyarrhythmia (VT) in control TAC mice. Asterisk (*) indicates the last burst paced (cycle length of 36 ms) complex. **B:** Activation maps from 3 numbered VT complexes indicated in the epicardial electrogram in **A**. Black isochronal lines of activation are 1 ms apart. Red colour represent earliest activation time and blue colour the latest. **C:** Incidence of arrhythmias in control and CTGF KO mice. **D:** CV measured by epicardial mapping on the left ventricle (LV) and right ventricle (RV) in longitudinal (left) and transverse (right) directions. *n* indicates the number of mice per group. # $p < 0.05$, ## $p < 0.01$, §§ $p < 0.01$.

Supplementary Figures 1C-D). Interestingly, vimentin immunolabeling was increased in TAC groups, with CTGF KO TAC hearts expressing significantly more vimentin than control TAC hearts ($p < 0.01$, Supplementary Figures 1E-F).

Ventricular tissue was further investigated on other determinants involved in conduction characteristics. The expression level of the gap junction protein Cx43 was significantly reduced after TAC surgery in control hearts by 43% when detected with immunoblotting and by 35% with immunohistochemistry ($p < 0.01$, Figures 5A-D). Similar reductions in Cx43 protein levels were observed on CTGF KO hearts. N-cadherin, a marker for intercalated disks was also analyzed with immunohistochemistry revealing unchanged levels between all groups (*n.s.*, Figure 5E). Additionally, there were no differences in Cx43 RNA levels after TAC or between control and CTGF KO hearts (*n.s.*,

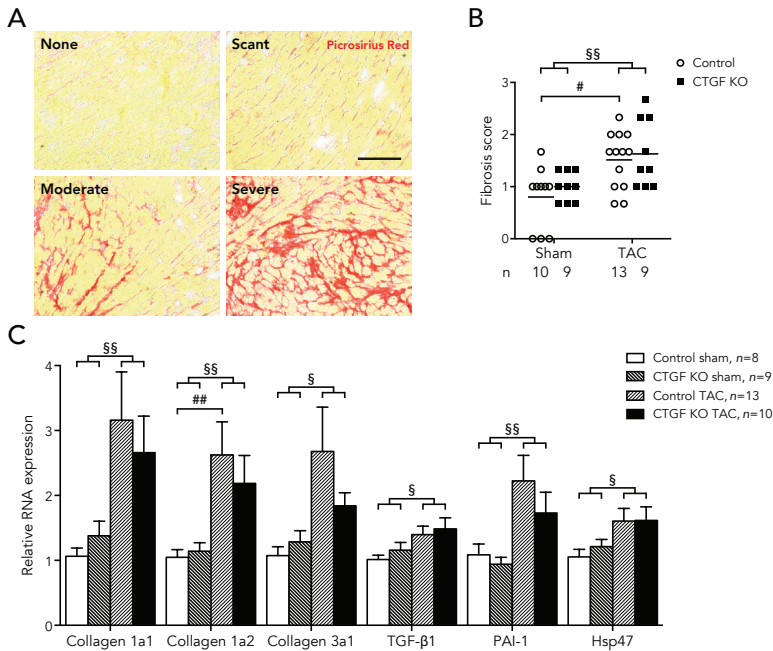


Figure 4. Fibrosis in isolated sham and TAC CTGF KO mouse ventricles compared with controls.

A: Picosirius Red representative images from gradations in severity of fibrosis into no fibrosis (none), scant amount of fibrosis (scant), moderate amount of fibrosis (moderate), and severe amount of fibrosis (severe). Scale bar represents 100 μ m. **B:** Average score of fibrosis determined by three observers. Black bars refer to CTGF KO mice and white bars to control mice. **C:** Collagen 1a1, Collagen 1a2, Collagen 3a1, TGF- β 1, PAI-1 and Hsp47 RNA expression in the ventricles assessed by TaqMan RT-qPCR in control and CTGF KO mice. n indicates the number of mice per group. # $p < 0.05$, ## $p < 0.01$, § $p < 0.05$, §§ $p < 0.01$. TGF- β 1, transforming growth factor beta-1; PAI-1, plasminogen activator inhibitor-1; Hsp47, heat shock protein 47.

Figure 5F). Finally, the sodium channel $\text{Na}_v1.5$ was analyzed for protein and RNA levels, revealing no changes in $\text{Na}_v1.5$ expression between sham and TAC hearts or between control and hearts with CTGF KO (*n.s.*, Figures 5G-I).

DISCUSSION

In this study we investigated the role of CTGF on cardiac fibrosis and hypertrophy using CTGF-deficient mice by conditional knockout in response to *in vivo* pathological stimuli of chronic pressure overload as induced by 16 weeks of TAC surgery. Additionally, the consequences of global CTGF deletion for functional, structural, and electrical remodeling in the mouse heart were also explored. The main finding of this study is that global conditional CTGF inhibition failed to prevent pressure overload induced: 1) increases in cardiac fibrosis and hypertrophy, 2) decreases in contractile function and in

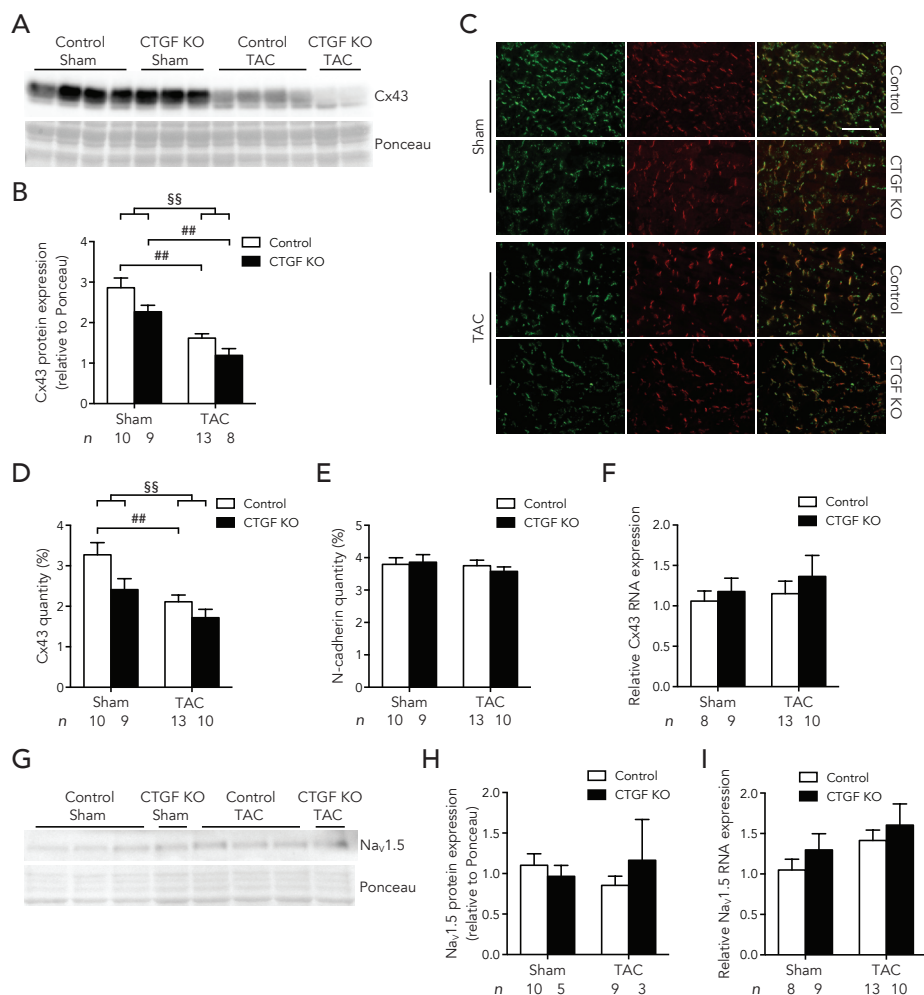


Figure 5. Connexin43 (Cx43) and Nav1.5 expression in isolated sham and TAC CTGF KO mouse hearts compared with controls.

A: Representative blot of Cx43 with respective ponceau staining below. **B:** Quantification of Cx43 protein expression (Cx43/ponceau) exemplified in **A**. **C:** Representative images of Cx43 expression (green), N-cadherin expression (red) and merged images in control and CTGF KO mice. N-cadherin was used as a marker for intercalated disks. Scale bar represents 100 μ m. **D:** Quantification of Cx43 immunolabeling exemplified in **C**. **E:** Quantification of N-cadherin immunolabeling exemplified in **C**. **F:** Cx43 RNA expression assessed by TaqMan RT-qPCR in control and CTGF KO mice. **G:** Representative blot of Nav1.5 with respective ponceau staining below. **H:** Quantification of Nav1.5 protein expression (Nav1.5/ponceau) exemplified in **G**. **I:** Nav1.5 RNA expression assessed by TaqMan RT-qPCR in control and CTGF KO mice. Black bars refer to CTGF KO mice and white bars to control mice; *n* indicates the number of mice per group. ## $p < 0.01$, §§ $p < 0.01$.

Cx43 protein expression. 3) In addition, there was a tendency towards a decrease in the incidence of pacing-induced ventricular arrhythmias and a tendency towards prevention of CV slowing in CTGF KO TAC hearts.

One of the most suggested roles of CTGF (in different organs like lungs, kidneys and heart) is the involvement in formation and/or maintenance of fibrogenic processes.^{6,27} Until recently, thorough *in vivo* functional analyses are scarce because of the lack of suitable animal models. Full CTGF KO mice die immediately after birth.²⁸ Therefore, we developed a new mouse model by global conditional knockout of CTGF, in which we show that the expression levels of CTGF are extremely low in both sham and TAC hearts. Moreover, we observed an increased expression of CTGF in control hearts after 16 weeks of pressure overload stimulation. This finding mirrors data from other studies that identified high CTGF expression levels under different cardiovascular pathological conditions as seen in patients and in experimental animal models, including applied pressure overload.⁸⁻¹⁴ These studies, including our control hearts, show that CTGF is upregulated in the fibrotic heart suggesting the connotation of CTGF as a pro-fibrotic factor. Besides that, CTGF can be regulated, among others, by the pro-fibrotic cytokine TGF- β 1.^{6,15} It would be anticipated that eliminating CTGF would reduce the amount of fibrosis in the heart, as was previously shown mainly in *in vitro* studies targeting CTGF.¹⁶ Strikingly in our study, eliminating CTGF in cardiomyocytes, fibroblasts and all other cell types that potentially are able to release CTGF did not prevent formation of cardiac fibrosis after TAC. This observation was confirmed by different approaches. Besides using Picrosirius Red staining, we also demonstrate that levels of collagen genes, fibronectin, TGF- β 1, PAI-1 and Hsp47 are not different in CTGF KO and control TAC hearts. This suggests that CTGF may not have a key role in the formation of cardiac fibrosis after all.

Contradicting findings from recent *in vivo* studies have raised uncertainty about the implication of CTGF in fibrosis, but also in hypertrophy. Szabo and colleagues²⁹ inhibited CTGF by monoclonal antibodies and found different outcomes depending on the type of cardiac injury; upon TAC there was evidence of reduced hypertrophy and collagen gene expression but no difference in collagen deposition, while with angiotensin II (Ang II) stimulation, another method to induce pressure overload, no effect on fibrotic or hypertrophic marker genes was detected. Studies using mice overexpressing CTGF specifically in cardiomyocytes have shown on one hand an increase in fibrosis but no effect on hypertrophy compared with controls upon pressure overload,³⁰ while another group that applied the same injury reported no effects on fibrosis deposition but attenuated hypertrophy.¹⁷ Using the same transgenic mouse model, but with applied myocardial infarction revealed a lower degree of hypertrophy with no aggravation on the amount of fibrosis,¹⁸ while Ang II-induced injury demonstrated an involvement of CTGF in hypertrophy but no change in fibrosis.¹⁹ All these contradicting findings questions whether CTGF is essential for fibrosis formation or hypertrophy. In fact, in the present

study we show that in addition to the lack of effect on fibrosis, CTGF KO did not alter the degree of hypertrophy after TAC, which was further strengthened by the unchanged levels of BNP in the ventricles and by echocardiography. Moreover, CTGF KO did not have an effect on contractility of the hearts after TAC, performing as poorly as control TAC mice. Again, independent studies using TAC mice with cardiac specific overexpression of CTGF showed different outcomes in terms of contractility.^{17,30} In our study, we observed an increased mortality in CTGF KO TAC mice compared with control TAC mice, although not statistically significant. This fits with the finding of Gravning and colleagues,¹⁸ who reported a reduction in mortality in their CTGF overexpressing myocardial infarction mouse model.

The gap junction protein Cx43, essential for cell-to-cell communication, is often reduced or abnormally localized in the diseased heart.³¹ Here, we show that Cx43 protein expression was decreased in control hearts after TAC, though RNA levels remained unchanged. Similarly, Cx43 protein but not RNA expression was downregulated in CTGF KO hearts. This suggests that CTGF is not involved in regulation of Cx43 expression. Nonetheless, it has been reported that recombinant CTGF added to cultured cardiomyocytes leads to acute upregulation of Cx43 and N-cadherin,³² which is in a setting that is hard to compare to our 16 weeks of pressure overload.

The sodium channel Nav1.5 is also very important for the normal propagation of the electrical impulse in the heart. Since there is no evidence that CTGF might influence or regulate Nav1.5 expression, also in this study, no differences were found in Nav1.5 protein and RNA expression after TAC in control or CTGF KO ventricles.

We previously showed that 16 weeks of pressure overload on *ex vivo* control hearts resulted in 18%⁵ or 44%²² of pacing-induced arrhythmias. Here we show a comparable percentage of arrhythmias (17%) in our control TAC hearts. Although increased fibrosis and reduced Cx43 expression were still present in CTGF KO mice, surprisingly these hearts did not show any arrhythmias under electrical stimulation on the Langendorff perfusion system. To speculate, the absence of arrhythmias in CTGF KO TAC hearts could maybe be attributed to the fact that we observed a tendency towards recovery of the longitudinal CV, although transversal CV was still decreased like control TAC. The tendency to recovery in longitudinal CV cannot be directly related to Cx43 or Nav1.5 as these proteins were not changed in CTGF KO TAC hearts when compared to control TAC. However, we cannot exclude a possible differential preservation of Cx43 at the intercalated disk, the actual site of intercellular conduction, since we did not separate our samples into junctional and non-junctional fractions. Neither we investigated potential changes in the phosphorylation status of Cx43, or in other post-translational modifications that could have affected the conduction velocity. In addition, increases in QRS and QTc of CTGF KO TAC hearts (significant when compared to control sham but not when compared to CTGF KO sham hearts) and increase in LV anisotropic ratio

points to an electrophysiological effect of CTGF, although this effect was rather small and probably not relevant for arrhythmia induction.

Our findings on the redundancy of CTGF on fibrosis, hypertrophy and cardiac function are supported by a very recent study that used different approaches to delete CTGF (or overexpress) and also subjected mice to pressure overload stimulation.²⁰ Although the overall conclusion of that study and ours strengthen each other, our data differ from that study since we followed mice chronically for 16 weeks instead of 2 or 8 weeks. Furthermore, effects on arrhythmogenesis and electrophysiological parameters were added and studied on the molecular level.

One limitation of this study that should be mentioned is that only mice surviving chronic pressure overload for 16 weeks were analysed, which might have influenced the obtained data considering that CTGF KO mice tended to die more (especially in the early phase upon TAC) than control mice.

CONCLUSION

Conditional CTGF inhibition failed to prevent TAC-induced cardiac fibrosis and hypertrophy. Additionally, other changes in response to TAC were comparable between CTGF KO and control TAC mice. With no profound effect of CTGF on fibrosis formation, other factors or pathways may be responsible for fibrosis development under these pathological conditions.

FUNDING SOURCES

We acknowledge the support from the Netherlands CardioVascular Research Initiative: the Dutch Heart Foundation, Dutch Federation of University Medical Centres, the Netherlands Organisation for Health Research and Development and the Royal Netherlands Academy of Sciences (CVON-PREDICT). In addition, this study was supported by the Dutch Heart Foundation (DHF, grant 2009B072) and by the Netherlands Institute for Regenerative Medicine (NIRM, grant FES0908).

REFERENCES

1. Swynghedauw B. Molecular mechanisms of myocardial remodeling. *Physiol Rev.* 1999;79:215-262
2. de Jong S, van Veen TA, de Bakker JM, Vos MA, van Rijen HV. Biomarkers of myocardial fibrosis. *J Cardiovasc Pharmacol.* 2011;57:522-535
3. Stein M, Boulaksil M, Jansen JA, Herold E, Noorman M, Joles JA, van Veen TA, Houtman MJ, Engelen MA, Hauer RN, de Bakker JM, van Rijen HV. Reduction of fibrosis-related arrhythmias by chronic renin-angiotensin-aldosterone system inhibitors in an aged mouse model. *Am J Physiol Heart Circ Physiol.* 2010;299:H310-321
4. Jansen JA, Noorman M, Musa H, Stein M, de Jong S, van der Nagel R, Hund TJ, Mohler PJ, Vos MA, van Veen TA, de Bakker JM, Delmar M, van Rijen HV. Reduced heterogeneous expression of Cx43 results in decreased Nav1.5 expression and reduced sodium current that accounts for arrhythmia vulnerability in conditional Cx43 knockout mice. *Heart Rhythm.* 2012;9:600-607
5. Jansen JA, van Veen TA, de Jong S, van der Nagel R, van Stuijvenberg L, Driessen H, Labzowski R, Oefner CM, Bosch AA, Nguyen TQ, Goldschmeding R, Vos MA, de Bakker JM, van Rijen HV. Reduced Cx43 expression triggers increased fibrosis due to enhanced fibroblast activity. *Circ Arrhythm Electrophysiol.* 2012;5:380-390
6. Daniels A, van Bilsen M, Goldschmeding R, van der Vusse GJ, van Nieuwenhoven FA. Connective tissue growth factor and cardiac fibrosis. *Acta Physiol (Oxf).* 2009;195:321-338
7. Shi-Wen X, Leask A, Abraham D. Regulation and function of connective tissue growth factor/CCN2 in tissue repair, scarring and fibrosis. *Cytokine Growth Factor Rev.* 2008;19:133-144
8. Chen MM, Lam A, Abraham JA, Schreiner GF, Joly AH. CTGF expression is induced by TGF-beta in cardiac fibroblasts and cardiac myocytes: A potential role in heart fibrosis. *J Mol Cell Cardiol.* 2000;32:1805-1819
9. Gabrielsen A, Lawler PR, Yongzhong W, Steinbruchel D, Blagoja D, Paulsson-Berne G, Kastrup J, Hansson GK. Gene expression signals involved in ischemic injury, extracellular matrix composition and fibrosis defined by global mRNA profiling of the human left ventricular myocardium. *J Mol Cell Cardiol.* 2007;42:870-883
10. Koitabashi N, Arai M, Kogure S, Niwano K, Watanabe A, Aoki Y, Maeno T, Nishida T, Kubota S, Takigawa M, Kurabayashi M. Increased connective tissue growth factor relative to brain natriuretic peptide as a determinant of myocardial fibrosis. *Hypertension.* 2007;49:1120-1127
11. Ruperez M, Lorenzo O, Blanco-Colio LM, Esteban V, Egido J, Ruiz-Ortega M. Connective tissue growth factor is a mediator of angiotensin II-induced fibrosis. *Circulation.* 2003;108:1499-1505
12. Way KJ, Isshiki K, Suzuma K, Yokota T, Zvagelsky D, Schoen FJ, Sandusky GE, Pechous PA, Vlahos CJ, Wakasaki H, King GL. Expression of connective tissue growth factor is increased in injured myocardium associated with protein kinase C beta2 activation and diabetes. *Diabetes.* 2002;51:2709-2718
13. Ohnishi H, Oka T, Kusachi S, Nakanishi T, Takeda K, Nakahama M, Doi M, Murakami T, Ninomiya Y, Takigawa M, Tsuji T. Increased expression of connective tissue growth factor in the infarct zone of experimentally induced myocardial infarction in rats. *J Mol Cell Cardiol.* 1998;30:2411-2422
14. Fontes MS, Raaijmakers AJ, van Doorn T, Kok B, Nieuwenhuis S, van der Nagel R, Vos MA, de Boer TP, van Rijen HV, Bierhuizen MF. Changes in Cx43 and Nav1.5 expression precede the occurrence of substantial fibrosis in calcineurin-induced murine cardiac hypertrophy. *PLoS One.* 2014;9:e87226

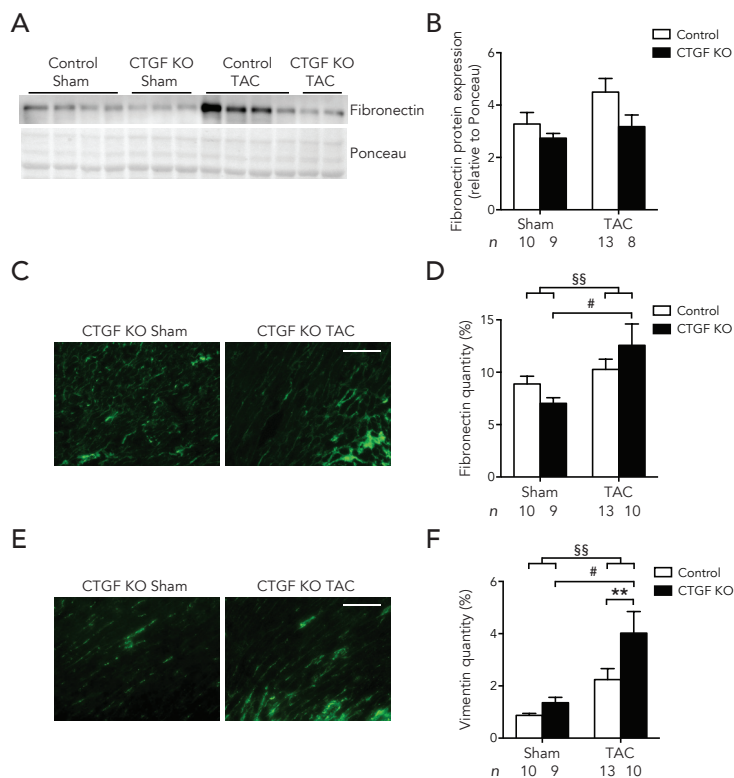
15. Ruiz-Ortega M, Rodriguez-Vita J, Sanchez-Lopez E, Carvajal G, Egido J. TGF-beta signaling in vascular fibrosis. *Cardiovasc Res.* 2007;74:196-206
16. Brigstock DR. Strategies for blocking the fibrogenic actions of connective tissue growth factor (CCN2): From pharmacological inhibition in vitro to targeted siRNA therapy in vivo. *J Cell Commun Signal.* 2009;3:5-18
17. Gravning J, Ahmed MS, von Lueder TG, Edvardsen T, Attramadal H. CCN2/CTGF attenuates myocardial hypertrophy and cardiac dysfunction upon chronic pressure-overload. *Int J Cardiol.* 2013;168:2049-2056
18. Gravning J, Orn S, Kaasboll OJ, Martinov VN, Manhenke C, Dickstein K, Edvardsen T, Attramadal H, Ahmed MS. Myocardial connective tissue growth factor (CCN2/CTGF) attenuates left ventricular remodeling after myocardial infarction. *PLoS One.* 2012;7:e52120
19. Panek AN, Posch MG, Alenina N, Ghadge SK, Erdmann B, Popova E, Perrot A, Geier C, Dietz R, Morano I, Bader M, Ozcelik C. Connective tissue growth factor overexpression in cardiomyocytes promotes cardiac hypertrophy and protection against pressure overload. *PLoS One.* 2009;4:e6743
20. Accornero F, van Berlo JH, Correll RN, Elrod JW, Sargent MA, York A, Rabinowitz JE, Leask A, Molkentin JD. Genetic analysis of connective tissue growth factor as an effector of transforming growth factor beta signaling and cardiac remodeling. *Mol Cell Biol.* 2015;35:2154-2164
21. Liu S, Shi-wen X, Abraham DJ, Leask A. CCN2 is required for bleomycin-induced skin fibrosis in mice. *Arthritis Rheum.* 2011;63:239-246
22. Boulaksil M, Winckels SK, Engelen MA, Stein M, van Veen TA, Jansen JA, Linnenbank AC, Bierhuizen MF, Groenewegen WA, van Oosterhout MF, Kirkels JH, de Jonge N, Varro A, Vos MA, de Bakker JM, van Rijen HV. Heterogeneous Connexin43 distribution in heart failure is associated with dispersed conduction and enhanced susceptibility to ventricular arrhythmias. *Eur J Heart Fail.* 2010;12:913-921
23. van Rijen HV, van Veen TA, van Kempen MJ, Wilms-Schopman FJ, Potse M, Krueger O, Willecke K, Opthof T, Jongsma HJ, de Bakker JM. Impaired conduction in the bundle branches of mouse hearts lacking the gap junction protein connexin40. *Circulation.* 2001;103:1591-1598
24. van Veen TA, van Rijen HV, Wiegerinck RF, Opthof T, Colbert MC, Clement S, de Bakker JM, Jongsma HJ. Remodeling of gap junctions in mouse hearts hypertrophied by forced retinoic acid signaling. *J Mol Cell Cardiol.* 2002;34:1411-1423
25. Falke LL, Dendooven A, Leeuwis JW, Nguyen TQ, van Geest RJ, van der Giezen DM, Broekhuizen R, Lyons K, Stoop R, Kemperman H, Schlingemann R, Joles JA, Goldschmeding R. Hemizygous deletion of CTGF/CCN2 does not suffice to prevent fibrosis of the severely injured kidney. *Matrix Biol.* 2012;31:421-431
26. Schneider CA, Rasband WS, Eliceiri KW. NIH Image to ImageJ: 25 years of image analysis. *Nat Methods.* 2012;9:671-675
27. Matsui Y, Sadoshima J. Rapid upregulation of CTGF in cardiac myocytes by hypertrophic stimuli: Implication for cardiac fibrosis and hypertrophy. *J Mol Cell Cardiol.* 2004;37:477-481
28. Ivkovic S, Yoon BS, Popoff SN, Safadi FF, Libuda DE, Stephenson RC, Daluiski A, Lyons KM. Connective tissue growth factor coordinates chondrogenesis and angiogenesis during skeletal development. *Development.* 2003;130:2779-2791
29. Szabo Z, Magga J, Alakoski T, Ulvila J, Piuhola J, Vainio L, Kivirikko KI, Vuolteenaho O, Ruskoaho H, Lipson KE, Signore P, Kerkela R. Connective tissue growth factor inhibition attenuates left ventricular remodeling and dysfunction in pressure overload-induced heart failure. *Hypertension.* 2014;63:1235-1240

30. Yoon PO, Lee MA, Cha H, Jeong MH, Kim J, Jang SP, Choi BY, Jeong D, Yang DK, Hajjar RJ, Park WJ. The opposing effects of CCN2 and CCN5 on the development of cardiac hypertrophy and fibrosis. *J Mol Cell Cardiol.* 2010;49:294-303
31. Fontes MS, van Veen TA, de Bakker JM, van Rijen HV. Functional consequences of abnormal Cx43 expression in the heart. *Biochim Biophys Acta.* 2012;1818:2020-2029
32. Adam O, Lavall D, Theobald K, Hohl M, Grube M, Ameling S, Sussman MA, Rosenkranz S, Kroemer HK, Schafers HJ, Bohm M, Laufs U. Rac1-induced connective tissue growth factor regulates connexin 43 and N-cadherin expression in atrial fibrillation. *J Am Coll Cardiol.* 2010;55:469-480

SUPPLEMENTARY MATERIALS

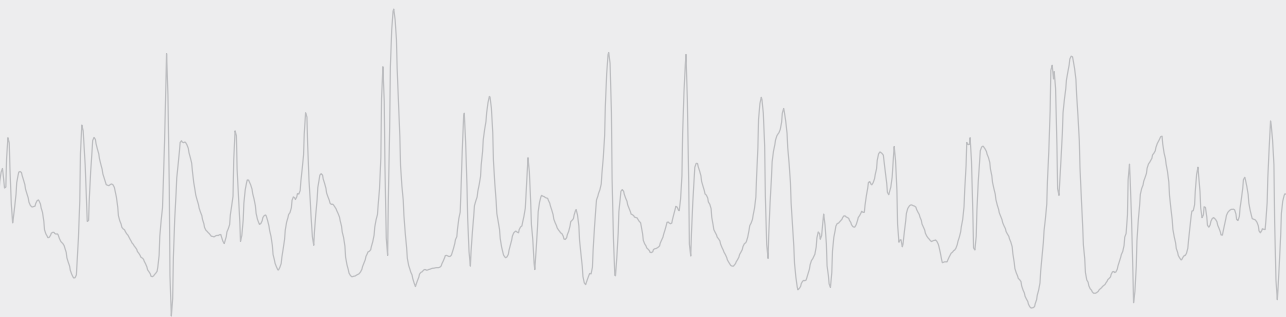
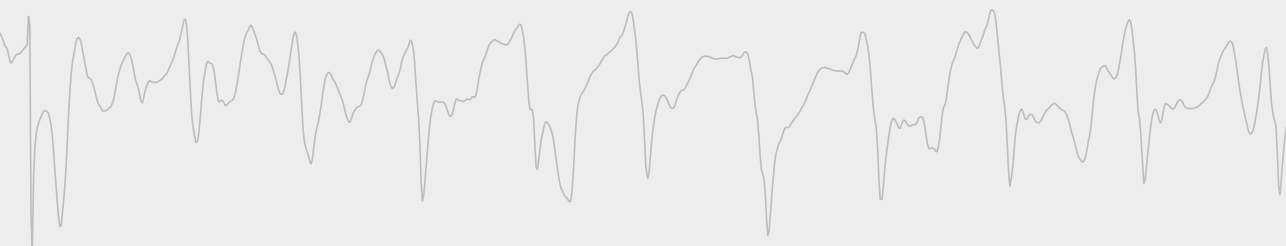
Supplementary Table 1 – References of the Applied Biosystems assays used in this study.

Protein	Gene	Assay ID
RPLP1	<i>Rplp1</i>	Mm02601846_g1
CTGF	<i>Ctgf</i>	Mm01192933_g1
BNP	<i>Nppb</i>	Mm01255770_g1
Collagen 1a1	<i>Col1a1</i>	Mm00801666_g1
Collagen 1a2	<i>Col1a2</i>	Mm00483888_m1
Collagen 3a1	<i>Col3a1</i>	Mm01254476_m1
TGF-β1	<i>Tgfb1</i>	Mm01178820_m1
PAI-1	<i>Serpine1</i>	Mm00435860_m1
Hsp47	<i>Serpinh1</i>	Mm00438058_g1
Cx43	<i>Gja1</i>	Mm00439105_m1
Na _v 1.5	<i>Scn5a</i>	Mm01342518_m1

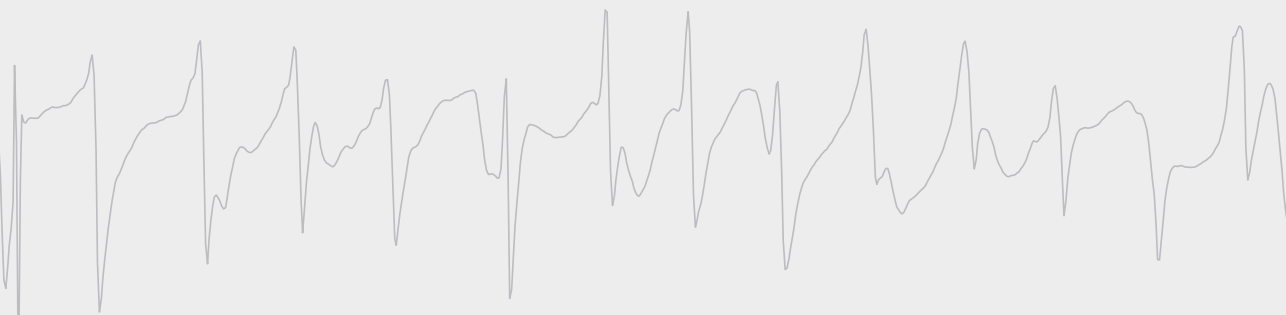


Supplementary Figure 1. Fibronectin and vimentin expression in isolated sham and TAC CTGF KO mouse ventricles compared with controls.

A: Representative blot of fibronectin with respective ponceau staining below. **B:** Quantification of fibronectin protein expression (fibronectin/ponceau) exemplified in **A**. **C:** Representative images of fibronectin (green) expression in sham and TAC CTGF KO mice. Scale bar represents 100 μ m. **D:** Quantification of fibronectin immunolabeling partly exemplified in **C**. **E:** Representative images of vimentin (green) expression in sham and TAC CTGF KO mice. Scale bar represents 100 μ m. **F:** Quantification of vimentin immunolabeling partly exemplified in **E**. Black bars refer to CTGF KO mice and white bars to control mice; n indicates the number of mice per group. # $p < 0.05$, §§ $p < 0.01$, ** $p < 0.01$.



Magda S.C. Fontes





Chapter 7



General discussion



DISCUSSION

Cardiovascular disease is a major cause of death in Europe, with a large percentage of heart failure patients still dying from sudden cardiac death, caused by fatal cardiac arrhythmias. The underlying mechanisms that lead to these arrhythmias are not fully clear. It is known, however, that most arrhythmias are perpetuated due to disturbances in electrical impulse conduction of the heart. This impulse conduction is mainly determined by 1) electrical cell-to-cell coupling between cardiomyocytes, 2) connective tissue architecture, and 3) excitability of individual cardiomyocytes. In this thesis we have investigated changes affecting electrical impulse conduction of the heart leading to arrhythmogenesis, and whether modifying some of these changes could prevent arrhythmias. The summarized results and conclusions from the different studies are as follows. In **Chapter 2** the gap junction protein connexin43 (Cx43), which primarily ensures electrical cell-to-cell coupling in the heart, was thoroughly reviewed in the background of hypertrophic, dilated and ischemic cardiomyopathy. In these cardiomyopathies, Cx43 is generally downregulated, heterogeneously redistributed throughout the heart, and in some cases lateralized. This abnormal Cx43 expression frequently results in a reduction in conduction velocity, which might increase the susceptibility to arrhythmias, especially in combination with increased fibrosis. In **Chapter 3**, we showed that in two mouse models of renal dysfunction a markedly increased susceptibility to arrhythmias was correlated with decreased Cx43 expression and increased fibrosis in the heart. In **Chapter 4** we provide evidence that acute or chronic inhibition of calmodulin/calcium-calmodulin protein kinase II (CaM/CaMKII) in different animal models leads to increased conduction velocity due to increased Cx43 at the intercalated disk. Additionally, acute CaM inhibition decreased the incidence of re-entry arrhythmias in rabbit hearts, while chronic CaMKII inhibition had no suppressive effect on induced arrhythmias in mouse hearts, and failed to prevent structural and contractile remodeling. In **Chapter 5**, using a mouse model of cardiac overexpression of continuously active calcineurin (CnA), we demonstrated that hypertrophy in these mice started as early as the first postnatal week, coinciding with reduction in Cx43 and $\text{Na}_v1.5$ expression. Furthermore, these changes preceded significant deposition of fibrosis, decreased phosphorylation of Cx43 and increased expression of pro-fibrotic genes amongst them connective tissue growth factor (CTGF). **Chapter 6** described the effects of absence of CTGF on cardiac remodeling upon chronic pressure overload in inducible and global CTGF knockout (KO) mice. Surprisingly, CTGF KO failed to prevent pressure overload-induced cardiac fibrosis and hypertrophy, as well as contractile remodeling and reduced Cx43 protein expression, suggesting that CTGF is not a critical player in fibrosis development. In summary, we have observed in the different studies that Cx43 expression and connective tissue architecture are altered in the maladaptive pathophysiological setting, as well as the activity of CaM, CaMKII and CnA, and all play important roles in arrhythmogenesis. These alterations found in the

Table 1. Summarizing results of the alterations found in the different animal models studied in this thesis.

	Cx43	Fibrosis	Nav1.5	CV	Arrhythmias
DOCA-salt model	↓	↑		↓	↑
SNx-salt model	↓	↑		=	↑
Acute CaM/CaMKII inhibition model	↑			↑	↓
Chronic CaM/CaMKII inhibition TAC model	↑	↑	=	↑	↑
CnA overexpression model	↓	↑	↓		↑
CTGF knockout TAC model	↓	↑	=	= / ↓	↓
Generalized pattern (review)	↓	↑		↓	↑

Abbreviations: Cx43, Connexin43; CV, conduction velocity; ↑, increased; ↓, decreased; =, not changed; DOCA, deoxycorticosterone acetate; SNx, 5/6-subtotal nephrectomy; CaM, calmodulin; CaMKII, calcium-calmodulin protein kinase II; TAC, transverse aortic constriction; CnA, calcineurin; CTGF, connective tissue growth factor.

different animal models studied will be discussed separately below and are summarized in Table 1.

Cell-to-cell coupling, connective tissue architecture, conduction velocity and arrhythmias

The general hypothesis of the arrhythmogenic mechanism in the diseased heart, such as in hypertrophic, dilated and ischemic cardiomyopathy has been described in **Chapter 2**: reduction of Cx43 expression and increased fibrosis result in a slowing down of the conduction velocity which predisposes the heart to reentrant arrhythmias.

In **Chapter 3**, we investigated the cardiac effects of renal dysfunction in 2 mouse models with different etiologies, an aldosterone-induced hypertension model using deoxycorticosterone acetate (DOCA) in combination with high salt diet in aged mice (DOCA-salt model), and a more severe model using 5/6-subtotal nephrectomy (SNx) in combination with high salt diet in adult mice (SNx-salt model). We observed that both of these mouse models with renal dysfunction were highly susceptible to cardiac arrhythmias. When we analyzed those hearts, we found that Cx43 expression was decreased in both models, and that there was also an increase of cardiac fibrosis, which is in agreement with previous studies.^{1,2} Furthermore, in the SNx-salt model, hypertension, cardiac hypertrophy and uraemia were not significantly increased, which suggests that these factors, under these circumstances, were not prerequisites for the development of arrhythmias.

CaMKII and its activity is usually upregulated in heart failure patients.^{3,4} Additionally, some studies have shown that CaM/CaMKII can regulate Cx43, mostly by regulating its

gating properties.⁵⁻⁷ Therefore, in **Chapter 4** we investigated the effect of acute and chronic CaM/CaMKII inhibition on rabbit (atrioventricular block and cryoablation) and mouse (chronic pressure overload) hearts, respectively, and found that total Cx43 protein expression was not changed in these hearts. The same was observed upon acute CaM/CaMKII inhibition in cultured dog cardiomyocytes. Instead, an increase in junctional Cx43 (most likely at the intercalated disk) was observed in these hearts. This suggests that the CaM/CaMKII pathway is important for controlling Cx43 localization, probably through post-translational modifications, since total Cx43 levels were unchanged. One of these modifications would be a shift in the phosphorylation status of Cx43. Although CaMKII phosphorylation sites have been identified on Cx43,⁶ no obvious differences were found between phosphorylated and non-phosphorylated Cx43 levels. Additionally, it has been shown that Cx43-mediated gap junction channels are closed by a CaM-dependent mechanism.⁵ This supports our observation of increased functional coupling after acutely inhibiting cardiomyocytes with the CaM inhibitor W7, as evidenced by the increases in functional dye transfer and in space constant of conduction. The increases in intercellular coupling and in Cx43 expression at the intercalated disk (junctional fraction) is in line with the observed increase of conduction velocity (CV) in both *ex vivo* hearts of acute and chronic CaM/CaMKII inhibition. When we looked at the possible anti-arrhythmic effect of CaM/CaMKII inhibition, we found that acutely inhibiting CaM by W7 in rabbit hearts resulted in a clear reduction of arrhythmias, although they were not completely abolished. This is in agreement with pharmacological studies in different animal models in which an anti-arrhythmic effect was observed after acute CaMKII inhibition.⁸⁻¹⁰ We speculate that the anti-arrhythmic effect in our study can be explained by the increase in CV, which in turn was a result of increased gap-junctional Cx43, although a contribution of additional factors should not be excluded given the rather small effect on conduction velocity. Perhaps surprisingly, this anti-arrhythmic effect was not observed upon chronic CaMKII inhibition during pathological chronic pressure overload (AC3-I TAC hearts). These hearts were similarly susceptible to arrhythmias as control TAC hearts from previous studies.^{11,12} The reason for the presence of arrhythmias in the AC3-I TAC hearts probably result from the fact that CaMKII inhibition did not prevent fibrosis formation after 16 weeks of pressure overload nor did it prevent the very poor contractility (due to mechanical remodeling) of these hearts. Although fibrosis is a likely candidate for the arrhythmogenic substrate in TAC mice, a previous study from our group showed no difference in degree of cardiac fibrosis between mice with or without ventricular arrhythmias.¹¹ Interestingly, two recent publications using CaMKII KO mice showed either no development of fibrosis or a further increase of fibrosis relative to controls after only 3 weeks of TAC.^{13,14} Although these studies reflect an earlier remodeling compared to our 16 weeks of TAC, it underlines the contradicting data on the direct role of CaMKII on fibrosis.

One possible reason for the presence of fibrosis in CaMKII-inhibited hearts could be the fact that CaM (not inhibited in this model) can still activate other proteins, like CnA. In the diseased heart, when CnA is activated through binding of calcium and calmodulin, it dephosphorylates members of the nuclear factor of activated T cells (NFAT) family, allowing NFAT to induce a hypertrophic response. In a previous study, our group has shown that mice overexpressing cardiac-specific CnA (MHC-CnA) were arrhythmogenic already at 4 weeks of age, with polymorphic ventricular tachyarrhythmias (VTs) and abnormal conduction, and that these hearts had reduced protein levels of Cx43.¹⁵ In our study as depicted in **Chapter 5**, we have shown that this reduction in Cx43 protein expression occurred and coincided with continuous activation of CnA at postnatal week 1, remaining reduced in the following weeks. The RNA levels of Cx43 did not follow a similar pattern, since they were downregulated at first, but later on normalized to WT values. This suggests that while the initial reduction of Cx43 protein levels was caused at the transcriptional level, the subsequent reduction was triggered by a different mechanism, most probably due to reduced Cx43 phosphorylation levels. In line with this, we have shown in **Chapter 5** that Cx43 at this stage was indeed less phosphorylated at a specific serine residue, which is a known target site for protein kinase C (PKC).¹⁶ Therefore, reduced Cx43 phosphorylation levels could possibly be attributed to reduced phosphorylation by PKC (indirectly by CnA) or to dephosphorylation by CnA itself, as CnA is a serine/threonine phosphatase, which we proved to be able to dephosphorylate Cx43 *in vitro*. The reduction in phosphorylation levels might trigger Cx43 for degradation, which would explain the observed decrease in Cx43 protein expression at the later analyzed stage of MHC-CnA hearts. Increased fibrosis in MHC-CnA hearts was reported in previous studies.^{17,18} In our study, we showed that fibrosis was significantly increased in MHC-CnA hearts from postnatal week 3 onwards. This increase in fibrosis was accompanied by increases in RNA levels of collagen, as well as other factors that have been previously linked to fibrosis: TGF- β 1, CTGF, TIMP-1 and miR-21. The RNA increase of these factors may have contributed to the increased collagen deposition observed in these hearts. In this study, the increased fibrosis and reduced Cx43 expression levels are likely forming the arrhythmogenic substrate of these hearts, which showed arrhythmias at 4 weeks of age.

Similarly as CTGF was increased in our MHC-CnA fibrotic hearts, CTGF is frequently increased in other cardiovascular pathological conditions as observed in patients and in experimental animal models, and is generally associated with formation and/or maintenance of fibrogenic processes.¹⁹⁻²⁶ Therefore, in **Chapter 6** we tried to eliminate fibrosis in a chronic pressure overload mouse model, in which we conditionally eliminated global CTGF before surgery (CTGF KO model). As expected, control hearts subjected to 16 weeks of pressure overload developed fibrosis as before,^{11,12} which was paralleled by increases in RNA levels of collagen, TGF- β 1 and CTGF. Strikingly, our new

global CTGF KO mouse model revealed the same amount of fibrosis after TAC as control mice. In line with this, in very recent literature evidence is cumulating that CTGF might not be as essential to cardiac fibrosis as originally thought, although a lot of controversy still exists.²⁷⁻³² In our study, although CTGF KO hearts still had increased levels of fibrosis and also reduced Cx43 expression, pacing-induced arrhythmias were absent in these hearts. Nevertheless, this absence of arrhythmias was not statistically different from the 17% of arrhythmias detected in control hearts. Additionally, the longitudinal impulse conduction velocity, which was reduced in control hearts, was near normal in CTGF KO hearts. Although this points to an electrophysiological effect from inhibition of CTGF, this effect is maybe too tiny to modify arrhythmia inducibility.

Previous studies from our group found no significant differences in Cx43 expression levels upon chronic pressure overload, but did find a heterogeneous redistribution of Cx43.^{11,12} This reflects our findings of similar Cx43 expression observed in sham vs. TAC AC3-I (CaMKII-inhibited) hearts. However, in the study described in **Chapter 6**, Cx43 protein expression was reduced in control TAC hearts, which is also in agreement with studies from others.^{33,34} Additionally, RNA levels for Cx43 were not changed, which means that phosphorylation levels or other post-transcriptional modifications could be behind the reduced Cx43 protein expression. Similarly, CTGF KO hearts had reduced levels of Cx43 protein but not RNA after TAC surgery, suggesting no additional involvement of CTGF on the regulation of Cx43. Though these observations might differ slightly from previous studies in our group, we cannot exclude minor differences in experimental approach as for example differences in the applied pressure gradient upon TAC, amount of animals and mode of analysis.

The arrhythmias detected in the different studies of this thesis were polymorphic ventricular tachyarrhythmias, with the exception of the spiral wave reentry observed in the rabbit CaM inhibition study. In the renal dysfunction models, while in DOCA-salt aged hearts there was CV slowing, in SNx-salt adult hearts CV was not changed, suggesting that CV was not necessary for arrhythmia inducibility in this model. In the CTGF KO study, there was a reduction in the transversal CV of control and CTGF KO TAC hearts. Also a reduction in the longitudinal CV was observed in control TAC hearts. In these situations, the presence of fibrosis and reduced Cx43 levels might have contributed to the arrhythmias. Therefore, we can conclude that on one hand, changes in conductional parameters and conduction slowing seem to be underlying arrhythmias in our cardiac disease models. On the other hand, the fact that TAC mice with CaMKII inhibition also had arrhythmias despite the increase in CV, unchanged total Cx43 and increase in junctional Cx43, points to triggered activity arrhythmias which support the nature of polymorphic VTs. Further research on action potential duration or ion currents would be necessary to confirm such statement. Most likely, arrhythmogenesis in these models relies on ectopic activity that is facilitated by increased deposition of fibrosis,

the heterogenetic character of this fibrosis and the additive effect of reductions in either transversal and/or longitudinal CV.

In conclusion, the combined results of this thesis indicate that in cardiac disease models Cx43 is downregulated and fibrosis is increased. However, we have not seen that CTGF and CaMKII are involved in fibrosis as is generally suggested in the literature. In addition, despite the changes in parameters primarily related to conduction, it seems that other factors like additional ion channels might contribute to the suspected triggered arrhythmias.

Excitability of cardiomyocytes

The excitability of cardiomyocytes is also an important aspect in assuring the proper impulse propagation throughout the heart. Relevance of changes in expression of Na_v1.5 during cardiac disease, with regard to impulse propagation, is not conclusive at this moment. For that, the sodium channel Na_v1.5 was investigated in the different studies of this thesis. In **Chapter 5**, the overexpression of CnA in the MHC-CnA mouse hearts coincided with a downregulation of Na_v1.5 expression at protein and RNA levels, suggesting that a NFAT-mediated transcriptional mechanism might be responsible for this downregulation. A recent study showed that a novel derivative of resveratrol, a known antioxidant, was able to inhibit the sodium current (among other currents) and also to reduce NFAT activity.³⁵ Still, there is no direct evidence for an association between NFAT activity and Na_v1.5. Therefore, in MHC-CnA hearts, Na_v1.5 downregulation might also have contributed to the arrhythmogenic substrate, in addition to fibrosis and reduced levels of Cx43.

Na_v1.5 has been shown to bind CaM, although its functional consequence is controversial in literature.³⁶ Furthermore, CaMKII can directly phosphorylate Na_v1.5, and inhibition of CaMKII leads to changes in the gating properties of Na_v1.5 thereby limiting channel availability, and causing a reduction in the upstroke velocity of action potentials.^{37,38} However, in our CaMKII-inhibited (AC3-I) mouse hearts, Na_v1.5 protein expression was not different from controls nor when compared with 16 weeks of pressure-overloaded TAC AC3-I hearts. Nevertheless, a study also subjecting mice to TAC surgery showed an increase in Na_v1.5 protein expression after 1 and 5 weeks of TAC.³⁹ This discrepancy could simply reflect an earlier remodeling of the heart upon pressure overload. Also, in our control mice from the CTGF study, there was no indication for differences in expression of Na_v1.5 at RNA or protein level between sham and 16 weeks of TAC. Likewise, no changes were found in CTGF KO hearts after TAC, indicating that CTGF does not regulate Na_v1.5 channel.

In conclusion, although Na_v1.5 protein levels were not changed in our TAC studies, we cannot conclude whether these channels were functional, since we did not

perform measurements of current density to confirm this. Additionally, excitability of cardiomyocytes is also dependent on other ion channels, which should be investigated in the future.

Research questions of this thesis

As postulated in the introduction, the central research questions of this thesis were:

- *How, and which changes in expression and localization of conduction parameters can be translated into an arrhythmogenic substrate?*
- *Can modification of one of those parameters prevent arrhythmias?*

Ad 1: Changes in conduction parameters that lead to arrhythmogenesis

The data of this thesis support the fact that a combination of abnormal conduction parameters is strongly associated with the arrhythmogenic substrate in the heart. In the MHC-CnA model, all three main parameters of conduction were disturbed, although this may also be due to the relatively high CnA expression in this transgenic model, which is beyond the increased levels usually observed in heart failure patients.^{40,41} In the remaining models that proved susceptible to arrhythmias, the most common finding was a combination of reduced Cx43 levels with increased fibrosis, or in the absence of reduced Cx43, the combination of fibrosis with hypertrophy and poor contractile function. Although in these models Nav1.5 protein expression was not changed, we cannot exclude possible changes in the gating/availability of the channel. This required combination of abnormal conduction parameters is strengthened by the fact that it was previously shown that reduced levels of Cx43 triggered formation of fibrosis, resulting in mice more arrhythmogenic than the ones having only increased fibrosis.¹² This finding is also proposed for the MHC-CnA model, in which fibrosis only developed after downregulation of Cx43. Furthermore, it was previously shown that a combination of heterogeneous Cx43 remodeling with a decrease of sodium current resulted in CV slowing, which likely can also contribute to the arrhythmogenic substrate.⁴² This brings us to the important topic of the localization of Cx43 in the cardiomyocyte. Cx43 is under physiological conditions primarily located in the intercalated disk, and when this distribution changes, it can contribute to abnormal intercellular coupling and therefore to arrhythmia susceptibility. In our CaM/CaMKII study, Cx43 was increased in the junctional membrane, contributing to the increase in CV. In the case of acute CaM inhibition this remodeling resulted in an anti-arrhythmic effect, understating the consequences of aberrant Cx43 distribution for the pathological phenotype. Likewise, it has been proposed that Nav1.5 channels are also localized in different pools within

the cardiomyocyte. They are found to a minor extend at the lateral membrane and predominantly at the intercalated disks, where $\text{Na}_v1.5$ interacts with different types of proteins, although their possible distinct physiological meaning is still unclear.³⁶

Ad 2: Can modification of one of those parameters prevent arrhythmias

There are currently different strategies to prevent arrhythmias, which include reduction of fibrosis, improvement of Cx43 expression, and improvement of excitability. One of the factors involved in cardiac arrhythmias is calcium signaling through CaM and CaMKII.^{10,43} Therefore, our aim for inhibiting acutely/chronically CaM/CaMKII was to prevent arrhythmias in two models of arrhythmogenesis. Indeed, by augmenting the localization of Cx43 in the intercalated disk, and therefore to increase intercellular coupling, we were able to increase CV and reduce the amount of arrhythmias in the acute CaM inhibition of rabbit hearts. Chronic CaMKII inhibition in TAC mice was not able to prevent arrhythmias which is probably due to the presence of fibrosis and functional/structural remodeling. This discrepancy could be due to the fact that the effects induced by inhibiting CaM and CaMKII are not the same, as CaM has other targets other than CaMKII, e.g. CnA. Nevertheless, it would be interesting to combine this chronic CaMKII inhibition mouse model with a treatment that would prevent formation of fibrosis and check if arrhythmias would then be suppressed.

Several approaches have been made in the literature to improve Cx43 expression and reduce arrhythmias, as discussed in **Chapter 2**. For example, dogs with atrial fibrillation administered with rotigaptide, an enhancer of gap junctional conductance, presented with increased CV.⁴⁴ In a different study, however, using explanted hearts of patients with heart failure, rotigaptide showed variable effects on conduction and arrhythmias.⁴⁵ Another avenue to improve Cx43 expression is by gene therapy. Anyukhovskiy and colleagues⁴⁶ demonstrated that adenoviral delivery of skeletal muscle Cx32 or $\text{Na}_v1.4$ directly into the left ventricle free wall preserved conduction and reduced arrhythmias in the setting of ischemia and reperfusion. Likewise, we tried to inject adenovirus encoding Cx43 directly into the left ventricle free wall although thus far this is still in a preliminary phase and no conclusions can be drawn with regard to the potential beneficial effects of this intervention. This because, the amount of adenovirus after 3 days of injection was extremely low and very local, besides the fact that a large area of the left ventricle was damaged due to the needle injection. This problem of needle injection could be avoided by intravenous injection of the virus, preferably using adeno-associated virus (AAV) that more specifically target to the heart like AAV9.⁴⁷ Important points of consideration when introducing Cx43 into the hearts is whether the phosphorylated state of these connexins will be maintained, whether the preferred localization at the intercalated disk will occur, and last but not least, whether these connexins indeed will form functional gap junctions.

Since fibrosis is one of the main contributors to pathological cardiac remodeling, preventing fibrosis was another goal in order to suppress arrhythmias.⁴⁸ As CTGF is generally considered to be extensively implicated in fibrosis, we used this target to suppress arrhythmias. Surprisingly, we found that, at least in the heart, CTGF is not essential for fibrosis formation (or hypertrophy). Therefore, we have to conclude that CTGF is not a future therapeutic target to suppress fibrosis-dependent arrhythmias. Since, to our surprise, these animals did not show any arrhythmias (although not statistically different from their controls), it would be tempting to investigate whether CTGF has anti-arrhythmic potency affecting other factors than the ones we have investigated thus far. Another pathway involved in fibrosis is the renin-angiotensin-aldosterone system (RAAS).⁴⁹ In a previous study from our group, chronic RAAS inhibition by losartan and eplerenone in aged mice significantly improved CV, reduced the amount of fibrosis, and one-to-one, reduced the incidence of arrhythmias.⁵⁰ Likewise, Qu and colleagues³⁴ have shown that treatment with spironolactone, an aldosterone receptor antagonist, reduced fibrosis and increased phosphorylation levels of Cx43 after TAC, without decreasing the degree of hypertrophy.

To follow up on the findings as described in this thesis, we have recently started a new study which is currently under investigation. In this study, we chronically treated AC3-I mice (CaMKII inhibition) with eplerenone in order to reduce fibrosis in a background of preserved Cx43 and Na_v1.5 levels at the intercalated disk. Thus far, this approach resulted in a promising reduction of ventricular tachyarrhythmias from 21% (3/14) to 7% (1/14) after 12 weeks of TAC, although this is not statistically significant yet. As such, more analyses are still necessary to substantiate these findings and to look further into the underlying mechanisms. Secondly, another new promising anti-arrhythmic target is a protein expressed in cardiomyocytes, called Carabin. A recent study showed that Carabin protects against cardiac hypertrophy and fibrosis through inhibition of CnA and CaMKII.⁵¹ Therefore, it would be very interesting to look into the electrophysiological parameters and arrhythmia inducibility in this model.

CONCLUSION

In conclusion, we have shown in this thesis that increased cardiac fibrosis and reduced Cx43 expression are strongly associated to the arrhythmogenic substrate in the diseased heart. Increased Cx43 at the intercalated disk is anti-arrhythmic under conditions that lack the maladaptive influence of fibrosis. Furthermore, we have shown that CTGF and CaMKII are not essential players in the development of cardiac fibrosis.

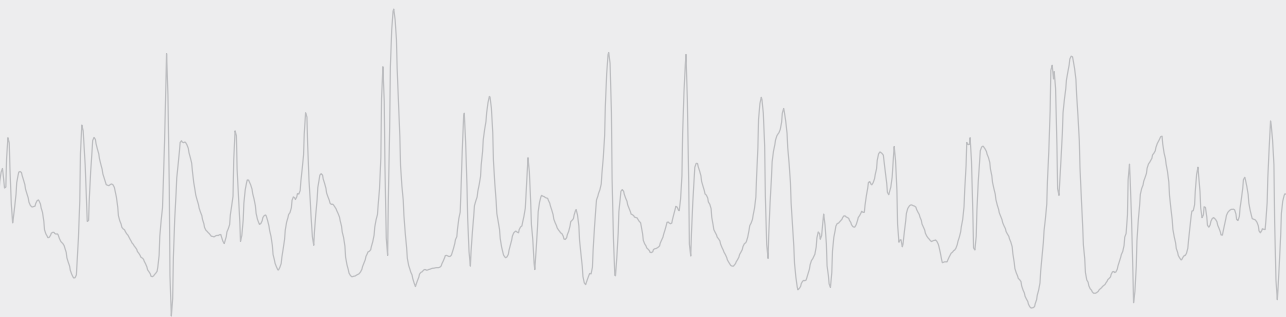
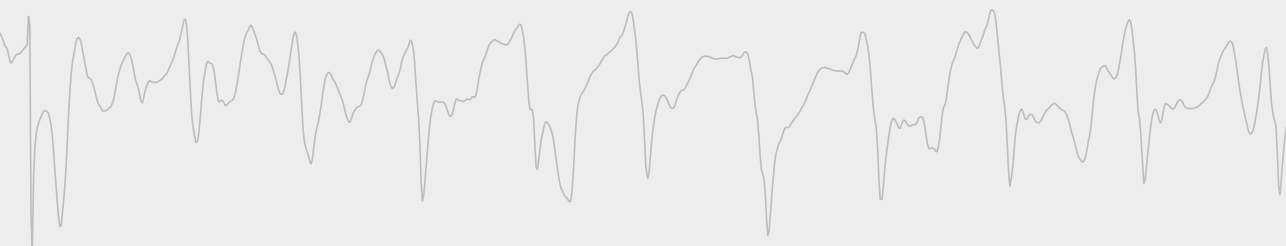
REFERENCES

1. Peng H, Carretero OA, Alfie ME, Masura JA, Rhaleb NE. Effects of angiotensin-converting enzyme inhibitor and angiotensin type 1 receptor antagonist in deoxycorticosterone acetate-salt hypertensive mice lacking Ren-2 gene. *Hypertension*. 2001;37:974-980
2. Young M, Head G, Funder J. Determinants of cardiac fibrosis in experimental hypermineralocorticoid states. *Am J Physiol*. 1995;269:E657-662
3. Anderson ME, Brown JH, Bers DM. CaMKII in myocardial hypertrophy and heart failure. *J Mol Cell Cardiol*. 2011;51:468-473
4. Kirchhefer U, Schmitz W, Scholz H, Neumann J. Activity of cAMP-dependent protein kinase and Ca²⁺/calmodulin-dependent protein kinase in failing and nonfailing human hearts. *Cardiovasc Res*. 1999;42:254-261
5. Xu Q, Kopp RF, Chen Y, Yang JJ, Roe MW, Veenstra RD. Gating of connexin 43 gap junctions by a cytoplasmic loop calmodulin binding domain. *Am J Physiol Cell Physiol*. 2012;302:C1548-1556
6. Huang RY, Laing JG, Kanter EM, Berthoud VM, Bao M, Rohrs HW, Townsend RR, Yamada KA. Identification of CaMKII phosphorylation sites in Connexin43 by high-resolution mass spectrometry. *J Proteome Res*. 2011;10:1098-1109
7. Toyama J, Sugiura H, Kamiya K, Kodama I, Terasawa M, Hidaka H. Ca²⁺-calmodulin mediated modulation of the electrical coupling of ventricular myocytes isolated from guinea pig heart. *J Mol Cell Cardiol*. 1994;26:1007-1015
8. Bell JR, Curl CL, Ip WT, Delbridge LM. Ca²⁺/calmodulin-dependent protein kinase inhibition suppresses post-ischemic arrhythmogenesis and mediates sinus bradycardic recovery in reperfusion. *Int J Cardiol*. 2012;159:112-118
9. Liu N, Ruan Y, Denegri M, Bachetti T, Li Y, Colombi B, Napolitano C, Coetzee WA, Priori SG. Calmodulin kinase II inhibition prevents arrhythmias in RyR2(R4496C+/-) mice with catecholaminergic polymorphic ventricular tachycardia. *J Mol Cell Cardiol*. 2011;50:214-222
10. Anderson ME, Braun AP, Wu Y, Lu T, Wu Y, Schulman H, Sung RJ. KN-93, an inhibitor of multifunctional ca²⁺/calmodulin-dependent protein kinase, decreases early afterdepolarizations in rabbit heart. *J Pharmacol Exp Ther*. 1998;287:996-1006
11. Boulaksil M, Winckels SK, Engelen MA, Stein M, van Veen TA, Jansen JA, Linnenbank AC, Bierhuizen MF, Groenewegen WA, van Oosterhout MF, Kirkels JH, de Jonge N, Varro A, Vos MA, de Bakker JM, van Rijen HV. Heterogeneous Connexin43 distribution in heart failure is associated with dispersed conduction and enhanced susceptibility to ventricular arrhythmias. *Eur J Heart Fail*. 2010;12:913-921
12. Jansen JA, van Veen TA, de Jong S, van der Nagel R, van Stuijvenberg L, Driessen H, Labzowski R, Oefner CM, Bosch AA, Nguyen TQ, Goldschmeding R, Vos MA, de Bakker JM, van Rijen HV. Reduced Cx43 expression triggers increased fibrosis due to enhanced fibroblast activity. *Circ Arrhythm Electrophysiol*. 2012;5:380-390
13. Cheng J, Xu L, Lai D, Guilbert A, Lim HJ, Keskanokwong T, Wang Y. CaMKII inhibition in heart failure, beneficial, harmful, or both. *Am J Physiol Heart Circ Physiol*. 2012;302:H1454-1465
14. Kreusser MM, Lehmann LH, Keranov S, Hoting MO, Oehl U, Kohlhaas M, Reil JC, Neumann K, Schneider MD, Hill JA, Dobrev D, Maack C, Maier LS, Grone HJ, Katus HA, Olson EN, Backs J. Cardiac CaM kinase II genes delta and gamma contribute to adverse remodeling but redundantly inhibit calcineurin-induced myocardial hypertrophy. *Circulation*. 2014;130:1262-1273
15. Bierhuizen MF, Boulaksil M, van Stuijvenberg L, van der Nagel R, Jansen AT, Mutsaers NA,

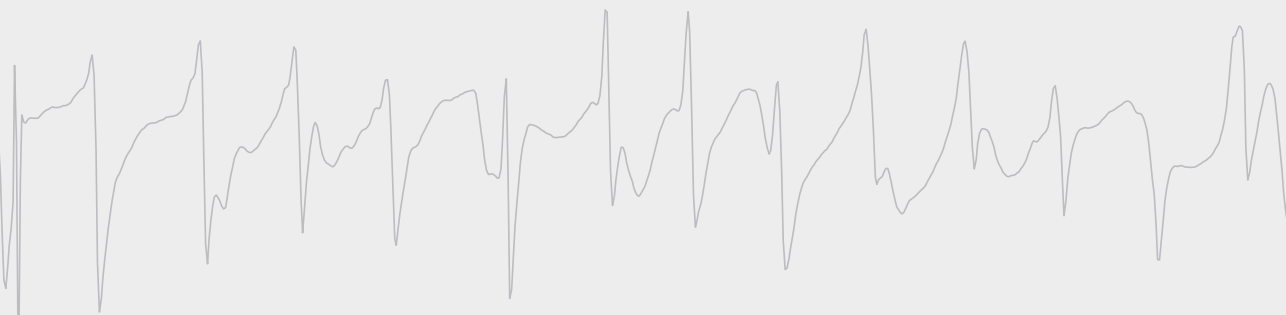
- Yildirim C, van Veen TA, de Windt LJ, Vos MA, van Rijen HV. In calcineurin-induced cardiac hypertrophy expression of Na_v1.5, Cx40 and Cx43 is reduced by different mechanisms. *J Mol Cell Cardiol.* 2008;45:373-384
16. Marquez-Rosado L, Solan JL, Dunn CA, Norris RP, Lampe PD. Connexin43 phosphorylation in brain, cardiac, endothelial and epithelial tissues. *Biochim Biophys Acta.* 2012;1818:1985-1992
 17. Molkentin JD, Lu JR, Antos CL, Markham B, Richardson J, Robbins J, Grant SR, Olson EN. A calcineurin-dependent transcriptional pathway for cardiac hypertrophy. *Cell.* 1998;93:215-228
 18. Chu G, Carr AN, Young KB, Lester JW, Yatani A, Sanbe A, Colbert MC, Schwartz SM, Frank KF, Lampe PD, Robbins J, Molkentin JD, Kranias EG. Enhanced myocyte contractility and Ca²⁺ handling in a calcineurin transgenic model of heart failure. *Cardiovasc Res.* 2002;54:105-116
 19. Chen MM, Lam A, Abraham JA, Schreiner GF, Joly AH. CTGF expression is induced by TGF-beta in cardiac fibroblasts and cardiac myocytes: A potential role in heart fibrosis. *J Mol Cell Cardiol.* 2000;32:1805-1819
 20. Gabrielsen A, Lawler PR, Yongzhong W, Steinbruchel D, Blagoja D, Paulsson-Berne G, Kastrup J, Hansson GK. Gene expression signals involved in ischemic injury, extracellular matrix composition and fibrosis defined by global mRNA profiling of the human left ventricular myocardium. *J Mol Cell Cardiol.* 2007;42:870-883
 21. Koitabashi N, Arai M, Kogure S, Niwano K, Watanabe A, Aoki Y, Maeno T, Nishida T, Kubota S, Takigawa M, Kurabayashi M. Increased connective tissue growth factor relative to brain natriuretic peptide as a determinant of myocardial fibrosis. *Hypertension.* 2007;49:1120-1127
 22. Ohnishi H, Oka T, Kusachi S, Nakanishi T, Takeda K, Nakahama M, Doi M, Murakami T, Ninomiya Y, Takigawa M, Tsuji T. Increased expression of connective tissue growth factor in the infarct zone of experimentally induced myocardial infarction in rats. *J Mol Cell Cardiol.* 1998;30:2411-2422
 23. Ruperez M, Lorenzo O, Blanco-Colio LM, Esteban V, Egido J, Ruiz-Ortega M. Connective tissue growth factor is a mediator of angiotensin II-induced fibrosis. *Circulation.* 2003;108:1499-1505
 24. Way KJ, Isshiki K, Suzuma K, Yokota T, Zvagelsky D, Schoen FJ, Sandusky GE, Pechous PA, Vlahos CJ, Wakasaki H, King GL. Expression of connective tissue growth factor is increased in injured myocardium associated with protein kinase C beta2 activation and diabetes. *Diabetes.* 2002;51:2709-2718
 25. Matsui Y, Sadoshima J. Rapid upregulation of CTGF in cardiac myocytes by hypertrophic stimuli: Implication for cardiac fibrosis and hypertrophy. *J Mol Cell Cardiol.* 2004;37:477-481
 26. Daniels A, van Bilsen M, Goldschmeding R, van der Vusse GJ, van Nieuwenhoven FA. Connective tissue growth factor and cardiac fibrosis. *Acta Physiol (Oxf).* 2009;195:321-338
 27. Szabo Z, Magga J, Alakoski T, Ulvila J, Piihola J, Vainio L, Kivirikko KI, Vuolteenaho O, Ruskoaho H, Lipson KE, Signore P, Kerkela R. Connective tissue growth factor inhibition attenuates left ventricular remodeling and dysfunction in pressure overload-induced heart failure. *Hypertension.* 2014;63:1235-1240
 28. Yoon PO, Lee MA, Cha H, Jeong MH, Kim J, Jang SP, Choi BY, Jeong D, Yang DK, Hajjar RJ, Park WJ. The opposing effects of CCN2 and CCN5 on the development of cardiac hypertrophy and fibrosis. *J Mol Cell Cardiol.* 2010;49:294-303
 29. Gravning J, Ahmed MS, von Lueder TG, Edvardsen T, Attramadal H. CCN2/CTGF attenuates myocardial hypertrophy and cardiac dysfunction upon chronic pressure-overload. *Int J Cardiol.* 2013;168:2049-2056

30. Gravning J, Orn S, Kaasboll OJ, Martinov VN, Manhenke C, Dickstein K, Edvardsen T, Attramadal H, Ahmed MS. Myocardial connective tissue growth factor (CCN2/CTGF) attenuates left ventricular remodeling after myocardial infarction. *PLoS One*. 2012;7:e52120
31. Panek AN, Posch MG, Alenina N, Ghadge SK, Erdmann B, Popova E, Perrot A, Geier C, Dietz R, Morano I, Bader M, Ozcelik C. Connective tissue growth factor overexpression in cardiomyocytes promotes cardiac hypertrophy and protection against pressure overload. *PLoS One*. 2009;4:e6743
32. Accornero F, van Berlo JH, Correll RN, Elrod JW, Sargent MA, York A, Rabinowitz JE, Leask A, Molkentin JD. Genetic analysis of connective tissue growth factor as an effector of transforming growth factor beta signaling and cardiac remodeling. *Mol Cell Biol*. 2015;35:2154-2164
33. Alesutan I, Voelkl J, Stockigt F, Mia S, Feger M, Primessnig U, Sopjani M, Munoz C, Borst O, Gawaz M, Pieske B, Metzler B, Heinzel F, Schrickel JW, Lang F. AMP-activated protein kinase alpha1 regulates cardiac gap junction protein connexin 43 and electrical remodeling following pressure overload. *Cell Physiol Biochem*. 2015;35:406-418
34. Qu J, Volpicelli FM, Garcia LI, Sandeep N, Zhang J, Marquez-Rosado L, Lampe PD, Fishman GI. Gap junction remodeling and spironolactone-dependent reverse remodeling in the hypertrophied heart. *Circ Res*. 2009;104:365-371
35. Baczko I, Liknes D, Yang W, Hamming KC, Searle G, Jaeger K, Husti Z, Juhasz V, Klausz G, Pap R, Saghy L, Varro A, Dolinsky V, Wang S, Rauniyar V, Hall D, Dyck JR, Light PE. Characterization of a novel multifunctional resveratrol derivative for the treatment of atrial fibrillation. *Br J Pharmacol*. 2014;171:92-106
36. Shy D, Gillet L, Abriel H. Cardiac sodium channel Nav1.5 distribution in myocytes via interacting proteins: The multiple pool model. *Biochim Biophys Acta*. 2013;1833:886-894
37. Ashpole NM, Herren AW, Ginsburg KS, Brogan JD, Johnson DE, Cummins TR, Bers DM, Hudmon A. Ca²⁺/calmodulin-dependent protein kinase II (CaMKII) regulates cardiac sodium channel Nav1.5 gating by multiple phosphorylation sites. *J Biol Chem*. 2012;287:19856-19869
38. Yoon JY, Ho WK, Kim ST, Cho H. Constitutive CaMKII activity regulates Na⁺ channel in rat ventricular myocytes. *J Mol Cell Cardiol*. 2009;47:475-484
39. Toischer K, Hartmann N, Wagner S, Fischer TH, Herting J, Danner BC, Sag CM, Hund TJ, Mohler PJ, Belardinelli L, Hasenfuss G, Maier LS, Sossalla S. Role of late sodium current as a potential arrhythmogenic mechanism in the progression of pressure-induced heart disease. *J Mol Cell Cardiol*. 2013;61:111-122
40. Diedrichs H, Chi M, Boelck B, Mehlhorn U, Schwinger RH. Increased regulatory activity of the calcineurin/NFAT pathway in human heart failure. *Eur J Heart Fail*. 2004;6:3-9
41. Haq S, Choukroun G, Lim H, Tymitz KM, del Monte F, Gwathmey J, Grazette L, Michael A, Hajjar R, Force T, Molkentin JD. Differential activation of signal transduction pathways in human hearts with hypertrophy versus advanced heart failure. *Circulation*. 2001;103:670-677
42. Wilders R. Arrhythmogenic right ventricular cardiomyopathy: Considerations from in silico experiments. *Front Physiol*. 2012;3:168
43. Bourgonje VJ, Schoenmakers M, Beekman JD, van der Nagel R, Houtman MJ, Miedema LF, Antoons G, Sipido K, de Windt LJ, van Veen TA, Vos MA. Relevance of calmodulin/ CaMKII activation for arrhythmogenesis in the AV block dog. *Heart Rhythm*. 2012;9:1875-1883
44. Shiroshita-Takeshita A, Sakabe M, Haugan K, Hennen JK, Nattel S. Model-dependent effects of the gap junction conduction-enhancing antiarrhythmic peptide rotigaptide (ZP123) on experimental atrial fibrillation in dogs. *Circulation*. 2007;115:310-318
45. Wiegerinck RF, de Bakker JM, Opthof T, de Jonge N, Kirkels H, Wilms-Schopman FJ, Coronel

- R. The effect of enhanced gap junctional conductance on ventricular conduction in explanted hearts from patients with heart failure. *Basic Res Cardiol.* 2009;104:321-332
46. Anyukhovskiy EP, Sosunov EA, Kryukova YN, Prestia K, Ozgen N, Rivaud M, Cohen IS, Robinson RB, Rosen MR. Expression of skeletal muscle sodium channel (Nav1.4) or connexin32 prevents reperfusion arrhythmias in murine heart. *Cardiovasc Res.* 2011;89:41-50
47. Inagaki K, Fuess S, Storm TA, Gibson GA, McTiernan CF, Kay MA, Nakai H. Robust systemic transduction with AAV9 vectors in mice: Efficient global cardiac gene transfer superior to that of AAV8. *Mol Ther.* 2006;14:45-53
48. Swynghedauw B. Molecular mechanisms of myocardial remodeling. *Physiol Rev.* 1999;79:215-262
49. Wright JW, Mizutani S, Harding JW. Pathways involved in the transition from hypertension to hypertrophy to heart failure. Treatment strategies. *Heart Fail Rev.* 2008;13:367-375
50. Stein M, Boulaksil M, Jansen JA, Herold E, Noorman M, Joles JA, van Veen TA, Houtman MJ, Engelen MA, Hauer RN, de Bakker JM, van Rijen HV. Reduction of fibrosis-related arrhythmias by chronic renin-angiotensin-aldosterone system inhibitors in an aged mouse model. *Am J Physiol Heart Circ Physiol.* 2010;299:H310-321
51. Bisserier M, Berthouze-Duquesnes M, Breckler M, Tortosa F, Fazal L, de Regibus A, Laurent AC, Varin A, Lucas A, Branchereau M, Marck P, Schickel JN, Delomenie C, Cazorla O, Soulas-Sprauel P, Crozatier B, Morel E, Heymes C, Lezoualc'h F. Carabin protects against cardiac hypertrophy by blocking calcineurin, Ras, and Ca²⁺/calmodulin-dependent protein kinase II signaling. *Circulation.* 2015;131:390-400



Magda S.C. Fontes





Addendum

Summary in English

Samenvatting in het Nederlands

Resumo em Português

Acknowledgements

List of publications

Curriculum Vitae



SUMMARY

Background

Cardiovascular disease (CVD) is the main cause of death in Western society and it is a global public health problem, particularly taking into account the ageing of the population in many countries. An important player in CVD is heart failure, which is a complex syndrome defined by insufficient pump function of the heart due to cardiac structural and functional abnormalities. Up to 50% of deaths in heart failure patients occur unexpectedly, due to sudden cardiac death, which is caused by fatal cardiac arrhythmias. Heart failure is also one of the final outcomes in the cardiorenal syndrome. This syndrome is characterized by the influence of the diseased heart on the kidney or by the influence of the diseased kidney on the heart, eventually causing failure of both organs. Patients with renal failure have an increased risk for CVD, with up to 25% of deaths in dialysis patients being caused by sudden cardiac death. Ventricular tachyarrhythmias are responsible for the vast majority of sudden cardiac deaths, however, the underlying mechanisms that lead to these arrhythmias are insufficiently understood. For this reason, more effort is needed to unravel the pathophysiological mechanisms of cardiac arrhythmias in the diseased heart.

Under normal conditions, the electrical activation pattern of the heart is initiated in the sinoatrial node, conducted by the atria, slowed in the atrioventricular node, further propagated through the ventricular conduction system, and finally terminating by activation of the ventricles. Three main parameters are responsible for proper electrical impulse propagation throughout the heart: 1. electrical cell-to-cell coupling between cardiomyocytes, 2. connective tissue architecture, and 3. excitability of individual cardiomyocytes. Any disturbance of this normal electrical impulse initiation and/or propagation may result in cardiac arrhythmias and thus underlie the sudden cardiac death frequently observed in CVD and the cardiorenal syndrome.

Aim

The aim of this thesis was to investigate changes affecting electrical impulse conduction in the diseased heart leading to arrhythmogenesis, and whether modification of the addressed changes proved to prevent arrhythmias (**Chapter 1**).

Results

A combination of genetically modified murine models, and models of applied (cardiac) disease have been analyzed with combined electrophysiological and molecular techniques to unravel key players of arrhythmogenesis in the diseased heart. In **Chapter 2**

the pathophysiological role of the gap junction protein connexin43 (Cx43), which primarily ensures electrical cell-to-cell coupling of cardiomyocytes in the heart, was thoroughly reviewed in the context of hypertrophic, dilated and ischemic cardiomyopathy. In these cardiomyopathies, Cx43 is generally downregulated, heterogeneously redistributed throughout the heart, and in some cases lateralized. This abnormal Cx43 expression and distribution frequently results in a reduction in conduction velocity, which might increase the susceptibility to arrhythmias, especially in combination with increased fibrosis (i.e. accumulation of connective tissue in the extracellular matrix). In **Chapter 3**, we showed that two mouse models of renal dysfunction, deoxycorticosterone acetate combined with high salt diet and 5/6-subtotal nephrectomy combined with high salt diet, had a markedly increased susceptibility to arrhythmias, which was correlated with decreased Cx43 expression and increased fibrosis in the heart. In **Chapter 4** we provided evidence that acute or chronic inhibition of calmodulin/calcium-calmodulin protein kinase II (CaM/CaMKII) in different animal models leads to increased conduction velocity due to increased presence of Cx43 at the intercalated disk. Additionally, acute CaM inhibition decreased the incidence of re-entry arrhythmias in diseased rabbit hearts, while chronic CaMKII inhibition had no suppressive effect on induced arrhythmias in mice subjected to pressure overload, and also failed to prevent structural and contractile remodeling. Since CaM is additionally involved in activation of calcineurin A (CnA), we further looked into a potential role for CnA. In **Chapter 5**, using a mouse model of cardiac overexpression of continuously active CnA, we demonstrated that hypertrophy in these mice started as early as the first postnatal week, coinciding with a reduction in Cx43 and in sodium channel $\text{Na}_v1.5$ expression. Furthermore, these changes preceded significant deposition of fibrosis, decreased phosphorylation of Cx43 and increased expression of pro-fibrotic genes amongst them connective tissue growth factor (CTGF). **Chapter 6** describes the effects of absence of CTGF on cardiac remodeling upon chronic pressure overload in inducible and global CTGF knockout (KO) mice. Surprisingly, CTGF KO failed to prevent pressure overload-induced cardiac fibrosis and hypertrophy, as well as contractile remodeling and reduced Cx43 protein expression, suggesting that CTGF is not a critical player in fibrosis development. Finally in **Chapter 7** the results and conclusions from preceding chapters were summarized and discussed.

Conclusion

In conclusion, we have shown in this thesis that increased cardiac fibrosis and reduced Cx43 expression are strongly associated with the arrhythmogenic substrate in the diseased heart. Increased Cx43 at the intercalated disk appears anti-arrhythmic under conditions that lack the maladaptive influence of fibrosis. Furthermore, we have shown that CTGF and CaMKII are not essential players in the development of cardiac fibrosis, though CaMKII affects the positioning of Cx43 in the intercalated disk.

Geleidingsveranderingen en ritmestoornissen in het zieke hart

SAMENSVATTING

Achtergrond

Hart- en vaatziekten zijn de voornaamste doodsoorzaak in Westerse samenlevingen en een wereldwijd probleem voor de volksgezondheid. In veel landen vergrijst daarbij de bevolking, wat het probleem waarschijnlijk zal vergroten in de toekomst. Een veelvoorkomend element bij hart- en vaatziekten is hartfalen, een complex syndroom dat gedefinieerd wordt door onvoldoende pompfunctie als gevolg van een verslechterde weefselstructuur en -functie van het hart. Tot 50% van de patiënten met hartfalen overlijdt plotseling (plotse hartdood) als gevolg van fatale hartritmestoornissen. Hartfalen komt tevens veel voor als gevolg van het cardiorenale syndroom. Bij dit syndroom verstoort een zieke nier de functie van het hart of omgekeerd, met als uiteindelijk gevolg hart- en nierfalen. Patiënten met nierfalen hebben een verhoogd risico op hart- en vaatziekten en tot 25% van de dialysepatiënten die overlijdt, sterft aan plotse hartdood. Ventriculaire tachyarritmieën zijn verantwoordelijk voor het merendeel van de sterfgevallen bij plotse hartdood, maar de onderliggende mechanismen van deze ritmestoornissen zijn nog niet goed opgehelderd. Meer onderzoek naar deze mechanismen is dus op zijn plaats.

Onder normale omstandigheden start, voorafgaande aan iedere slag, elektrische activatie van het hart in de sinoatriale knoop, waarna de impuls via de atria, de atrioventriculaire knoop (waar een vertraging optreedt) en het ventriculaire geleidingssysteem de ventrikels activeert. Drie factoren zijn bepalend voor goede geleiding van de elektrische impuls: 1. elektrische geleiding tussen hartspiercellen, 2. bindweefselstructuur van het hart, en 3. de prikkelbaarheid van de individuele hartspiercellen. Verstoring van normale impulsvorming of -geleiding kan hartritmestoornissen veroorzaken en ligt daarmee vaak ten grondslag aan de plotse hartdood die optreedt bij hart- en vaatziekten en het cardiorenale syndroom.

Doel

Het doel van dit proefschrift was om veranderingen in elektrische impulsgeleiding in het zieke hart te bestuderen die leiden tot hartritmestoornissen, en om te onderzoeken of herstel van de veranderingen ook leidt tot het voorkomen van hartritmestoornissen (hoofdstuk 1).

Resultaten

De factoren die ten grondslag liggen aan arritmogenese in zieke harten zijn onderzocht in verscheidene genetisch gemanipuleerde muismodellen en in diermodellen waarin hartziekte was geïnduceerd. Deze diermodellen zijn bestudeerd met een combinatie van elektrofysiologische en moleculair biologische technieken. In **hoofdstuk 2** is de rol van het gap junction eiwit connexin43 (Cx43) uitvoerig bediscussieerd in de context van hypertrofe, gedilateerde en ischemische cardiomyopathie. In deze ziekten is de expressie van Cx43 over het algemeen verlaagd, heterogeen verdeeld in het hart en in sommige gevallen verschuift het op cellulair nivo van de intercalair schijven aan de uiteinden van de hartspiercel naar de zijanten (lateralisatie). Deze abnormale verdeling en expressie van Cx43 eiwitten resulteert vaak in een verlaging van de geleidingssnelheid van de elektrische impuls, wat de vatbaarheid voor hartritmestoornissen verhoogd, vooral wanneer het samengaat met toegenomen fibrose (collageendepositie in het weefsel). In **hoofdstuk 3** hebben we in twee diermodellen van renale dysfunctie (deoxycorticosteron acetaat met een hoog zout dieet of 5/6 resectie van de nier met hoog zout dieet) een duidelijk verhoogde gevoeligheid voor hartritmestoornissen gevonden, welke gecorreleerd was met een verlaagde Cx43 expressie en toegenomen fibrose in het hart. In **hoofdstuk 4** hebben we aangetoond dat acute of chronische remming van calmoduline/calcium-calmoduline eiwit kinase II (CaM/CaMKII) in verscheidene diermodellen de snelheid van impulsgeleiding verhoogd door toegenomen expressie van Cx43 in de intercalair schijf. Bovendien zorgde acute remming van CaM voor een afname van re-entry arritmieën in zieke konijnenharten, terwijl chronische CaMKII remming in muizen met verhoogde drukbelasting van het hart het aantal geïnduceerde ritmestoornissen niet verlaagde en ook structurele en contractiele veranderingen niet voorkwam. Omdat CaM ook betrokken is bij activatie van calcineurine (CnA), hebben we de rol van CnA verder onderzocht. In **hoofdstuk 5** hebben we middels een transgeen muismodel met hartspecifieke overexpressie van constitutief actief CnA aangetoond dat hypertrofie in deze muizen al in de eerste postnatale week begint, wat samenvalt met een reductie in expressie van Cx43 en het natrium ionkanaal $\text{Na}_v1.5$. Bovendien gaan deze veranderingen vooraf aan significante fibrose, afgenomen fosforylatie van Cx43 en toegenomen expressie van pro-fibrotische genen, waaronder de bindweefselgroeifactor CTGF. **Hoofdstuk 6** beschrijft het effect van afwezigheid van CTGF bij chronische drukbelasting van het hart in transgene knock-out muizen waarin CTGF expressie in het gehele lichaam uitgeschakeld kan worden. Verrassend was dat uitschakeling van CTGF de standaard veranderingen bij drukbelasting (fibrose, verminderde Cx43 expressie, contractiele remodellering en hypertrofie) niet voorkwam, wat suggereert dat CTGF geen belangrijke rol speelt bij fibrose in het hart. In **hoofdstuk 7** worden tot slot de resultaten en conclusies van de voorgaande hoofdstukken samengevat en bediscussieerd.

Conclusie

In dit proefschrift hebben we aangetoond dat in zieke harten toegenomen fibrose en afgenomen expressie van Cx43 sterk geassocieerd zijn met het arritmogeen substraat. Toegenomen expressie van Cx43 in de intercalair schijven lijkt een anti-arritmogeen effect te hebben onder omstandigheden waarin de fibrose niet ook toegenomen is. Bovendien hebben we aangetoond dat CTGF en CaMKII geen essentiële rol spelen bij het ontstaan van fibrose in het hart, maar dat CaMKII wel de positionering van Cx43 beïnvloedt in de intercalair schijf.

Remodelação da condução e arritmias no coração com patologia associada

RESUMO

Contexto

A doença cardiovascular (DCV) é a principal causa de morte na sociedade Ocidental, sendo um problema global de saúde pública, especialmente tendo em conta o envelhecimento da população em muitos países. Um fator importante na DCV é a insuficiência cardíaca, uma patologia complexa caracterizada por um bombeamento insuficiente do coração, que resulta de anomalias cardíacas estruturais e funcionais. Até 50% das mortes em doentes com insuficiência cardíaca ocorrem de forma inesperada por morte súbita, devido a arritmias fatais. A insuficiência cardíaca é também uma das consequências da síndrome cardiorrenal. Esta síndrome é caracterizada pela influência que um coração com patologia provoca nos rins ou pela influência que os rins com patologia provocam no coração, causando eventualmente falha de ambos os órgãos. Os pacientes com insuficiência renal têm um risco acrescido para a DCV. As mortes de doentes em diálise ocorridas por morte súbita causada por paragem cardíaca pode chegar aos 25%. As taquiarritmias ventriculares são responsáveis pela grande maioria das mortes súbitas cardíacas, contudo, os mecanismos subjacentes que levam ao aparecimento destas arritmias são pouco compreendidos. Por esta razão, é necessário mais trabalho de investigação para desvendar os mecanismos fisiopatológicos das arritmias cardíacas.

Em condições normais, o impulso elétrico cardíaco inicia-se no nódulo sinusal, propaga-se pelas aurículas e desacelera no nódulo auriculoventricular. Este impulso elétrico prossegue através do sistema de condução dos ventrículos onde termina com a ativação dos mesmos. Os três parâmetros principais responsáveis pela propagação adequada do impulso elétrico no coração são: 1. acoplamento elétrico célula-a-célula entre cardiomiócitos, 2. estrutura do tecido conjuntivo e 3. excitabilidade de cada cardiomiócito. Qualquer distúrbio na geração ou propagação do impulso elétrico pode resultar em arritmias e, por isso, estar na base da morte súbita por paragem cardíaca frequentemente observada na DCV e na síndrome cardiorrenal.

Objetivo

O objetivo desta tese foi o de investigar as alterações que afetam a propagação do impulso elétrico no coração com patologia e que conduzem a arritmogénese. Também foi investigado se a modificação de algumas dessas alterações conduz à prevenção das arritmias (**Capítulo 1**).

Resultados

De forma a encontrar os fatores chave da arritmogénese no coração com patologia foi analisada uma combinação de modelos de murganhos geneticamente modificados e modelos de doença (cardíaca) induzida, juntamente com técnicas electrofisiológicas e moleculares. No **Capítulo 2** a função fisiopatológica da proteína de junção comunicante conexina43 (Cx43), que assegura principalmente o acoplamento elétrico célula-célula entre cardiomiócitos no coração, foi exaustivamente estudada no contexto da miocardiopatia hipertrófica, dilatada e isquémica. Nestas miocardiopatias, a expressão da proteína Cx43 está geralmente reduzida, redistribuída por todo o coração de forma heterogénea, e em alguns casos expressa na zona lateral das membranas dos cardiomiócitos. Esta expressão e distribuição anormal da Cx43 resulta frequentemente numa redução da velocidade de condução, o que poderá aumentar a susceptibilidade para arritmias, especialmente em combinação com um aumento da fibrose (ou seja, acumulação de tecido conjuntivo na matriz extracelular). No **Capítulo 3** demonstrámos que dois modelos de murganhos com disfunção renal: um modelo com acetato de desoxicorticosterona combinado com uma dieta rica em sal e um modelo com nefrectomia parcial (remoção de 5/6 dos rins) combinado com uma dieta rica em sal, tiveram um aumento notório da susceptibilidade para arritmias que foi correlacionada com a diminuição da expressão da Cx43 e o aumento da fibrose no coração. No **Capítulo 4** concluímos que a inibição aguda ou crónica da proteína calmodulina (CaM) ou da proteína cínase dependente de cálcio e de calmodulina do tipo II (CaMKII) em diferentes modelos animais resulta num aumento da velocidade de condução que por sua vez se deve ao aumento da presença da Cx43 ao nível dos discos intercalares. Adicionalmente, a inibição aguda da CaM diminuiu a incidência das arritmias de reentrada nos corações de coelhos com patologia, enquanto a inibição crónica da CaMKII não revelou efeitos inibitórios nas arritmias induzidas em murganhos submetidos a uma sobrecarga de pressão, como também não preveniu a remodelação estrutural e de contração dos corações destes corações de murganhos. Como a CaM está também envolvida na ativação da calcineurina A (CnA), investigámos melhor uma potencial função para a CnA. No **Capítulo 5**, usando um modelo de murganho a sobreexpressar uma forma continuamente ativa da CnA no coração, demonstrámos que a hipertrofia nestes murganhos começa logo na primeira semana pós-natal, coincidindo com uma redução na expressão da proteína Cx43 e do canal de sódio $\text{Nav}1.5$. Além disso, estas alterações precederam uma deposição significativa de fibrose, uma diminuição na fosforilação da Cx43 e um aumento da expressão de genes pró-fibróticos, entre os quais o fator de crescimento de tecido conjuntivo (CTGF). O **Capítulo 6** descreve os efeitos da ausência do CTGF na remodelação cardíaca após sobrecarga de pressão crónica em murganhos com um *knockout* (KO) global induzido do CTGF. De forma surpreendente, o CTGF KO não impediu o desenvolvimento de fibrose cardíaca e a hipertrofia induzidos pela sobrecarga de pressão, assim como não impediu a remodelação de contração e a

redução da expressão da proteína Cx43. Isto levou-nos a concluir que o CTGF não é um fator crítico para o desenvolvimento da fibrose. Por fim, no **Capítulo 7** os resultados e conclusões dos capítulos precedentes foram resumidos e discutidos.

Conclusão

Em conclusão, nesta tese demonstrámos que o aumento da fibrose cardíaca e a redução da expressão da Cx43 estão fortemente associados ao substrato arritmogénico. Nas situações em que não se verificou a influência anormal da fibrose, o aumento da Cx43 nos discos intercalares revelou uma tendência para ser anti-arritmico. Além disso, demonstrámos que o CTGF e a CaMKII não são fatores essenciais no desenvolvimento de fibrose cardíaca, apesar de a CaMKII afetar o posicionamento da Cx43 nos discos intercalares.

ACKNOWLEDGEMENTS

This journey of my PhD in Utrecht would not have been possible without the help and support from many many people, which I am deeply thankful for. I would like to thank everyone (also the ones I forgot to mention) that contributed in any way to my accomplishments at work or personal level!

I would like to start by thanking my supervisor **Harold**. Thank you for welcoming me in your group, for the constant help and support with everything, and for everything I learned from you. I really appreciate how you are always so enthusiastic and positive about everything, keeping the hopes up even when experiments fail. It was also great to see you every once in a while in the mouse lab to solve issues with the ECG or Langendorff. And thank you also for the gadget talks. I wish you the best of luck with your new job outside MedPhys! **Marc**, it was nice to work with you and I also learned a lot from you. Thank you for the advice on future perspectives and *gezelligheid* in congresses. And I was really surprised that after a long time you remembered what I said in my master's internship, that I would go home when I would finish my experiments! (how naive I was). To my daily supervisors, **Marti** and **Teun**, thank you for the fruitful discussions and suggestions to improve my work, and how to progress step by step, I really appreciated. **Toon**, it was a pleasure to work with you, especially these past few years where we've started to collaborate more and more on different projects and I started to bother you with more and more questions. You've helped me a lot on several topics and I truly value all the support you have given me. And I look forward to work another year with you! **Jacques**, your knowledge on science and especially on arrhythmias is remarkable. Thank you for accepting being a part of my Assessment Committee. Many thanks also to the rest of the members of the Assessment Committee for critically reading my thesis.

My journey in the Netherlands actually started thanks to **Marcel**, who accepted me for a Master's internship. Thanks to you, my interest for the heart but also for research really kicked in. It was such a pleasant experience and nice work environment with great people that I didn't think twice when the opportunity came to continue working in the same lab. **Martin** and **Marien**, it was already a while ago, but I really have to thank you for teaching me how to patch and all the basic techniques on the cell culture/molecular lab.

I want to express my sincere gratitude to **Tonny**, famously known as the mother of our department, for your help, guidance and kindness for all sort of things. The coffee/tea breaks in your office are definitely appreciated and cherished by everyone in the department, along with the cookies/sweets you always have, and that I always eat! My tummy also thanks you :)

Sanne, it was great to work together with you all these years. We helped each other a lot and I also learned a lot from you, especially with your organization skills,

which always left me amazed. It was always a pleasure to be around you, with you always smiling and laughing!

Leonie and **Bart**, super *bedankt* for all your help and commitment in the lab, in all different projects. We had really nice talks and you definitely made work more enjoyable. **Roel** and **Maike**, all my 'mouse skills' I learned from you, thank you so much! The many many hours we spent together in the GDL were definitely easier and more fun with you.

Siddarth, what can I say? I definitely had a lot of fun and great time with you inside but especially outside the lab in many many occasions. I really hope you'll be as successful as you have always aspired.

Vincent, I really appreciate our many conversations, especially on our bikes back home. Your interest for different cultures and history is remarkable. Good luck with your upcoming books! **Thom**, I learned a lot from you but especially about photography. Thank you for all your help when I was buying my first real camera. I really enjoyed visiting and being a tourist in Lisbon with both of you.

Hanneke (Hannie), you are such an amazing and fun person. I really enjoyed working with you but also partying with you. I'm sure you'll do great in Australia, good luck with the rest of your PhD! **Hannie**, **Bastiaan**, **Alex**, **Ivar**, **Helen** and **Elise**, we had a good time on Olivier Tuesdays, so we should come back to it ;)

Thanks for other members in the lab **Mohamed**, **Peter**, **Lukas**, **John**, **Christian**, **Linda**, **Hiroki**, **Malin**, **Maartje**, **Rosanne**, and the 'newer ones' **Rianne**, **Sofieke**, **Bastiaan**, **Albert**, **Yuan**, **Alex**, **Lotte**, **Elise**, **Helen**, **Iris** for making work environment a very pleasant one to work, but also for the very nice time we had in parties or congresses. I wish you all a successful and bright career and for the 'newer ones', also a successful path to finish your PhDs. **Maria**, it was nice to work together with you on the website. Thank you for all the suggestions and help. **Jet**, it was good to learn from your nice administration.

Thank you also to my students **Tessa** and **Sanne K**, who really did a great job with experiments that ended up in 2 publications! Also thank you to **Marieke** and **Bianca**, who also helped me a lot.

Arianne and **Diana**, it was great to work with you on the cardiorenal study. Thank you for all your help, especially your patience to answer all my many questions. **Lucas**, it was also nice to collaborate with you on the CTGF study. And good luck with finishing up your PhD. **Judith**, **Dries** and **Marcel Nederhoff**, thank you for the nice discussions, suggestions and tips in the mouse lab. It's nice to have a big mouse lab with so many skilled people around.

I would also like to thank several people from the GDL for all their help with the mice, including **Kelly**, **Kiki**, **Anja**, **Herma** and **Helma**. Especially to **Paul** for the nice discussions and interest in my research.

Dr. Flavien Charpentier, thank you for receiving me in your lab in Nantes to guide me with the intracardiac pacing tricks. And also thank you to **Martine de Boer**, who came all the way from Rotterdam to help us. I hope I will still use the knowledge I learned from you in the future.

Besides my colleagues, I really appreciate all the other people who helped me these past years.

I want to thank my Paranympths, **Renata** and **Susana**, for being such amazing girls and for the nice friendship we have built over the past few years. We have spent so many nice and crazy moments together that I truly treasure.

To the wonderful people and friends I made in Lange Nieuwstraat, thank you for making my life much easier in Utrecht! **Natasha, Wouter, Joana, Saskia, Thomas, Welling, Susana, Roberto, Pradeep, Isa, Casper, Alex, Erik, Anshu** and a few others, I really enjoyed and still enjoy all the nice and fun moments together either in dinners (amazing food!), parties, birthdays, burning Christmas trees or traveling around like Barcelona or the unforgettable trip to India! It's also nice to see that in the end we all have the same kind of 'struggles' during our PhDs. And now that LN babies started, my babysitting skills are also improving... ;)

Also a big thank you to my other family in Utrecht, everyone from the English community of St. Augustine's church, who welcomed me with open arms. **Renata, Ratna, Maria, Chantal, Vítor, David, Rosa, Rohan, Andrew, Loraine, Carmie, Paulius, Jesse** and **Saruné** just to name a few, really amazing the time we spend together in the choir, park, afternoons, celebrations, etc... I think we already had lunch almost everywhere in Utrecht! (Or at least in the center...)

Ana Isabel, Ana Miranda, Raquel, Filipa, Débora e Filipe já vos conheço há tantos anos! Adoro estar com vocês, apesar de ultimamente serem só umas quantas vezes ao ano... Mas eu sei que posso contar sempre com vocês para tudo o que precisar e que a nossa amizade continuará por muitos muitos anos. E a seguir à minha defesa, estou prontíssima para o grande evento do ano em Sintra :)

Ché, Carolina, Kathy e Ricardo, although the past years we are all spread in different countries (Central African Republic/Portugal/Iraq/Greece, Denmark, Portugal and Germany) I love the fact that we are still always in touch, with constant updates about everything in our lives! And of course I enjoy even more when we actually meet in person every time I come to Portugal. I think I can repeat myself with *los quiero mucho y los echo de menos!*

It would have been impossible to do this PhD without the unconditional love and support of my family. Quero agradecer a todos os meus **tios, tias, primos, primas** e querida **avó Bia** por todo o apoio. Em especial aos meus **pais** e à minha maninha

Mafalda pelo apoio constante e dedicação, mas também pela paciência estes anos todos por detrás do ecrã, através das infinitas horas que passámos a falar pelo skype. E eu sei como sou muito mimada por vocês, com as minhas comidas preferidas sempre que vou a casa :) Um muitíssimo obrigada a todos por tudo!

Thank you all,

Magda :)

Utrecht, 2015

LIST OF PUBLICATIONS

Publications in this thesis:

Fontes MSC*, Kessler EL*, van Stuijvenberg L, Brans MA, Falke LL, Kok B, van Rijen HVM, Vos MA, Goldschmeding R, van Veen TAB. CTGF knockout does not affect cardiac hypertrophy and fibrosis formation upon chronic pressure overload. *Submitted*

Takanari H*, Bourgonje VJA*, **Fontes MSC***, Raaijmakers AJA, Driessen H, Jansen JA, van der Nagel R, Kok B, van Stuijvenberg L, Boulaksil M, Takemoto Y, Yamazaki M, Tsuji Y, Honjo H, Kamiya K, Kodama I, Anderson ME, van der Heyden MAG, van Rijen HVM, van Veen TAB*, Vos MA*. Calmodulin/CaMKII inhibition augments the localization of cardiac Connexin43 in the intercalated disk: consequences for conduction velocity and arrhythmogenesis. *Submitted*

Fontes MSC, Papazova DA, van Koppen A, de Jong S, Korte SM, Bongartz LG, Nguyen TQ, Bierhuizen MFA, de Boer TP, van Veen TAB, Verhaar MC, Joles JA, van Rijen HVM. Arrhythmogenic remodeling in DOCA-salt and SNX-salt induced murine models of cardiorenal disease. *Cardiorenal Med* 2015; 5: 208-18

Fontes MSC, Raaijmakers AJA, van Doorn T, Kok B, Nieuwenhuis S, van der Nagel R, Vos MA, de Boer TP, van Rijen HVM, Bierhuizen MFA. Changes in Cx43 and Nav1.5 expression precede the occurrence of substantial fibrosis in calcineurin-induced murine cardiac hypertrophy. *PLoS One* 2014; 9(1): e87226

Fontes MSC, van Veen TAB, de Bakker JMT, van Rijen HVM. Functional consequences of abnormal Cx43 expression in the heart. *Biochim Biophys Acta* 2012; 1818(8): 2020-9

* Authors contributed equally

Other publications:

de Jong S, Kok B, van Wijk MC, **Fontes MSC**, Brans MA, de Bakker JMT, Vos MA, van Rijen HVM, Bierhuizen MFA. In cardiac pressure overloaded mice fibrosis is correlated to miR-21, miR-30c, and miR-133a in tissue but not in plasma. *In preparation*

Vale FF, Saraiva-Pava KD, **Fontes MSC**, Vieira H. Microbiologic quality of an untreated water sample analyzed by a novel DNA chip for simultaneous detection of microorganisms. *Microbiology Research* 2012; 3: e11

Conference presentations (selection):

Fontes MSC, Kessler EL, van Stuijvenberg L, Brans MA, Falke LL, Kok B, van Rijen HVM, Vos MA, Goldschmeding R, van Veen TAB. The role of CTGF in cardiac remodeling upon pressure overload. *Oral presentation, Meeting of the European Heart Rhythm Association / 39th European Working Group on Cardiac Cellular Electrophysiology Meeting 2015, Milan, Italy*

Fontes MSC, Takanari H, Bourgonje VJA, Raaijmakers AJA, Driessen H, Jansen JA, van der Nagel R, Kok B, Takemoto Y, Tsuji Y, Honjo H, Kodama I, Anderson ME, van der Heyden MAG, van Rijen HVM, van Veen TAB, Vos MA. Calmodulin/CaMKII inhibition accelerates conduction velocity by augmenting the localization of Cx43 in the intercalated disk. *Oral presentation, Symposium of the Dutch Physiological Society 2014, Rotterdam*

Fontes MSC, Raaijmakers AJA, van Doorn T, Kok B, Nieuwenhuis S, van der Nagel R, Vos MA, de Boer TP, van Rijen HVM, Bierhuizen MFA. Arrhythmogenic remodeling in calcineurin-induced cardiac hypertrophy. *Oral presentation, Meeting of the European Heart Rhythm Association / 37th European Working Group on Cardiac Cellular Electrophysiology Meeting 2013, Athens, Greece*

Fontes MSC, van Koppen A, de Jong S, Bongartz LG, Joles JA, Nguyen TQ, van Rijen HVM, Verhaar MC. Cardiac remodeling in DOCA-salt induced mouse model of cardiorenal disease. *Meeting of the European Heart Rhythm Association / 37th European Working Group on Cardiac Cellular Electrophysiology Meeting 2013, Athens, Greece*

Fontes MSC, de Boer TP, Bierhuizen MFA, van Veen TAB, van Rijen HVM. Modification of electrical coupling in cultured cardiac slices. *35th European Working Group on Cardiac Cellular Electrophysiology Meeting 2011, Oslo, Norway*

CURRICULUM VITAE

Magda Fontes was born on November 12, 1987 in Lisbon, Portugal. After completing secondary education in Lisbon, she started a bachelor in Biomedical Engineering at Catholic University of Portugal. In September 2008, she continued with a master in Biomedical Engineering in the same university where she did a 4-month research project on "The validation of a novel DNA chip for detection of microorganisms in water samples". In February 2010, she moved to the Netherlands for a 6-month research internship combined with Masters' thesis at the department of Medical Physiology in the UMC Utrecht where she worked with Dr. Marcel van der Heyden on "Pharmacological regulation of the inward rectifier ion channel protein Kir2.1". After she obtained her MSc in 2010, she started as a PhD candidate the same year with Prof. Dr. Marc Vos, Prof. Dr. Harold van Rijen, Dr. Marti Bierhuizen and Dr. Teun de Boer at the department of Medical Physiology. The results of her research are described in this thesis. During her PhD she was a member of the PhD candidates committee from the Cardiovascular Research Track of UMC Utrecht and Utrecht University.



Magda will publicly defend her thesis entitled "Conductional remodeling and arrhythmias in the diseased heart" on the 3rd of September 2015. Currently, she continues in Utrecht in the same department working as a post-doctoral researcher with Dr. Toon van Veen.

